

THE DURNESS GROUP OF NW SCOTLAND: A STRATIGRAPHICAL AND
SEDIMENTOLOGICAL STUDY OF A CAMBRO-ORDOVICIAN PASSIVE MARGIN
SUCCESSION

by

ROBERT JAMES RAINE

A thesis submitted to
The University of Birmingham
for the degree of
DOCTOR OF PHILOSOPHY

School of Geography, Earth and
Environmental Sciences
The University of Birmingham
June 2009

UNIVERSITY OF
BIRMINGHAM

University of Birmingham Research Archive

e-theses repository

This unpublished thesis/dissertation is copyright of the author and/or third parties. The intellectual property rights of the author or third parties in respect of this work are as defined by The Copyright Designs and Patents Act 1988 or as modified by any successor legislation.

Any use made of information contained in this thesis/dissertation must be in accordance with that legislation and must be properly acknowledged. Further distribution or reproduction in any format is prohibited without the permission of the copyright holder.

ABSTRACT

The Cambrian to Ordovician Durness Group was deposited on the Scottish sector of the passively-subsiding, continental margin of the Laurentian craton, and now forms part of the Hebridean terrane, lying to the west of the Moine Thrust zone. It represents c. 920 m of shallow marine, peritidal carbonates with minor siliciclastic and evaporitic strata. Facies analysis shows that the carbonates represent deposition within coastal sabkha, intertidal and shallow subtidal to shelfal environments and sedimentary logging of all available sections has revised the thicknesses of the lithostratigraphic formations within the Durness Group. A diverse array of microbialites is documented, and their application for interpreting the sea-level and palaeoenvironmental history is discussed. The enigmatic ‘leopard rock’ texture is here concluded to represent a thrombolite, thus significantly increasing the abundance of microbial facies within the section. A revised conodont biostratigraphy for the Ordovician upper five formations of the Durness Group allows more precise correlation with the once contiguous sections in western Newfoundland and Greenland and dating of the lithostratigraphical and sequence stratigraphical subdivisions for the first time. Based upon the new conodont biostratigraphy, a sequence stratigraphical model for the Cambro-Ordovician strata in Scotland is proposed, comprising four depositional megasequences, which correlate well with the Sauk sea level sequence recognised across Laurentia. This study allows for further correlation with Laurentian margin sections and the global sea-level record.

ACKNOWLEDGEMENTS

I would like to thank all the help and support from my supervisors Paul Smith (Birmingham) and Maarten Krabbendam (BGS). Paul is particularly thanked for tireless reading of paginated ramblings, trying to explain the finer points of en- and em-dash usage to deaf ears and for much assistance, culinary delights and enthusiasm in the field. John Repetski, Dave Evans and Tim Palmer have been good company in the field and always showed interested in my project.

Thanks are also due to Rosie, Lauren, Kate and Liam, Neil (for camping barn trips and painting a 6' chaffinch on my wall), Tom Challands, Giles Miller, Nick, Luis (BGS), Mark Dean (BGS), Ross, Jenny, Chris, Tim, Andy, Helen, Carl, Ruth, Karen, Aruna, Pete Turner, Beth, Leyla, Jason, Paul Hands, Donald the Highland Ranger, and any others who deserve a mention. Lil and Helen are thanked greatly for their friendship, encouragement and joint enthusiasm for curry. Russel is thanked for breaking the boredom with cider making and drinking.

My parents and sisters deserve special mention for their support and financial assistance and whose recurring greeting over the past few years has been 'have you finished your thesis yet?'

For the many housemates and Geology vagrants at [REDACTED] who have been both a help and a welcome distraction at times and who now have jobs in the real world. Dr Liam Herringshaw, Emma Nichols, Dr Simon Holford and Gui the French guy.

The work was funded primarily by the School of Geography, Earth and Environmental Sciences. and the British Geological Survey (BUFI Grant E2152S60). The Palaeontological Association (Sylvester Bradley Award) and the BSRG (Farrell Fund) are acknowledged for financial assistance with fieldwork and conference attendance.

The school funding has involved the opportunity to work as assistant curator (and for a brief stretch conservator) within the Lapworth Museum, whilst spinning out my PhD. The main benefit of which has been working with Jon Clatworthy, who is perhaps one of the most helpful and kind persons around. I have to thank him for never putting fine specimens of dolomite in the skip.

Finally thanks to all at Ichron Ltd., who always assumed that I slept in the office whilst writing.

‘It is not that I object to the work, mind you; I like work: it fascinates me. I can sit and look at it for hours.’

Jerome K. Jerome (1859–1927): *Three Men in a Boat (To Say Nothing of the Dog)* 1889

‘Stands Scotland where it did?’

William Shakespeare (1564–1616): *Macbeth* 1606

TABLE OF CONTENTS

	Page
Abstract	i
Acknowledgements	ii
Chapter 1.	
INTRODUCTION AND STRATIGRAPHICAL REVISION OF THE DURNESS GROUP, NW SCOTLAND	
1.1 Geological setting of the Durness Group	1
1.2 Study areas	2
1.2.1 An t-Sròn, Loch Eriboll	2
1.2.2 Smoo Inlet and Leirinmore	4
1.2.3 Balnakeil Bay	4
1.2.4 Inland exposures between Loch Borrallie and Loch Caladail	6
1.2.5 The Kyle of Durness	8
1.2.6 Grudie	8
1.2.7 Ardvreck Castle and Inchnadamph, Loch Assynt	9
1.2.8 Ord, Skye	9
1.2.9 Strath Suardal and Loch Lonachan, Skye	9
1.3 Previous research on the Cambro-Ordovician of northwest Scotland	10
1.3.1 Sedimentology	11
1.3.2 Sequence stratigraphy and correlation	11
1.3.3 Palaeontology and biostratigraphy	11
1.3.4 Chemostratigraphy	14
1.4 Lithostratigraphical revision of the Durness Group	15
1.4.1 Durness Group	16
1.4.2 Ghrudaidh Formation	17
1.4.3 Eilean Dubh Formation	17
1.4.4 Sailmhor Formation	18
1.4.5 Sangomore Formation	20
1.4.6 Balnakeil Formation	20
1.4.7 Croisaphuill Formation	21
1.4.8 Durine Formation	22
1.5 Recent developments in Cambrian and Ordovician chronostratigraphy	22
1.5.1 Current Cambrian stratigraphy	22
1.5.2 The Cambrian–Ordovician boundary	26
1.5.3 Current Ordovician stratigraphy	26
Chapter 2.	
FACIES ANALYSIS OF THE IAPETUS PASSIVE MARGIN SEDIMENTS IN NW SCOTLAND: THE CAMBRO-ORDOVICIAN DURNESS GROUP	
2.1 Introduction	27

2.2	Lithofacies	27
2.2.1	Ooidal grainstone/wackestone	30
2.2.2	Oncoidal grainstone/packstone	33
2.2.3	Burrowed mudstone/wackestone	35
2.2.4	Ribbon carbonate	37
2.2.5	Bioclastic wackestone/packstone	39
2.2.6	Stromatactoid carbonate	40
2.2.7	Peloidal grainstone	42
2.2.8	Thrombolite boundstone	44
2.2.9	Columnar stromatolite boundstone	46
2.2.10	Hemispheroidal stromatolite boundstone	46
2.2.11	Intraclast rudstone	47
2.2.12	Parallel laminated carbonate	50
2.2.13	Ripple laminated carbonate	53
2.2.14	Quartz arenaceous carbonate	55
2.2.15	Fenestral carbonate	57
2.2.16	Crinkly laminated and planar stromatolite boundstone	58
2.3	Facies associations	59
2.3.1	Shallow subtidal facies association	59
2.3.2	Intertidal flat facies association	60
2.3.3	Sabkha/supratidal facies association	60
2.4	Stratigraphic trends	76
2.5	Conclusions and environmental interpretations	85

Chapter 3.

TEMPORAL TRENDS OF CAMBRO-ORDOVICIAN MICROBIALITES: A CASE STUDY FROM THE DURNESS GROUP OF NW SCOTLAND

3.1	Introduction	87
3.2	Development of terminology	88
3.3	Histry of research	91
3.3.1	Stromatolites	91
3.3.2	Thrombolites	92
3.3.3	Dendrolites and leiolites	93
3.4	Methods	94
3.5	Stromatolites from the Durness Group	94
3.5.1	Stratiform stromatolites	94
3.5.2	Encrusting stromatolites	97
3.5.3	Hemispheroidal stromatolites	97
3.5.4	Columnar stromatolites	98
3.5.5	Oncolites	102
3.6	Leiolites from the Durness Group	104
3.7	Thrombolites from the Durness Group	104
3.7.1	Reinterpretation of the 'leopard rock'	105

3.7.2	Domal and columnar thrombolite bioherms	109
3.7.3	Stratiform thrombolite biostromes	109
3.8	Microbialites as environmental indicators	111
3.8.1	Stromatolites	111
3.8.2	Thrombolites	113
3.9	Durness Group microbialites and palaeoenvironment	114
3.10	Temporal trends of palaeoenvironmental change	116
3.10.1	Short term temporal trends	116
3.10.2	Long term temporal trends	118
3.11	The rise and demise of Cambro-Ordovician microbialites	121
3.12	Conclusions	125

Chapter 4.

CONODONT BIOSTRATIGRAPHY OF THE DURNESS GROUP

4.1	Introduction	127
4.2	Sampling and processing methods	127
4.3	Previous research	130
4.3.1	Early studies concerning the upper Durness Group	130
4.3.2	The Cambrian–Ordovician boundary interval	131
4.4	Conodont zonation	133
4.4.1	North American midcontinent zones	133
4.5	Conodont biostratigraphy of the Durness Group	137
4.5.1	<i>Rossodus manitouensis</i> Zone	137
4.5.2	‘Low diversity interval’	139
4.5.3	<i>Macerodus diana</i> Zone	139
4.5.4	<i>Acodus deltatus</i> – <i>Oneotodus costatus</i> Zone	140
4.5.5	<i>Oepikodus communis</i> Zone	141
4.5.6	? <i>Reutterodus andinus</i> Zone	145
4.5.7	<i>Tripodus laevis</i> Zone	146
4.5.8	<i>Histiodela altifrons</i> Zone	147
4.6	Palaeobiogeography	150
4.6.1	Extent of the Tropical Domain	150
4.6.2	A multivariate statistical analysis of Laurentian faunas at the time of maximum flooding	152
4.7	Conclusions	157

Chapter 5.

SEQUENCE STRATIGRAPHY OF THE SCOTTISH LAURENTIAN MARGIN AND RECOGNITION OF THE SAUK MEGASEQUENCE

5.1	Introduction	158
5.2	Terminology	162
5.3	Metre-scale, shallowing upward parasequences within the Durness Group	163
5.3.1	Subtidally dominated parasequences	165
5.3.2	Peritidally dominated parasequences	165

5.3.3	Origin of metre-scale parasequences	167
5.3.4	Alloyclic model	168
5.3.5	Autocyclic model	169
5.3.6	Parasequence sets and accommodation curve	171
5.4	SLM I Supersequence	175
5.5	SLM I–II boundary	177
5.6	SLM II Supersequence	178
	5.6.1 SLM IIa Sequence	179
	5.6.2 SLM IIb Sequence	180
5.7	SLM II–III boundary	181
5.8	Cambrian Grand Cycles and correlation with the Durness Group (SLM IIa, IIb & IIIa)	184
5.9	SLM III Supersequence	185
	5.9.1 SLM IIIa Sequence	186
	5.9.2 SLM IIIb Sequence	186
	5.9.3 SLM IIIc Sequence	189
5.10	SLM IV Supersequence	194
5.11	The end of the SLM Megasequence in Scotland	198
5.12	Conclusions and relative sea-level history	201
Chapter 6.		
SUMMARY OF CONCLUSIONS		205
REFERENCES		208
APPENDICES		
	APPENDIX 1 List of localities	238
	APPENDIX 2 Biostratigraphical samples	239

LIST OF FIGURES

		Page
Text-fig. 1.1	Schematic sedimentary log of the Cambro-Ordovician succession in NW Scotland.	3
Text-fig. 1.2	Palaeogeographical maps of the Lower Ordovician globe and the Laurentian margin.	4
Text-fig. 1.3	Location map showing the distribution of Cambro-Ordovician rocks in NW Scotland.	5
Text-fig. 1.4	Simplified geological map of the east side of Loch Eriboll.	6
Text-fig. 1.5	Simplified geological map of the area around Durness.	7
Text-fig. 1.6	Simplified geological map of the area around Assynt.	10
Text-fig. 1.7	Published stratigraphical subdivisions and thicknesses of the Cambro-Ordovician succession in NW Scotland.	19
Text-fig. 1.8	Cambrian global series and stages and their correlation.	24
Text-fig. 1.9	Ordovician global series and stages and their correlation.	25
Text-fig. 2.1	The interpreted distribution of lithofacies described in relation to tidal range.	28
Text-fig. 2.2	The classification of carbonate rocks by their depositional texture.	29
Text-fig. 2.3	Exposure indices for tidal flat features.	30
Text-fig. 2.4	Photographs and photomicrographs showing ooidal grainstone/wackestone facies.	31
Text-fig. 2.5	Photographs showing oncoidal grainstone/packstone facies.	34
Text-fig. 2.6	Photographs showing burrowed mudstone/wackestone facies.	37
Text-fig. 2.7	Photographs showing ribbon carbonate facies.	39
Text-fig. 2.8	Photographs showing stromatactoid carbonate facies.	41
Text-fig. 2.9	Photographs and photomicrograph showing peloidal grainstone facies.	43
Text-fig. 2.10	Photographs showing stromatolite and thrombolite boundstone facies.	45
Text-fig. 2.11	Photographs showing carbonate and chert intraclast rudstone facies.	49
Text-fig. 2.12	Photographs showing parallel laminated carbonate facies.	52
Text-fig. 2.13	Photographs showing ripple laminated carbonate facies.	54
Text-fig. 2.14	Photographs and photomicrographs showing quartz arenaceous carbonate facies.	56
Text-fig. 2.15	Photographs showing fenestral carbonate facies.	57
Text-fig. 2.16	Photographs showing crinkly laminated and planar stromatolite boundstone facies.	58
Text-fig. 2.17	Photographs and photomicrograph showing crystalline gypsum pseudomorphs.	63

Text-fig. 2.18	Photographs showing nodular and bedded evaporate pseudomorphs	65
Text-fig. 2.19	Photomicrographs of replaced evaporate textures in thin section	68
Text-fig. 2.20	Photographs showing sabkha facies and halite pseudomorphs.	69
Text-fig. 2.21	Photographs showing evaporate dissolution breccias.	72
Text-fig. 2.22	Annotated photograph displaying a sabkha cycle	75
Text-fig. 2.23	Sedimentary logs of the An t-Sròn and Ghrudaidh formations, including legend.	78
Text-fig. 2.24	Sedimentary logs of the Eilean Dubh Formation.	79
Text-fig. 2.25	Sedimentary logs of the Sailmhor Formation.	80
Text-fig. 2.26	Sedimentary logs of the Sangomore and Balnakeil formations.	81
Text-fig. 2.27	Sedimentary logs of the Croisaphuill Formation.	82
Text-fig. 2.28	Sedimentary logs of the Durine Formation.	83
Text-fig. 3.1	Diagram showing the scales of observation used in the study of microbialites.	93
Text-fig. 3.2	Terminology used in the description of microbialites.	95
Text-fig. 3.3	Photographs showing stratiform and encrusting stromatolites.	96
Text-fig. 3.4	Photographs showing hemispheroidal stromatolites.	99
Text-fig. 3.5	Photographs showing columnar stromatolites (Eilean Dubh Formation).	100
Text-fig. 3.6	Photographs showing columnar stromatolites (Sailmhor to Balnakeil formations).	101
Text-fig. 3.7	Photographs showing oncolites.	103
Text-fig. 3.8	Photographs showing the features of burrow mottled carbonate.	107
Text-fig. 3.9	Photographs showing the microbialitic features of the ‘leopard rock’.	108
Text-fig. 3.10	Photographs and photomicrograph showing thrombolites.	110
Text-fig. 3.11	Palaeocurrent data for the Durness Group.	113
Text-fig. 3.12	Photographs and sketches showing the internal arrangement of thrombolites maceriae.	117
Text-fig. 3.13	Graphs showing microbialite abundance and morphological diversity.	119
Text-fig. 3.14	Graph showing the interval studied in the context of global climate.	124
Text-fig. 3.15	Graph showing literature based microbialite diversity and abundance through time.	124
Text-fig. 4.1	Photographs showing conodont CAI values for the Durness Group.	129
Text-fig. 4.2	Geological map displaying the locations of Higgins’ conodont localities.	131
Text-fig. 4.3	Range chart spanning the Cambrian–Ordovician boundary interval.	132
Text-fig. 4.4	Laurentian conodont zonation and its correlation.	134
Text-fig. 4.5	Chart showing the ranges of recovered conodont taxa.	136

Text-fig. 4.6	SEM images of selected conodont taxa from the Sangomore and Balnakeil formations.	138
Text-fig. 4.7	SEM images of selected conodont taxa from the Croisaphuill Formation.	142
Text-fig. 4.8	SEM images of selected conodont taxa from the Croisaphuill Formation.	143
Text-fig. 4.9	SEM images of selected conodont taxa from the Croisaphuill Formation.	144
Text-fig. 4.10	SEM images of selected conodont taxa from the Durine Formation.	148
Text-fig. 4.11	SEM images of conodont taxa from Higgins' localities D-15 and D-16.	149
Text-fig. 4.12	Ordovician conodont realms domains and provinces.	151
Text-fig. 4.13	Palaeogeographical map showing cluster analysis localities.	153
Text-fig. 4.14	Dendrograms comparing conodont faunas from across Laurentia.	155
Text-fig. 5.1	Simplified graphical log showing the SLM megasequence and subdivisions.	159
Text-fig. 5.2	Parasequence stacking patterns and their relation to sea-level change.	164
Text-fig. 5.3	Chart showing the classification of Durness Group parasequences.	166
Text-fig. 5.4	Diagram explaining construction of a Fischer plot.	173
Text-fig. 5.5	Fischer plot for the Durness Group.	174
Text-fig. 5.6	Photographs showing the SLM I–II sequence boundary.	177
Text-fig. 5.7	Photographs showing the SLM IIa–b sequence boundary	180
Text-fig. 5.8	Sedimentary log of the interval spanning the SLM II–III boundary	182
Text-fig. 5.9	Photographs of features observed at the SLM II–III boundary.	183
Text-fig. 5.10	Photographs of features observed at the SLM IIIa–b boundary.	187
Text-fig. 5.11	Photograph showing the flooding within SLM IIIb at the Cambrian–Ordovician boundary	188
Text-fig. 5.12	Parasequences within the upper Sailmhor Formation (SLM IIIb).	189
Text-fig. 5.13	Photographs showing the SLM IIIb–c boundary.	191
Text-fig. 5.14	Sedimentary log of the SLM III–IV boundary	192
Text-fig. 5.15	Photographs of the SLM III–IV sequence boundary	193
Text-fig. 5.16	Photographs displaying the MFS of SLM IV and parasequences within the upper member of the Croisaphuill Formation	196
Text-fig. 5.17	Correlation of the Cambro-Ordovician of northwest Scotland with western Newfoundland and North-east Greenland.	197
Text-fig. 5.18	Relative sea level curve for the Durness Group	202

LIST OF TABLES

	Page	
Text-table 4.1	Abundance table of conodont taxa abundance within samples.	135
Text-table 4.2	List of localities and publications used for cluster analysis.	152
Text-table 4.3	Presence/absence data matrix.	154
Text-table 4.4	Biogeographical units and their classification	157

Chapter 1

INTRODUCTION AND STRATIGRAPHICAL REVISION OF THE DURNESS GROUP, NW SCOTLAND

1.1 GEOLOGICAL SETTING OF THE DURNESS GROUP

The Hebridean terrane includes the part of northwest Scotland lying west of the Moine Thrust zone. It represents a fragment of the Laurentian craton where Archaean and Palaeoproterozoic gneissic basement is unconformably overlain by a thick succession of unmetamorphosed, red arkosic sandstones and conglomerates (alluvial fan, fluvial and lacustrine) of Meso- to Early Neoproterozoic age (Sleat, Stoer and Torridon groups) (Text-fig. 1.1). After rifting of the palaeocontinent Rodinia in the late Neoproterozoic (Torsvik *et al.* 1996), these rocks were peneplaned and formed a broad but shallow marine shelf, upon which a succession of Cambro-Ordovician rocks was deposited. Subsidence and deposition on the margin was continuous from south-eastern USA, through maritime Canada and Newfoundland to North Greenland (a distance of several thousand kilometres). The subsidence history and stratigraphical record in the Newfoundland–Scotland–East Greenland sector of the margin shows remarkable similarity (Swett & Smit 1972a, Wright & Knight 1995, Higgins *et al.* 2001). Durness Group carbonates conformably overlie dominantly siliciclastic, Cambrian (late Terreneuvian or early C₂; see section 1.5) rocks assigned to the Ardvreck Group (Text-fig. 1.1).

The Durness Group comprises at least 920 m of peritidal and shallow subtidal limestones and dolostones, deposited on the Laurentian passive margin of the Iapetus Ocean. These carbonates record deposition within a tropical setting – microbialites are common, ooids are locally abundant, and evidence of former evaporites and early dolomite formation are found in parts of the succession. This is consistent with available palaeogeographical reconstructions, which indicate that Laurentia lay between 30° N and 30° S (Text-fig. 1.2), with Scotland situated at a palaeolatitude of approximately 20° S (Cocks & Torsvik 2006). Rocks of Cambro-Ordovician age crop out in a narrow, almost continuous belt, rarely more than 10 km wide that stretches 180 km southwest from Loch Eriboll to Skye (Text-fig. 1.3). The Durness Group crops out to the west of the Moine Thrust Zone and eastwards the rocks are overlain by allochthonous metamorphic rocks of the Moine Supergroup. The Ardvreck

Group and the overlying lowest two formations of the Durness Group are widely exposed along the Moine Thrust zone. Only in the vicinity of Durness is the full succession of the Durness Group (seven formations) represented, where the upper boundary is truncated by a thrust fault. On Skye all but the uppermost formation of the Durness Group crops out, but there is a lack of continuous section for detailed study.

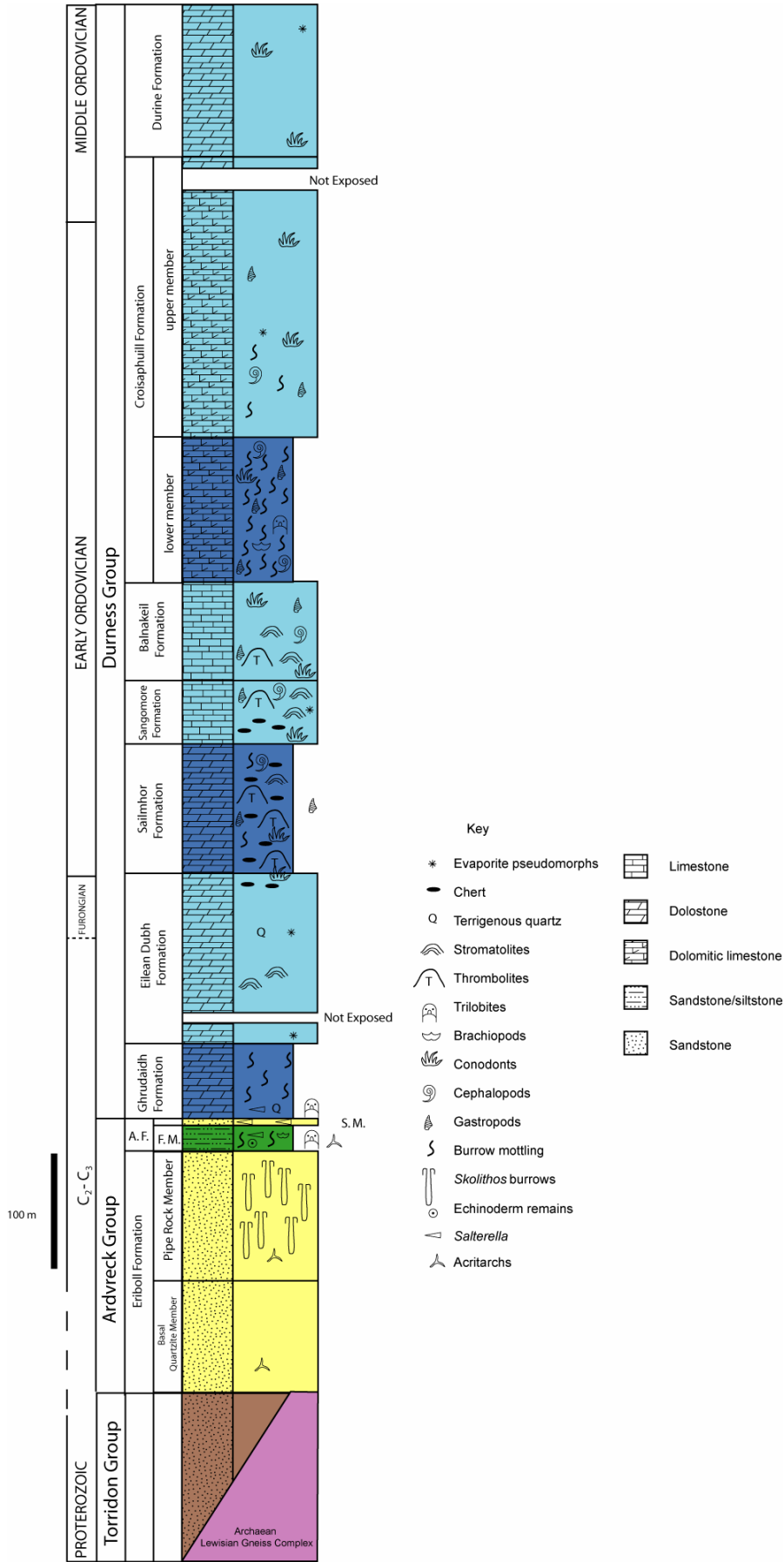
This thesis presents the first facies analysis of the whole Durness Group (Chapter 2); it introduces a new conodont biostratigraphy for the Durness Group (Chapter 4) and examines the microbialite successions and their relation to palaeoenvironmental changes through time (Chapter 3). The thesis also includes a new sequence stratigraphical model for the Cambro-Ordovician succession (Chapter 5). The latest Cambrian and earliest Ordovician was an important time in earth history, metazoans were diversifying rapidly, sea-level is interpreted to have been at its highest for the Phanerozoic, and study of the Laurentian shelf in Scotland lends much information on the environmental and evolutionary history of the Cambrian–Ordovician.

1.2 STUDY AREAS

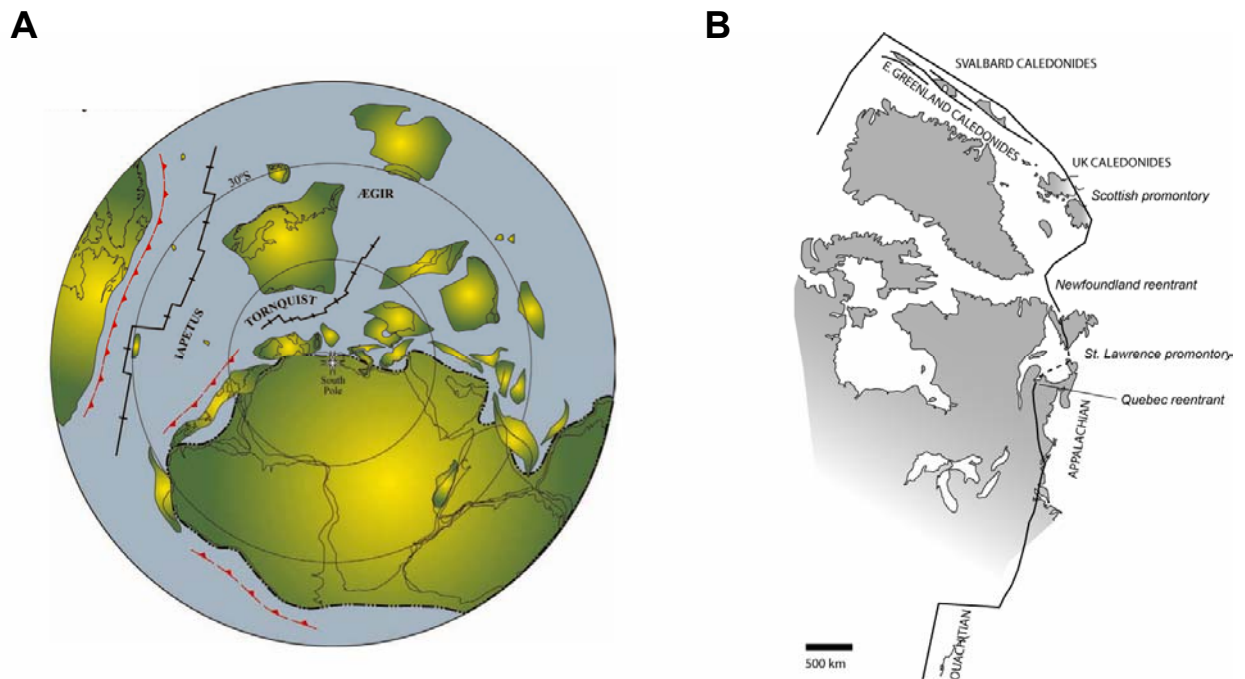
Despite the extensive outcrop along the Moine Thrust zone (Text-fig. 1.3), there are few areas in which strata above the lowest two formations are preserved. The main areas of study have been around Durness, Loch Eriboll, Assynt and Skye. The divisions of the Ardvreck and Durness groups show remarkable consistency, both in terms of their thickness and sedimentological nature along the whole outcrop length (probably indicating a margin parallel outcrop).

1.2.1 An t-Sròn, Loch Eriboll

This area represents the only locality in the entire outcrop belt where the An t-Sròn, Ghrudaidh and lower part of the Eilean Dubh formation are well-exposed without major structural complication (Text-fig. 1.3, 1.4). The coastal section displays the upper Pipe Rock Member (Eriboll Formation) [NC 4417 5812] and exposure is near continuous (including the complete Furoid Member, Salterella Grit Member and Ghrudaidh Formation) along the shore of Loch Eriboll to NC 4396 5798, where the Ghrudaidh–Eilean Dubh formation boundary and an overlying 12 metres of strata are exposed. The boundary between the Furoid and Salterella Grit members is exposed at NC 4401 5808 and the boundary between the Salterella Grit



Text-figure 1.1 Schematic sedimentary log of the Cambro-Ordovician succession in NW Scotland. The lithostratigraphy, lithology and the principal fossil groups recorded are shown. The An t-Sròn Formation is indicated by A.F., the Fucooid Member by F.M. and the Salterella Grit Member by S.M.



Text-figure 1.2 Palaeogeographical reconstructions showing the position of Laurentia during the Early Ordovician; **(A)** Plate reconstruction (Cocks & Torsvik 2006); **(B)** Close up of the Laurentian margin, showing the position of Scotland and the principal promontories and re-entrants (modified after Cawood *et al.* 2007).

Member and the Ghrudaidh Formation is seen a short distance along the coast [NC 4400 5807].

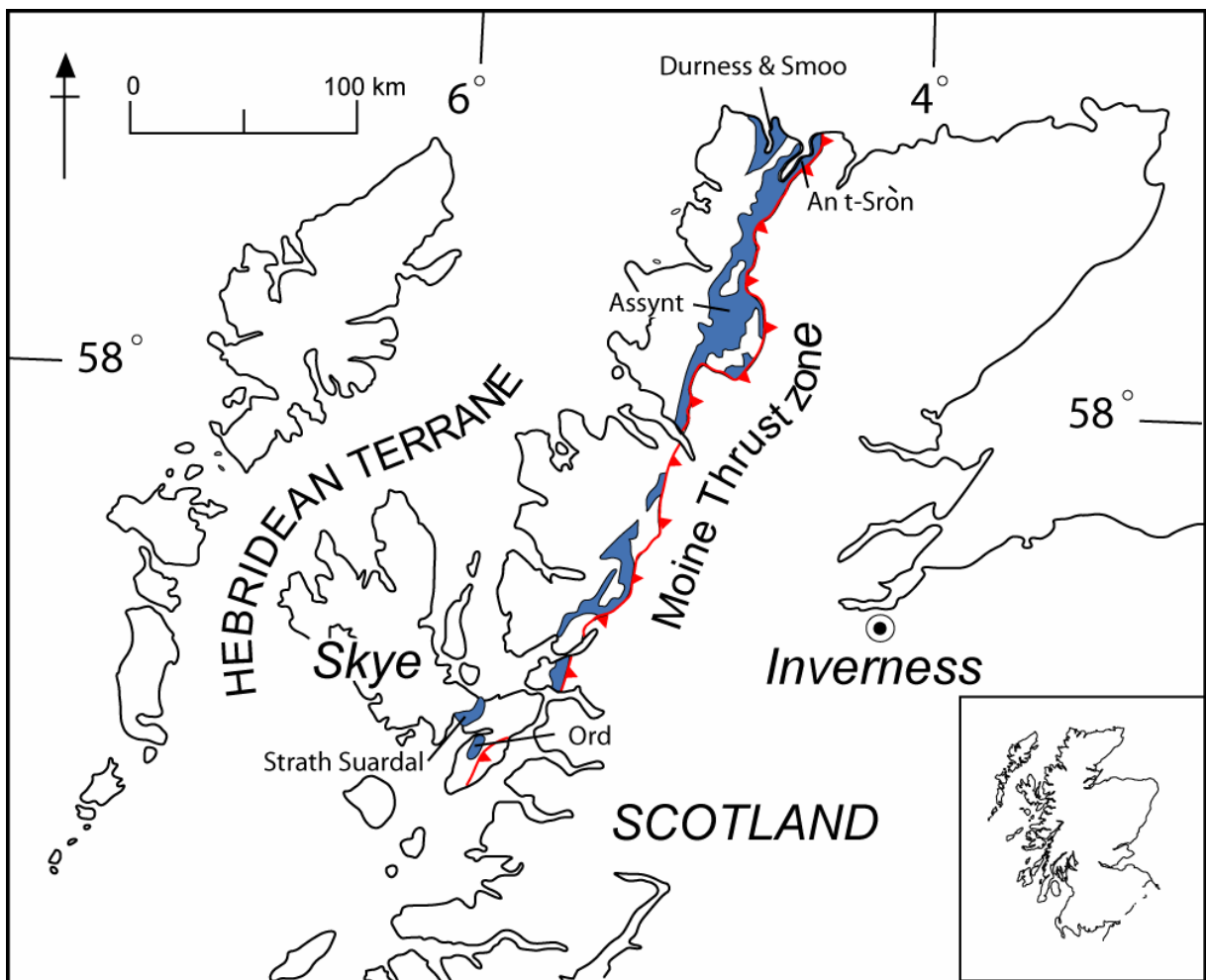
1.2.2 Smoo inlet and Leirinmore

In the cliffs at Smoo inlet, the boundary between the Sailmhor and Sangomore formations is well exposed. The actual boundary is high up in the cliff but can be traced around the headland at Pocaan Smoo, where it is accessible at NC 4248 6730; 49 m of strata across the boundary were logged (Text-fig. 1.3, 1.5). The boundary is almost identical in nature to that exposed at Balnakeil Bay and along the Kyle of Durness.

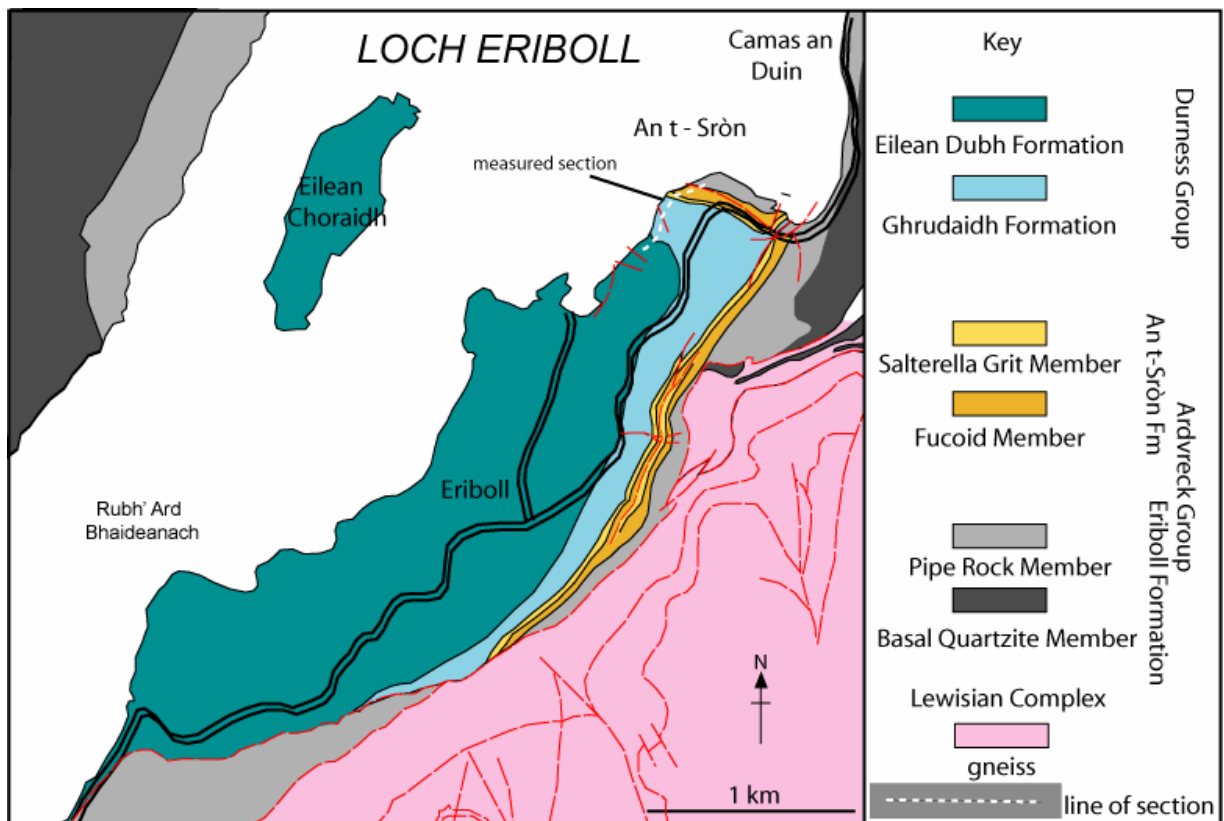
1.2.3 Balnakeil Bay

The section at Balnakeil Bay (Text-fig. 1.3, 1.5) stretches from NC 3738 6858, on the edge of the Kyle of Durness to 3918 6851. It affords the best exposures of the middle and upper

Eilean Dubh Formation and the Saimhor, Sangomore and Balnakeil formations. The boundaries between formations are well exposed and accessible. The Eilean Dubh–Saimhor formation boundary is seen at NC 3783 6877, and the Saimhor–Sangomore formation boundary is well exposed at NC 3835 6886. The boundary between the Sangomore and Balnakeil formations is well exposed at NC 3887 6876 and some 65 metres thickness of the Balnakeil Formation are exposed along the shore before outcrop is covered by sand. The section through the lower part of the formation ends at NC 3196 6869, and this has been supplemented by exposures at Balnakeil House, and in a small lay-by [NC 3913 6855 to 3918 6851].



Text-figure 1.3 Location map showing the outcrop pattern of the Cambro-Ordovician rocks in NW Scotland and the principal structural elements and terranes. The principal localities discussed in this thesis are indicated, An t-Sròn, Loch Eriboll, Durness and Assynt.



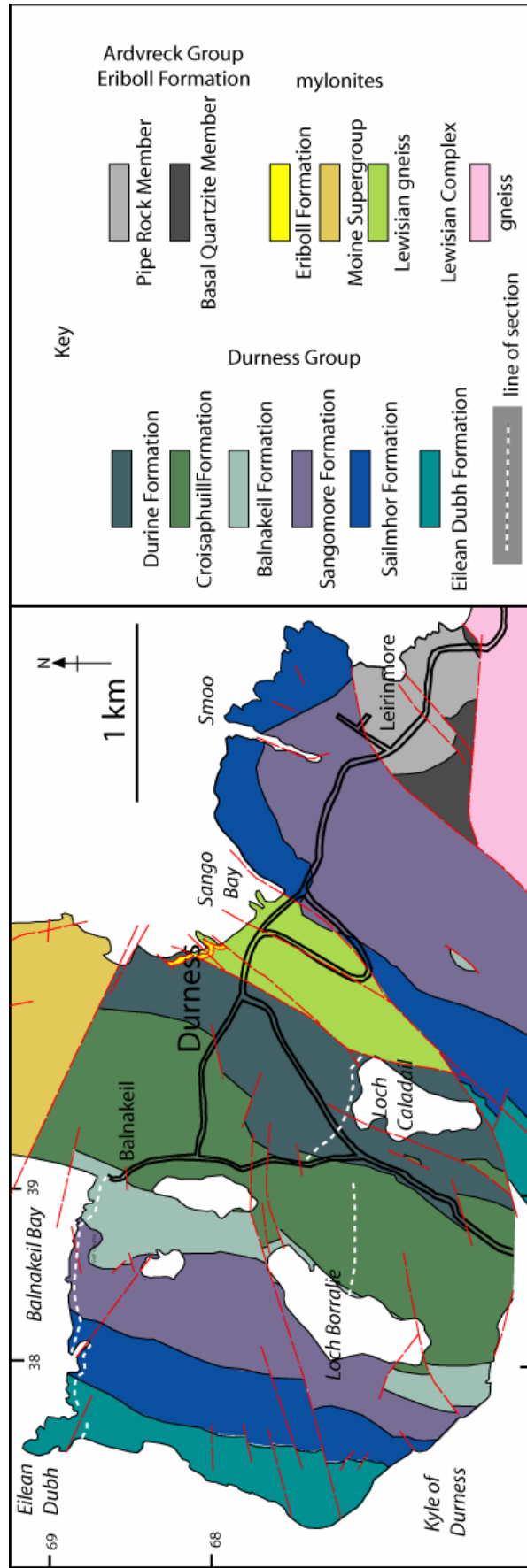
Text-figure 1.4 Simplified geological map of the east side of Loch Eriboll, showing the outcrop of the Durness Group and the sections described (modified after BGS 2002) .

Although the Eilean Dubh Formation is exposed around the whole peninsula of Eilean Dubh [NC 375 690], sedimentological logging was not possible due to the presence of abundant thrust faults and the peninsula affords only a repetition of strata, which was logged along the main shore.

1.2.4 Inland exposures between Loch Borralie and Loch Caladail

The upper two formations (Croisaphuill and Durine) of the Durness group are solely exposed in scattered inland outcrops. There was, however, enough continuous outcrop to allow sedimentary logging and to construct a composite section to derive a minimum thickness for the two formations.

The Croisaphuill Formation (350 m) is well exposed in cliffs along the shore of Loch Borralie [NC 3857 6730 and 3851 6717 – 3858 6714] (85 m) and a composite section for the overlying 124 m was measured across the hillside east of Loch Borralie.



Text-figure 1.5 Simplified geological map of the area around Durness, showing the lines of section and the principal localities mentioned within the text (modified after BGS 2002).

The outcrop width of the upper part of the formation was measured using GPS and the true thickness (132 m) worked out from the tectonic dip of the beds [NC 38871 67019 – 38994 66964] (Text-fig. 1.5). What is interpreted to be the upper 10 metres of the Croisapuill Formation and the lower 55 m of the Durine Formation are exposed along a trackway leading to the old manse at Glebe [NC 3927 6749 – 3929 6732]. A small roadside quarry afforded a further section of 12 m [NC 3949 6719], and sections were measured between NC 3952 6701 and 3958 6704 (24 m), 3967 6701 and 3972 6697 (41.7 m) along the shore of Loch Caladail. The sections differed sufficiently to suggest that there is no repetition of strata by major faulting. The separate sections were then joined to form a composite section of 132 m.

Supplementary inland sections were logged through the lower Balnakeil Formation (28 m) at [NC 3857 6772], the lower Croisaphuill Formation (17 m) at Loch Croispol [NC 3907 6836 – 3910 6834] (Appendix 1), and a few outcrops of the Durine Formation were examined at Durness village [4035 6772]. Many other small outcrops were examined but provided little additional information.

1.2.5 The Kyle of Durness

The Kyle of Durness exposes the same formations as at Balnakeil Bay (Text-fig. 1.5), but they are much faulted and subsequently only one section, 30 m thick was measured across the Eilean Dubh–Sailmhor formation boundary (Appendix 1). The boundary between the Sailmhor and Sangomore formations was also examined at NC 3733 6664.

1.2.6 Grudie

The upper part of the Ghrùdaidh Formation (24 m) was logged at Grudie [NC 3599 6316 – 3628 6319] (Appendix 1), but the section is poorly exposed and neither the lower or upper boundary was observed. Pale grey beds of dolostone occur at the top of the section indicating that the boundary with the Eilean Dubh Formation lies a short stratigraphical height above this (if compared to its expression at An t-Sròn, and this is supported by the presence of scattered outcrops of Eilean Dubh Formation type lithofacies around the headland of Rubh' a' Ghrùdaidh).

1.2.7 Ardvreck Castle and Inchnadamph, Loch Assynt

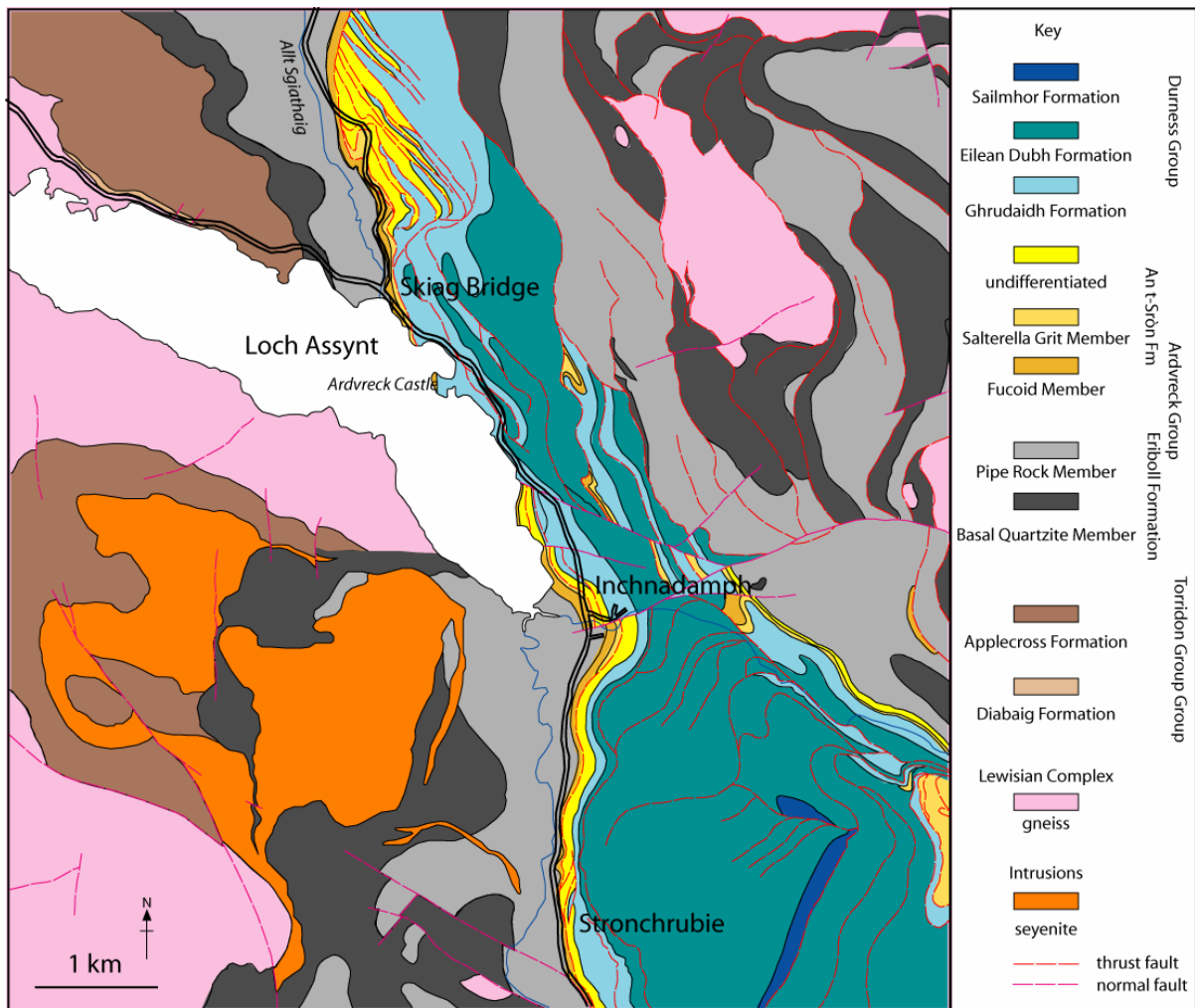
The upper 8.6 m of the Pipe Rock Member and 8 m of the overlying Furoid Member were logged at Skiag Bridge along a road cutting from NC 2355 2427 to 2360 2420. The uppermost 1.8 m of the Furoid Member were seen further along the road [NC 2368 2410] and a measured section was undertaken through the Salterella Grit Member (8.3 m) and 5 m up into the Ghrudaidh Formation [NC 2373 2405]. Near Ardvreck Castle and further east towards Inchnadamph, thrusts have repeated much of the strata making logging difficult. Strata across the Ghrudaidh–Eilean Dubh formation boundary were logged at NC 2448 2335 (18 m) and also at NC 2454 2321. East of Inchnadamph at Bad na Bà Duibhe a section c. 26 m in thickness was logged [NC 2663 2006 – 2668 2001], and spans the upper 2.7 m of the Eilean Dubh Formation and the lower 23 of the Sailmhor Formation. Additionally, a small 2 m section also exposes the boundary on the slopes of Creag nan Cnaimhseag [NC 26406 18706] (Text-fig. 1.3, 1.6).

1.2.8 Ord, Skye

At Ord (Text-fig. 1.3), blocks of Furoid Member are seen on the foreshore [NG 622 139], and rocks typical of the Salterella Grit Member and Ghrudaidh Formation crop out nearby. A section through part of the Eilean Dubh Formation is exposed along the shore but is cut by a fault that juxtaposes it with the Sailmhor Formation [NG 6177 1365]. The section was not logged but microfossil samples were collected through the Sailmhor Formation. The outcrop is poor and much faulted but continues along the coast to NG 61667 13470. Lithology typical of the Sangomore Formation was exposed in a stream bank [NG 6146 1282] and comprised cream and pink coloured dolostone with cherts. A thrust occurs to the north of the outcrop and brings the Eriboll Formation into contact.

1.2.9 Strath Suardal and Loch Lonachan, Skye

Small outcrops of the unit that Peach *et al.* (1907) called the Ben Suardal Limestone (given formation status by Whittington 1972) cover a large area around Strath Suardal. These outcrops were examined around Ben Suardal itself and Loch Lonachan, SSW of Broadford (Text-fig. 1.3). The rocks correlate well with the Croisaphuill Formation at Durness, based upon the fossil content and lithology.



Text-figure 1.6 Simplified geological map of the Assynt area showing the localities mentioned within the text (modified after BGS 2007).

1.3 PREVIOUS RESEARCH ON THE CAMBRO-ORDOVICIAN OF NORTHWEST SCOTLAND

The Cambro-Ordovician of NW Scotland represents a unique sequence of rocks in Britain in that it formed part of the Laurentian margin. Correlation with British stages is therefore problematic and of limited relevance. Ideally correlation with North American and global series and stages should be used, and this has been attempted by Rushton (2000). International stage correlation is used wherever possible in this thesis.

1.3.1 Sedimentology

The sedimentology of the Cambro-Ordovician in NW Scotland has been studied by Swett (1965; 1969), Swett *et al.* (1971), Wright (1985), and Wright (1993). Wright (1997) suggested an organogenic origin for the dolomite within the Eilean Dubh Formation and evaporites were recorded from the Sangomore Formation by Young (1979), and from the Furoid Member by Allison & Russell (1985). Compared to the Durness Group, the sedimentology of the Ardvreck Group has been studied in more detail (McKie 1990a, b, c, 1993).

1.3.2 Sequence stratigraphy and correlation

The Cambro-Ordovician succession in northwest Scotland is remarkably similar to sections in western Newfoundland, Spitsbergen and East Greenland, and the stratigraphy correlates well across these areas (Cowie 1974, Swett & Smit 1972a, b, Swett 1981, Wright & Knight 1995, Smith & Rasmussen 2008). The sequence stratigraphy of the Ardvreck Group has been interpreted by McKie (1993), but a similar study for the whole of the Durness Group has not previously been attempted and a new sequence stratigraphical model for sedimentation within the Durness Group is proposed in Chapter 5.

1.3.3 Palaeontology and biostratigraphy

In 1854–5, fossils from the Durness Group were first discovered by Charles Peach (Peach 1855). Murchison originally identified the fossils as Devonian (Oldroyd 1991), but later concluded that they were ‘lower Silurian’ based upon the descriptions by Salter (1859). It has long been established that the fauna from the Durness Group bears a close similarity to that recorded from other parts of Laurentia and comparison of the fauna by Salter (1859), Peach (1913), Peach & Horne (1930), and Grabau (1916) with the Cambro-Ordovician of the USA, and western Newfoundland, allowed diagnosis of the ages of some of the formations for the first time.

Previous biostratigraphical studies have been limited, and this is mostly due to the scarcity and poor preservation of the fauna. Only the Balnakeil and Croisaphuill formations are comparatively rich in fossil remains. During the present study, new collections have provided material from the Sailmhor and Sangomore formations. The Balnakeil and Croisaphuill afforded Peach *et al.* (1907) some one hundred species, 66 of which are present within the Balnakeil Formation (15 being restricted to the Balnakeil Formation). Peach *et al.*

(1907) also interpreted the Ben Suardal Formation on Skye as being a correlative of both the Balnakeil and Croisaphuill formations.

Cephalopods were first described from the Durness Group by Salter (1859), and Foord (1887, 1888) also examined the cephalopods and species lists were published by Peach *et al.* (1907), based upon material recovered during mapping by the Geological Survey. Recent revision of the cephalopod fauna by D. H. Evans has shown that although cephalopods are scarce and poorly preserved, they are present within the Sailmhor, Sangomore, Balnakeil and Croisaphuill formations. Over 30 species have been recorded representing some 11 families (D. H. Evans *pers. comm.* 2006).

Salterella is an enigmatic small shell of uncertain, but possible stem-molluscan, affinity (Yochelson 1983). This fossil was first mentioned by Macculloch (1814) and later described and named by Salter (1859). Peach *et al.* (1907) recorded *Salterella* from the middle Pipe Rock Member, and the overlying Furoid Member, Salterella Grit Member and Ghrudaidh Formation. Yochelson (1983) reviewed the taxonomy of *Salterella* and concluded it was of use as a biostratigraphic indicator, due to it having a short range, being widespread across Laurentia and often present in large numbers. Fritz & Yochelson (1988) concluded that *Salterella maccullochi* (Salter) is diagnostic of the middle *Olenellus* Zone of North America (this equates to mid Stage 4, C₂; Text-fig. 1.8).

Trilobites are rare within the Cambro-Ordovician of northwest Scotland. They are most common within the An t-Sròn Formation, but the Durness Group has yielded only a handful of specimens. The North American biozonal trilobite *Olenellus* was first recovered from the Scottish succession during systematic collecting of potential fossiliferous horizons (identified by the Geological Survey's mapping), by the survey fossil collector A. Macconochie in 1891. This afforded evidence of a Cambrian age for these rocks for the first time. Species of *Olenellus* were then described from the Furoid and Salterella Grit members (Peach & Horne 1892; Peach 1894). More recently, the olenellid fauna was taxonomically revised by Cowie & McNamara (1978), based upon more recent collections from Loch Awe quarry [NC 2499 1578]. They gave revised descriptions of *O. lapworthi*, *O. reticulatus*, *O. intermedius*, *O. (Olenelloides) armatus* and described a new species *O. hamoculus*. A single *Olenellus* has since been discovered in the basal bed of the Ghrudaidh Formation (Huselbee & Thomas 1998) giving a maximum age (*Bonnia – Olenellus* Zone) for the base of the Durness Group. The olenellid trilobites have been subjected to cladistic analysis by Lieberman (2001),

who included *O. lapworthi* Peach & Horne and *O. intermedius* Peach in a new genus; *Fritzolenellus*. Lieberman also concluded that *O. (Olenelloides) armatus* is a separate genus, *Olenelloides*, rather than a subgenus of *Olenellus*.

Trilobites were first recorded from the Durness Group by Peach *et al.* (1907) (Sailmhor and Croisaphuill formations). The single species from the Sailmhor Formation; *Asaphus canalis* Conrad was not figured in their monograph and the specimen is now lost (Cowie *et al.* 1972; Fortey 1992). Provided Peach *et al.* identified the trilobite correctly, the genus would not be assignable to *Isoteloides*, according to Fortey (1992). *Petigurus nero* (Billings) was also recorded by Peach *et al.* (1907) from the Croisaphuill Formation, and later figured by Fortey (1992). Fortey also recorded the occurrence of *Jeffersonia timon* (Billings) and *Cybelopsis* sp. nov from the Croisaphuill Formation. *P. nero* is age diagnostic of the *Strigigenalis caudata* trilobite zone (Boyce & Stouge 1997) of the North American, upper Ibexian Stage. This equates with the mid-Floian in global terms (Text-fig. 1.9). It also occurs in the lower part of the Catoche Formation of western Newfoundland (Fortey 1979).

Conodonts were first recorded from the Durness Group by Higgins (1967). Out of 19 sample localities, 5 produced conodont faunas, but only selected taxa were figured as line drawings. Higgins (1985) additionally reported conodonts from the underlying Croisaphuill Formation (at heights of 3 m and 20 m above the base) 100 m east of Loch Croispol. Other conodont studies primarily concern the Cambro-Ordovician boundary strata spanning the Eilean Dubh–Sailmhor Formation boundary (Huselbee 1998, Huselbee & Thomas 1998). A more complete conodont biostratigraphy will be presented in Chapter 4.

Acritarchs were recorded from the Fucoïd Member by Downie (1982) and by a more recent study (Molyneux 2006), based upon samples collected during the undertaking of this project. Acritarchs from the Basal Quartzite and Pipe Rock members were not age diagnostic, but those from the Fucoïd Member compare well with floras from East Greenland and Siberia suggesting a position within the North American *Nevadella* Zone or mid-Tommotian (Siberian Cambrian stage) (Text-fig. 1.8). These ages are discrepant with the co-occurrence of *Salterella* and *Olenellus* in the member and suggest that the application of these floras as a correlative tool may be limited.

Elements of the macrofauna, considered to be of less biostratigraphical potential have been briefly studied or only referred to in passing. Hinde (1889) recorded the sponges *Archeoscyphia minganensis* and *Calathium* sp. from the Durness Group, and Palmer *et al.*

(1980) were the first to record fossils from the Sangomore Formation; the only unit in which Peach *et al.* (1907) recovered no fossil remains. Palmer *et al.* recorded *Murchisonia* sp. *Pleurotomaria* sp. and *Orthoceras* sp. Recently Herringshaw & Raine (2007) recorded a machaeridian sclerite from the middle part of the Sangomore Formation and this represents the earliest recorded machaeridian.

One paper has been published concerning the brachiopods from the Croisaphuill Formation (Ben Suardal Formation) on Skye (Curry & Williams 1984). The brachiopod fauna was recovered by the acid digestion of limestone blocks. Seven known genera and one species, assignable to a new genus along with several new species were recorded. Some 62% of the brachiopod fauna from Skye can be recognised within the Arbuckle Group of Oklahoma (Curry & Williams 1984).

A single species of rostroconch, *Euchasma blumenbachi* (Billings) has been recorded from the Croisaphuill Formation (Peach *et al.* 1907), and it is also present in equivalent strata in western Newfoundland, where it has been shown to have a short range spanning the lower half of the *Oepikodus communis* conodont zone within the Catoche Formation (Rohr *et al.* 2008).

Silicified gastropod opercula, now attributable to the genera *Maclurites* Le Sueur and *Ceratopea* Ulrich are common within the Croisaphuill Formation. The opercula figured by Salter (1859) as *Maclurea peachii* was subsequently assigned to a new species of a different genus (*Ceratopea billingsi*) by Yochelson (1964). Peach *et al.* (1907) made reference to four opercula of '*Maclurea*' in their species list, but did not figure the specimens.

Whilst developing a biostratigraphy for the Durness Group, all available material, from both museum and new field collections, was examined but proved to be only of limited utility for biostratigraphy. By far the most biostratigraphically useful fossils within the Durness Group are the conodonts. It is now known that they occur throughout most of the Durness Group (with the exception of the Ghrudaidh Formation and most of the Eilean Dubh Formation). A high resolution conodont biostratigraphy is introduced in Chapter 4.

1.3.4 Chemostratigraphy

Nicholas (1994) collected 48 samples for strontium isotope analysis through the Eilean Dubh to Balnakeil formations along Balnakeil Bay. Nicholas used the global Sr curve to test if there was a major unconformity at the Sailmhor/Sangomore formation boundary (as suggested by

Palmer *et al.* 1980). In contrast to the views of Palmer *et al.*, Nicholas concluded that there was no evidence of a major break at the formation boundary and that the Eilean Dubh Formation exposed at Balnakeil Bay is not early Cambrian but probably middle or late Cambrian age, with the possibility of some minor non-sequences within the Eilean Dubh Formation recognised from the Sr isotope curve.

1.4 LITHOSTRATIGRAPHICAL REVISION OF THE DURNESS GROUP

The lithostratigraphy of the Durness Group is fairly well established and the divisions of Peach & Horne (1884) are still used. Lapworth (1883) was first to construct an accurate but simple stratigraphy (Text-fig. 1.7), and this was expanded and further subdivided by Peach & Horne (1884), and Peach *et al.* (1907). Although the formation names have been stable, published thicknesses for the Durness Group have been variable (Robertson *et al.* 1949; Walton 1965) and have ranged from 460 m (Peach *et al.* 1907) to almost 1600 m (Phemister 1948). Swett (1965, 1969) recorded 1250 m and Wright (1985) gave a thickness of around 770 m for the group (Text-fig. 1.5).

Recent logging (Chapter 2; Appendix 1) has amended many of the thicknesses of the formations within the Durness Group, and it is because of this that a revision of the lithostratigraphy is considered desirable. During the present period of research much time was spent tracing marker beds across the many faults that are present along Balnakeil Bay. Only the largest faults obstructed correlation across them and appear to be cutting out strata and thus the thicknesses given are minimum thicknesses. However, they are the most accurate thickness measurements to date for the Durness Group.

Peach *et al.* (1907) established a 'Calcareous Series' and divided it into seven 'groups' (Ghrudaidh, Eilean Dubh, Sailmhor, Sangomore, Balnakeil, Croisaphuill and Durine). Swett (1969) reduced the groups to member status, but this was emended by Cowie *et al.* (1972) and Whittington (1972) to the Durness Group and its constituent formations (Text-fig. 1.5). Whilst the standard divisions of the Durness Group can be recognised on Skye, the nature of outcrop and the presence of Palaeogene igneous intrusions have greatly complicated matters. Following current work, it is clear that equivalents of all but the Durine Formation occur on Skye. The Ghrudaidh Formation, Eilean Dubh, Sailmhor and Sangomore formations are all present in sections around Ord (see Section 1.2). The division of the succession on Skye into the six members of Holdroyd (1994), used on recent British Geological Survey (BGS) maps is

not followed here as they lack lithostratigraphical consistency and integrity and in part, they may represent different grades of contact metamorphism.

The Cambro-Ordovician rocks of northwest Scotland can be divided into two distinct groups. The lower group (Ardvreck) has recently been proposed (BGS 2007) and represents a predominantly siliciclastic sequence of rocks, comprising the Eriboll and An t-Sròn formations. The overlying Durness Group is predominantly composed of carbonate rocks. The formations and members within the Durness Group are here revised, based upon recent sedimentary logging of the whole available thickness. The original spelling of the divisions is maintained where possible and the principal locations and minimum thicknesses are given. The three members within the Eilean Dubh Formation (Wright 1993, Wright & Knight 1995, Park *et al.* 2002) are abandoned based upon recent logging and a lack of application for correlation (Text-fig. 1.5).

1.4.1 Durness Group

The Durness Group takes its name from the village of Durness [NC 677 403], NW Scotland, where the group is particularly well-exposed. Lapworth (1883) referred to the succession (Durness or Eriboll Limestone), and the rocks were described in more detail by Peach & Horne (1884) and Peach *et al.* (1907) as the ‘Calcareous Series’. Later Cowie *et al.* (1972) proposed group status for the Durness carbonates.

The measured thickness of the Durness Group is around 920 m and the lithologies within the group represent a spectrum of subtidally to supratidally deposited limestones, dolostones, and dolomitic limestones with some cherts and minor evaporate pseudomorphs. Microbialites are abundant and diverse, and a variety of morphological forms of stromatolites and thrombolites are present. The type area for the Durness Group is the Peninsula at Durness, with the most complete section at Balnakeil Bay [NC 3738 6858 – 3918 6851] (Text-fig. 1.5) where the Eilean Dubh, Sailmhor, Sangomore and Balnakeil formations are well-exposed. The lower boundary of the group is conformable with the Salterella Grit Member, but is marked by a flooding surface. The upper boundary is truncated by a thrust fault, as seen at Sango Bay [NC 6792 4068].

1.4.2 Ghrudaidh Formation

The Ghrudaidh Formation (Peach & Horne 1884) takes its name from the farmhouse at Grudie (spelt Ghrudaidh on the old Ordnance Survey maps), and probably not from the promontory of Rubh' a' Ghrùdaidh as Wright (1985) suggested. The type section at Grudie exposes the upper 24 m, however, the section at An t-Sròn [NC 4400 5807 – 4396 5798] provides the most complete sequence, where 63 m were recorded, although there are some thrust faults. The lower boundary of the formation is marked by a change from siliciclastic sedimentation to carbonates and is taken at the first dolomitic siltstone or dolostone. Sand grains persist up into the Ghrudaidh Formation for a few metres, and around Loch Assynt thin quartz arenites (<50 cm) are present in the lower part of the formation. Other lithologies include mottled dolostone, oolites and local mud flake breccias towards the top. Although the Ghrudaidh Formation has a large outcrop area, it is often seen in thrust slices at Assynt and the monotonous nature of the formation makes correlation difficult. The formation is also exposed at Ord, Skye [NG 622 139], and the base is well exposed at Skiag Bridge, Assynt [NC 2373 2405].

1.4.3 Eilean Dubh Formation

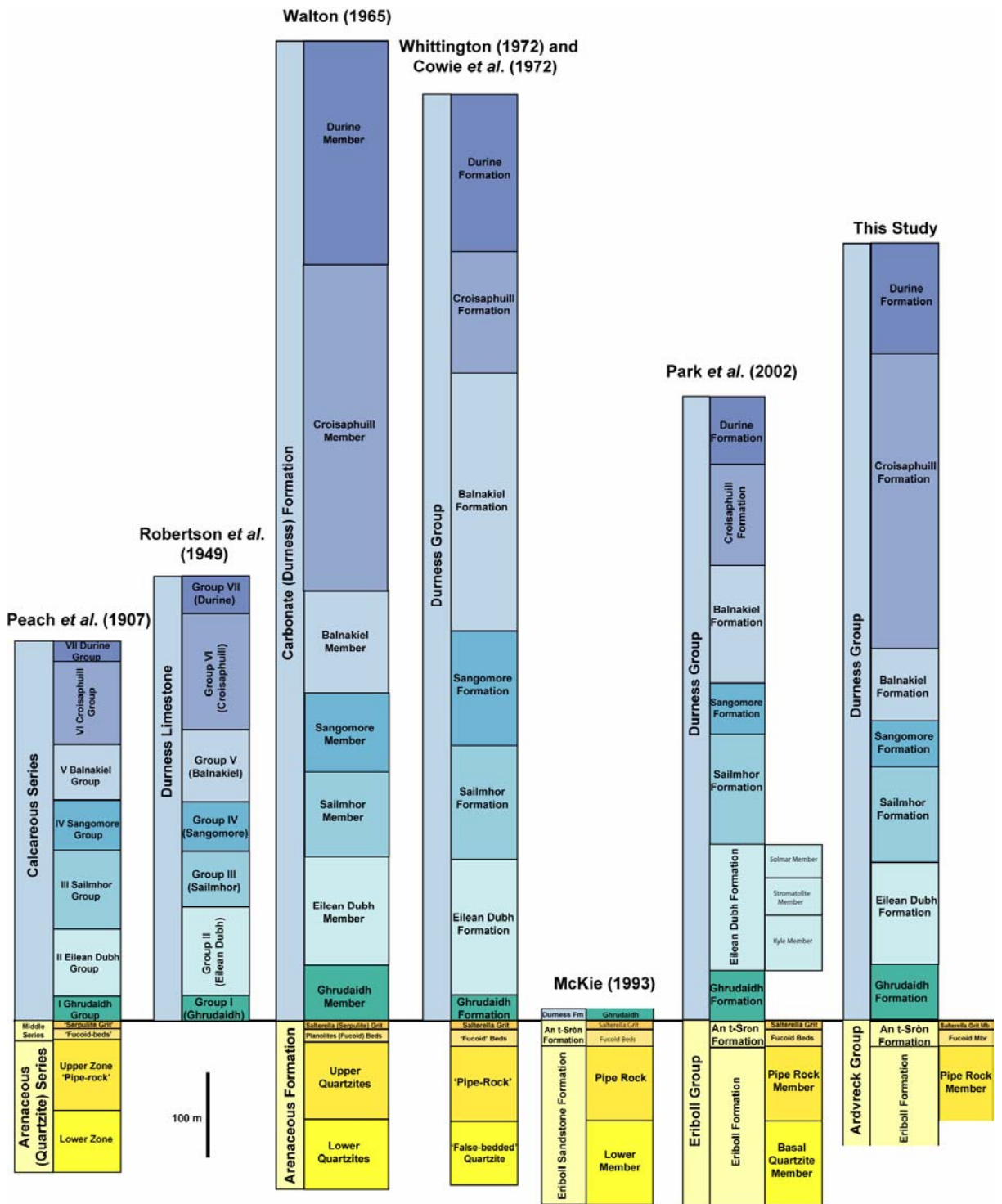
The Eilean Dubh Formation (Peach & Horne 1884) takes its name from the peninsula of Eilean Dubh [NC 374 689], at the west end of Balnakeil Bay. Its type section is along Balnakeil Bay from NC 3738 6758 to 3783 6877. Exposures are also seen at An t-Sròn, and at Stronchrubie, but they are significantly disrupted by thrusting. The formation is present on the Isle of Skye, at Ord [NG 6176 1361] but the upper boundary with the Sailmhor Formation is faulted. The lower boundary is seen at An t-Sròn [NC 4394 5791] and Grudie [NC 3626 6320], where light-grey and cream weathering dolostones overly intercalated light-grey dolostones and sucrosic, mottled, dark-grey dolostones of the Ghrudaidh Formation (although some fine-grained, cream coloured dolomite beds are present in the upper part of the formation). The upper boundary is seen at Stronchrubie [NC 2640 1870 and 2662 2006], Balnakeil Bay and on the shores of the Kyle of Durness [NC 3718 6688], but at Ord, Skye it is faulted. At all these localities the boundary is remarkably consistent in nature. Wright (1993) divided the formation into three members (Kyle, Stromatolite and Solmar), but these were not fully defined, and the bases of the lowest two members were placed above sections of non-exposure. During this research no comparable divisions were recognised in the Eilean

Dubh Formation at Assynt. However this may be a result of the thrust faulting and coarse recrystallisation of many of the outcrops. The thickness of the Eilean Dubh Formation at Assynt is difficult to ascertain due to these structural complications. Wright (1993) recognised the lower and upper members but did not recognise a stromatolite member in the Assynt area. Some 121 m have been logged at Balnakeil Bay, where lithologies include stromatolites fine-grained ripple laminated dolostone, mud-flake breccia and minor amounts of clastic sediment and evaporates pseudomorphs. The basal 12 m of the unit are exposed at An t-Sròn, and their difference to the lowest logged section at Balnakeil Bay suggests no overlap and hence a minimum thickness for the formation is 133 m.

1.4.4 Sailmhor Formation

The Sailmhor Formation (Peach & Horne 1884) was named after the abandoned settlement of Sailmhor (now Solmar). The formation consists of a 113 m succession of mostly dark mottled dolostone forming metre-scale parasequences with pale-grey tops exhibiting stromatolites. White cherts are particularly abundant in the lower half of the formation. The formation is well exposed at its type section along the shores of Balnakeil Bay [NC 3783 68877 – 3806 6875] but is heavily faulted. The section along the Kyle of Durness is also faulted, but not complete. At Inchnadamph the basal 23 metres are exposed in a thrust horse, whilst at Ord, Skye the formation is partly exposed along the shore. The upper half of the formation is best exposed on the shore near Leirinmore [NC 4262 6739 – 4248 6730], where some 37 m were logged. A thicker but more structurally complex section through the upper part of the unit is also seen along the shores of Balnakeil Bay [NC 3811 6882 – 3835 6886]. At both localities the uppermost part contains a thick bed of white chert c. 2.5 m thick.

The base of the formation is taken at a sharp colour and lithological change from light-grey, peritidal, finely crystalline dolostones to dark grey dolostones exhibiting locally common cherts. At Balnakeil Bay the basal boundary is exposed low in a cliff at NC 3783 6877. The distinctive colour change and distribution of cherts are recognisable along the shores of the Kyle of Durness [NC 3718 6688] 1.1 km to the southwest.



Text-figure 1.7 Published stratigraphical subdivisions and thicknesses of the Cambro-Ordovician succession in NW Scotland.

A colour change is also seen at Inchnadamph, but the boundary is faulted in the section on Skye. Oolite beds are common in the basal half of the formation, thrombolites become more common up section and the parasequences are often capped by ripple- and parallel-laminated, pale-grey dolostones displaying stromatolites.

1.4.5 Sangomore Formation

The Sangomore Formation (Peach & Horne 1884) takes its name from the hamlet of Sangomore, to the east of Durness. The formation (55 m) is exposed in its entirety along the type section at Balnakeil Bay [NC 3835 6886 – 3887 6876]. At 3850 6886, a small section of the formation was not accessible due to the shear cliff, and at 3875 6880 a vertical fault cuts strata out on the east side of a bay. The Sangomore Formation is distinguished by light-grey and buff, finely laminated dolostones, with some mid-grey, thrombolitic limestones, stromatolites and bioclastic, peloidal and ooidal wackestones or packstones occurring locally. The Sangomore Formation crops out on Skye, where a small outcrop buff weathering finely crystalline dolostone is seen at Ord [NG 6146 1282].

The lower boundary is gradational, with a series of chert breccias and dolomite sands spanning the boundary. The junction between the two formations is taken at the top of a 60 cm thick dolomite sand, which forms a distinctive notch in the cliff at Balnakeil Bay [NC 3835 6886]. Above this the dolostones become lighter in colour and the cherts are dominantly orange in colour. An identical bed of carbonate sand is seen at NC 3733 6664 along the Kyle of Durness, and although at Leirinmore the boundary is covered, the distribution of thick chert beds above and below indicates its location.

1.4.6 Balnakeil Formation

The Balnakeil Formation (Peach & Horne 1884) takes its name from the village of Balnakeil [NC 391 686]. It has a minimum thickness of 86 m at the type location of Balnakeil Bay [NC 3887 6876 – 3906 6870]. The formation is exposed inland at [NC 3839 6750] where some 28 m have been recorded but it is fairly certain that this is a repetition of the basal part. Wright (1985) cited a thickness of 140 m for the formation; however, this was based on the assumption that the inland exposure recorded an upper part of the formation. The lower boundary is marked by an oncoid and pebble bed at Balnakeil Bay, but the boundary is seen nowhere else. Lithologies defining the Balnakeil Formation include; mid- to dark-grey

coloured, stromatolitic and thrombolitic dolostones and limestones, with ribbon carbonates and bioclastic wackestones and packstones.

1.4.7 Croisaphuill Formation

The Croisaphuill Formation (Peach & Horne 1884) is a succession of purplish-grey, burrow-mottled, dolomitic-limestones, and occasional dark-grey dolostones. In the upper part of the formation, laminated dolostone becomes more abundant and light-grey, un-burrowed, dolomitic-limestones provide good marker beds. The formation takes its name from Loch Croisaphuill [NC 390 680] (now Loch Croispol). In its type section (cliff to the east of Loch Borrallie [NC 383 665–388 674]) a composite measured section provides a minimum thickness 350 m. However, many of the recent published thicknesses have been based upon the work of Wright (1985), who apparently logged to the top of the cliff at Loch Borrallie and no further, disregarding the large area of outcrop of different lithology to the east.

Although the lower boundary is not seen, the lithologies of the Croisaphuill Formation mark a change from those observed within the Balnakeil Formation. On the first edition British Geological Survey map of Durness, the boundary is marked as a fault at Balnakeil, and this interpretation is supported by the present study, with fracturing seen along a small roadside cutting. A small section at Loch Croispol [NC 3907 6836–3910 6834] exposes 17 m of what is likely to be basal Croisaphuill Formation, but this was not included in the measured section. A fault is probably present with a north-south trend, immediately to the west of the section but it is nowhere exposed.

The lower part of the formation comprises some 135 m of strongly burrow mottled, purplish-grey, dolomitic limestones. Fossils are commonly found within brownish black cherts in the basal 30 m and include rostroconchs, cephalopods, gastropods, local brachiopods and sponges. Most of the fossils are poorly preserved, with some replaced by dolomite, but the majority by chert (beekite).

The upper part of the formation is exposed on the hillside to the south of Glebe where 215 m have been logged, but outcrop width suggests it may be thicker. The upper part is distinct from the underlying succession and marks a unit in which dolostone is more abundant. Several light-grey, structureless, dolomitic-limestone beds up to 3 m thick are present at various levels and burrow-mottled, dolomitic-limestone beds persist. Parasequences become increasingly apparent, with lighter, parallel-laminated dolostones capping the cycles.

1.4.8 Durine Formation

The Durine Formation (Peach & Horne 1884) takes its name from the hamlet of Durine [398 678]. It is not exposed in any one complete section but in a series of inland sections providing a minimum thickness for the formation of 132 m. The track to the Old Manse at Glebe [NC 3927 6749–3929 6732] exposes 55 m. A small roadside quarry [NC 3949 6719] exposes 12 m and the section along Loch Caladail [NC 3952 6701–3972 8697] exposes a further 66 m. These sections can not be correlated and although they may be separated by faults, show no repetition and therefore offer a minimum thickness for the formation. The basal boundary is gradational and seen at [NC 3927 6749], where light-grey, fine-grained dolomites become abundant after 10 metres of the uppermost Croisaphuill Formation. The basal part of the Durine Formation contains some beds of burrow-mottled carbonate, a higher proportion of dolostone, a change in the colour of the cherts from black to orange-pink and an increasing proportion of parallel and ripple-laminated, light-grey dolostones.

1.5 RECENT DEVELOPMENTS IN CAMBRIAN AND ORDOVICIAN CHRONOSTRATIGRAPHY

The International Commission on Stratigraphy (ICS) has recently completed a revision of the international stratigraphical division of the Ordovician, and that of the Cambrian is underway. A summary of the subdivisions formalized so far is included. The succession in NW Scotland correlates well with North American stratigraphy (Chapter 5) and so these subdivisions are used. However, the international chronostratigraphy is referred to where possible.

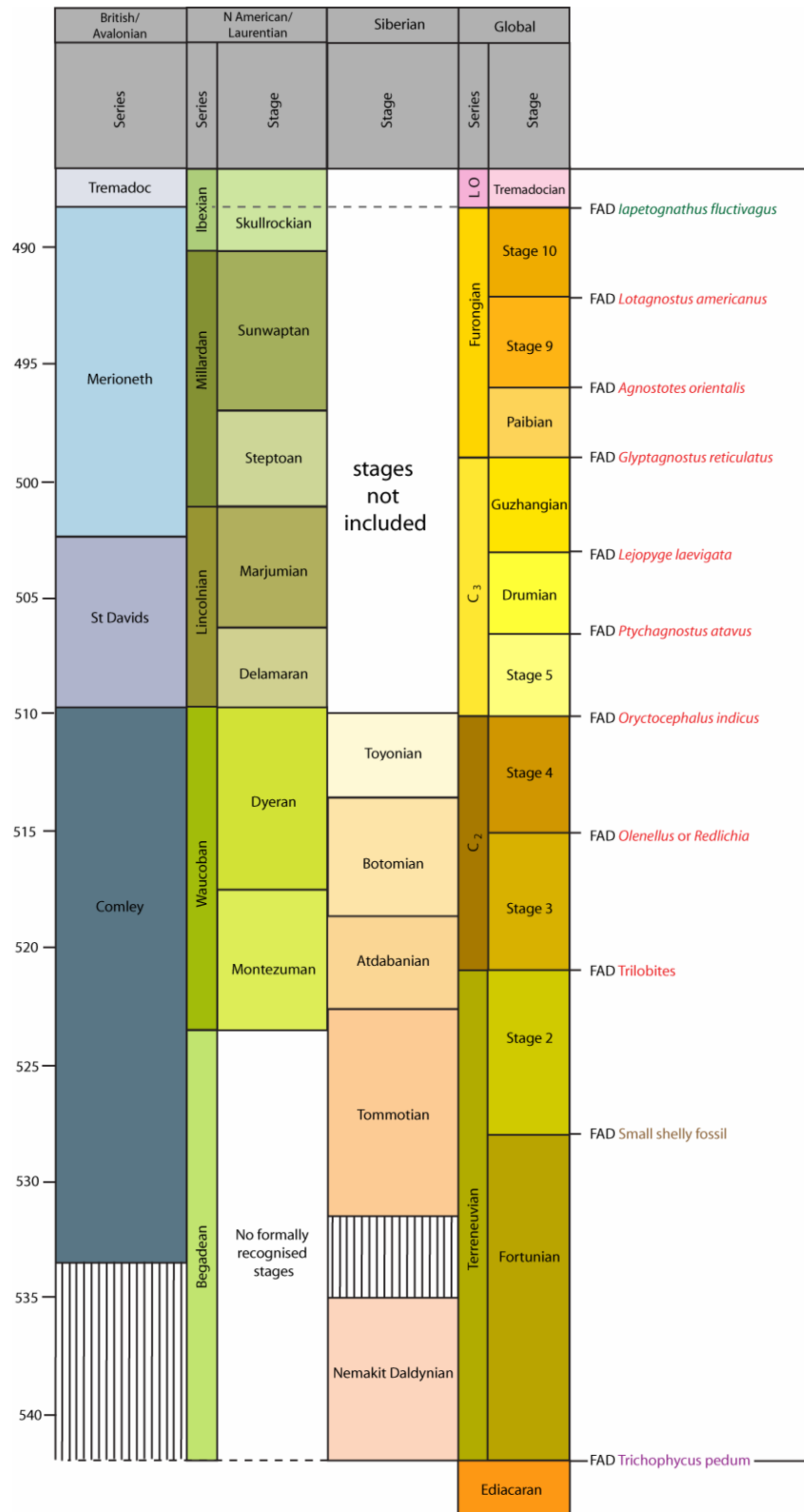
1.5.1 Current Cambrian stratigraphy

The subdivision of the Cambrian into globally recognized subdivisions is difficult, and the Cambrian System currently lacks some formally agreed international series and stages. This partly reflects the scarcity of suitable biostratigraphic markers for intercontinental correlation at the stage level and a strong faunal provincialism. The restriction of faunal groups to particular climatic belts and facies confined many genera and species of Cambrian organisms to single continents, and diachronous occurrences of key groups between the continents often limits the precision of biostratigraphy in global correlation, especially in the Early Cambrian. Correlations based on international comparison of improved radiometrical dating techniques

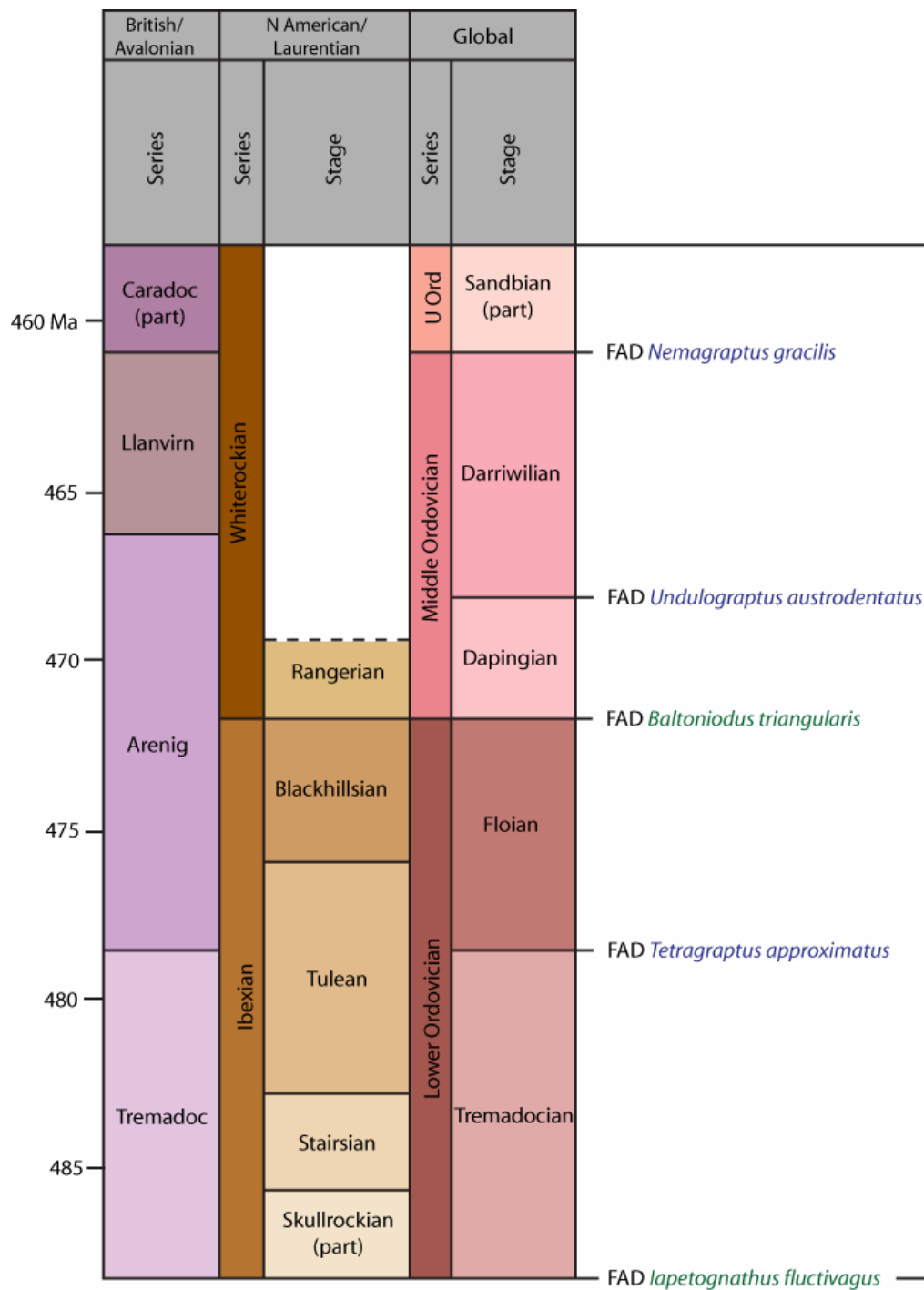
will improve correlations, particularly of the uppermost Proterozoic to pre-trilobitic Early Cambrian interval.

A stratotype for the Proterozoic–Cambrian boundary was formalized in 1991. It is placed at the first occurrence of the trace fossil *Trichophycus* (formerly *Treptichnus* or *Phycodes*) *pedum* (Seilacher) (Text-fig. 1.7). The Global Stratotype Section and Point (GSSP) is within the Chapel Island Formation, at Fortune Head, southeastern Newfoundland (Brasier *et al.* 1994, Landing 1994, Gehling *et al.* 2001).

Some of the series and stages within the Cambrian have been named, whilst others are still to be formally ratified. The Cambrian is now divided into four series (replacing the former three-fold division of Early, Middle and Late). The lowest series has been named Terreneuvian (Landing *et al.* 2007) and the boundary (which is defined by a brief but significant carbon isotope excursion) has been dated at 542 ± 1 Ma (Amthor *et al.* 2003). The Terreneuvian Series is divided into two constituent stages, the Fortunian at the base, and an as yet undefined and un-named stage (Stage 2) (Text-fig. 1.6). The base of this stage will probably be defined by the first occurrence of small shelly fossils (Ogg 2008). The second series within the Cambrian remains un-named and comprises two stages (3 and 4) and the base of the series is likely to be taken at the first occurrence of trilobites. Series 3 of the Cambrian comprises, in ascending order, un-named Stage 5, the Drumian Stage (Babcock *et al.* 2007) and the Guzhangian Stage (Ogg 2008). The base of the series is marked by the first occurrence of the trilobite *Oryctocephalus indicus* (Reed). The fourth and final series of the Cambrian, the Furongian consists of the Pabian Stage (Peng *et al.* 2004) at the base and is overlain by un-named stages 9 and 10 (Ogg 2008). In order to simplify matters somewhat whilst the two series remain un-named, un-named Series 2 and 3 will be referred to within this study by the abbreviations; C₂ and C₃ (Text-fig. 1.7).



Text-figure 1.8 Global series and stages within the Cambrian, the zonal fossil defining the base of each and showing correlation with Avalonian, Laurentian and Siberian series and stages. Index fossils in red represent trilobites, graptolites are represented in green and trace fossils in purple. Based upon Ogg (2008) and Babcock & Peng (2007).



Text-figure 1.9 Global series and stages within the Lower and Middle Ordovician and the zonal fossil defining the base of each. Correlation with Avalonian and Laurentian series and stages is shown. Conodont zonal taxa are displayed in green, whilst graptolite zonal taxa are in blue. Based upon Ogg (2008) and Webby *et al.* (2004).

1.5.2 The Cambrian–Ordovician boundary

Since 1998 the base of the Ordovician has been placed at the base of the *Iapetognathus fluctivagus* conodont zone (Text-fig. 1.8), which approximates to the *Cordylodus lindstromi* conodont zone elsewhere, the *Rhabdinopora flabelliforme* zone and the (first appearance datum) FAD of the trilobite *Jujuyaspis*. The GSSP for this boundary is the section at Green Point section, Newfoundland (Cooper *et al.* 2001). The base of the Ordovician System (base of Lower Ordovician Series and Tremadocian Stage) (Cooper *et al.* 2001) at Green Point has been dated to 488.3 ± 1.7 Ma (Gradstein *et al.* 2004).

1.5.3 Current Ordovician stratigraphy

The Ordovician Period spans the time interval between 488.3 ± 1.7 to 443.7 ± 1.5 million years ago (Ma) (Ogg 2008) and was originally defined by Charles Lapworth (1879), to resolve a longstanding dispute between followers of Adam Sedgwick and Roderick Murchison, who were placing the same units in northern Wales into both the Cambrian and Silurian periods respectively. Lapworth, recognised that the fossil fauna in the disputed strata were different from those of either the Cambrian or the Silurian periods, and that they should be placed in a time period of their own.

The Ordovician is formally divided into three series (Lower Ordovician, Middle Ordovician and Upper Ordovician). The two constituent stages of the Lower Ordovician are the Tremadocian and the Floian (Text-fig. 1.9) (Bergström *et al.* 2004, 2006). The base of the Floian is marked by the first occurrence of the widespread graptolite species *Tetragraptus approximatus* Nicholson, and the GSSP for the base of the Floian Stage is within the Tøyen Shale of Diabastbrottet, southwestern Sweden. The base of the overlying Dapingian Stage (Middle Ordovician) is marked by the FAD of the conodont *Baltoniodus triangularis* as defined by Wang *et al.* (2005).

Chapter 2

FACIES ANALYSIS OF THE IAPETUS PASSIVE MARGIN SEDIMENTS IN NW SCOTLAND: THE CAMBRO-ORDOVICIAN DURNESS GROUP

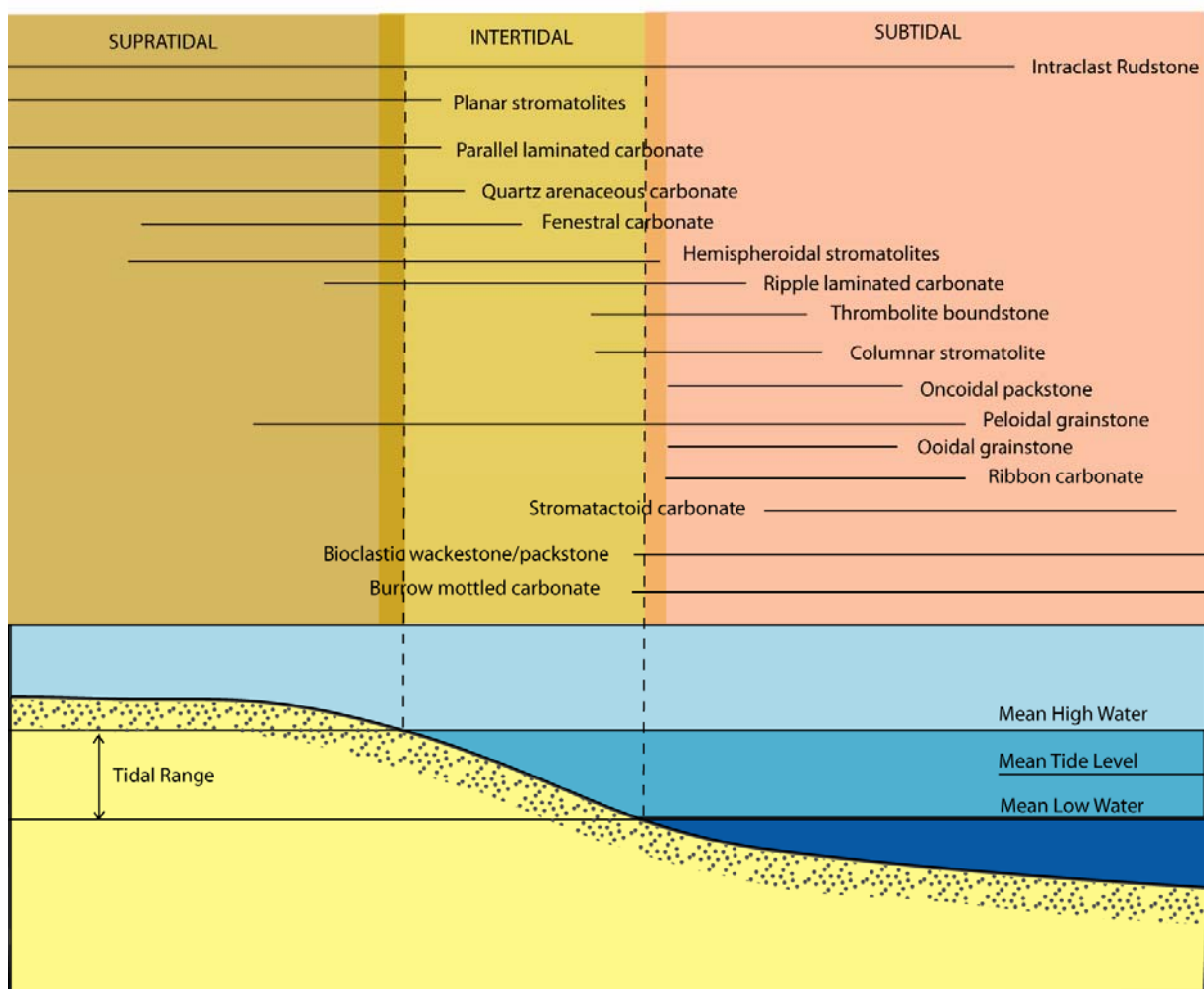
2.1 INTRODUCTION

The Durness Group has been little studied in comparison with other Laurentian margin sections in Newfoundland and North America; this is particularly the case for sedimentological and facies analyses. This study represents the first detailed description of facies from the Durness Group. The sedimentology of the underlying group (Ardvreck) has been comparatively well studied (for example, McKie 1990a, b, c, 1993)

The Durness Group is subdivided into seven formations, which are, in ascending order, the Ghrudaidh, Eilean Dubh, Sailmhor, Sangomore, Balnakeil, Croisaphuill, and Durine formations. The Durness Group represents a succession of shallow-water carbonate strata of Cambrian to early Middle Ordovician age. It is exposed in a semi-continuous belt some 170 km in length, from Loch Eriboll in the north to Skye in the south. It crops out along the foreland and within thrust sheets of the Moine Thrust zone. The most complete section includes the coastal type section at Balnakeil Bay, near Durness and other inland localities. A composite section for the whole of the Durness Group was constructed using sedimentary logs from Balnakeil Bay, Loch Borralie, Loch Caladail, An t-Sròn and Ardvreck (Appendix 1; Text-figs 1.3 –1.6). Sections on Skye were also examined but proved to be of little use for facies analysis, due to thermal alteration by the Beinn an Dubhaich granite.

2.2 LITHOFACIES

The rocks of the Durness Group have been divided into 16 separate lithofacies (Text-fig 2.1), and genetically or environmentally related lithofacies grouped together in a facies association, representing a gross depositional environment. The individual lithofacies are transitional between lithofacies associations and each lithofacies commonly comprise a variety of lithologies, but is identified and distinguished by a dominant lithology, lithological association, sedimentary structure or a particular fauna.



Text-figure 2.1 Lithofacies described and their interpreted distribution across the supratidal, intertidal and subtidal zones, based upon the relative position within shallowing upward parasequences and associated sedimentary structures observed within the Durness Group. The tidal zones are defined by the mean low water and mean high water marks.

Dolomite and limestone comprise much of the sequence. Where the dolomite is coarsely crystalline the recrystallisation makes sedimentary structures difficult to distinguish. In contrast early diagenetic dolomite is also present and preserves structures to a better degree, due to its fine crystal size.

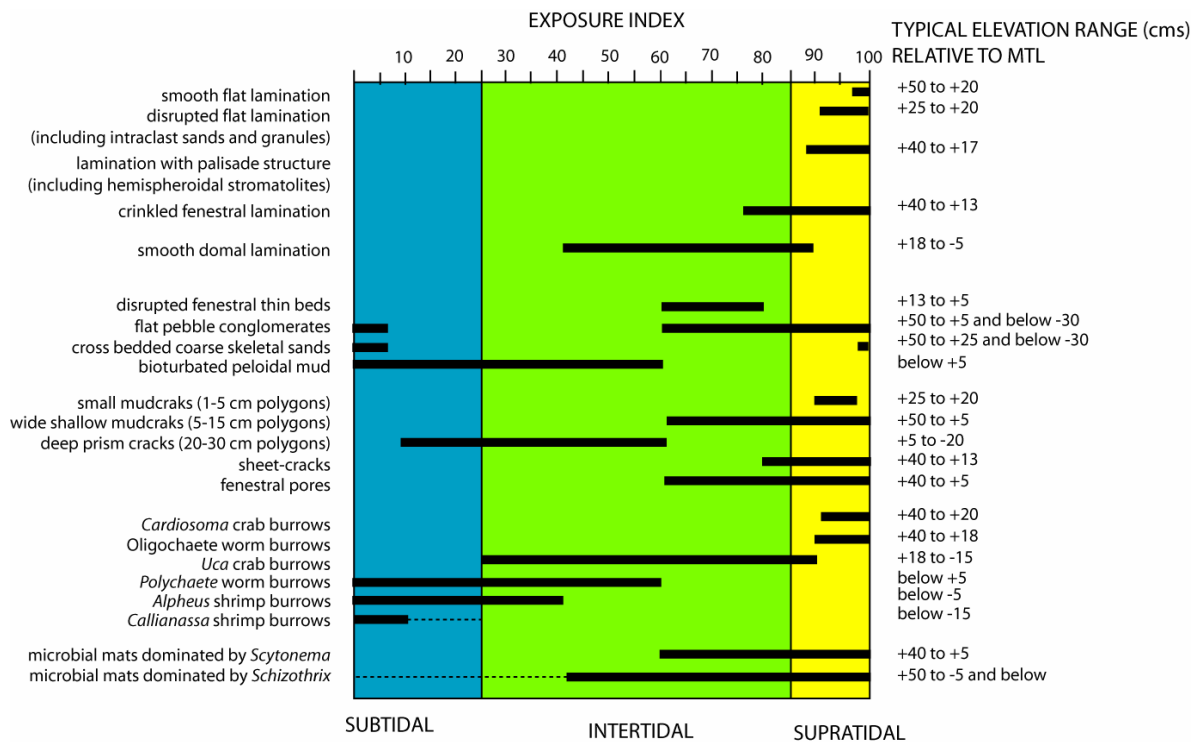
Chert has been excluded from the lithofacies analysis, as it does not represent depositional bedded-chert, but appears to be an early diagenetic phenomenon. The cherts within the Durness Group commonly occur at the top of shallowing-upward cycles and often

replace and preserve sedimentary fabrics. Chert is observed replacing burrows, microbialites, evaporates and ooids.

The carbonate classification largely follows that introduced by Dunham (1962) and added to by Embry & Klovan (1971) (Text-fig. 2.2). The environmental interpretation of the lithofacies comes from many sources, but principal references include, Hardie (1986), Shinn (1983), Ginsburg *et al.* (1977) and Flügel (2004). Ginsburg *et al.* (1977) used an exposure index to more accurately define the depositional setting of sedimentary structures, which is an invaluable source of quantitative data. The exposure index is essentially the percentage of time that an area at certain elevation relative to mean tide level stays dry (this is often complicated by wind however on tidal-flats with a small tidal range). Different features of tidal-flats have a specific exposure index range, and also a height range in relation to mean tide level (Text-fig. 2.3).

original components not organically bound together during deposition						Boundstones: original components organically bound during deposition		
contains lime mud			lacks mud and is grain-supported	>10% grains >2 mm		organisms act as baffles	organisms encrust and bind	organisms build a rigid 3-D framework
mud-supported		grain-supported with muddy matrix		matrix-supported	supported by >2 mm component			
< 10% grains	> 10% grains							
mudstone	wackestone	packstone	grainstone	floatstone	rudstone	bafflestone	bindstones	framestone

Text-figure 2.2 The Dunham classification of carbonates (mudstone–grainstone) based on the textural relationship between grains, mud matrix and intergranular pore space, and the Embry & Klovan classification for coarse grain sizes (floatstone and rudstone and reefal or organically bound carbonate rocks (bafflestone to framestone) (Tucker & Wright 1990 based on Dunham 1962 and Embry & Klovan 1971).

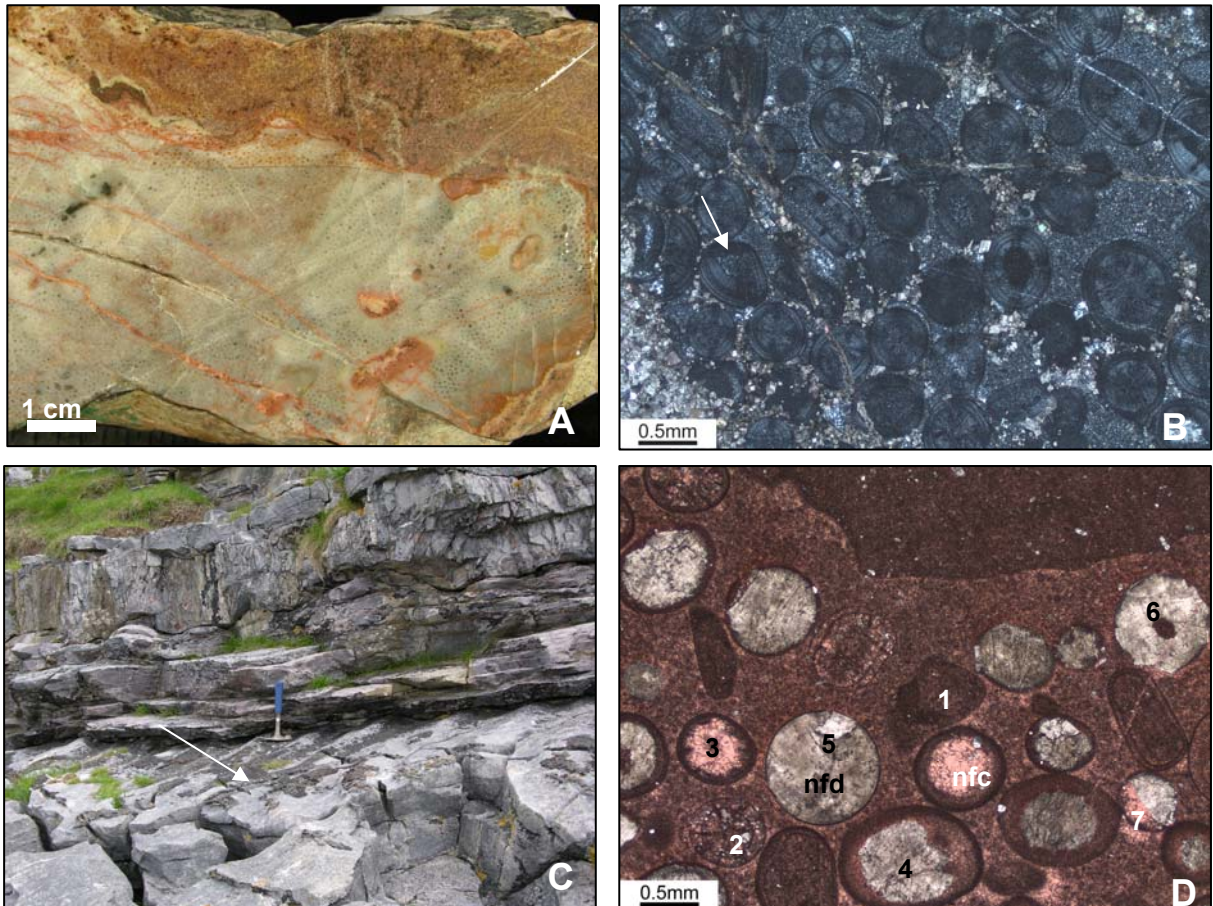


Text-figure 2.3 Chart displaying quantitative data for the exposure indices of selected tidal flat features. The tidal elevation range relative to mean tide level (MTL) is also shown (after Ginsburg *et al.* 1977).

2.2.1 Ooidal grainstone/wackestone

Beds of ooidal grainstone and wackestone occur in all but the Balnakeil, Croisaphuill and Durine formations. The distribution may be a preservational artefact however as much of the succession is heavily dolomitised, and primary depositional texture is commonly difficult to distinguish. In beds without pervasive dolomitisation or which have been subjected to early silicification, the ooids are well preserved. Although it is often possible to deduce that some coarse dolostone beds were once ooidal grainstone, the majority of this description comes from those preserved in chert. The dolostones surrounding the cherts show little structure but allow us to interpret those beds of faintly cross stratified coarsely recrystallised (but commonly with ghost ooids) and grey dolostone as ooidal grainstones. Good examples of ooidal grainstone occur within the upper Ghrudaidh (47.5 m), upper Eilean Dubh (122 m), Sailmhor (43 m) and lowest Sangomore (7.5 m) formations.

Ooidal grainstone beds are commonly tabular in shape, and locally exhibit an upper rippled surface (Text-fig. 2.4C). Beds in the Eilean Dubh Formation are observed to be infilling the space between stromatolite bioherms (116–118.5 m). Bed thickness ranges between 0.1 and 1.2 m but the majority are c. 30 cm thick. This lithofacies is often associated with intraclast rudstone, peloidal grainstone and oncoidal packstone.



Text-figure. 2.4 Examples of ooidal grainstone and wackestone. **(A)** Chert nodule from the upper Eilean Dubh Formation (122 m height) preserving ooids. **(B)** Thin section micrograph of ooids shown in A. Silicification has preserved the concentric nature of the cortices. A regenerated ooid is marked by an arrow. **(C)** Rippled ooidal wackestone bed (arrowed) which shows a silicified upper surface (Sangomore Formation, 49.5 m height). Hammer for scale **(D)** Thin section photomicrograph of a sample of the bed in C, showing ooids and peloids within a matrix of non-ferroan calcite microspar. The ooids have commonly been replaced by non-ferroan dolomite (nfd) and locally by non-ferroan calcite spar (nfc). Ooids numbered refer to preservational styles discussed in the text.

Due to coarse dolomitisation of the succession, ooids are rarely preserved, but locally some cherts preserve them in large numbers, especially in the upper Eilean Dubh Formation (122 m) (Text-fig 2.4A, B) and middle Sangomore Formation (31 and 32 m). This suggests that ooids were more abundant than can be interpreted by solely observing the dolostone succession. In one limestone within the upper Sangomore Formation (49.5 m; Text-fig. 2.4C, D) ooids are observed in different modes of recrystallisation. They occur as; 1) unaltered micrite, 2) micrite with small quartz crystals, 3) micrite, with a nucleus replaced by non-ferroan calcite spar, 4) nucleus replaced by dolomite, 5) complete replacement by dolomite with an intact margin to the ooid, 6) dolomite crystals completely replace and extend beyond the margin, 7) replacement by both dolomite and non-ferroan calcite spar.

The ooids from the Durness Group are rarely more than 1.5 mm in diameter and the majority range from 0.5 to 1 mm. They are commonly spherical or ovoid in shape, but this largely depends upon the nature of the nucleus around which it formed. Both single and compound ooids are represented, and broken and regenerated ooids are observed in the Eilean Dubh Formation (Text-fig 2.4B). The majority of nuclei are composed of micritic or peloidal intraclasts, however the original nucleus is commonly destroyed by dolomitisation prior to silicification (compare Text-fig. 2.4B and 2.4D). In the uppermost Eilean Dubh Formation some superficial ooids are noted (cortex less than half the diameter of the entire ooid) (Text-fig. 2.4D), however, most are ‘normal’ (cortex/nucleus ratio of 4:1) *sensu* Flügel (2004).

Ooids which are not silicified and are un-dolomitised are seen to be composed of non-ferroan calcite, and most of the ooids have a concentric–tangential cortex, but radial–fibrous forms are sometimes observed. A small proportion of the ooids are composed of structureless micrite (micritic ooids). This largely results from micro-boring or recrystallisation, but can also occur when aragonitic ooids become calcitised (Flügel 2004).

The depositional environment of the ooidal grainstone facies is interpreted to have been a high-energy, shallow subtidal setting (Moshier 1986; Flügel 2004). Modern marine ooids commonly occur in intertidal and shallow marine environments of places such as the Bahamas, Persian Gulf and on the Great Barrier Reef (Hine 1977, Loreau & Purser 1973, Marshall & Davies 1975). Modern ooid deposits accumulate at or above fair-weather wave base (FWWB), under high-energy conditions. Extensive linear marine sand belts and tidal bars upon which ooids are produced and deposited have been well documented in the Bahamas (Ball 1967, Hine 1977) and in the Persian Gulf (Loreau & Purser 1973) in water

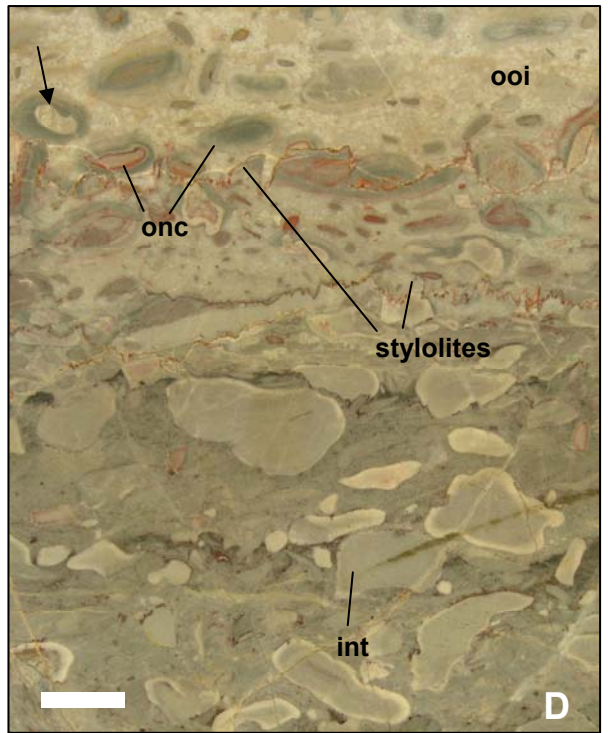
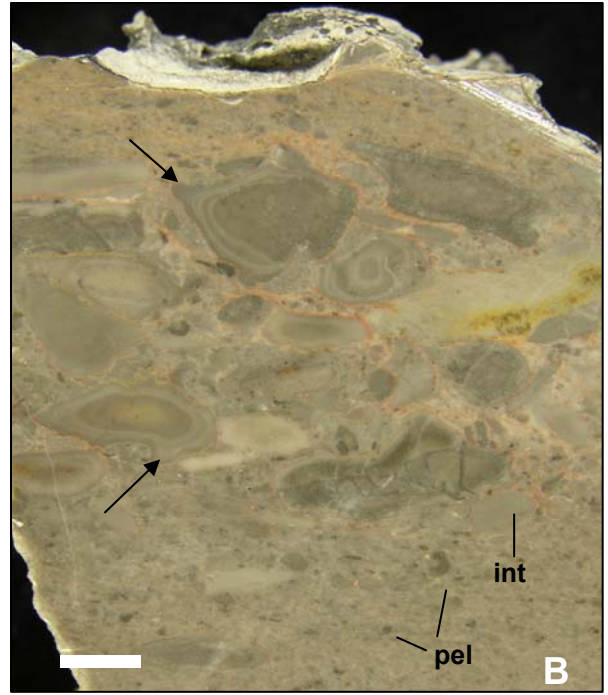
depths of 0–5 m. The Quaternary ooid sand shoals of the Bahaman Bank originate and accumulate in a range of different sub-environments, including mobile fringes, sand flats, tidal channels, platform shelves, open margins and platform interiors (Flügel 2004).

Tidal current generated sands are characterised by ooid growth in water depth ranging from less than 1 m to as much as 10 m (Flügel 2004). Based upon the size of the ooids and the thickness of the cortices, the ooids of the Durness Group are interpreted to have formed ooid shoals in the shallow subtidal zone (Steinhoff & Strohmenger 1996).

2.2.2 Oncoidal grainstone/packstone

Oncoidal grainstone and packstones are recorded only from the Sailmhor, Sangomore and Balnakeil formations, however they are perhaps the most distinctive lithofacies present within the Durness Group. They commonly occur at the base of parasequences. Silicification has preserved 20 cm of oncoidal packstone, surrounding columnar stromatolites, 47 m above the base of the Sailmhor Formation. The oncolite is preserved by selective silicification of the microbial structures and parts of their surrounding inter-reef facies by black and white chert. Oncoids also occur with peloids in a 5–21 cm thick bed, approximately 80 m above the base of the Sailmhor Formation. The Sangomore and lowest Balnakeil formations contain two horizons within which oncoidal packstone beds occur. Between 37 and 39 m above the base of the Sangomore Formation at Balnakeil Bay, a 30 cm oncolite bed is associated with other thin beds containing oncoids. The thickest bed displays oncoids which are discoid in shape, up to 2 cm in diameter and 1 cm thick (Text-fig. 2.5A, B). Within the beds above this, oncoids are much smaller in size (2–4 mm).

Text-figure 2.5 Oncoidal grainstone and packstone. **(A)** weathered surface of a limestone containing oncoids comprised of dolomite; Sangomore Formation 37 m above the base. **(B)** polished slab of the same bed shown in **(A)** displaying oncoids within a matrix of peloidal grainstone (pel) and small intraclasts (int). The oncoids are up to 2 cm in diameter and have lobate surfaces (arrowed). Scale bar is 1 cm. **(C)** basal bed of the Balnakeil displaying weathered oncoids, surrounded by a patchy silica cement. Coin for scale. **(D)** polished slab showing a close up view of the bed figured in **(C)**. The sample comes from a part of the bed which is not silicified and intraclasts (int) are observed at the base. The intraclasts commonly have a pale margin, suggesting weathering. Styloites cross the sample and overlying the intraclasts oncoids (onc) are noted in a matrix of ooidal grainstone (ooi). One oncoid is observed to have a cortex comprising ooidal grainstone (arrowed). Scale bar is 1 cm.



The second horizon containing oncoids marks the base of the Balnakeil Formation. It comprises a tabular (20 cm) bed, overlying parallel-laminated dolostone, and overlain by quartz sand and hemispheroidal stromatolites. Ooids are observed in the upper half of the bed, and clasts of oolite form the nuclei of some oncoids (Text-fig. 2.5C). The nuclei of the oncoids show evidence of weathering (lighter grey margin), and laminae have formed around intraclasts identical to those in the lower part of the bed.

The oncoids from the Durness Group range from 0.5 to 3 cm in diameter (macro-ocoid) and are non-skeletal (spongiostromate). They are distinctly laminated, with laminae having formed around carbonate intraclasts. The laminae are mostly uniform however some are asymmetrical, or non-continuous. All laminae comprise micrite and sparite alternations, sometimes with a fenestral fabric. The surfaces of the oncoids are locally lobate (Text-fig. 2.5B) but the majority are smooth. Smaller nuclei tend to have larger cortices than large intraclasts, which commonly have a reduced and more asymmetrical cortex. The oncoids can be classified as 'type c' oncoids (concentrically stacked) (Logan *et al.* 1964). Oncoidal grainstones are commonly associated with intraclast rudstones, peloidal grainstone and ooidal grainstones. They commonly occur as inter- reef facies, associated with columnar stromatolite bioherms and thrombolite bioherms/biostromes.

The oncoids result from the sediment trapping and calcification of microbial or algal filaments, followed by rapid decomposition, leaving only the laminae visible (Flügel 2004). Marine oncoids most commonly form in agitated shallow subtidal settings, forming shoals, and are often used as indicators of high-energy, lower intertidal to shallow subtidal environments and locally of hiatal surfaces (Tucker & Wright 1990; Flügel 2004). The regular concentric lamination and symmetrical shape of oncoids from the Durness Group suggest high agitation and constant turning of the grains and they commonly characterise the bases of parasequences and larger sequences within the Durness Group.

2.2.3 burrowed mudstone/wackestone

Burrow mottled carbonate is most common lithofacies within the Durness Group, and it accounts for a large proportion of the Ghrudaigh and Croisaphuill formations. Beds of burrow mottled carbonate are always tabular and are thicker, on average than beds of any other facies (partly due to an inability to recognise changes in bedding due to homogenisation). The burrows commonly occur in lime micrite or peloidal/bioclastic wackestones. Beds of up to 10

m in thickness occur in the Croisaphuill Formation, but those occurring within shallowing upward parasequences are commonly less than 2 m thick. Where the burrow fill is distinguishable they are generally 0.5 cm to 2 cm in diameter. Where the burrows are visible they commonly show overprinting of successive periods of burrowing and the burrows within the Durness Group show a high degree of branching and interconnection (Text-fig. 2.6A, B). The burrow fills are sometimes silicified but more commonly are distinguished by paler dolomite (with the surrounding sediment remaining as limestone). Any primary sedimentary structures were subsequently destroyed by burrowing.

Associated lithofacies include ribbon carbonate with which burrow mottling is gradational in shallowing upward sequences (Text-fig. 2.7B). Thrombolites are associated in some beds with burrow-mottled carbonate and following pervasive dolomitisation it becomes difficult to distinguish tabular thrombolite biostromes from beds of burrow mottled carbonate, for example the 'leopard rock' of the Sailmhor Formation (see Chapter 3).

In recent environments, burrowing occurs in the intertidal- to subtidal zone, and is especially common in subtidal settings (Ginsburg *et al.* 1977, Tucker & Wright 1990). Infaunal burrowing organisms are particularly frequent in calcareous muds deposited in shallow-marine, quiet water, sheltered embayments (e.g. lagoons and muddy tidal flats), and deeper water environments below fair-weather- and storm-wave base (Flügel 2004). Recent shallow marine carbonate environments in Florida and the Bahamas are dominated by burrows of the shrimp *Callianassa*, which bioturbate as much as 75% of the sediment, and repetition of burrow excavation and storm infilling results in the formation of storm-derived sediment textures dominated by mottled packstone with coarse skeletal patches (Shinn 1968; Tudhope & Scoffin 1984; Curran & White 1991; Wanless & Tedesco 1993). Sedimentation rate is a major factor affecting the nature of burrows and overprinting implies a slow rate of sedimentation (Text-fig. 2.6C) (Taylor *et al.* 2003).

The high degree of branching and interconnectivity (Text-fig. 2.6A, B) implies a well oxygenated environment. Vertical burrows are most common in intertidal settings, but anastomosing burrows are generally subtidal (Flügel 2004). Differences in permeability and porosity influence the style and course of dolomitisation, and the crystal size of burrow fills may be one factor controlling the often observed selective dolomitisation of the burrows (Zenger 1992, Morrow 1978, Gingras *et al.* 2004).



Text-figure 2.6 Strongly bioturbated dolomitic limestone, (A) Croisaphuill Formation. The burrows comprise a fill of light grey sucrosic dolomites within a lime rich, muddy carbonate. (B) *Planolites* isp. observed on a bedding plane, 33 m above the base of the Ghrudaigh Formation, An t-Sròn. (C) silicified burrows within a subtidal limestone, showing evidence of tiering, indicating a complex deposit feeding community, 39.5 m above the base of the Sangomore Formation. Pen is 14 cm long. (D) silicified *Thalassinoides* isp. burrows displaying branching networks in plan view. upper Sangomore Formation (44 m).

The intensely bioturbated bioclastic wackestones represents deposition in a protected, shallow marine shelf of normal salinity and well oxygenated conditions. This is supported by the most diverse fossil fauna and conodont assemblages (Chapter 4). The networks of burrows and the overall shape and thickness would normally be referred to *Thalassinoides* (Text-fig. 2.6D), but in carbonates it is more difficult to assign names to trace fossils without the sand/mud contrast exhibited in most well preserved siliciclastic preserved trace fossils.

2.2.4 Ribbon carbonate

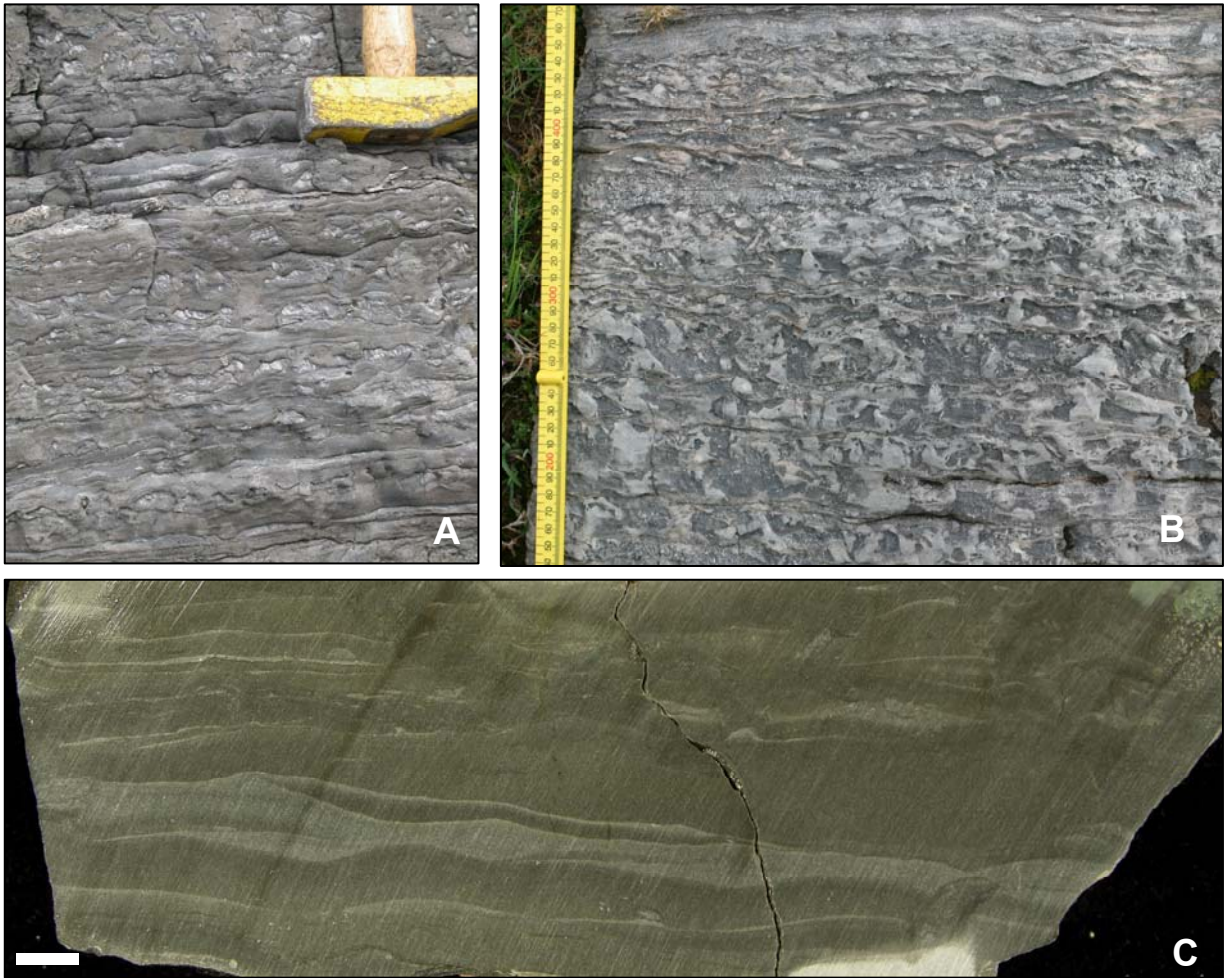
Ribbon carbonate ('Ribbon rock') comprises a distinctive heterolithic alternation of cm-scale beds of coarse-grained laminae and mm-scale inter-laminae of finer grained carbonate mud.

In general the coarser-grained constituents are dolomitic, commonly silt grade and the finer-grained constituents are calcareous (Demicco 1983). The ribbon rock in the Durness Group commonly shows burrow networks on bedding planes.

Ribbon carbonate is most common in the Balnakeil Formation and the upper Croisaphuill Formation, and comparatively rare in the other formations within the Durness Group. This lithofacies forms tabular beds 30–90 cm thick and the best examples occur between 30 m and 42 m above the base of the Balnakeil Formation (Text-fig. 2.7A), where beds are tabular but often have a gradational lower boundary with underlying burrow mottled carbonate. There is commonly a gradation from strongly bioturbated, dolomitic-limestone to ripple-laminated carbonate (Text-fig. 2.7B).

Ribbon carbonate is closely associated with burrow-mottled carbonate, which it commonly overlies. There is a gradation between the two facies, as the burrow fills become reworked by ripple laminae. Preferentially dolomitised burrow fill has been described by Morrow (1978) from the Upper Ordovician of the Canadian Arctic. The dolomitisation was influenced by differences in porosity and permeability during deposition and the eroded burrow-fill was most likely similar. It does not prove that burrows were dolomitised contemporaneously as sedimentation progressed, only that the ripple laminated burrow fills and the burrows themselves were similarly affected by diagenetic dolomitisation. The ribbon carbonate is locally associated with intraclast rudstones which are commonly dark grey, matrix supported and contain clasts of the ribbon carbonate within them. Good examples of intraclast breccias within ribbon carbonate are seen at 17.80 m and 36 m above the base of the Balnakeil Formation.

The interpreted depositional environment for the ribbon carbonate is below FWFB and above SWB. Ribbon carbonate has previously been interpreted as a shallow subtidal deposit (Demicco 1983, Osleger & Read 1991, Chow & James 1992). The association of flat pebble conglomerates suggests that there was reworking of early cemented ribbon carbonate into brittle intraclasts. The intraclast conglomerates may represent storm deposits, a view supported by Sepkoski (1982), Demicco (1985) and Whisonant (1987).



Text-figure 2.7 Photographs of ribbon carbonate. **(A–B)** close association with burrow mottled facies; **(A)** Balnakeil Formation 41 m above the base. Hammer for scale. **(B)** burrowed dolomitic limestone grading into ripple laminated ribbon rock upper Croisaphuill Formation. rule for scale. **(C)** polished slab of ribbon carbonate from the Balnakeil Formation. Scale bar is 1 cm.

2.2.5 Bioclastic wackestone/packstone

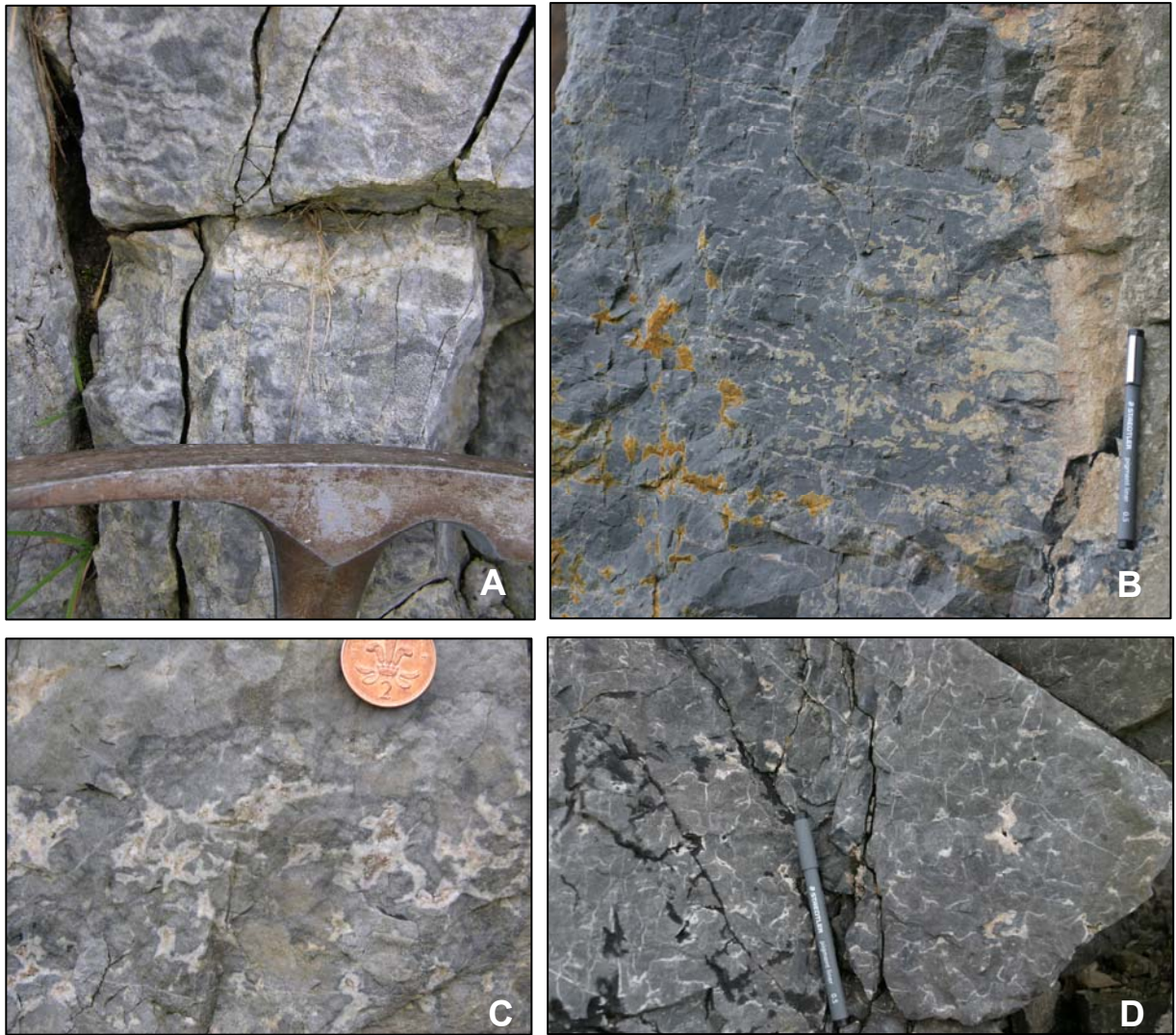
Bioclastic wackestones and packstones are observed within the lower part of the Ghrudaidh Formation and the Sailmhor, Sangomore, Balnakeil and Croisaphuill formations. They form tabular beds up to 2 m thick, but also occur as isolated inter-reef facies, between thrombolite and columnar stromatolite bioherms. The bioclasts are more easily recognised when the shell debris is silicified, however coarse dolomitisation makes some bioclasts difficult to distinguish. Beds within the Croisaphuill Formation contain the most diverse fauna, including gastropods, cephalopods, sponges, rostroconchs, brachiopods and trilobites.

2.2.6 Stromatactoid carbonate

Large, complex fenestral structures found within the Durness Group are here assigned to a stromatactoid texture, as they bear a superficial similarity to features described as stromatactis. Horizontal, stromatactis-type fenestral structures were first recorded by Dupont (1881), and later defined more fully by Bathurst (1982). The Durness Group fenestrae differ from true stromatactis, which comprise flat-bottomed, reticulate pores, with digitate and dendrate roofs by being more irregular and commonly not concentrated along discrete horizons. The Durness Group stromatactoid fabrics are very variable (Text-fig. 2.8). Only the textures present within the lowest Sailmhor Formation bear a strong similarity to true stromatactis (Text-fig. 2.8B).

Stromatactoid cavities occur in the Eilean Dubh, Sailmhor and Sangomore formations. They occur at the bases of parasequences and are commonly observed in dark grey coarsely crystalline dolostone. Beds of stromatactoid carbonate up to 1.3 m thick are noted and are tabular and generally have a gradational upper boundary. Stromatactoid carbonate commonly underlies thrombolite bioherms and biostromes.

The stromatactoid texture is closely associated with coarse grained dolostone, possibly suggesting a diagenetic origin for some of the 'cavities'. The stromatactoid texture within the Durness Group is different to true stromatactis, in that they are more irregular. Different stages of infilling/growth are evident, for some of the most irregular shapes, found within the Sailmhor Formation (Text-fig. 2.8C, D). The features appear to start as a network of intersecting veins of dolomite, at the intersections of these veins large irregular patches of spar are now present. It is still not known if these formed by displacement of sediment or by passive means, but they seem to be a late diagenetic feature. Other structures resembling stromatactis are found within coarsely recrystallised ooidal grainstones and are also interpreted to be features formed during recrystallisation. Several papers have suggested that stromatactis is closely associated with the formation of carbonate mud mounds (Monty *et al.* 1995, Reitner & Neuweiler 1995, Riding 2002) but the precise mechanism of formation has still not been determined.



Text-figure 2.8 Stromatactoid textures. **(A)** a recrystallised ooidal grainstone displaying stromatactoid texture, lower Sangomore Formation (7.5 m above the formation base), Balnakeil Bay. Hammer head for scale. **(B)** ‘true’ stromatactis observed within a dark grey, fine grained dolostone. Photograph taken 1.8 m above the base of the Sailmhor Formation, Balnakeil Bay. Pen is 14 cm long. **(C)** dolomite spar-filled vugs displaying an irregular stromatactoid texture. several phases of cement infill are visible. Thrombolite bed, 1 m above the base of the Sangomore Formation. Voin for scale. **(D)** irregular stromatactoid vugs within dark grey, mottled dolostones. The texture is observed towards the base of a parasequence from the middle of the Sailmhor Formation. It comprises white dolomite spar-filled vugs with numerous interconnecting veins. Pen for scale.

Hladil (2005) suggested that not all the documented occurrences of stromatactis fit with the mud mound formation hypothesis. Organisms have been proposed as agents for some stromatactis formation and these include sponges (Bourque & Gignac 1983), non-skeletal algae (Coron & Textoris 1974), microbial accretions (Tsien 1985) and bryozoans (Textoris & Carozzi 1964). The cavities have also been attributed to a variety of inorganic processes,

including slumping (Schwarzacher 1961), dewatering and collapse (Heckel 1972), dynamic metamorphism (Logan & Semeniuk 1976), recrystallisation of carbonate mud (Ross *et al.* 1975) and submarine crust formation (Bathurst 1982).

The stromatactoid textures within the Durness Group vary in terms of their size, shape and internal composition. It is therefore proposed that they may have had different origins although to elucidate these is difficult. They all appear to be closely associated with the distribution of dark-grey, subtidal carbonates.

2.2.7 Peloidal grainstone

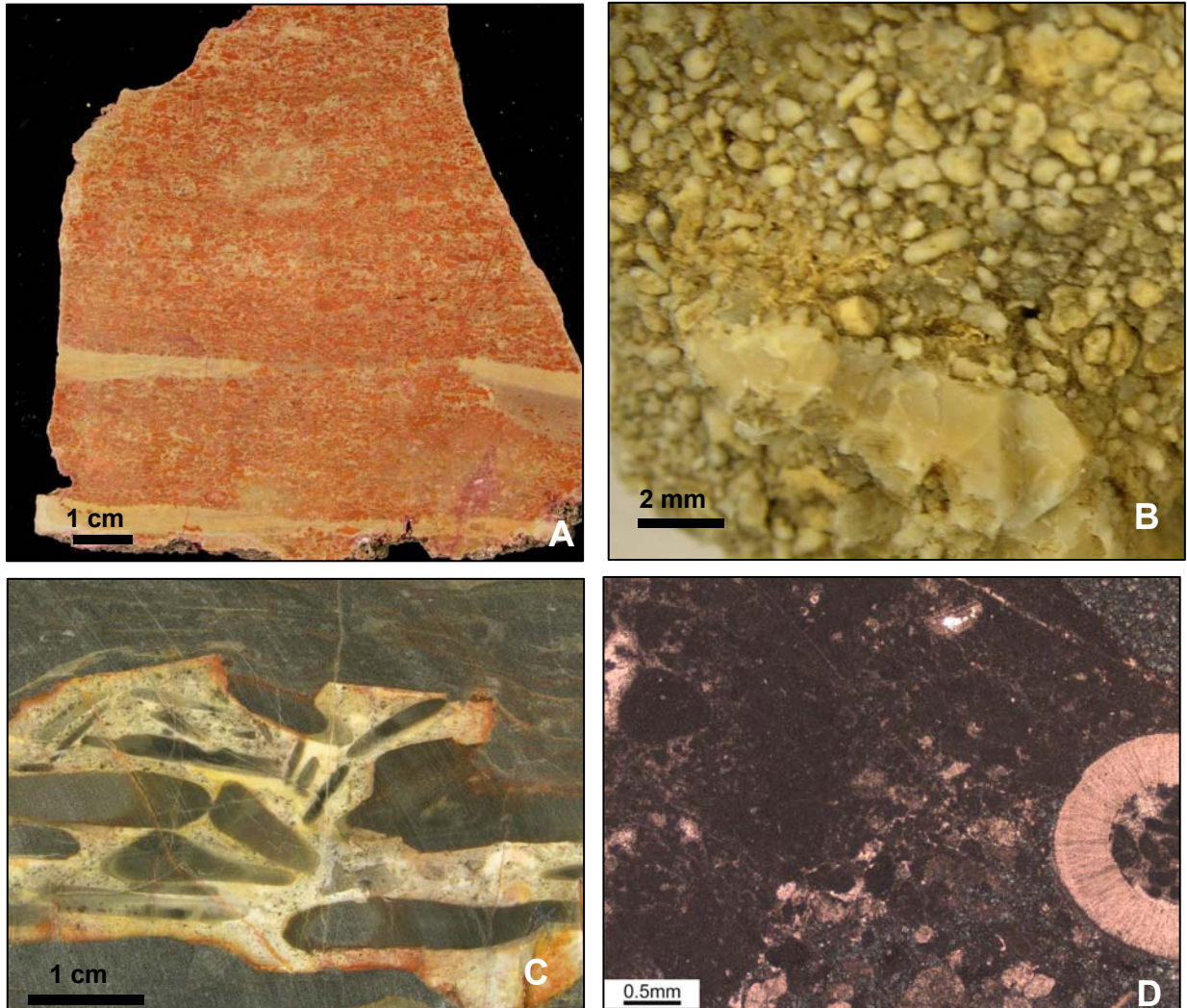
Peloids are grains of micrite which may form in a variety of different ways and occur in a wide variety of environments (Flügel 2004). Peloids comprise an important constituent of many of the carbonates within the Durness Group. The peloids range from 80 μm to 2 mm and are commonly associated with other facies, but locally form entire beds (Text-fig. 2.9A). Durness Group peloids can be subdivided into two principal types, based upon size and interpreted origin: faecal pellets and mud peloids.

Faecal pellets are recorded from the Sangomore, Balnakeil and Croisaphuill formations, they are closely associated with bioclastic wackestones and sometimes burrows. They range in diameter from 400 μm to 2 mm and are rounded, elongate or rod shaped. Faecal pellet grainstone often forms inter-reef facies associated with columnar stromatolites or thrombolites (Text-fig. 2.9B). They are interpreted as lower intertidal to subtidal in origin, based on their common association with thrombolites and marine fauna. These peloids are interpreted primarily as the faecal matter of gastropods but may also include those of crustaceans and worms.

Mud peloids are comparatively smaller than faecal pellets and they are composed of micrite varying in size from 80 μm to 200 μm . Those over 200 μm are termed small intraclasts (Flügel 2004). They are associated with tidal flat facies (intraclast rudstones and stromatolites) although they are rarely preserved following dolomitisation. The peloids result from the reworking of mud and grains, commonly by deflation of the supratidal flats. They are variously shaped micritic grains, commonly without internal structure. The absence of burrowing and the occurrence in layers or laminations (Text-fig. 2.10B) supports the interpretation that these peloids formed in an upper intertidal to supratidal environment. Peloids are sometimes reworked within intraclast rudstones at the bases of parasequences

(Text-fig. 2.9C). Locally small peloids of uncertain origin comprise clotted textures interpreted to be thrombolites (Text-fig. 2.9D).

In recent settings, peloids are most common in tropical carbonates but are rare or absent in non-tropical settings. In the Bahamas peloids comprise 75% of the total sand fraction over an area of 10 000 km² of the restricted interior platform (Flügel 2004).



Text-figure 2.9 Peloidal grainstone facies in polished section, hand specimen and thin section. **(A)** stained polished slab displaying non-ferroan calcite peloids and small intraclasts within a non-ferroan dolomite matrix, forming a laminated fabric. They probably form part of a stromatolite, upper Sangomore Formation (45 m). **(B)** detailed view of subrounded and rod-shaped peloids, which have been silicified. Inter-reef facies within a thrombolite bioherm, Sangomore Formation (24 m). **(C)** faecal pellets forming the matrix of a chert replaced intraclast rudstone. Specimen from the lower Balnakeil Formation, Loch Borrallie. **(D)** thin section micrograph displaying a peloidal texture to micritic mud. Thrombolite inter-reef facies, upper Sangomore Formation.

2.2.8 Thrombolite boundstone

Thrombolites are microbialites with a clotted mesostructure (Kennard & James 1986) and although comparatively rare at the modern day, they were abundant during Cambrian and Ordovician (Shapiro 2000). They commonly form mound shaped bioherms (Text-fig. 2.10E) or tabular biostromes. The morphology and structure of these build-ups is described in more detail in Chapter 3.

Thrombolites are rare within the Eilean Dubh Formation and only one candidate is a 65 cm bed, 108 m above the formation base, although in plan view the bed is seen to comprise multiple syneresis cracked laminae. This bed therefore represents a thrombolitic texture but not a true thrombolite. Thrombolites *sensu stricto* become more abundant in the Sailmhor, Sangomore and Balnakeil formations, but have not recorded from the Croisaphuill and Durine formations. The morphologies vary (Chapter 3) and they range in height from 30 cm to as much as 4 m (the majority are 1–2 m thick). Thrombolite boundstone commonly overlies intraclast rudstone facies, and is closely associated with peloidal grainstone and bioclastic wackestone, which often forms the inter-reef facies.

Based upon the common association with open marine fossils (trilobites and cephalopods), and the common occurrence of peloidal grainstones and intraclast rudstones, the thrombolites are interpreted to have formed in agitated subtidal waters, forming patch reefs. The intraclast rudstones may have provided a firm substrate on which the microbialites could grow.

Feldmann & Mckenzie (1997), Pratt & James (1982), and Aitken (1967, 1978) interpret thrombolites to have formed in a subtidal environment under more or less normal marine conditions. This is supported by the diverse fauna often associated with them, the burrowing that the bioherms/biostromes are commonly associated with and the flanking beds not exhibiting desiccation cracks. Modern thrombolites in Lake Clifton, Western Australia grow in waters which are below seawater salinity (15–35‰) for most of the year, but may be up to 40‰ (Moore & Burne 1994). In view of the grazing habits of much of the associated fauna it is reasonable to assume that thrombolites provide both a source of food as well as a refuge. The thrombolites are not attached to hard substrates but lie partly buried in the unconsolidated sediments.

Text-figure 2.10 Examples of stromatolite and thrombolite boundstones. **(A)** stromatolite biostrome comprising linked hemispheroidal mounds, which are overlain by lower relief stromatolites. Eilean Dubh Formation 27 m above the base of the formation. Hammer is 33 cm long. **(B)** hemispheroidal stromatolite bioherms from the upper Sangomore Formation (45 m). Hammer for scale. **(C)** bioherm comprising columnar branching stromatolites. The stromatolites are more lime rich and the dolomitic limestone inter-reef facies weathers proud. Hammer for scale. **(D)** plan view of a 3 m wide domed biostrome comprising columnar stromatolites. The bed lies 79 m above the base of the Eilean Dubh Formation. Hammer for scale. **(E)** thrombolite boundstone facies within the upper Sangomore Formation (35 m).



2.2.9 Columnar stromatolite boundstone

The facies is characterised by laminated, non-linked, vertically stacked columns of cylindrical or branching stromatolites. They vary in diameter from 1 cm to 10 cm as both biostromes and bioherms (see Chapter 3). Bioherms occur as complex structures up to 1.2 m high, but most are simple un-branching forms around 30 cm high. Biostromes are most common within the middle Eilean Dubh Formation (Text-fig. 2.10D) form continuous beds 30 cm thick, which follow the topography of underlying domes of vuggy dolostone 1–3 m wide and are also observed within karstic hollows. Within the Sailmhor Formation, the columnar stromatolites are commonly 25 cm high and 10–15 cm wide, they persistently occur at the bases of parasequences and overly flooding surfaces. The largest columnar stromatolite bioherms are present within the upper Sangomore Formation, where they attain a height of 1.2 m and are overlain by a rippled bed of oolitic grainstone 70 cm thick (Text-fig. 2.10C).

The size and shape of the stromatolites may reflect particular conditions at the time of formation. However columnar stromatolites all represent deposition in an agitated- to protected, lower intertidal to shallow subtidal environment. This interpretation is based upon similar morphological forms presently forming around exposed headlands at Shark Bay, Western Australia (Logan 1961), where they form in turbulent environments. The turbulence causes scour of originally planar microbial mats, and the disrupted mats acts as new loci for further microbial colonisation (Aitken 1967, Logan 1961).

2.2.10 Hemispheroidal stromatolite boundstone

A range of microbial bioherms are seen within the Durness Group (Chapter 3) (Text-fig. 2.10). Within the succession, hemispheroidal stromatolites are particularly abundant in the Eilean Dubh and Sailmhor formations, but become less frequent up section. No hemispheroidal stromatolites have been recorded from the Croisaphuill Formation and they are uncommon within the Durine Formation. The Eilean Dubh Formation at Assynt preserves some stromatolites but they are rare in comparison to the section at Balnakeil Bay.

The stromatolites form isolated domes or tabular beds with a domed upper surface (Text-fig. 2.10A, B). Stromatolite beds may be as much as 70 cm thick but the stromatolites show domes with an amplitude of around 10 cm, and a wavelength of 40 cm. Associated lithofacies include intraclast rudstones which often infill hollows between the stromatolites. An upward or lateral gradation is often seen into parallel or ripple laminated carbonate and

into planar stromatolites. The hemispheroids are composed of crinkly, sub mm-scale laminated micrite, displaying small desiccation cracks and fenestrae.

The interpreted environment of deposition is in agitated to protected intertidal mudflats, where microbial mats flourished. In Shark Bay, the microbial mats and stromatolites are limited in distribution to the intertidal zone where conditions are hypersaline with salinities 56–65‰ (Logan 1961).

Conditions needed for the development of microbial mats in the present day are a low to moderately smooth gradient $0.8\text{--}0.1\text{ m km}^{-1}$, and restricted tidal influx with well defined tidal zonation (Logan *et al.* 1974). Mats at Hamelin Pool, Western Australia form from the supratidal (2 m above prevailing low water level) to lower intertidal zone (c. 4 m depth). In areas of less than 53‰ salinity (metahaline) they are browsed and reduced to thin films and are therefore less likely to be preserved in normal marine settings. The hypersaline concentration is also important in penecontemporaneous lithification which acts to lower the aragonite precipitation threshold (Logan *et al.* 1974).

2.2.11 Intraclast rudstone

This lithofacies has been identified within the Eilean Dubh, Sangomore, Sailmhor and Balnakeil formations. Intraclast breccias can be divided into two categories; those that comprise chert clasts and those that comprise carbonate intraclasts. Most beds are tabular or show scoured bases and are commonly continuous over the observed outcrop. The lithofacies is also seen to infill channels 20 cm deep and around 1 m wide. It also infills surface palaeokarstic hollows, and fills hollows between thrombolite and stromatolite bioherms.

Carbonate flake breccias are best displayed within the middle and upper part of the Eilean Dubh Formation, exposed along Balnakeil Bay, and they are also present within the Balnakeil Formation at some horizons. Other than these occurrences they are locally preserved at the base of parasequences within all of the other formations. The beds of carbonate flake breccia are mostly within the range of 5 to 40 cm thick and are mostly tabular (with planar to irregular bases), to lens shaped and locally the facies forms discrete isolated channel fills (Text-fig. 2.11C). The channel may be a result of the genesis of the clasts or the fill may have superseded the formation of the scour. The carbonate intraclast rudstones commonly form one of two end members, clast supported breccias and matrix supported breccias.

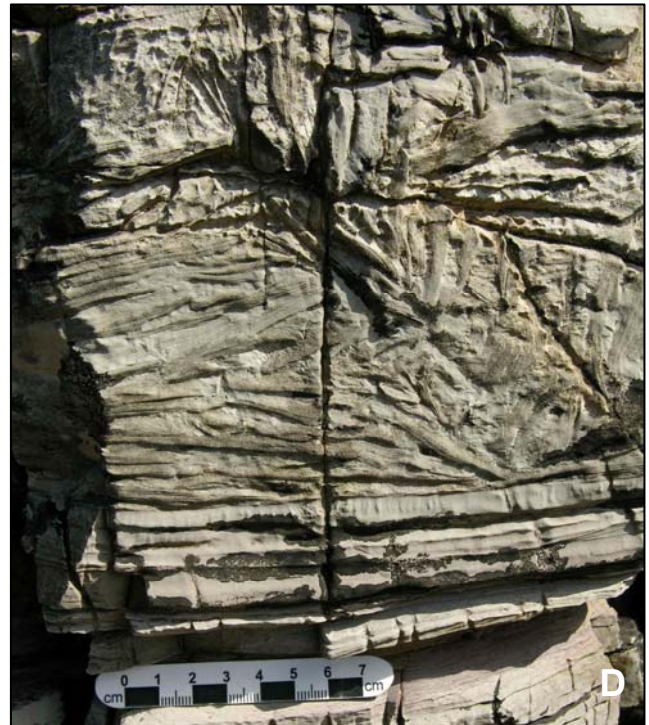
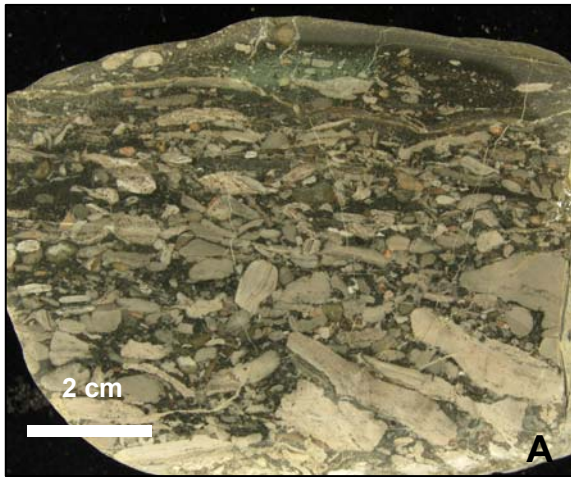
The clast supported breccias commonly occur within the upper part of parasequences. The clasts are thin (less than 5 mm thick) with diameters commonly in the range of 0.5 to 5 cm (although locally reaching 10 cm). Shapes vary from elliptical (most common) to polygonal or irregular, most with rounded edges but some being angular. Nearly all intraclasts are composed of parallel-laminated or structureless, micritic dolostone, identical in composition and fabric to the associated facies. There is no evidence of soft sediment deformation within the clasts, suggesting they were completely lithified before erosion. The clasts are mostly flat lying but sometimes are arranged in rosette (fan shaped) structures comprising clasts in a variety of angles and stacked together (Text-fig. 2.11D, E). This facies is locally intermixed with quartz sand rich- and ripple laminated carbonates and is associated with thrombolites, which commonly colonise the upper surfaces.

Beds of matrix rich conglomerates (5–20 cm thick) are commonly found at the base of parasequences and contain smaller, dominantly pebble grade clasts (2–20 mm long), which are subrounded. The matrix is composed, primarily of peloidal grainstone and small intraclasts (Text-fig. 2.9C; 2.11B). Imbrication is seen in one conglomerate in the upper Ghrudaidh Formation (Text-fig. 2.11A), where pale grey clasts of fine grained dolostone rest within a dark grey matrix of peloidal grainstone.

The carbonate mud flakes probably derive from the supratidal zone, where the hardening and cementation of muds is common and sedimentation occurs above the influence of most tides. The supratidal laminites then become eroded and redeposited during storm events. Mud polygons are highly susceptible to erosion, and brecciation of these cemented crusts is a common feature of the supratidal zone (Assereto & Kendall 1977). During storms or cyclones, widespread flooding of the inner part of the tidal flats and subsequent transport of indurated crust debris into channels and other localised depressions occurs (Davies 1970). Shinn (1983) noted that a flat pebble conglomerate was deposited almost instantaneously on supratidal flats after a hurricane. The presence of steeply inclined intraclasts within the Durness Group conglomerates indicates that pivoting must have occurred during transport (Mount & Kidder 1993).

The matrix (peloidal grainstone) supported conglomerates are interpreted to have been deposited during subtidal storm events or the result of increased energy, following base-level rise over an exposed carbonate platform. Clasts are disc shape but have rounded margins and are smaller than clasts occurring within breccias at the top of parasequences.

Text-figure 2.11 Intraclastic rudstones comprising both carbonate and chert varieties. **(A)** flat pebble conglomerate displaying clasts of fine grained dolomicrite within a dark grey matrix. The clasts show imbrication towards the base of the bed. Ghrudaigh Formation 34 m above the base. **(B)** matrix supported conglomerate comprising dark grey subrounded clasts within a mid to dark grey peloidal grainstone matrix. Balnakeil Formation (41 m). Tape measure for scale **(C)** mud flake conglomerate within a channel feature, middle Eilean Dubh Formation. Hammer is 33 cm long. **(D)** clast supported edgewise orientation of carbonate clasts in a mud flake conglomerate, Eilean Dubh Formation, Balnakeil Bay. **(E)** radiating clasts seen in plan view within a flake conglomerate, Balnakeil Formation. **(F)** chert breccia from the lower Sangomore Formation, Kyle of Durness. **(G)** polished slab of the bed shown in (F), showing irregular and angular chert clasts within a matrix comprising sand and granule grade chert material.



Chert breccias are most common at the Sailmhor–Sangomore formation boundary and persist up into the Sangomore Formation for a few metres. They are observed along the Kyle of Durness [NC 3733 6664] and occur at the formation boundary at Balnakeil Bay [NC 3835 6886] and at Smoo, Leirinmore [NC 4248 6730]. The bed of chert breccia at the Kyle of Durness (lower Sangomore Formation) is 30 cm thick (Text-Fig. 2.11F, G). It is tabular with sharp upper and lower boundaries. Clasts are irregular, angular and range in diameter from 2 cm to 6 cm. Locally, clasts show a relict peloidal grainstone texture but most are structureless. The breccia is matrix supported with a matrix consisting of coarse sand to granule grade, angular chert fragments (Text-Fig. 2.11G). The chert breccias at the Sailmhor-Sangomore formation boundary are similar in their clast and matrix composition, but are thicker bedded (up to 2 m).

The chert breccias are interpreted to represent extensive periods of sediment removal associated with the erosion and fracturing of what must have been syngenetically-formed, brittle chert (Carozzi & Gerber 1978). At the top of the Sailmhor Formation a bed of silicified columnar stromatolites has been eroded into a series of pinnacles. Within the hollows, chert clasts rest in a matrix of coarse dolomite sand with small angular chert granules. Clasts sizes range up to 3 cm diameter and are commonly angular, showing no preferred orientation.

2.2.12 Parallel laminated carbonate

Parallel laminated carbonate can be easily mistaken for planar stromatolites. Beds of parallel laminated carbonate may be up to 1 m thick and are commonly associated with ripple lamination, crinkly lamination and intraclast rudstones. Laminations occur on a sub mm to mm-scale (Text-fig. 2.12A) and are often disrupted by desiccation features. The environmental interpretation of much of the parallel laminated carbonate relies upon associated sedimentary structures, as parallel lamination can form in a variety of different environments and by a variety of different means. Parallel laminated carbonate locally shows tepee structures and desiccation cracks. Associated facies include hemispheroidal stromatolite bioherms, which it commonly overlies. Crinkly laminated microbial mats and fenestral carbonate which it is inter-bedded. Parallel laminated carbonate sometimes contains pseudomorphed evaporites of gypsum/anhydrite. As these are interpreted to be largely the replacement of secondary evaporates (early diagenetic) they will be discussed separately in section 3.

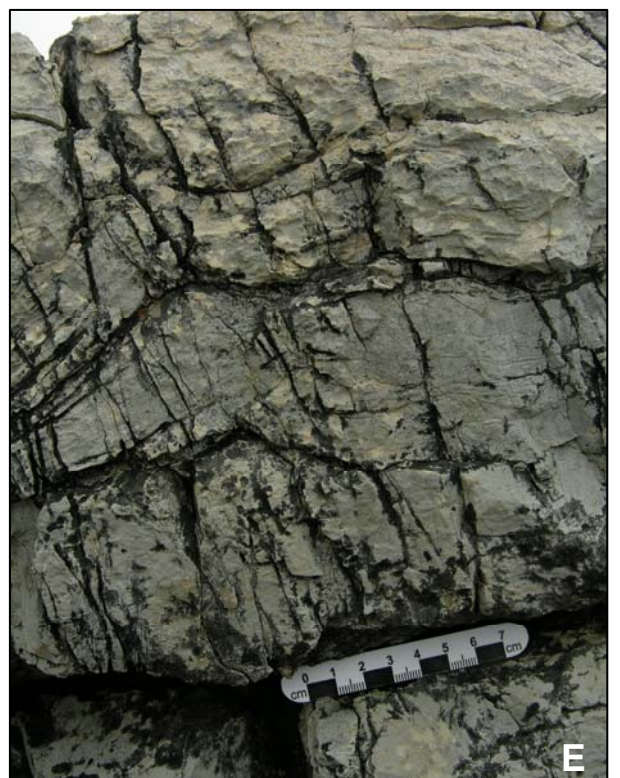
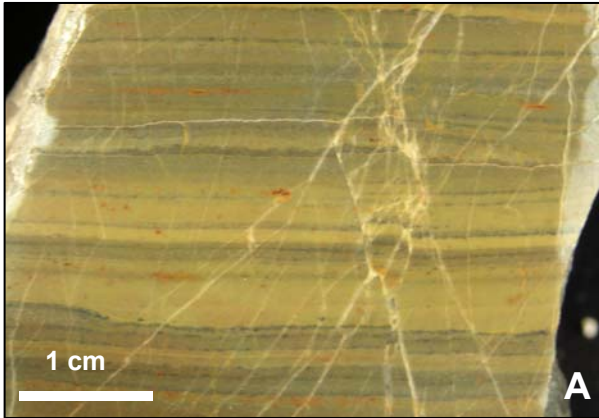
In the lower Eilean Dubh Formation, sub-hexagonal polygons, formed by desiccation cracks are seen on bedding planes in parallel laminated light grey dolostone (Text-fig. 2.12B), they are localised to an area 30 cm wide. The crack infill comprises terrigenous quartz sand and polygons are up to 5 cm in diameter. Within the Sangomore Formation mud crack polygons are more common and range from 7 cm to 60 cm in diameter. They locally show multiple stages of sediment infilling (healed desiccation cracks).

Tepees within the Durness Group are only present within the Eilean Dubh and Sangomore (Text-fig. 2.12C–E) formations. They sometimes deform up to 30 cm thickness of sediment and sheet cracks (parallel to laminae) are sometimes associated with particularly well developed tepees in the Eilean Dubh Formation (Text-fig. 2.12D).

Most of the laminated sediments forming on modern tidal flats occur in the supratidal zone. Windblown dust collected in the tidal flats of the Arabian Gulf (Shinn 1968) is typically 60% detrital dolomite c. 30 μm across and clay minerals, however, sediment is also deposited by storms and the highest spring tides. Studies of modern environments by Hardie (1986) showed that small mud-cracks (1–5 cm polygons) represent an exposure index greater than 90 and a height of 20–25 cm above mean tide level (upper intertidal) (Text-fig. 2.3). Wide, shallow mud-cracks (5–15 cm diameter) indicate heights of 5–50 cm above mean tide and an exposure index of 60–100. Deep prism cracks (20–30 cm in diameter) suggest an exposure index of 10–60 and a height of 5 cm above to 20 cm below mean tide level (Text-fig. 2.3).

Tepees form on indurated supratidal crusts and formation is thought to involve either of the following; salt hydration, slow dehydration then wetting during spring tides or storms or thermal expansion or moisture swelling within desiccation cracks. Tepees have been studied and described by Assereto & Kendall (1977), Burri *et al.* (1973) and Kendall & Warren (1987). Two types occur within the Durness Group. In the present day tepees are forming in Shark Bay (Davies 1970) and the Persian Gulf (Kendall & Skipwith 1968, Assereto & Kendall 1971, Evamy 1973).

Text-figure 2.12 Sedimentary features observed within parallel laminated carbonate facies. **(A)** mm- and sub mm-scale lamination within a fine grained dolostone, upper Sangomore Formation, Balnakeil Bay. **(B)** loose block of parallel laminated, light grey dolostone with desiccation cracks forming polygons and extending over an area 30 cm in diameter. Lower Eilean Dubh Formation. Lens cap for scale. **(C)** larger, well developed desiccation cracks within the upper Sangomore Formation. **(D)** tepee structure from 79 m above the base of the Eilean Dubh Formation, Balnakeil Bay. Scale is 7 cm in length. **(E)** tepee structure from the upper Sangomore Formation.



The depositional environment of this facies is interpreted to be upper intertidal to supratidal based upon the fine grained pale dolomite, mm to sub-mm scale lamination, the associated underlying intertidal lithofacies, the close association with evaporite pseudomorphs and the sedimentary structures present, and their known exposure indices.

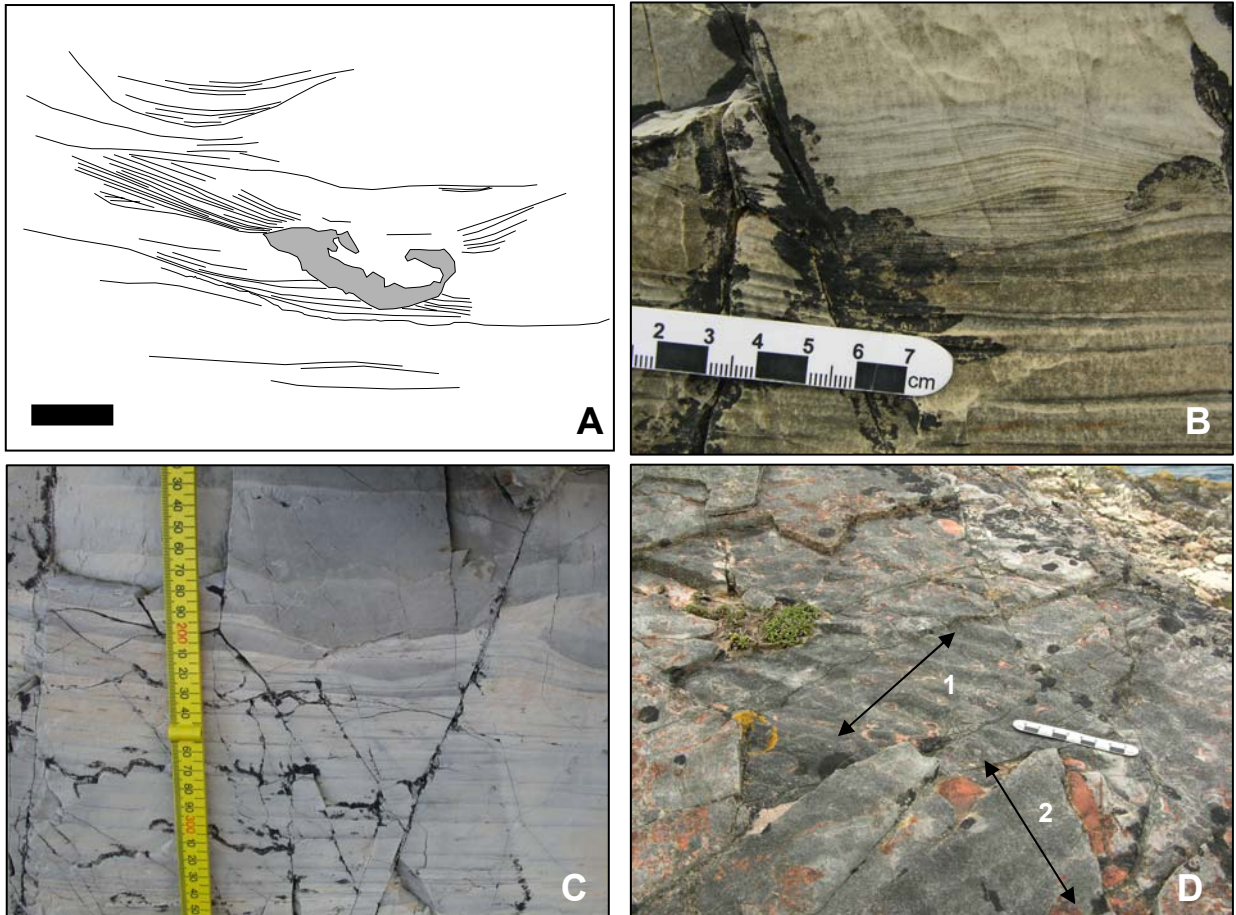
2.2.13 Ripple laminated carbonate

Ripple laminated carbonate is often difficult to distinguish within the Durness Group. Dolomitisation has commonly destroyed evidence of lamination. Ripple lamination occurs in many of the shallowing upward parasequences within the Sailmhor and upper Croisaphuill Formation. Thick successions of ripple laminated carbonate are present within the upper Eilean Dubh Formation, where they form the dominant lithofacies between 78–109 m above the formation base. Bedsets may be up to 9.4 m in thickness. Beds are tabular and have gradational upper and lower boundaries, commonly overly burrow mottled carbonate and are in turn overlain by stromatolites.

The ripple lamination comprises a mixture of low-amplitude, wavy, lenticular and flaser lamination. The ripples are dominantly wave generated, but some subordinate current ripples are noted. Some of the rippled beds contain a high proportion of terrigenous quartz silt especially in the middle part of the Eilean Dubh Formation. Ripple amplitude is rarely more than 5 cm, with a wavelength of less than 10 cm. In plan view, ripple crests are rounded and usually straight, sinuous (Text-fig. 2.13D) or out of phase. There is commonly an irregular erosive and undulating lower boundary of sets (Text-fig. 2.13A, B). The ripple forms are associated with flat lamination and low and high angle cross lamination. Sets are often seen to be swollen and lens like, with offshooting and draping foresets (Text-fig. 2.13B).

Tidal flat sediment of both modern and ancient sediments is deposited as layers of sand size mud pellets, and although they may be destroyed by dolomitisation or compaction, the ripple lamination is often still visible. Ripples may form in the supratidal zone (Shinn 1983). Horizontal laminations, with or without cross bedding are mostly restricted to supratidal and upper intertidal settings (Shinn 1983). Couplets of mechanical laminites form on storm, wave and tide dominated intertidal flats. Within the Durness Group, ripple laminated carbonate is often associated with quartz sand and silt, intraclast rudstones and hemispheroidal stromatolites. The small size of the ripples and the lack of subtidal features suggest an intertidal setting on muddy tidal flats. The ripple lamination represents deposition

of carbonate silt, with the mud deposited in the slack water of receding tides. The mixture of wavy, flaser and lenticular bedding, with muddy drapes suggests intertidal flat deposition. Palaeocurrent directions from limited ripple crust orientation indicate both northwest–southeast and east–west directions.



Text-figure 2.13 (A) tracing of laminae within a rippled bed, Eilean Dubh Formation. 85 m above the formation base. Balnakeil Bay. The grey shaded area represents quartz silt and sand, which rests in a scour. Scale bar is 1 cm. **(B)** phtography from the same horizon. Ripples display asymmetrical crests and have erosive bases. **(C)** lenticular bedding, passing upwards into flaser bedding. 95 m above the base of the Croisaphuill Formation. **(D)** plan view of bed at 79.5 m, which displays symmetrical wave ripples (arrowed 1), which are immediately overlain by the successive bed containing ripples of a different palaeocurrent (arrowed 2). Scale is 7 cm long.

2.2.14 Quartz arenaceous carbonate

Quartz sand is most common between 55 m and 80 m height within the Eilean Dubh Formation, it also occurs at the boundary between the Sangomore and Balnakeil formations, and within the basal 5 m of the Ghrudaidh Formation. It commonly occurs at the top of parasequences. This lithofacies forms/fills channels and small scours (Text-fig. 2.14F), occurs as discontinuous beds a few millimetres thick and infills surface microkarst in the middle Eilean Dubh Formation. It also occurs as a matrix for intraclast rudstones (Text-fig. 2.14E).

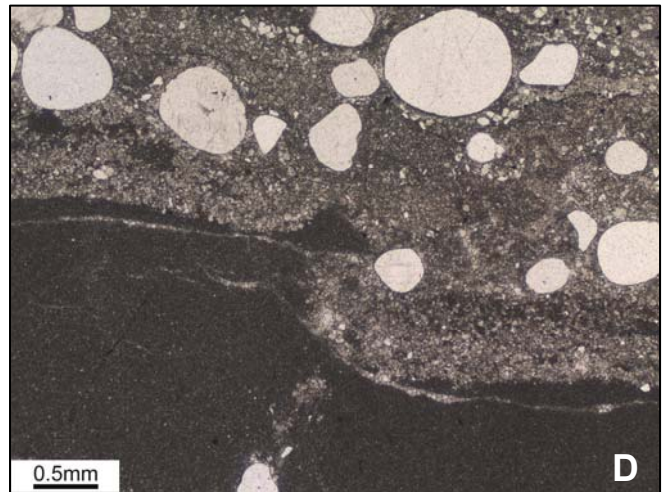
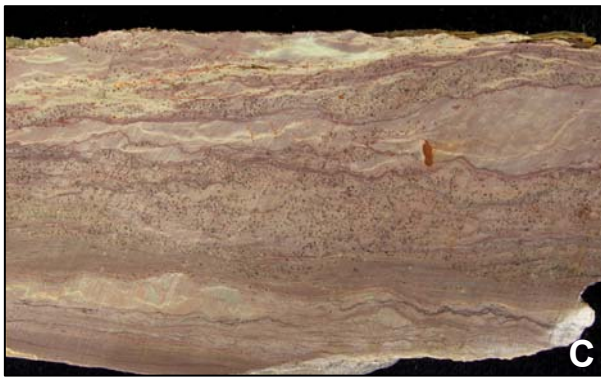
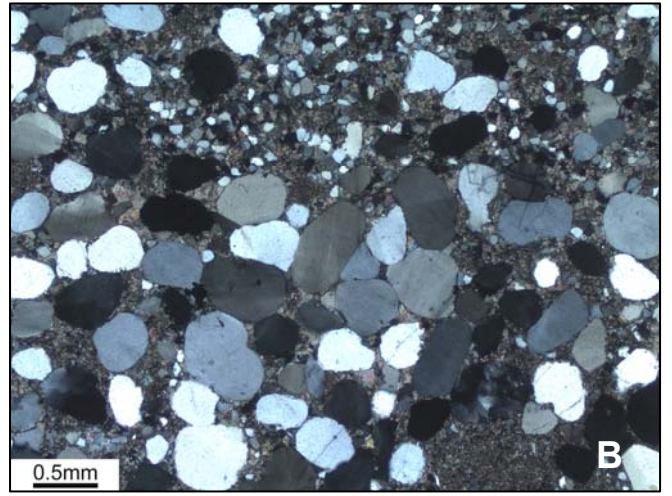
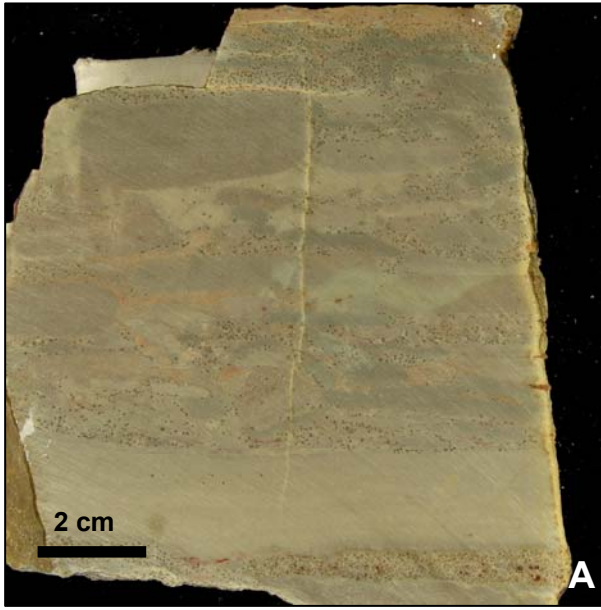
The grains comprise largely unstrained, monocrystalline quartz and are well rounded to rounded and range in size from 0.4 mm to 1.3 mm (medium to very coarse sand). Commonly associated lithofacies include intraclast carbonate breccias, ripple laminated carbonate, parallel laminated carbonate, hemispheroidal stromatolite boundstone (which it caps) and crinkly laminated microbialites with which it is sometimes admixed (Text-fig. 2.14).

The quartz silt and sand is interpreted to be aeolian in origin (due to the smooth and well rounded shape and well sorted nature), blown or migrated onto the carbonate flats as they are today in the sabkhas of the Persian Gulf (Shinn 1986). Larger grains may have migrated onto the shelf by the progradation of dunes (ergs). They were then reworked by tidal action ('eolo-marine' deposition *sensu* Fischer & Sarnthein 1988). A lack of rooted vascular plants on the near-by Cambrian craton probably contributed to the generation of large volumes of material (Dalrymple *et al.* 1985). Because the quartz sand is found in thinly bedded horizontal and cross laminated lenses, infilling channels, karst and associated with desiccation cracks, stromatolites, intraclasts and evaporite pseudomorphs, this suggests deposition by supratidal to upper intertidal storm deposits.

This facies has been recorded along the entire shelf in the upper Cambrian (Saltzman *et al.* 2004). The presence of the quartz sand suggests that extensive dunes were present on the craton, which migrated basinward when sea-level fell.

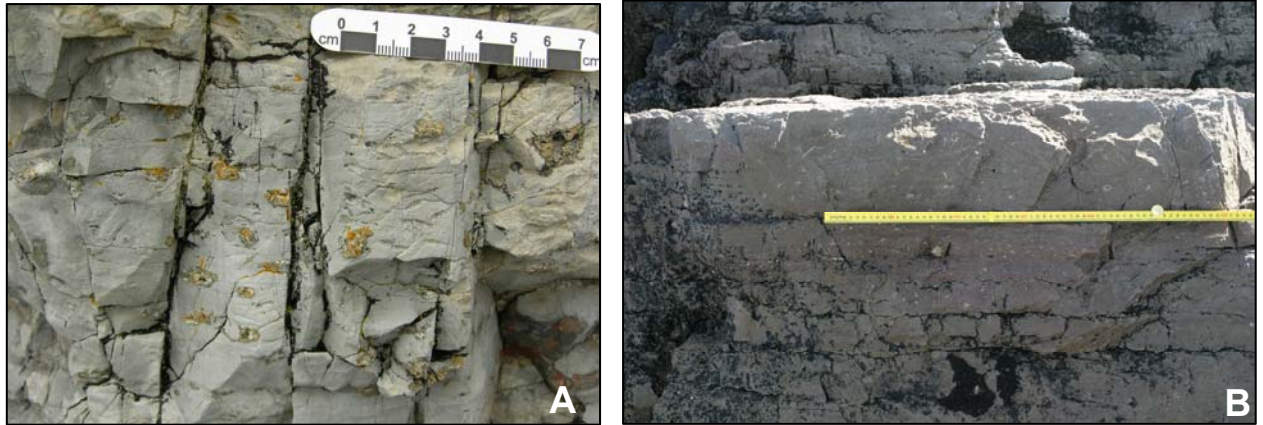
In modern environments ergs migrate into the ocean bordering the Saharan Desert. Ergs are concentrated in two broad belts between 20° N to 40° N and 20° S to 40° S. Active ergs are restricted to regions that receive no more than 150 mm annual precipitation (Wilson 1971). Some of the quartz grains show strain, indicating a erosion from a metamorphic source rock, although secondary reworking is possible.

Text-figure 2.14 Quartz arenaceous carbonate from the Eilean Dubh Formation. **(A)** intraclast rudstone with a matrix rich in millet seed quartz sand. **(B)** thin section photomicrograph showing well rounded quartz grains, with point and long grain contacts, overlain by more angular silt grains. **(C)** microbial crinkly laminae interspersed with millet seed quartz. **(D)** floating quartz grains within a matrix of dolomite microspar (possibly representing a dolomite grainstone) overlying dolomicrite. A desiccation crack extends down from the quartz rich facies and is filled by microspar. **(E)** abundant millet seed quartz occurring between light grey dolostone clasts within a matrix supported conglomerate. **(F)** fine sand displaying a distinctive brown weathering colour and lying within a channel feature. Other thin quartz rich laminae and stringers are observed above this.



2.2.15 Fenestral carbonate

Fenestral facies are most common within the Eilean Dubh Formation and the Sangomore Formation. Beds of fenestral carbonate are predominantly formed of fine-grained, light grey dolomite. Beds are tabular and range in thickness from 10 to 50 cm (Text-fig. 2.15).



Text-figure 2.15 Fenestral carbonates from the Durness Group. **(A)** sub cm-scale, irregular vugs with a lining of quartz. The surrounding rock is a finely crystalline dolomite which is dominantly structureless but shows local, weak contorted laminae. (possibly indicating evaporite growth). Upper Sangomore Formation (41 m up). Scale bar is 7 cm long. **(B)** smaller-scale vugs, filled with white quartz, which are stratified, but lie within a structureless dolomite. Eilean Dubh Formation 15 m above the formation base.

The fenestrae range in size from 1 mm to 1 cm (too large to be classed as birdseye fenestrae *sensu stricto*) and are usually filled with calcite or with chert (Text-fig. 2.15). It is interpreted here that they have a similar origin to birdseyes, they are circular, oval or slightly irregular, to laminar and are filled with calcite or white chert and quartz crystals, presumably after evaporites. They are isolated and occur in groups roughly parallel to bedding.

Associated lithofacies include parallel laminated carbonate, ripple laminated carbonate, stromatolites, microkarst and teepees and occur within fine grained pale grey dolostones, suggesting an intertidal to supratidal setting. Hardie (1986) showed fenestral fabrics were forming +40 to +5 cm above mean tide level with an exposure index of 60–100.

Fenestrae (Tebbutt *et al.* 1965) are a diagnostic feature of supratidal sediments, but only when occurring with mud cracks and stromatolites. They are often filled with calcite, forming ‘bird’s eyes’, but fenestral fabric is a more appropriate term. Fenestrae have been formed experimentally by Shinn (1968, 1983) and numerous modern examples from supratidal environments have been described (Ginsburg & Hardie 1975, Hardie 1977, Shinn 1983). Fenestrae can be subdivided into three types; spherical or bubble-like, planar, and

irregular. Gas bubbles trapped in sediment/microbial slime or by air coalescing as the tide rises causes voids, which are preserved by the rapid cementation in such environments may preserve the voids. Planar voids probably result from shrinkage and swelling, some may represent the flattened blisters, which occur in microbial mats (Shinn 1983).

2.2.16 Crinkly laminated and planar stromatolite boundstone

This facies is common in the Sailmhor, Sangomore, Balnakeil and locally the upper Durine Formation. Desiccation cracks are common within this facies, lenses with peloids, ooids and quartz silt grains are noted and fenestrae are common, along with evaporite pseudomorphs. Beds have a thickness of less than 80 cm (Text-fig. 2.16). This facies is described in more detail in Chapter 3.



Text-figure 2.16 Crinkly laminated and planar stromatolites. **(A)** crinkly laminated stromatolites from the lowest Sangomore Formation, Balnakeil Bay. Pencil for scale. **(B)** crinkly planar stromatolites from a limestone bed within the upper Durine Formation, Loch Caladail. **(C)** planar stromatolites displaying crinkly laminae, middle Balnakeil Formation, Balnakeil Bay. Pen for scale. **(D)** planar stromatolites from the upper Sangomore Formation, displaying a pseudocolumnar pattern.

Measurements of sediment movement by Gebelein (1969) demonstrate that microbial mats can form only in areas of less than $1.97\text{-}2.62\text{ g hr}^{-1}\text{ m}^{-1}$ bottom sediment movement. The thickness of the algal mat increases as the rate of sediment movement decreases. Microbial domes can form only between 0.26 and $1.97\text{ g hr}^{-1}\text{ m}^{-1}$ bottom sediment movement (Gebelein 1969). In very clear waters around Bermuda, microbial mats have been observed to depths of 50 m . In general however, growth is most rapid in depths of less than 10 m (Gebelein 1976). These superficial mats represent a dynamic interface at which sediments shoreward and offshore of the mat are continuously reworked (i.e. laminations are not produced). The boundary between laminated sediment and un-laminated varies from place to place depending upon the presence of microbes and invertebrates. At Andros Island in the Bahamas it is represented by the 50% flooding isograd and in Florida by the 25 % flooding isograd (Gebelein 1976).

2.3 FACIES ASSOCIATIONS

Diagenesis and tectonism have severely altered original fabric in many of the beds. In spite of this, a range of depositional features are preserved. The sixteen lithofacies have been grouped into three lithofacies associations; shallow subtidal, intertidal flat and sabkha/supratidal. However, due to the limited outcrop it has not been possible to subdivide these associations into depositional environments, such as lagoon, tidal channel etc. Exposure is the factor defining the supratidal zone. Because this exposure is so important, Ginsburg *et al.* (1977) made careful measurements of exposure duration in different zones to establish the exposure index. This is essentially the percent of time during which any particular environment is exposed above tide level (Text-fig. 2.3).

2.3.1 Shallow subtidal facies association

Lithofacies interpreted to form in subtidal environments include: 1) intraclast rudstones, 2) ribbon carbonate, 3) burrow mottled carbonate, 4) columnar stromatolite boundstone, 5) bioclastic wackestone/packstone, 6) ooidal grainstone, 7) oncoidal wackestone, 8) stromatolite carbonate, 9) peloidal grainstone, 10) thrombolite boundstone.

The subtidal zone represents the environment below mean low tide and is rarely, if ever exposed to the air. Subtidal environments occur in ponds, channels and offshore. The sediments are dark grey in colour (reflecting organic content) and commonly lack

sedimentary structures. In modern environments, pond sediments are bioturbated by mangrove roots, are fine grained, and contain gastropods, they are commonly less than one metre thick (Shinn 1986). Within Ordovician sediments it is difficult to recognise this sub-environment without these key characteristics.

Tidal channels are an important part of modern tidal flats. The migration of tidal channels results in a point-bar sequence that is cross bedded and the tidal flats become reworked during the lateral migration of the channels. Tidal channels are recorded on the tidal flats of the Persian Gulf (0–15 m deep), but they are comparatively more common on Andros Island flats, where they are 0–3 m deep. There is no evidence for channels within the Durness Group, and they have been rarely described from tidal flat carbonates of this nature (Cloyd *et al.* 1990).

The subtidal zone acts as an important source of the sediment needed for accretion of the flats, including; ooid bars, reefs, dominantly pelletal muds and the resulting sediment is almost always homogenised by burrowing and a lack of sedimentary structures (Shinn 1983).

2.3.2 Intertidal flat facies association

The intertidal region is sometimes referred to as the foreshore or littoral zone. It is exposed to the air at low tide and is commonly submerged at high tide. This lithofacies association is recognised from its occurrence above subtidal facies within metre-scale shallowing upward parasequences. It underlies sabkha/supratidal facies association sediments where they are present. It includes the following facies: 1) ripple laminated carbonate, 2) parallel laminated carbonate, 3) hemispheroidal stromatolites, 4) crinkly and planar stromatolites, 5) intraclast rudstone and 6) peloidal grainstone.

2.3.3. Sabkha/supratidal facies association

The supratidal environment experiences fluctuations in salinity, and therefore bioturbation is limited but microbial mats thrive. These mats may extend down into the upper intertidal zone in arid environments (Shinn 1986). Mud cracks are also diagnostic of the supratidal zone (Shinn 1983, 1986, Hardie 1977). The third diagnostic feature of supratidally deposited rocks is the presence of fenestrae. Lithofacies representing deposition within the supratidal zone include: 1) intraclast rudstone, 2) quartz arenaceous carbonate, 3) parallel laminated carbonate

and 4) fenestral carbonate. They are also characterised by the presence of desiccation cracks, teepees, evaporate pseudomorphs and evaporate dissolution breccias.

The vertical succession of peritidal facies is complex but a few patterns emerge. The observation that different successions of facies are preserved in the shallowing upward sequences suggests lateral discontinuity and not a straightforward linear facies belt.

Landward of the intertidal flats, deposits representing supratidal conditions occur. In humid climates such as the Bahamas, a supratidal marsh develops. However in more arid settings such as the Arabian Gulf, a coastal sabkha commonly develops. Sulphates such as gypsum and anhydrite form on humid tidal flats during the dry season, but disappear during the wet season and therefore are rarely preserved. In the Arabian Gulf, where the annual rainfall is less than 2 cm, evaporates are much more common and include sulphates and minor halite (Alsharhan & Kendall 2003).

Previously there has only been one record of evaporites from the Durness Group, but new discoveries in this present study indicate that at several points in the stratigraphical succession, a coastal sabkha has been preserved. This provides evidence to suggest that throughout much of the deposition of the Durness Group a coastal sabkha may have been present in more inboard depositional settings.

Lath shaped vugs – a preserved gypsum mush?

Beds and lenses are observed in which there are concentrations of largely euhedral crystal vugs (Text-fig. 2.19). They range in length from 1 to 8 mm, and commonly show no particular orientation. They may comprise up to c. 50% of the total rock volume and are locally associated with pseudomorphed nodules, interpreted to be after anhydrite. The shape of the crystals varies from barrel/keg shaped to acicular twinned in some cases (Text-figure 2.17H). They bear a close resemblance to gypsum crystals grown experimentally in bentonite muds (Cody 1976). Within the middle Eilean Dubh Formation at Balnakeil Bay the pseudomorphs are closely associated with teepee structures.

The crystals bear close similarity to those described by Kennard (1981) from the Upper Cambrian of the Georgina Basin, Central Australia, where single crystals of calcite represent pseudomorphed gypsum. In thin section the crystals are seen to be ferroan sparry calcite very similar in size and habit to those recorded by Lucia (1961) from the Permian Tansill Formation, Texas.

In Recent microbial mat facies, gypsum crystals are observed to precipitate (up to 2 mm long) (Handford *et al.* 1982). This is replaced landward by gypsum mush facies, representing lower supratidal deposition. This facies belt extends inland for some 2.5 km and is up to 30 cm thick in the coastal sabkha at Abu Dhabi (Handford *et al.* 1982). In the mid-supratidal zone, anhydrite replaces subsurface gypsum mush and forms nodules and beds, where there is extensive dolomitisation

The crystal shaped vugs from the Durness Group interpreted to originally have been sulphate crystals, which grew within the sediment and they bear close similarity with the gypsum mush (recorded from recent coastal sabkhas). It is not certain whether the growth of the evaporites led to the formation of the teepee but it is more likely that the teepee existed prior to the growth of the crystals but that it allowed brine into the sediment, which then became concentrated.

Pseudomorphs of anhydrite

Young (1979) recorded anhydrite nodule pseudomorphs from the Sangomore Formation. During this study, further examples have been found throughout the Durness Group and are described. The size, shape and modes of preservation vary from those mentioned by Young (1979). Anhydrite nodules and beds are commonplace in the middle and upper sabkha of the Arabian Gulf. In this study the classification of nodular and bedded anhydrite of Maiklem *et al.* (1969) is followed.

Pseudomorphs of anhydrite are locally present at certain horizons and examples show that replacement is usually by white silica but also by calcite, dolomite and a mixture of both quartz and calcite. Replacement of anhydrite nodules by silica is a relatively common phenomenon in the rock record, and many cases have been recorded (e.g. West 1964, Milliken 1979, Siedlecka 1972, 1976, Tucker 1976a, b, Folk & Pittman 1971, Radke & Mathis 1980, Arbey 1980, Friedman & Shukla 1980 and Chowns & Elkins 1974).

Text-figure 2.17 Occurrences of crystalline evaporate pseudomorphs within the Durness Group. **(A)** bed at Ardvreck, within the lowest Eilean Dubh Formation containing abundant crystal-shaped vugs. **(B)** bed from the same interval as (A) displaying larger vugs. Pencil for scale. **(C)** brecciated and deformed, laminated dolostone clasts within a matrix of crystal-vug rich dolostone. The growth of crystals within the sediment may be responsible for the observed deformation. Middle Eilean Dubh Formation, Balnakeil Bay. **(D)** crystal shaped vugs and larger spar filled nodules within a very fine-grained dolostone. The laminae are deflected around the nodules suggesting either displacive growth or differential compaction. Lowerst Eilean Dubh Formation, An t-Sròn. **(E)** crystal shaped vugs within a columnar stromatolite biostrome, middle Eilean Dubh Formation, Balnakeil Bay. **(F)** lens shaped bed comprising crystallotopic vugs, which is overlain by contorted laminae and tepee structures; middle Eilean Dubh Formation, Balnakeil Bay. **(G)** thin section photomicrograph of the crystal vugs and their infilling mineral. The vugs are observed to be filled with non-ferroan calcite, but are interpreted to have originally been gypsum. **(H)** acicular and lath shaped vugs, middle Eilean Dubh Formation, Balnakeil Bay.



Silicified evaporate nodules have also been recorded from the Durness Group (Young 1979). The quartz nodules were recorded from two separate horizons, 3 metres apart, 46 and 49 metres height above the base of the Sangomore Formation at Balnakeil Bay. Recent logging of the formation has proved a minimum thickness of 55 m, but the succession is crossed by three faults. The faults are not seen to repeat strata, indicating an unknown thickness is missing. Based upon detailed logging, the evaporite pseudomorphs are within a 1.57 m parasequence, 33.5 m above the formation base. As described by Young, the nodules rest within dolostone, but these dolostone lenses lie within a 12–32 cm thick, mottled orange, red and black chert (Text-fig. 2.18A), which is repeated by faulting. The succession and thickness of the chert beds above and below are identical, suggesting repetition. The majority of the nodules are 1–2 cm in diameter, but rarely up to 3.5 cm. The bed comprises clusters of nodules, which display an un-distorted to distorted nodular mosaic, partially separated by a dolomite matrix. Void filling quartz and calcite is noted within the centre of some nodules in thin section and the quartz displays a variety of textures indicative of an evaporate precursor (outlined below).

Nodules are also recorded from the lower and middle Eilean Dubh Formation. Those from the lower Eilean Dubh Formation at Ardvreck (9 m and 15 m above the formation base) are now filled with calcite spar and quartz, but some of the nodules retain their original shape and irregular ‘cauliflower’ margin. Quartz nodules are also observed at a height of 80 m within the Eilean Dubh Formation, Balnakeil Bay. They range up to 3 cm in diameter and up to 1.5 cm in thickness and display an ovoid shape, with an irregular knobbly margin. In hand specimen the nodules comprise white, massive quartz, however in thin section they display a felted lath texture (Text-fig. 2.19C) around the margin, characteristic of the anhydrite precursor. The quartz crystals contain inclusions of highly birefringent anhydrite up to 90 μm in length. The successive inner parts of the nodule contain length-slow chalcedony, which forms spherules, up to 1 mm in diameter (Text-figs. 2.19B, E, F). The centre of the nodule commonly comprises void-filling megaquartz (Text-fig. 2.19A).

Text-figure 2.18 Nodular and bedded evaporate pseudomorphs from the Durness Group. **(A)** white quartz nodules preserving a texture similar to chicken wire anhydrite 33 m above the base of the Sangomore Formation. **(B)** dolomite bed with a texture attributable to a contorted anhydrite nodule. The anhydrite is now replaced by fine grained dolomite, but the texture is visible within a haematite staining. Middle Eilean Dubh Formation, Balnakeil Bay. **(C)** white pink quartz nodule preserving an anhydrite macrocell structure. Middle Eilean Dubh Formation, Balnakeil Bay. **(D)** plan view of chert nodules which form a circular feature attributed to deflation of the sabkha. The bed represented is seen in side profile in **(E)** where a dolostone bed and red cherts show a folded texture. The enterolithic' texture is observed in bedded anhydrite in modern coastal sabkhas. Middle Eilean Dubh Formation, Balnakeil Bay.



The nodules are often surrounded by fine grained dolostones with dispersed crystallotopic pseudomorphs. Rare examples are observed within the Eilean Dubh Formation of replacement via finely crystalline dolomite. The nodule shows an original distorted nodular mosaic texture, picked out by haematite rich seams (Text-fig. 2.18B).

Many sulphate nodules are silicified in a multistage process that involves both replacement and void filling (West 1964, Chowns & Elkins 1974).

Stage 1

Chalcedony mimics or pseudomorphs the felted lath textures of the precursor anhydrite in the outer portion of the nodules (Text-figs. 2.19A–C). The pseudomorphs occur as radiating or decussate and flow textures are noted in laths that make up sabkha anhydrite nodules and define their explosive mode of growth. As well as the lath microtexture, outlines of larger crystals that predated anhydritisation and silicification may also be preserved by the nodule margin, these crystal outlines vary from prismatic to bladed. Many silicified nodules still retain the knobbly cauliflower outline of its precursor anhydrite. Other nodule edges preserve the interfacial outlines of gypsum precursor (Chowns & Elkins 1974).

Stage 2

Microquartz and quartz fill can assume euhedral faces as they grow into voids created by the dissolution of the nodule. At the same time the quartz may continue to engulf and pseudomorph small areas of residual anhydrite (Text-fig. 2.19D) or other less common evaporite salts. Quartz crystals precipitated at this time are commonly zoned with more anhydrite inclusions within the inner zone of the pseudomorph. Some quartz crystals are doubly terminated and probably grew via the support of a dissolving meshwork of anhydrite. With the final dissolution of the supporting mesh these quartz crystals sometimes dropped to the floor of the void to create a geopetal indicator.

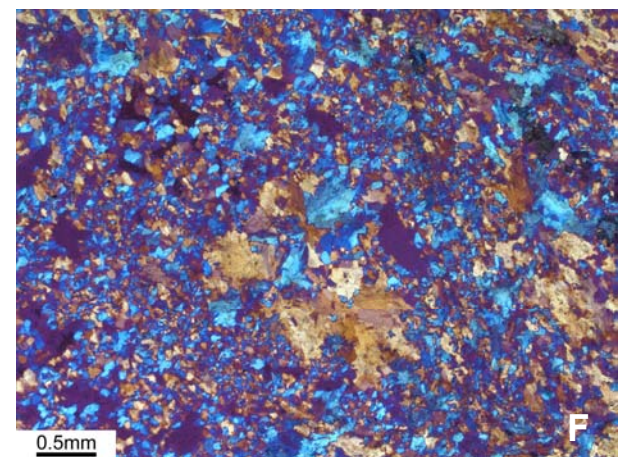
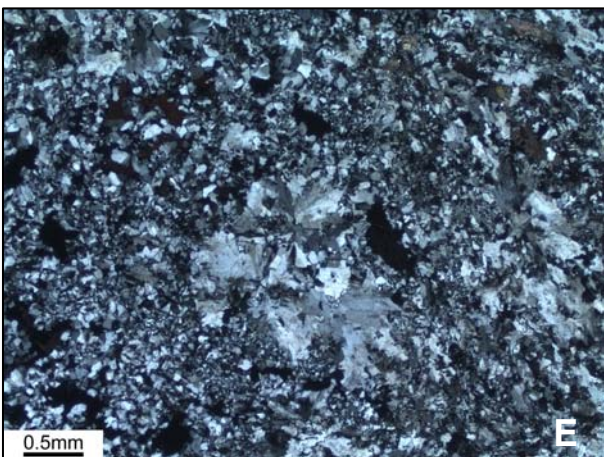
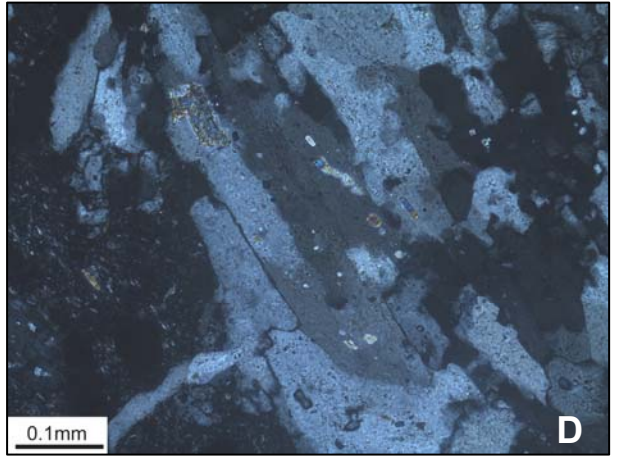
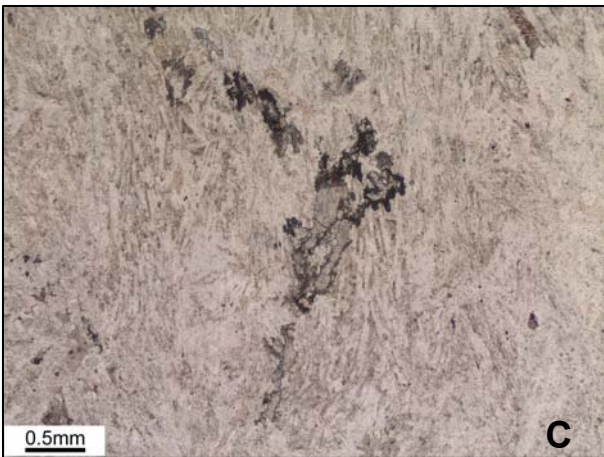
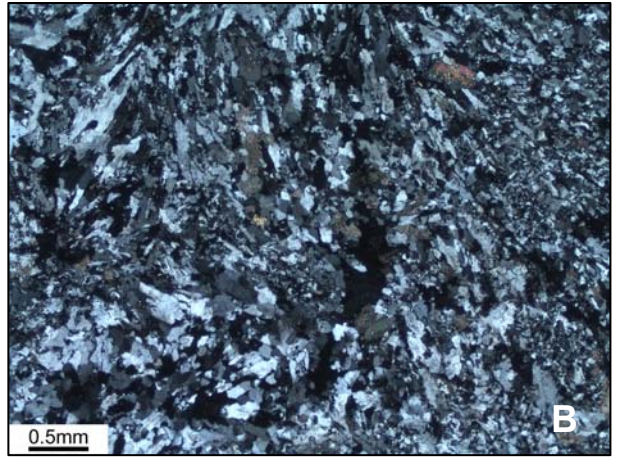
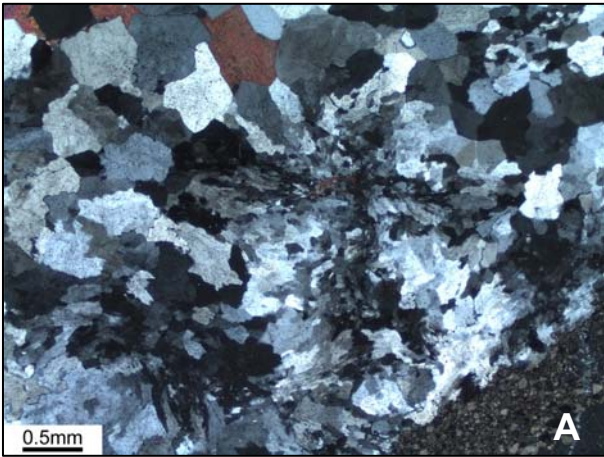
Stage 3

The final stage of the void fill is typified by the precipitation of coarse, drusy, euhedral quartz and minor non-ferroan calcite, lacking inclusions of anhydrite. This coarse quartz resembles coarse vein quartz (Text-fig. 2.19A). Sometimes the process of void fill may be arrested to leave a hollow core in the silica lined geode.

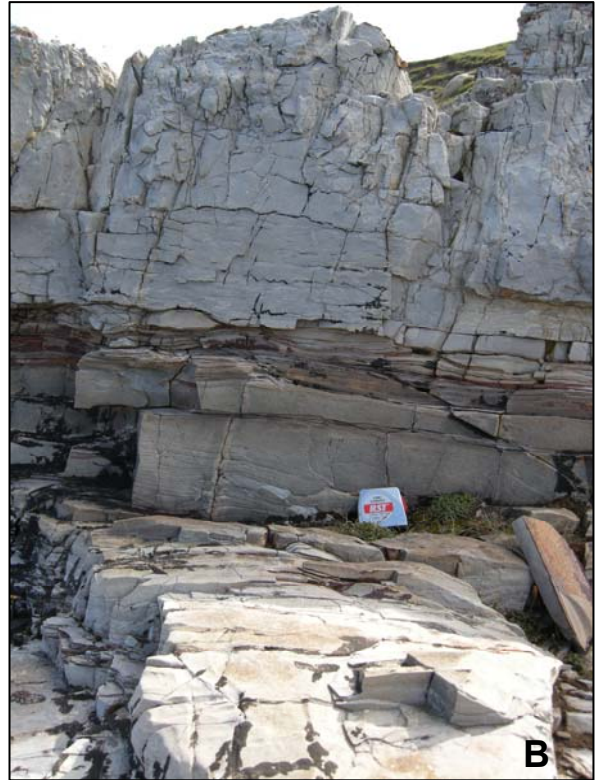
Work on diagenetic timing of silicified CaSO₄ nodules (e.g. Milliken 1979, Geeslin & Chafetz 1982, Gao & Land 1991 Ulmer-Scholle & Scholle 1994) shows that most silica replacement begins with shallow burial, either in the zone of active phreatic flow or in the upper portion of the zone of compactional flow (probably at depths of less than 500–1000 m) early silica replacement in the zone of phreatic flow is indicated by a lack of compressional flattening of the nodule, by the preservation of delicate surface ornamentation, such as ‘cauliflower chert’ surfaces, and the preservation of compactional drapes around subspherical replaced nodules. If replacement of an anhydrite nodule occurs later in the burial cycle, many nodules have then become flattened. Due to the soluble nature of sulphates, replacement may also occur during exhumation.

Overall the texture of silica infill or replacement in a nodule is dependent on the rate of sulphate dissolution, the timing of the silica precipitation and the rate of silica supply (Chowns & Elkins 1974). Some nodules are dominated by the early high fidelity replacement textures others have textures indicating silica cements growing into an open phreatic void left after the complete dissolution of the CaSO₄. Such nodules may still retain a hollow centre where the anhydrite once resided, seen in nodules from the lowest Eilean Dubh Formation at Ardvreck. When a silica-filled geode did not start to accumulate silica until after all the CaSO₄ dissolved, the main evidence for an evaporite precursor comes from the shape of the replaced nodule and its stratigraphical position within the evaporitic depositional sequence (supratidal, intertidal in a sabkha peritidal cycle). More recently megaquartz crystals have been observed infilling voids in a dolomite matrix, as well as forming overgrowths on detrital quartz grains, in a gypsum- and anhydrite bearing Pleistocene sabkha dolomite sequence in the Arabian Gulf, forming within meters of the present surface (Chafetz & Zhang 1998).

Text-figure 2.19 Thin section micrographs displaying the textures observed within the evaporate replacing nodules. **(A)** nodule margin displaying a transition from chalcedony (lutecite) to megaquartz and minor non ferroan calcite (showing red). XPL. **(B)** radially arranged lutecite crystals. XPL **(C)** dusty margins of the quartz crystals preserve the ‘felted lath’ texture of the original precursor anhydrite. PPL. **(D)** detailed view of highly birefringent inclusions of anhydrite within a quartz crystal. **(E)** spherules of lutecite. XPL **(F)** same view as previous but with the sensitive tint plate. The spherules are seen to be comprised of length-slow chalcedony. XPL All the samples come from either the middle Eilean Dubh or the middle Sangomore formations.



Text-figure 2.20 Halite pseudomorphs and other features of the upper parts of the sabkha cycle. **(A)** lenses of fine-grained dolomite within quartz sand rich dolomite. The lenses are mottled and interpreted to be after anhydrite. **(B)** parallel laminated and ripple laminated quartz-silt rich, fine grained dolomites from which halite pseudomorphs have been recovered. **(C)** desiccation cracks and halite pseudomorphs. **(D)** impression of a halite hopper in quartz sand rich dolomite. **(E)** bedding plane displaying texture interpreted to be the pseudomorph of a halite crust. All photographs are from the middle Eilean Dubh Formation, Balnakeil Bay.



Bedded anhydrite

One occurrence of pseudomorphed bedded anhydrite (Text-fig. 2.18E) is recorded from 80 m above the base of the Eilean Dubh Formation at Balnakeil Bay. The bed (7–14 cm thick) shows an enterolithic folded cross section and is replaced by mottled, light grey dolomite. The shape of the bed is highlighted by orange cherts, without which an interpretation as pseudomorphed anhydrite would be difficult.

Pseudomorphs of halite

Casts of equant halite hoppers were found at one horizon (82 m) within the Eilean Dubh Formation. They range in size from 0.3 to 2.0 cm and form single, and more rarely casts of composite halite crystals (Text-fig. 2.20E). Some loose blocks of dolomite show a mass of poorly developed halite pseudomorphs covering the bedding plane (Text-fig. 2.20D).

The occurrences most likely represent halite precipitation by concentration of sea water at ephemeral pools. Halite crystals commonly form in the modern sabkha environment but are seldom preserved, due to their high solubility. The multiple halite pseudomorphs may represent a halite crust which is recorded from sabkha environments (Warren 2006).

Evidence for once more extensive evaporites, solution breccias

Breccias interpreted to have formed by the dissolution of evaporites span the Ghrudaidh – Eilean Dubh Formation boundary at An t-Sròn and Ardvreck Castle and are locally developed within the Eilean Dubh Formation at Balnakeil Bay. There are more preserved evaporite dissolution breccias within the rock record than there are preserved evaporite beds (Warren 2006). The breccias recorded here indicate that extensive beds of soluble salts were once developed within the succession. Bed dissolution as well as nodule and crystal replacement, can be syndepositional and driven by active phreatic flow or can occur later, driven by compactional and thermobaric flushing. Dissolution can also occur during uplift associated with collision, inversion and over-thrusting (Warren 2006). The different types of breccia that can result are packbreccia (clast supported) and floatbreccia (clasts float in a finer matrix of granules, sand or mud). These may be further classified in terms of the orientation of the clasts into crackle (fitted clasts), mosaic (mildly disorientated) and rubble (totally independent) (Morrow 1982).

Evaporite solution breccias have been previously described by McWhae (1953), Middleton (1961), Stanton (1966) and Swennen *et al.* (1990). Their identification is often problematic but a number of criteria, suggested by Morrow (1982) can be used to imply an origin from evaporite solution.

- Planar to slightly irregular, continuous lower contact, which is commonly coated with insoluble residues.
- Beds below the breccia are locally veined by satin spar.
- They commonly show a gradational upper boundary, locally grading into crackle breccia.
- Pseudomorphs of now dissolved evaporite minerals and nodules, composed of calcite silica or celestite may also remain within matrix or within clasts.
- Locally the breccias correlate laterally with evaporite beds.
- The breccias are found within a sequence containing other evaporites and supratidal indicators.

It is the flat base and gradational top that distinguishes the evaporite breccias from cataclasites (which have symmetrical contacts). The breccias from the Durness Group are all oligomict, crackle to mosaic breccias (Text-fig. 2.21) and the lithic fragments are similar to the rocks surrounding the breccia (dolomicrite). The clasts are generally fitted and appear to have been brittle, implying they were cemented prior to formation of the breccia. The spaces between the clasts are largely filled with cements, which are dominated by calcite and chert. There is no indication of weathering and the clasts are angular to sub angular. Clast size varies from 0.4 cm to 6.0 cm. There is no imbrication, alignment or grading observed. The overall shape of the breccia body varies from tabular (Text-fig. 2.21A, C), lensoid (Text-fig. 2.21D) (concordant/interstratal) or irregular and locally has a vertical trend (discordant/transtratal) (Text-fig. 2.21B), in relation to the surrounding beds. Examples of both packbreccia and floatbreccia are observed (Text-fig. 2.21A). These can be further classified into crackle, mosaic and rubble breccias (Text-fig. 2.21). Some of the breccias show a flat base and irregular upper boundary (Text-fig. 2.21D).



Text-figure 2.21 Breccias interpreted to be formed during the dissolution of evaporites. **(A)** rubble floatbreccia of clasts within a haematite-rich chert replaced matrix. Tape measure is 9 cm in diameter. **(B)** discordant, mosaic packbreccia, lowest Eilean Dubh Formation, Ardvreck, Assynt. Pencil is 14 cm long. **(C)** bedding parallel crackle packbreccia displaying weakly disorientated clasts. The bed lies 34.5 m above the base of the Ghrudaidh Formation, An t-Sròn. cm rule for scale. **(D)** lens-shaped bed of rubble packbreccia displaying a planar bed base and an irregular upper surface. The breccia lies 8 m above the base of the Eilean Dubh Formation, An t-Sròn. Cm rule for scale.

If the cavity is only a few millimetres or centimetres high the overburden founders gradually and gently, and so clast orientation is fitting and little disturbed by the process of dissolution, crackle and mosaic breccias will be commonplace, as is the case in the Durness Group. If large local cavities develop the collapse is more likely to produce disturbed rubble- or packbreccias. Clast supported packbreccias result from pure evaporites, interbedded with indurated dolomites and other non-evaporite strata. Whilst evaporite sequences interbedded with, or underlying non-consolidated sediments, or evaporites with a high content of dispersed impurities tend to produce matrix supported float-breccias (Warren 2006).

Environmental interpretation

A sabkha is a low, arid plain of carbonate sediment, built at supratidal level by a prograding shoreline (Kendall 1984). Although commonly a metre or so above normal high tide, the sabkha is liable to flooding by abnormal tides and storms. It is thus exposed to the effects of wind and sun for much of the time but is occasionally flooded by meteoric freshwaters and saline marine storm waters. This combination of different depositional and diagenetic conditions results in a characteristic sequence of sediments and diagenetic mineral layers, particularly anhydrite. The best modern examples of sabkha sedimentation occur around the shores of the Arabian Gulf and particularly between the northern Emirates and eastern Qatar. They have been studied in detail and are described in numerous papers (Evans *et al.* 1969; Purser 1973; Kendall & Skipwith 1969; Kendall 1984; Alsharhan & Kendall 1994, 2003; Al-Farraj 2005). The supratidal portion of the Sabkha may be divided into three subzones, the lower, middle and upper. Each of these has a distinct set of physical characteristics (Patterson & Kinsman 1981; Butler *et al.* 1982).

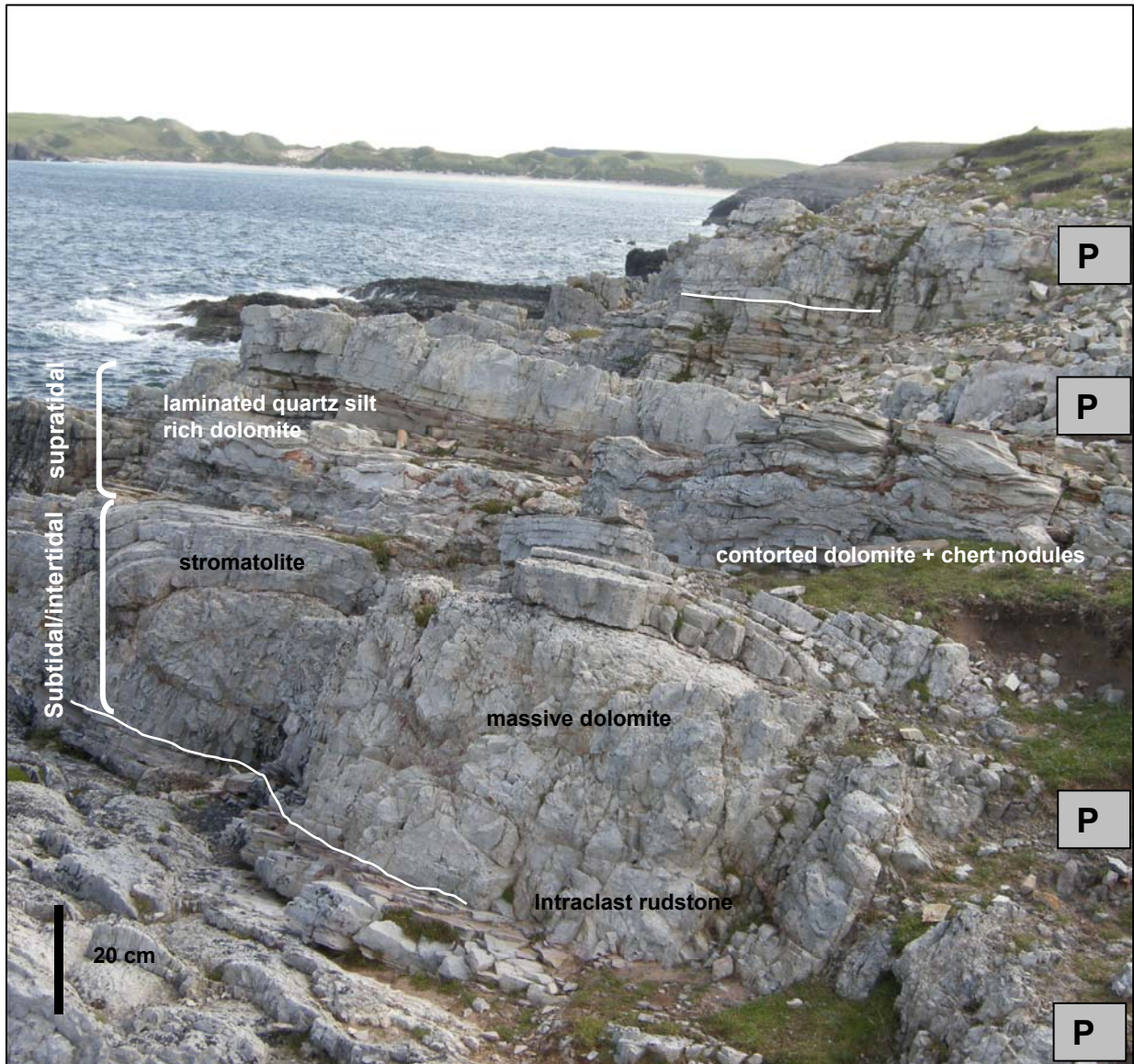
The Durness Group at this time is interpreted to have been deposited on a wide, restricted tidal flat, covered by extensive microbial mats. Evaporite moulds and desiccation cracks are common in some lithofacies indicating increased salinity and subaerial exposure. Lack of abundant evaporite deposition suggests a semi-arid climate, where periods of subaerial exposure produced erosional surface palaeokarst (Choquette & James 1988, Chow & James 1992).

The most complete sabkha cycle (1.53 m) in the Durness Group is preserved at a height of 79 m above the base of the Eilean Dubh Formation (Text-fig. 2.22). It comprises a locally rippled, basal intraclast rudstone (18 cm) containing fine-grained, laminated clasts of dolomite (which are clast supported and commonly vertically orientated, see Text-fig. 2.11D). Overlying this is a 10–70 cm thick bed of light grey dolomite within which there are veins of silica and small cherts. This is in turn overlain by stromatolite biostromes (45 cm) which follow the topography of the underlying bed (Text-fig. 2.22), which are interpreted to have formed in a subtidal to intertidal setting. The biostromes consist of many cm-scale digitate and columnar stromatolites, which within the top 20 cm of the bed commonly exhibit small lath-shaped vugs (Text-fig. 2.17E). Overlying the stromatolites are parallel laminated dolomites with lenses of more dense vugs (Text-fig. 2.17F) (20–35 cm) and this is in turn overlain by mottled pale grey dolomite with orange chert nodules and bands. Although the

dolomite is structureless the shape of the chert which overlies it indicates that the bed is tectonically folded and this shape bears close similarity with bedded anhydrite documented from recent sabkha environments (Kendall 1984). Quartz nodules after anhydrite also occur in this bed. On the upper surface the cherts are observed to be circular in plan (20 cm diameter) The upper parts of the parasequence comprise a 30–55 cm thick bed of finely-laminated and locally rippled dolomite within which well developed tepee structures are observed. Laminae and lenses of quartz sand and silt become increasingly common towards the top of the parasequence (Text-fig. 2.22). In some of the overlying parasequences these laminites contain halite pseudomorphs (Text-fig. 2.22).

In the upper portion of the upper intertidal and in the lower supratidal zone a significant measure of syndiagenesis takes place. Interstitial precipitation of aragonite and of small lenticular gypsum crystals begins within the microbial mats and surface sediments are locally cemented by aragonite, magnesite and protodolomite (Butler *et al.* 1982). In some areas the upper intertidal areas may also include a complex of embayed ponds, water-filled deflation areas and restricted lagoons in which thicker and more extensive microbial peats accumulate. In the most seaward portion of the supratidal zone, the microbial mats are gradually disrupted by the growth and accumulation of gypsum crystals. The crystal growth becomes extensive and may develop into a discrete layer, up to 30 cm in thickness, termed the gypsum-crystal mush (Kinsman 1964; Alsharhan & Kendall 1994). This zone may extend inland across a 2.5 km area centred on the high water zone of the tidal flats. As the lower supratidal zone progrades slightly, the gypsum crystals of the mush become more and more disruptive and microbial peat loses its coherence and structure and becomes a loose matrix squeezed between the new formed crystals.

In the mid-portion of the supratidal zone (mid-salt flat of Butler *et al.* 1982) evaporation causes salinity of the pore waters to rise sharply. Flooding by marine waters is less common and diurnal temperature fluctuations may exceed 40° C (Alsharhan & Kendall 2003). The carbonates in this zone are strongly dolomitised. The high salinities plus the high temperatures cause precipitation of ephemeral halite and a gradual change in the earlier-formed gypsum, which alters to massive to nodular anhydrite either through a single series of dehydration steps. Anhydrite is added to the initial nodules by further concentration of the pore waters and the gypsum crystal shapes are wholly lost. The general morphology of the middle part of the supratidal zone is quite variable.



Text-figure 2.22 View of a well developed sabkha parasequence within the Eilean Dubh Formation. The parasequences are marked (P) and the top and base of the units is shown. The features labelled are described in the text.

The anhydrite layers are developed as polygonal structures which possibly began as desiccation features. Initially the anhydrite in this layer appears as small nodules above the crystal mush zone (above the water table). The small nodules increase in size and concentration towards the landward side of the supratidal zone, forming an interlocking surface of polygonal saucers 0.3–1 m in diameter. This surface may become overlain by reworked aeolian sands. The upper surface of the polygons is commonly planed by storm-driven floods from the lagoons and new layers of sediment are then formed above the

polygonal saucers. As the underlying gypsum mush is also gradually altered to anhydrite, the volume decrease causes slumping and compaction, and the original layers are distorted.

The upper part of the supratidal zone is inundated only rarely (every 4 or 5 years) and may extend in a broad depositional belt nearly 5 km in width (Alsharhan & Kendall 1994). Many if not all the features developed in this portion of the sabkha are syngenetic. They include the addition of near surface nodular anhydrite layers and the alteration processes are accomplished by ground waters composed of both marine and continental components, which have been concentrated by rapid evaporation, both at the surface and within the soil profile. The gypsum mush is not only dehydrated, but develops into folded or enterolithic beds, anhydrite diapers and small disharmonic folds. Halite is precipitated locally in this zone as displacive hopper crystals and cements and substantial aeolian sediment is also present.

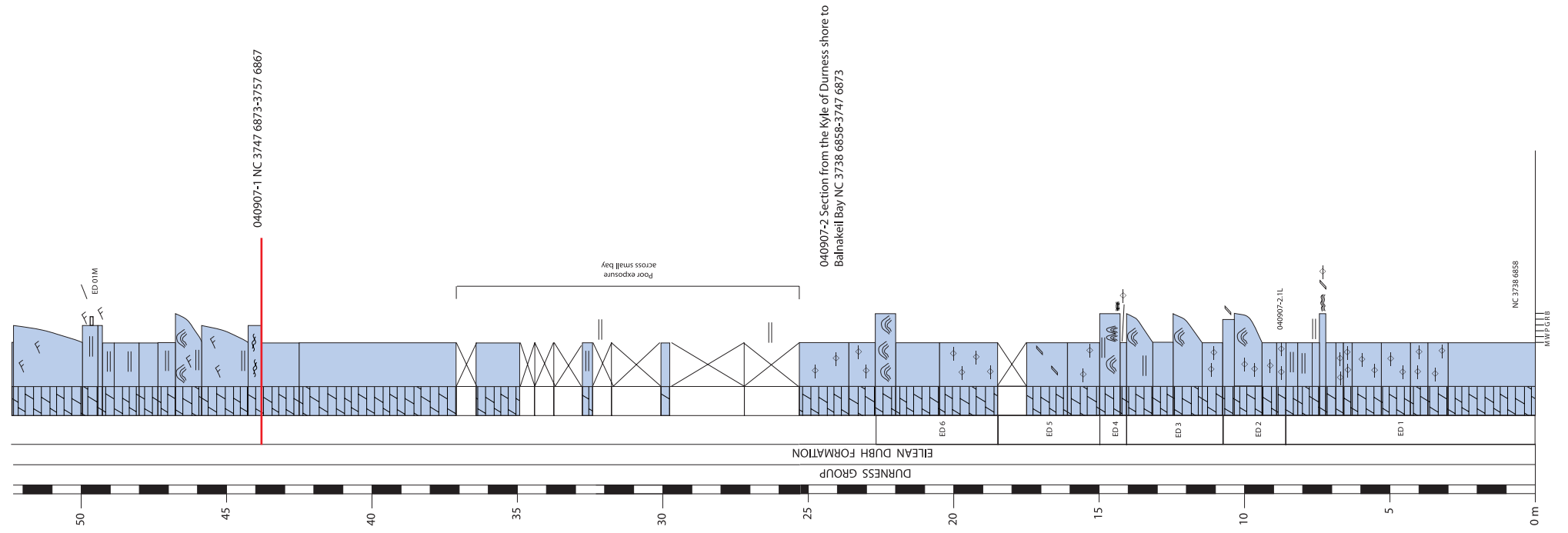
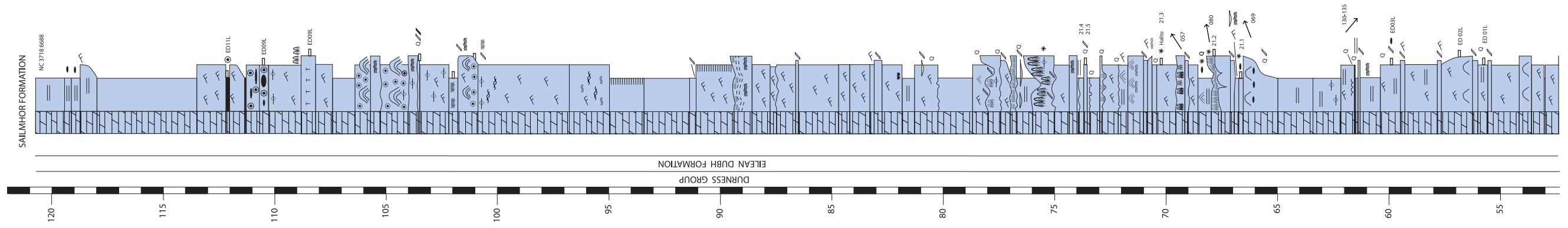
2.4. STRATIGRAPHIC TRENDS

The basal 5 metres of the lowest unit in the Durness Group, the Ghrudaidh Formation contain quartz sand within burrow mottled dark grey dolostone (Text-fig. 2.23). Coarsely crystalline dolostone with locally common small intraclasts is interpreted as a recrystallised ooidal grainstone. The entire Ghrudaidh Formation represented deposition within the shallow subtidal zone. The scarce fauna either reflects the coarse recrystallisation of much of the dolomite or an original paucity of fauna. There are local bioclastic grainstones and wackestones containing the small shelly fossil *Salterella*. The lack of fauna within much of the succession may suggest that conditions on the shelf were restricted or may represent deposition within a lagoon. Salinity may have fluctuated causing evaporites to fill vugs within the sediment. Burrow mottled dolostones occupy the basal 31 m of the formation. Above this, paler more fine grained carbonate suggests that the environment was shallower and early cementation took place. At this stratigraphical level at Grudie, rare hemispheroidal stromatolites are observed, suggesting an intertidal depositional environment. At An t-Sròn, light grey coloured, parallel laminated dolostones are observed within the upper part, suggesting deposition on supratidal flats and the presence of crystallotopic evaporites within the sediment at the top of the formation and into the lowest Eilean Dubh are associated with dissolution breccias and large nodules of sparry calcite (possibly after anhydrite) suggest that a coastal sabkha was well developed. Ooidal grainstones, ripple lamination, planar

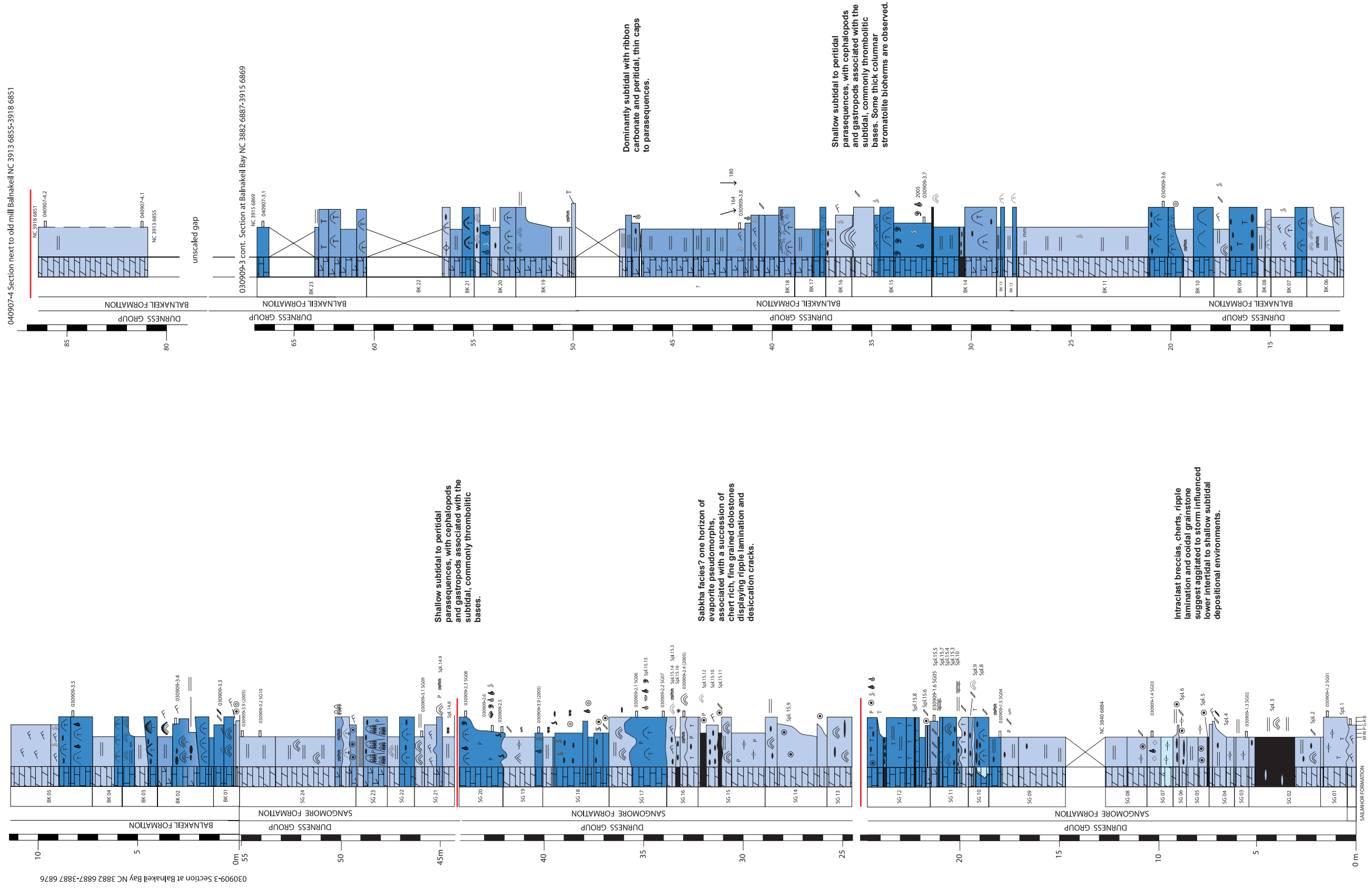
stromatolites, suggest agitated shallow subtidal to supratidal setting, beds of fenestral carbonate.

Within the lower Eilean Dubh Formation, muddy tidal flats develop and the thick succession of ripple laminated and structureless or fenestral carbonate with stromatolites and flake breccias towards the top of the succession suggest aggrading tidal flats with deposition between the lower intertidal and lower supratidal zones. The section is poorly preserved and the complete thickness is not known (Text-fig. 2.24). The middle part of the Eilean Dubh Formation represents deposition on supratidal flats, with channels, karst and microbialites, evaporates, quartz rich sand recorded and sabkha cycles prominent. (Text-fig. 2.24). This is overlain by aggrading tidal flat facies typified by flaser and lenticular bedded intertidal flats without evaporates (Text-fig. 2.24).

During deposition of the Sailmhor Formation regular alternations of subtidal and peritidal facies were deposited in shallowing upward sequences. The regular facies makeup of the parasequences suggests that facies belts were laterally extensive and uniform. Dark subtidal dolostones with columnar stromatolites lie at the base of the parasequences and are surrounded by oncoidal packstone and peloidal grainstone. They have colonised the sea floor following base level rise. They are overlain by a repetitive succession of facies, from thrombolites and bioclastic wackestone (subtidal facies association) then ripple laminated mid grey dolostone and hemispheroidal stromatolites, (Text-fig. 2.25). Within this formation there is little evidence for both evaporite deposition or desiccation features suggesting either a preservational bias or that most of these parasequences comprise upper intertidal rocks in the upper parts, or that the climate was more humid. In the top 10 m of the formation chert breccias and ooidal grainstones suggest that the tidal flats are more agitated by current or wave activity.

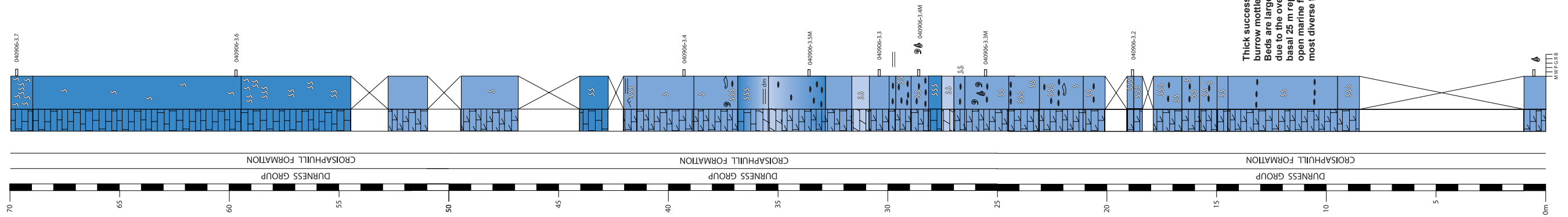
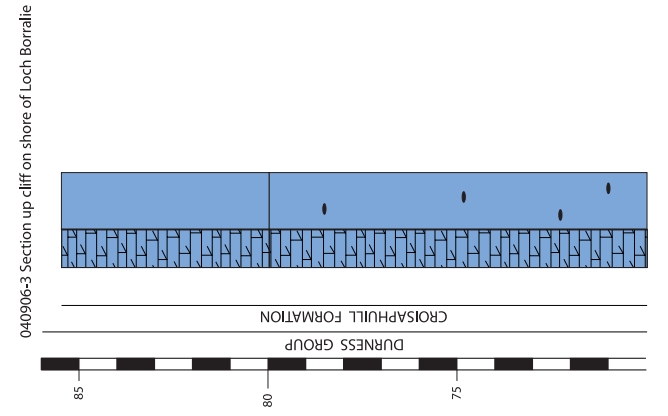
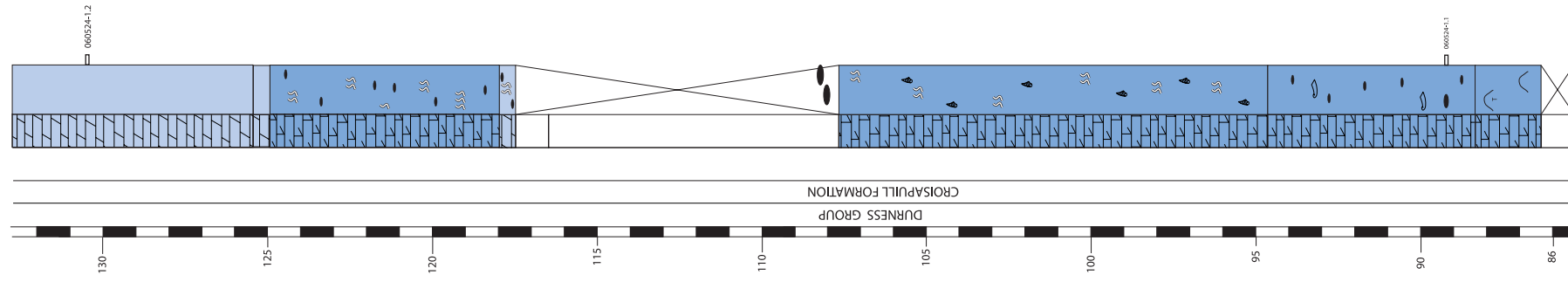
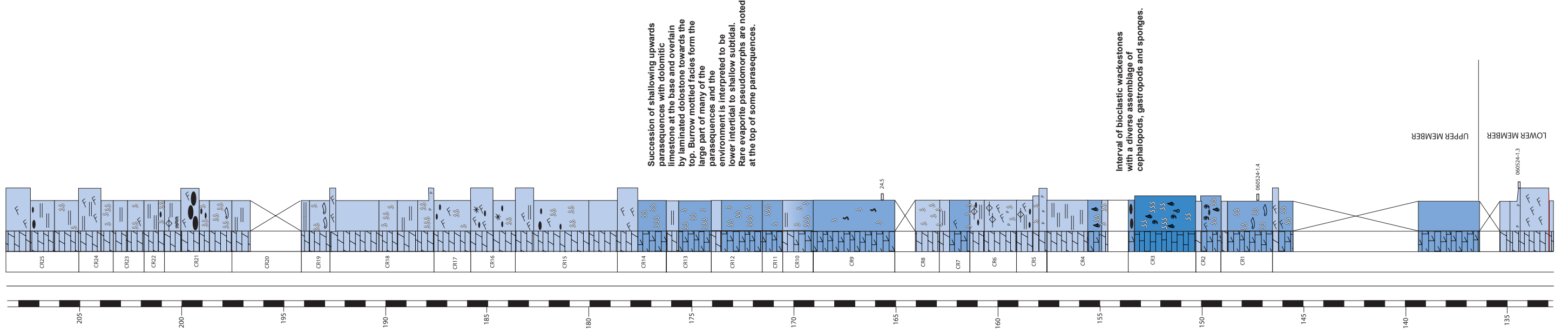


Text-figure 2.24 1:200 sedimentary log of the Eilean Dubh Formation, Balnakeil Bay

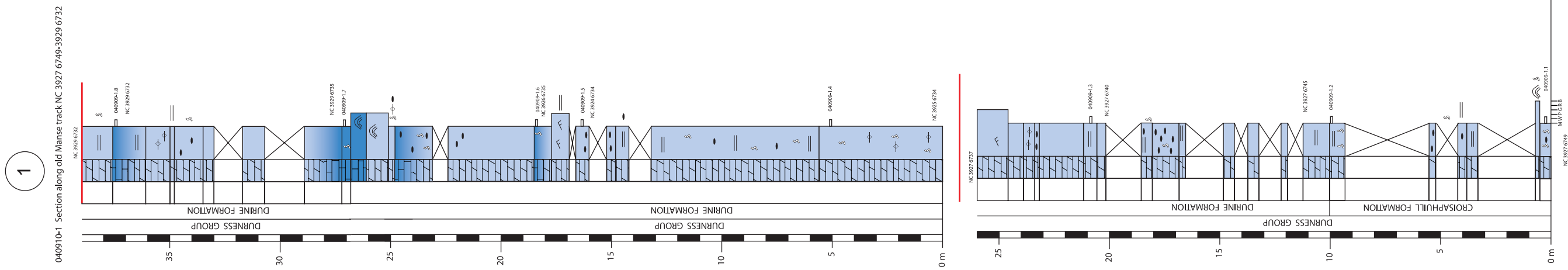


Text-figure 2.26 1:200 sedimentary log of the Sangomore and Balnakeil formations, Balnakeil Bay

132 m vertical distance inferred from a measured transect, with stratigraphical dip data taken



Text-figure 2.27 1:200 sedimentary log of the Croisaphuill Formation near Loch Borrallie (for key, see Text-fig. 2.23).



Facies interpretation is made difficult by diagenetic alteration and faulting of the beds. The lower part comprises shallowing upward parasequences similar to those of the upper member of the Croisaphull Formation. The bases are dominantly composed of dolomitic limestone with burrow mottling. Higher in the sequence, fine grained, parallel laminated dolostones dominate, suggesting upper intertidal to supratidal depositional environments and evaporite pseudomorphs are recorded.

Text-figure 2.28 1:200 sedimentary log of the Durine Formation, comprising a series of sections, which are arranged in order (1-4) to produce the composite section (for key, see Text-fig. 2.23).

Deposition of the Sangomore and Balnakeil formations resulted in a mosaic of facies, probably representing shoals, channels and lagoons on a wider shelf environment, subject to wave influence. The Sangomore Formation (Text-fig. 2.26) contains the most diverse array of lithofacies and stacking patterns of lithofacies within parasequence are less ordered than those seen in the underlying Sailmhor Formation. Shallowing upward sequences are still recognisable but their internal facies makeup varies. This lends support to the theory that the intertidal environment consisted of facies belts that varied laterally, giving rise to differences in the facies composition of cycles. In the lower part of the formation dark fenestral carbonate or ooidal grainstone represents shallow agitated patches of shallow subtidal shoals. Thrombolites are common in the middle part of the formation and form amalgamated sequences up to 4 m. But most are tabular and occur at the base of parasequences. Ooidal and peloidal grainstone is common beneath and surrounding the thrombolite biostromes (up to 2.3 m). Hemispheroidal stromatolites are not as abundant in the intertidal facies as in the Eilean Dubh Formation. The peritidal facies are represented by ripple laminated dolostone (intertidal zone) and planar crinkly stromatolites, parallel laminated dolostone with desiccation cracks and occasional tepees, and intraclast rudstones (supratidal zone). Evaporite pseudomorphs occur at 33.50 m and indicate that the supratidal zone was a coastal sabkha but succeeding marine inundation of the supratidal flats at the start of the overlying parasequence removed any record of evaporites.

The boundary between the Balnakeil Formation and Croisaphuill Formation is faulted but facies change seems to be gradational either side of the boundary. At the top of the Balnakeil, lithofacies belonging to the subtidal facies association constitute an increasing proportion of individual parasequences. The lower part of the overlying Croisaphuill Formation is composed entirely of burrow mottled dolomitic limestone (Text-fig. 2.27). The abundance of the burrows within these beds suggests that the depositional environment was subtidal. A ramp margin build-up may have dampened the effect of storms upon the shelf but was clearly not influencing ocean circulation or salinity. The Croisaphuill Formation has yielded the majority of the fauna described from the group and studies of the museum collections suggest that the fauna was moderately diverse, with a high proportion of gastropods, but also cephalopods, brachiopods, rostroconchs, ostracods, trilobites and sponges. The depositional setting is thought to be outboard of marine sand shoals into open marine shelf.

The nature of the tidal flats at this time can be taken from the upper Croisaphuill Formation and overlying Durine Formation (Text-fig. 2.28) which mark a change to peritidal facies association rocks representing deposition on a restricted tidal flat and coastal sabkha.

2.5 CONCLUSIONS AND ENVIRONMENTAL INTERPRETATIONS

Tidal flats differ from beaches in that they are protected from open ocean waves. They may therefore occur in settings, which are:

- a) Separated from the open ocean by a wide, shallow shelf lagoon that dampens the incoming waves, as for example, Andros Island tidal flats, Great Bahaman Banks.
- b) Behind barrier islands that separate back barrier lagoons from the open ocean waves, as for example, Abu Dhabi in the Persian Gulf.
- c) In restricted embayments, as in Shark Bay, Western Australia.

Suitable recent analogues are not common but include the humid tidal flats of Andros Island, Bahamas and the more arid Caicos Islands, West Indies (Shinn 1983). The largest tidal flats are those along the southern shore of the Persian Gulf (Kendall 1984), and the tidal flats of Western Australia (Logan *et al.* 1964). But tidal flats in low latitudes on the scale of whole cratonic margins are not represented in the modern day. Modern tidal flats are greatly influenced by the activity of fauna and flora which modify the sediment. There are no plants recorded at this time and fauna which could tolerate high salinity has not been recorded.

Recent environmental analogues include Shark Bay (latitude 25° S). Lee Stocking Island, Bahamas (latitude 24° N). Sediments within the Durness Group bear close similarity to those forming in the Bahamas, which experience a semi-arid climate. Sedimentary structures such as burrows, ripple lamination, tepees, desiccation cracks and evaporites all occur on the tidal flats. Ooids, peloids and intraclasts form an important part. The succession of stromatolites and thrombolites within the Durness Group most closely resemble that occurring within Shark Bay, Western Australia.

The lithofacies from the Durness Group represent supratidal to shallow subtidal deposition. Microbialites were both abundant, diverse and were present in all depositional environments (Chapter 3).

The recognition of true sabkha facies within the Durness Group for the first time gives a better understanding of the depositional environment on the Laurentian margin in NW

Scotland. The observation that most parasequences within the Durness Group terminate with upper intertidal facies implies that a coastal sabkha may have existed for much of the time spanning deposition of the Durness Group and that its preservation at major sequence boundaries preserves a snapshot of facies that existed inboard of the preserved depositional section. Sabkha facies have not to date been recorded from western Newfoundland (Chapter 5) despite the similarity of the lithostratigraphy. The section appears to have lain in a more outboard setting from the continental margin and true offshore facies are preserved along with a higher proportion of subtidal ooid shoals and metazoan reefs (Pratt & James 1986). It is reasonable to assume that a coastal sabkha was developed along much of the southeastern margin of the Laurentian craton, and that this sabkha represents the most extensive and largest to have existed during the Phanerozoic.

Palaeocurrent data for the Durness Group carbonates are scarce and are only displayed in the peritidal facies association. Ripple lamination is present but is poorly preserved. Occasionally bedding planes show ripples but these are wave, rather than current ripples and because the water is interpreted to be very shallow, the prevailing winds may have had more of an effect than the tides. Stromatolite bioherms often show current alignment (Text-fig. 3.11). Within the Eilean Dubh Formation karst at the top of parasequences sometimes shows a preferential alignment and these may represent draining of the supratidal flats, causing dissolution. The long axes of karst hollows show a preferential elongation in a NW/SE trend. This would fit with current palaeogeographical reconstructions, which place NW Scotland on the southeastern margin of the Laurentian craton. If the coast was orientated perpendicular to the long axes of the palaeokarst, it would imply that the ripples reflect the prevailing wind or current direction in a NE or SE direction (Text-fig. 3.11).

Chapter 3

TEMPORAL TRENDS OF CAMBRO-ORDOVICIAN MICROBIALITES: A CASE STUDY FROM THE DURNESS GROUP OF NW SCOTLAND

3.1 INTRODUCTION

In this present study, microbialites are recorded from all but the Ghrudaidh and Croisaphuill formations, but they are particularly abundant in the middle Eilean Dubh to uppermost Balnakeil formations. They are best exposed and best preserved at the type locality for the Durness Group in Balnakeil Bay (Text-fig. 1.5) and a supplementary section was included for study at Smoo (Text-fig. 1.5).

Microbialites from the Durness Group have never been documented in detail, partly due to the poor preservation. Microbialites (stromatolites in particular) commonly show palaeocurrent directions in sections where other current indicators may not be visible and they have been used as a tool for correlation and chronostratigraphy (Shapiro & Awramik 2000, Cloud & Semikhatov 1969).

The proportion of Earth's history for which stromatolites were the dominant biota spans some 2.9 billion years (Riding 2006). They have a use in interpreting past biotic activity, depositional environment, correlation, palaeocurrent, and may be a proxy for palaeotidal range, palaeolatitudes and rates of sediment accumulation (Hofmann 1973). Study of microbialite gross morphology may indicate past environmental fluctuations and has not previously been applied to thrombolites, its potential usefulness is discussed within this chapter (Section 3.9.1). The Durness Group contains a great variety of microbialite forms and this period in their history remains understudied in comparison with Precambrian examples. During the Cambrian–Ordovician, shallow water carbonate rocks were deposited along most of the Laurentian margin, much of which was dominated by microbialites in terms of both rock volume and morphological diversity, these display a wide range of fabrics, morphology and inter-relationships (Rowland & Shapiro 2002; Webby 2002). The microbialite deposits represent a complex interplay of the photic and nutrient requirements of the community that formed them, and are further constrained by salinity, energy levels, sedimentation rate and accommodation space (Riding 2006). Ecosystems dominated by microbialites suffered a major decline after the Ordovician, and these ecosystems constitute the last major peak of

microbialite abundance (both in Laurentia and worldwide), after a period of domination from the Palaeoproterozoic onwards (Rowland & Shapiro 2002; Riding 2005). The Ordovician thus represents a major shift within carbonate environments and their associated ecosystems. Nevertheless, at this time, microbialites exhibit one of their greatest levels of disparity in form, associated with their occurrence across a wide range of bathymetries (Webby 2002). A number of interacting factors may have been responsible for both the success and the demise of microbial communities during the Cambro-Ordovician. These include metazoan grazing pressure, the Phanerozoic sea-level maximum, competition for ecospace, and the existence of a large continental landmass, Laurentia, which was anchored in the tropics throughout this interval (Rowland & Shapiro 2002).

It is the aim of this study to document the microbialites from the Durness Group for the first time, and to assess the abundance of microbialite facies within these strata. The abundance and diversity through the whole succession will be quantified and the causal factors leading to both 'short' and 'long' term changes within this dataset will be examined.

3.2 DEVELOPMENT OF TERMINOLOGY

Different and often confusing classifications of microbialites have led to a plethora of different terms, often perpetuating the confusion. The use of separate terms for ancient and present day examples such as 'potential stromatolite' (*sensu* Krumbein 1983 and Gerdes & Krumbein 1994) is likely to increase this confusion and should not be used. There has been little attempt to classify types of thrombolite, however in contrast there exists a diverse array of terms concerning stromatolites. The classification used by Krylov (1976) followed a Linnaean-type of binomial nomenclature but Chafetz (1973) pointed out that microbial mound morphology and internal structure can be related to changes in environmental conditions and is therefore physically controlled. Stromatolites are highly variable and within a complex bioherm, the different morphological components would be given separate names if found in isolation. It can also not be known whether different morphotypes were constructed by the same group of microbes. Given this uncertainty it seems better to apply a descriptive terminology in the classification of stromatolites. Logan *et al.* (1964) proposed a purely descriptive classification, based on geometric shapes. This included LLH-C (close-linked laterally linked hemispheroids), LLH-S (space-linked), SH-C (stacked hemispheroids), SH-V (vertically expanded stacked hemispheroids) and SS (discrete spheroids). Spherical

stromatolites were classified by Logan *et al.* (1964) as modes I (inverted), R (randomly stacked) and C (concentrically stacked). Kendall & Skipwith (1968) introduced an additional acronym for microbial desiccation polygons, SH-I (inverted stacked hemispheroids). This method is not used here, due to the potential long list of acronyms needed to describe a continuously variable stromatolite.

Shapiro (2000) usefully argued that a distinction should be made between megastructure (large scale features, such as development of bioherms), macrostructure (gross form of the microbialites), mesostructure (visible to the naked eye) and microstructure (visible under microscope or SEM) (Text-fig. 3.4). These definitions serve to highlight problems with previous work on thrombolites in which poor figuring of specimens has led to confusion concerning the scale of 'clots' referred to. Branching stromatolites in which lamination may have been recrystallised during dolomitisation may superficially resemble large, branching mesoclots, or alternatively, small branching thrombolites which have lost their mesoclotted texture. It was noted by Shapiro (2000) that many specimens are often too poorly preserved to show a good, 'true' mesostructure.

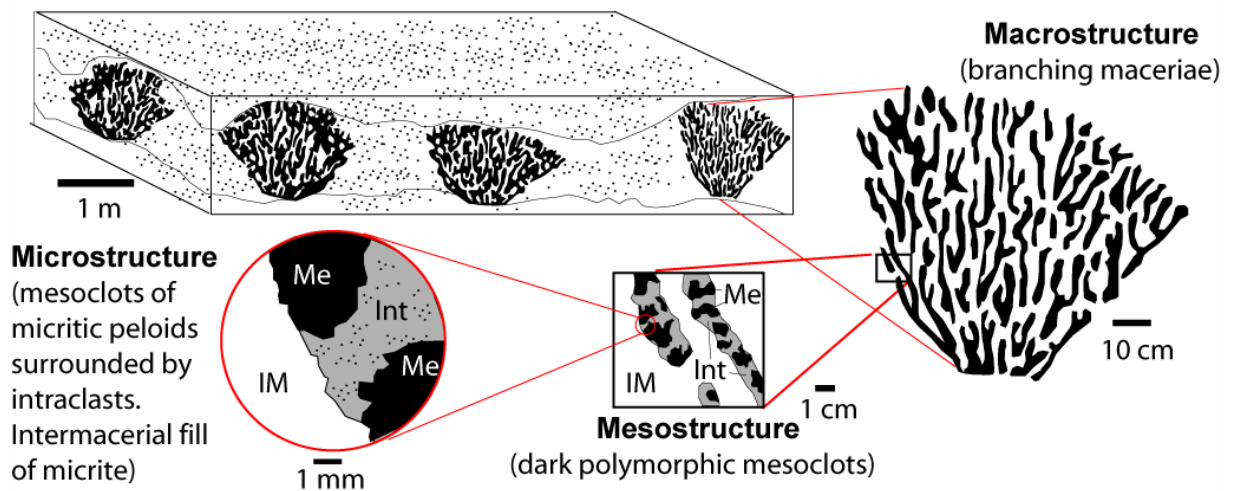
Although there are many classification schemes for stromatolites, the systematic description of thrombolites has largely been ignored and there is a lack of consistent terminology for describing thrombolite textures and morphologies, which in turn has hampered comparative analyses (Shapiro 2000). There are some similarities between the shapes of thrombolite and stromatolite bioherms and also some current stromatolite terminology can be used. There have been some attempts to describe thrombolite mesostructure and Shapiro & Awramik (2006) gave the first description and name to a thrombolite form.

Kennard & James (1986) and Kennard (1994) termed the internal clots of bioherms thromboids, with mesoclot the term given to the macroscopic clotted texture. These mesoclots were more suitably termed maceriae (the mazelike pattern of the microbialite at the macrostructural scale) by Shapiro & Awramik (2006), who also used the term mesoclot solely to refer to the mesostructural clotted texture (Text-fig. 3.1). Poorly preserved thrombolites may have diffuse maceriae visible, thus leading to confusion, particularly true if the columns are complex and form part of larger bioherms or biostromes. The structure of microbialites can thus be described in terms of the scale of the characters (mega-, macro-, meso- and microstructural (Grey 1989; adapted by Shapiro 2000). Shapiro & Awramik (2006) were the

first to apply a binomial (group and form) name to a thrombolite. The thrombolite *Favomaceria cooperi* is similar to those from the Sailmhor Formation and Shapiro & Awramik (2006) recorded it from the Skullrockian–Tulean (Tremadocian to lower Floian) aged strata of the St. George Group, western Newfoundland. Many of the thrombolites described so far were placed in this new group, including those from the Argentine Precordillera, the Appalachians and the Mississippi Valley (Shapiro & Awramik 2006).

Megastructure

(thrombolitic bioherms enclosed by grainstone, bounded by erosion surfaces)



Text-figure 3.1 Schematic diagram showing examples of the spatial relationships between the different scales of observation used in microbialite studies (after Shapiro & Awramik 2006).

Kennard & James (1986) recognised that some bioherms comprised mixtures of laminated and clotted textures, and therefore introduced a new classification based upon the relative proportion of these features. Stromatolites constitute microbialites with greater than 75% stromatoids. A mixture of mesoclots and stromatoids may produce a thrombolitic stromatolite (50–75% stromatoids) or a stromatolitic thrombolite (25–50% stromatoids). True thrombolites represent microbialites with less than 25% stromatoids and if no structures are visible it is termed a leiolite (following Riding 2000). The term cryptomicrobial was proposed for structures which were neither thrombolites or stromatolites *sensu stricto*. This included textures previously described as ‘cryptalgal’, ‘thrombolitic’ and ‘stromatolitic’. Irregularly mottled, patchy, massive non-laminated and non-clotted microbial structures represent

stromatolites and thrombolites that have been disrupted or modified by inorganic or organic processes, or both (Kennard & James 1986).

3.3 HISTORY OF RESEARCH

Burne & Moore (1987) first proposed the term microbialite for organosedimentary deposits, which accreted as a result of a benthic, microbial community trapping and binding detrital sediment and/or forming the locus of mineral precipitation. This term replaced ‘cryptalgal’, which was misleading (blue-green algae are now more appropriately termed cyanobacteria and preservation of the constituent microbes is rare).

Microbialites are generally subdivided into four morphologically distinct types, based upon the internal structure of a build-up. These are; stromatolites (laminated), thrombolites (clotted), leiolites (structureless) and dendrolites (dendritic) (Riding 1991). The literature concerning microbial carbonate deposits has been reviewed by many authors (e.g. Hofmann 1973; Monty 1977, Krumbein 1983 and Riding 2000) and only a brief summary of the main morphological groups is provided here. Microbialites from the Cambro-Ordovician have received little study in comparison to forms from the Precambrian, which have, in contrast, been studied for many decades.

3.3.1 Stromatolites

The term stromatolite was first introduced by Kallowsky (1908) as ‘stromatolith’ (Greek *stromat*, to spread out, Greek *lithos*, stone) for lacustrine examples from the lower Triassic of Germany. Some workers have restricted the term to dome- and column-shaped structures, but stromatolites may also be flat or spherical deposits. They are not necessarily composed of carbonate either, and siliceous, evaporitic or siliciclastic examples also occur (Riding 2000).

There is currently no generally accepted definition of stromatolites but that of Riding (1991) (‘a stromatolite is a laminated benthic microbial deposit’) is perhaps the most concise and is in agreement with much current thinking. Some previous descriptions avoided the biogenic nature of stromatolites and were purely descriptive, allowing the term stromatolite to apply to abiogenic structures (Semikhatov *et al.* 1979). Problems with the definition have stemmed from the fact that the biological process of formation of stromatolites has not been accepted by all workers. However recent work by Allwood *et al.* (2006) suggested that even some of the earliest stromatolites discovered (Strelley Pool Chert, Western Australia)

represent morphologies too complex to not have been formed by biological activity. This interpretation indicates that microbes (at least in the form of bacteria) were present on the earth and constructing bioherms almost 3.5 billion years ago, long before they came to dominate the biosphere.

Stromatolites were most abundant during the Proterozoic and subsequently declined in both numbers and diversity until the present day, where their occurrence is now relatively restricted. It was not until 1961 that Recent stromatolites were fully documented for the first time from Hamelin Pool (Shark Bay), Western Australia (Logan 1961).

3.3.2 Thrombolites

The term thrombolite was first introduced by Aitken (1967) for microbialites ('cryptalgal rocks') that lacked lamination and which exhibited a cm-scale, clotted texture. The word thrombolite takes its name from the Greek *thrombos*, clot; *lithos*, stone. Aitken described the thrombolites from the Cambro-Ordovician of the southern Rocky Mountains. Thrombolites range in age from the Neoproterozoic (Aitken & Narbonne 1989) to the Recent (Moore *et al.* 1984; Moore & Burne 1994), however, they were at their most abundant, diverse and widespread during the Cambro-Ordovician (Kennard & James 1986, Armella 1994). Thrombolite 'clots' (mesoclots of Kennard & James 1986) are more or less discrete rounded to irregular patches (> 500 µm), that differ in colour and/or texture from intervening areas creating a blotchy, un-layered micro-scale fabric.

The origin of thrombolites remains less certain than that of stromatolites. Walter & Heys (1985) viewed thrombolites as bioturbated stromatolites but this is at odds with the evident skeletal nature described by Kennard & James (1986), Pratt & James (1982) and Walter (1994). However, Burne & Moore (1987) agreed with Walter & Heys, that at least some structures interpreted as thrombolites may have formed by bioturbation. These textures are better termed 'thrombolitic', when the mode of formation is less certain.

Modern thrombolites are rare but do exist and Moore & Burne (1994) described thrombolites from Lake Clifton, Western Australia. These thrombolites occur as conical, domical, discoidal and tabular forms (locally forming reefs extending over 6 km along shore). Modern thrombolites have also been described from Great Salt Lake, Utah (Halley 1976), Green Lake, New York (Eggleston & Dean 1976) and Lee Stocking Island (Planavsky & Ginsburg 2009). Fossil thrombolites have been recorded from the Ediacaran of NW Canada

(Aitken & Narbonne 1989), but the oldest reported occurrence of thrombolites are from the 1.9 Ga (Palaeoproterozoic) (Kah & Grotzinger 1992). Despite this, they are primarily a Cambrian and Early Ordovician phenomenon (Kennard & James 1986), whilst forming a significant part of some reefs during the Silurian, Carboniferous and Permian (Kennard & James 1986).

Many thrombolite mesoclots (Section 3.3) consist of a peloidal texture of uncertain origin (the bacteria responsible for this are seldom preserved). Kennard & James (1986) argued that the fundamental difference between stromatolites and thrombolites is that the former were constructed by filamentous bacteria and the latter by coccoid bacteria. This may be the case in some, but certainly not all thrombolites, as examples from Lake Clifton, Western Australia demonstrate that not all examples exhibit mesoclots with diverse and complex microstructures, nor are they necessarily the product of *coccus*-dominated benthic microbial communities (Moore & Burne 1994). Braga *et al.* (1995) studied microbialites from the Miocene of Spain and concluded that thrombolites were the result of neither disturbance nor calcification and that both thrombolites and stromatolites can form by agglutination as well as microbial calcification, with thrombolites resulting from episodic but uneven accumulation of sediment. Formation of thrombolites by metazoan activity and early diagenetic changes was documented by Planavky & Ginsburg (2009).

3.3.3. Dendrolites and leiolites

Dendrolites (Riding 1991) (Greek, *dendron*, tree; *lithos*, stone) have a centimetre scale, bush-like fabric and form large domes similar to stromatolites and thrombolites. They differ from thrombolites in having bushy or tree-like mesoclots in a vertical or radiating fashion, unlike the rounded or irregular clots of thrombolites (Riding 2000). The microfossils *Epiphyton-Renalcis-Angulocellularia* (ERA) are common constituents of dendrolites. The affinities of these microfossils with modern groups are still not certain, but have been suggested by Riding (1991) to be forms of cyanobacteria.

Leiolites of Riding (2000) (Greek *leios*, uniform or smooth; *lithos*, stone) have a relatively structureless, 'aphanitic' macrofabric lacking clear lamination, clots or dendritic fabrics. They most likely result from destruction (evaporate precipitation, diagenesis or bioturbation) of texture.

3.4 METHODS

Microbialites within the Durness Group were described, photographed and where necessary, samples were taken. Selected samples were cut, acid etched and stained with alizarin red and potassium ferrocyanide. Preservation is generally poor at both the mesostructural and microstructural scale and many features have been obscured by dolomitisation. No attempt has here been made to apply a rigorous binomial classification to the microbialites studied. Instead the structures have been described in morphological terms, chiefly following those used by Hofmann (1969), Preiss (1976), Shapiro & Awramik (2006) and Armella (1994) (Text-fig. 3.2).

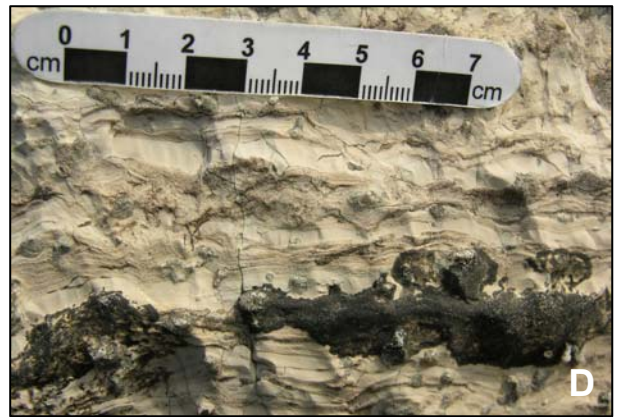
3.5 STROMATOLITES FROM THE DURNESS GROUP

The stromatolites observed from the Durness Group display a range of forms from domed, discoidal and elongate bioherms that are several decimetres to one metre thick, to mounded, gently domed and tabular biostromes a few decimetres or less thick, and to large digitate bioherms measuring up to 1.2 m thick. The stromatolites commonly display greater lateral continuity and lower synoptic relief than the thrombolites.

3.5.1 Stratiform stromatolites

Stratiform stromatolites within the Durness Group have an average thickness of 25 cm. They commonly show crinkly lamination, producing small laterally linked hemispheroids with up to 1 cm of relief. There is sometimes a moderate or high degree of inheritance, with successive laminae following the shape of those below, producing pseudocolumnar and columnar-layered structure (Text-fig. 3.2, 3.3A, B). Within the upper Eilean Dubh Formation (height) bioherms are observed to comprise flat stromatolitic laminae, which are undulatory and show a low degree of inheritance. It appears that the planar stromatolites have been eroded into a nodular morphology (Text-fig. 3.3C, D).

Text-figure 3.3 Planar and encrusting stromatolites from the Durness Group. **(A)** planar stromatolites, showing crinkly microbial laminae, middle Balnakeil Formation. **(B)** planar stromatolites from the upper Sangomore Formation, displaying a pseudocolumnar pattern. **(C)** planar stromatolites, interpreted to have been eroded into mounds, upper Eilean Dubh Formation, Balnakeil Bay. **(D)** detailed view of the stromatolites in (C) showing crinkly laminae and a fenestral fabric. **(E)** encrusting stubby stromatolite biostromes which rest above a karstic surface. The upper surface of the karst is marked by silicification, and silica filled fissures extend downwards (upper Eilean Dubh Formation). **(F)** encrusting stromatolites overlying a karstified surface, upper Eilean Dubh Formation. Pencil for scale. **(G)** encrusting stromatolite overlying a thrombolite boundstone, upper Sangomore Formation. Hammer is shown for scale.



There are a wide variety of mat morphologies observed in present day settings, however following evaporite growth, compaction, and bacterial decay, the result is an almost monotonous display of planar laminate stromatolites with occasional polygonal cracks (Gebelein 1976). Any laminated sediment lacking cross lamination is therefore suspected as being of possible microbial origin, although this may be hard or impossible to prove.

3.5.2 Encrusting stromatolites

Encrusting stromatolites are relatively rare within the Durness Group (Text-fig. 3.3E–G). The bioherms are less than 10 cm thick and on first inspection appear to be standard hemispheroidal bioherms, but they are commonly seen to overlie karst, and maintain the shape of the underlying eroded surface (Text-fig. 3.3E, F). The stromatolites occur at 84 m height within the Eilean Dubh Formation, they are partially linked, and form nodular domes up to 20 cm in diameter. In one bed (Text-fig. 3.3E) the stromatolites overlie a chertified surface, down from which chert-filled fissures extend. Laminae are visible in the lower half of the bed, but they become more diffuse towards the top. Lamina thickness ranges from 0.5 to 2 mm. Encrusting stromatolites occur at 84 m height within the Eilean Dubh Formation. They also are observed to locally overly thrombolites and digitate stromatolites (Text-fig. 3.3G). The laminae are most commonly even, but crinkled (wavy) lamination is observed in some examples.

3.5.3 Hemispheroidal stromatolites

Within the succession, hemispheroidal stromatolites (Text-fig. 3.4) are particularly abundant in the Eilean Dubh and Sailmhor formations, but become less frequent up section. No hemispheroidal stromatolites have been recorded from the Croisaphuill Formation and they are uncommon within the Durine Formation. The Eilean Dubh Formation at Assynt preserves some stromatolites but they are rare in comparison to the section at Balnakeil Bay.

The stromatolites form isolated, low relief domes (bioherms) or tabular and domed biostromes (Text-fig. 3.4A). Stromatolite beds may be as much as 70 cm thick but the stromatolites show domes with an amplitude of around 10 cm, and a wavelength of 40 cm. The hemispheroids are commonly linked and composed of even, crinkly or dentate microbial laminae. The laminae comprise sub mm-scale laminated micrite, displaying small desiccation cracks and fenestrae.

Domed stromatolites may develop due to:

- 1) Upward yielding of the mat to growth expansion.
- 2) Doming over pre-existing irregularities, mud cracks, breccia fragments, domes.
- 3) Preferential microbial growth on surface highs.
- 4) Differentiation of relief features under the mat by more active growth and sediment binding on the highs (Logan 1961).

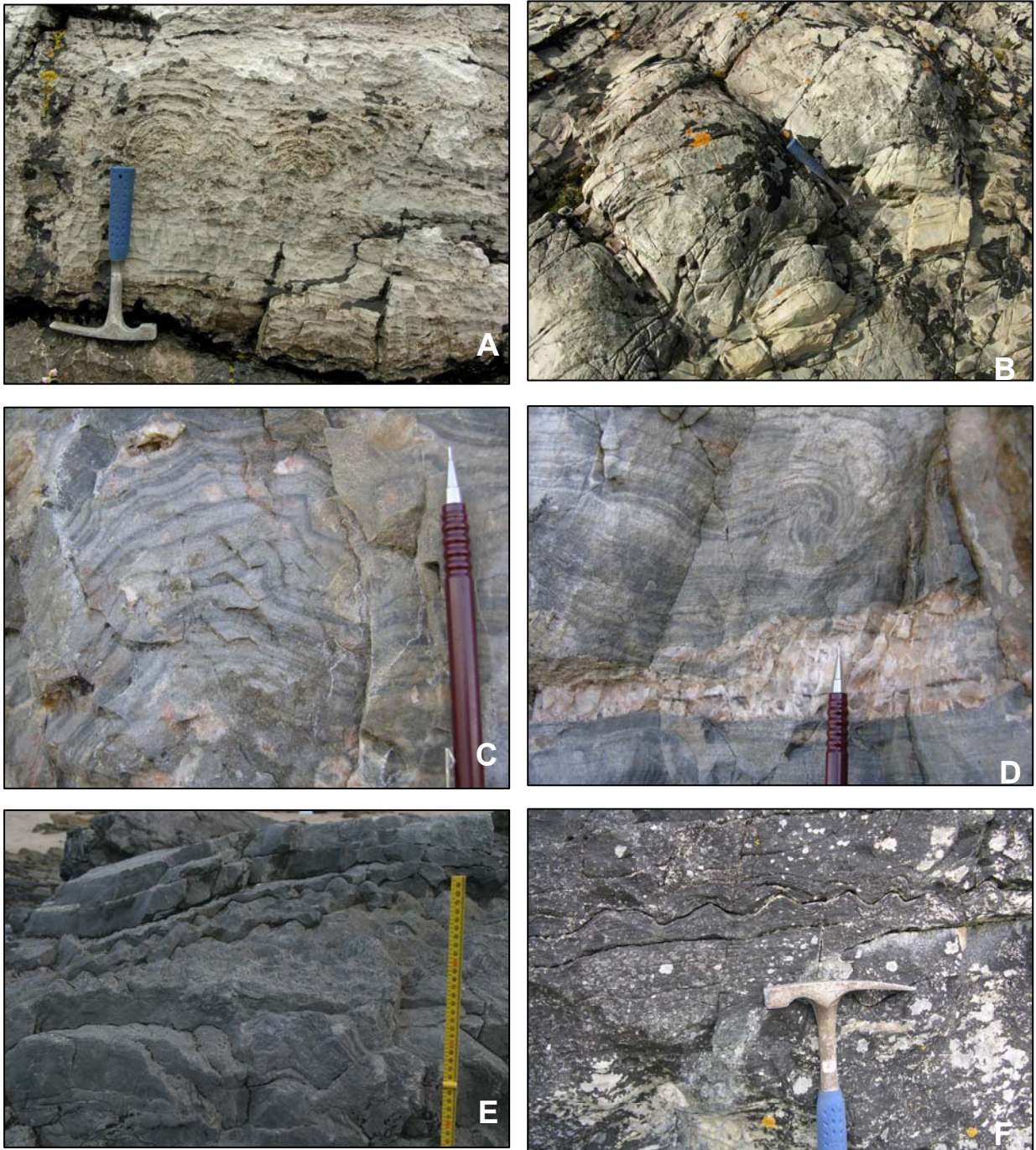
3.5.4 Columnar stromatolites

The stromatolites comprise laminated, non-linked, vertically stacked columns with a branching, cylindrical morphology. They vary in diameter from 1 cm to 10 cm and are seen to form both domed biostromes and subspherical bioherms. Bioherms may be up to 1.2 m high, and biostromes commonly 40 cm thick. Biostromes within the middle Eilean Dubh Formation form continuous beds 30 cm thick, which follows the topography of underlying domes of vuggy dolostone 1–3 m wide.

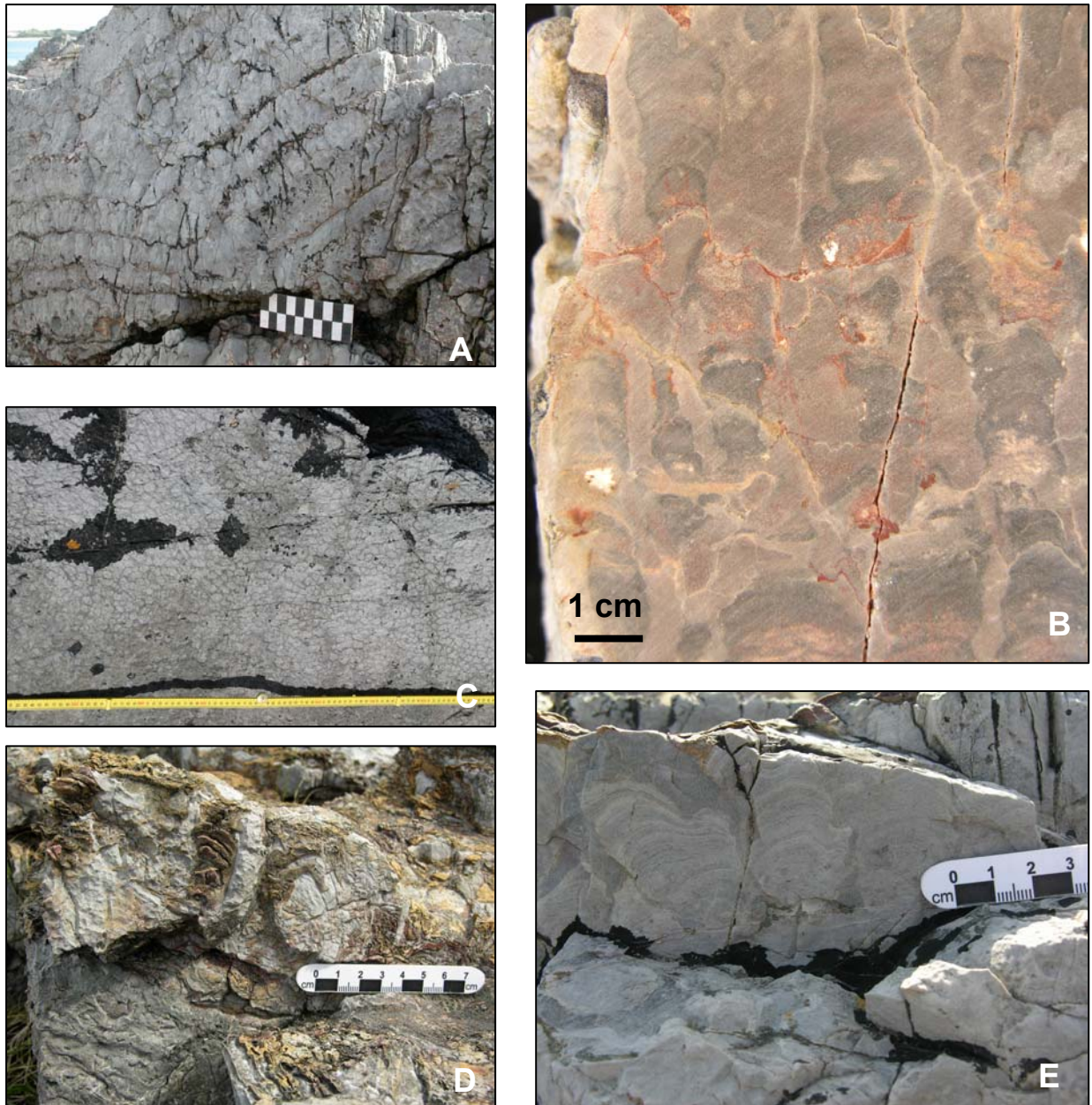
Within the Eilean Dubh Formation (Text-fig. 3.5, 3.6A,B) and Sailmhor Formation the columnar stromatolites are cylindrical and unbranching, commonly 25 cm high and 10–15 cm wide. They persistently form at the bases of parasequences and rest on flooding surfaces. The largest columnar stromatolite bioherms are present within the upper Sangomore Formation and are overlain by a rippled bed of oolitic grainstone 70 cm thick (Text-fig. 3.6C).

Beds of columnar, turbinate and digitate stromatolites are a common part of parasequences within the middle part of the Eilean Dubh Formation between heights of 78–88 m above the base of the Balnakeil Bay section 040907-2. Six horizons are recognised comprising contiguous domes up to 3 m in diameter. The basal surface of the stromatolite bioherms has a relief of up to 15 cm. The main body of the stromatolite unit is composed of columnar, commonly bifurcating (digitate) stromatolites, locally constricted and turbinate, with typical diameters of 1–2 cm. (Text-fig. 3.5B). The columns are divided into layers 3–10 cm thick, by thin, more easily eroded ‘bedding planes’, which appear to be stylolitic (Text-fig. 3.5A). These bedding planes may represent breaks in microbial growth. In some cases the stromatolite (column) growth appears to be continuous through the break whereas in others it is not. Apparent continuity of the columns may reflect nucleation of the renewed microbial mat on a previously existing column. The stromatolitic columns (as seen in the vertical

section; Text-fig. 3.5A) are commonly orientated approximately at right angles to the enveloping surface of that dome so that, at the dome edges, the columns are almost horizontal.

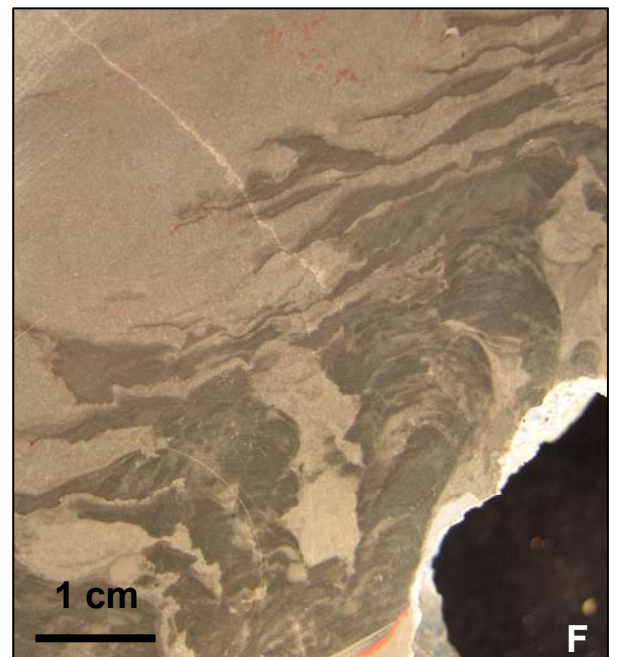
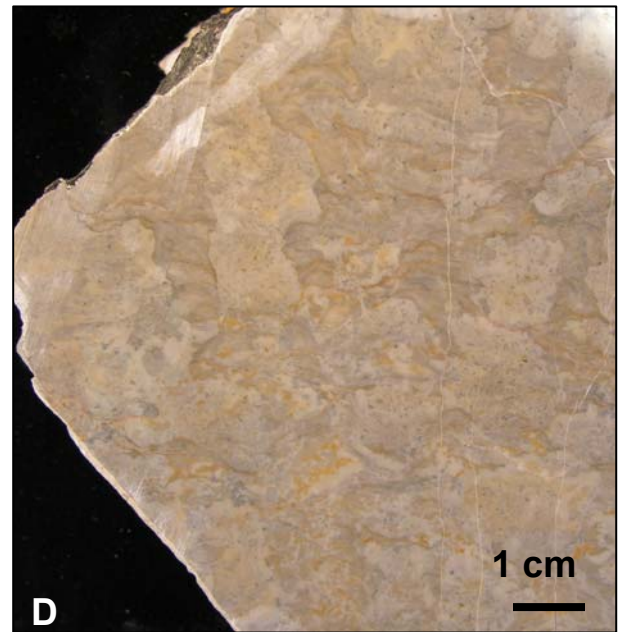
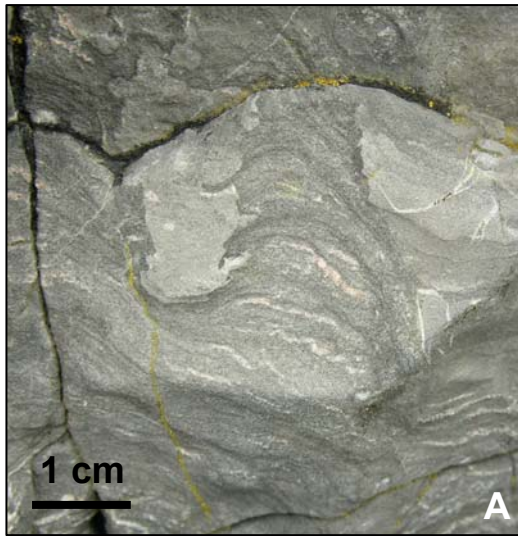


Text-figure 3.4 (A) hemispheroidal stromatolites forming a biostrome, lower Eilean Dubh Formation, Kyle of Durness. (B) contiguous, aligned and elongated stromatolite bioherms in plan view, Eilean Dubh Formation. (C) hemispheroidal stromatolite displaying laminae with a dentate cross section, lower Sangomore Formation. (D) isolated cusperate stromatolite bioherms overlain by a hemispheroidal stromatolite, lower Sangomore Formation, (E) large stromatolite bioherms in plan view, displaying parasitic linked hemispheroids, Balnakeil Formation. (F) cross section of the same bed.



Text-figure 3.5 Examples of columnar stromatolites from the Eilean Dubh Formation. **(A)** large domed biostromes with multiple layers of columnar stromatolites. **(B)** plan view of the same bed. **(C)** polished slab of the same bed displaying individual columnar, digitate stromatolites. **(D)** Small chert replaced columnar stromatolites resting on an eroded upper bed boundary. **(E)** stubby digitate, columnar stromatolites locally displaying a karstified upper surface.

Text-figure 3.6 Columnar stromatolites from the Sailmhor and Sangomore formations. **(A)** columnar stromatolites from the Sailmhor Formation. The columns display a ragged margin. **(B)** turbinate columns preserved in chert at the base of a parasequence within the Sailmhor Formation. The chert preferentially preserves the stromatolites and parts of the surrounding oncoidal and peloidal grainstone. **(C)** 1.2 m thick bioherm of columnar stromatolites within the upper Sangomore Formation. **(D)** polished slab from the same bed shown in (C). The stromatolites display bridges between adjacent columns. **(E)** nodular bioherm of columnar stromatolites from the upper Sangomore Formation. **(F)** close up view of a polished slab from the bioherms depicted in **(E)**. The stromatolites comprise small turbinate forms which become increasingly ranges towards the top and grade into planar stromatolites.



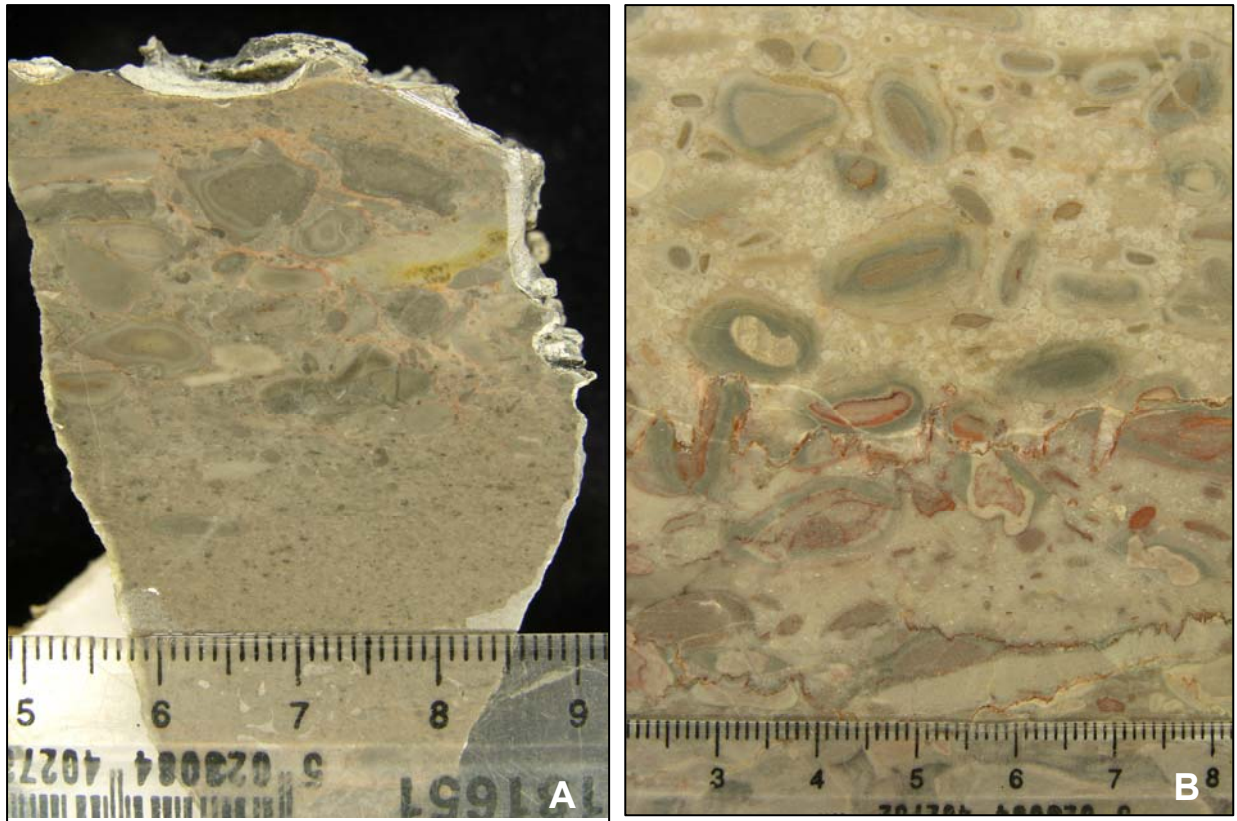
The upper surface of the bioherms shows many columns with minor inter-stromatolite material (Text-fig. 3.5C).

The mesostructure of the columnar stromatolites comprises non-linked, vertically stacked, highly arched hemispheroids. The stacked hemispheroids form cylindrical shaped, non-branching columns 1.5 cm in diameter and up to 8 cm high. The columnar stromatolites are gregarious, forming extensive biostromes consisting of many hundreds of columnar stromatolites. In these, the stromatolites form broad domes up to 3 m wide with up to 50 cm of relief.

Columnar stromatolites are more varied within the Sangomore and Balnakeil formations. Towards the top of the Sangomore Formation (48 m height), a 1.2 m thick bed of bioherms (up to 45 cm in diameter) contains columnar digitate and anastomosed stromatolites with ragged margins (Text-fig. 3.6C, D). Laminations often form bridges between adjacent stromatolites columns. Columns are mostly 1.5 cm in diameter. In another bed at 50 m height above the base of the Sangomore Formation comprises small bioherms, which upon first inspection appear to be thrombolites, in polished section however display faintly laminated, constricted, turbinate columns at the base. Towards the top the columns become increasingly ragged and laminations extend outwards some 2 cm from the columns (Text-fig. 3.6E, F).

3.5.5 Oncolites

Oncoids commonly occur at the bases of parasequences. Silicification has preserved 20 cm of oncoidal packstone, surrounding columnar stromatolites, 47 m above the base of the Sailmhor Formation, where the oncolite is preserved by selective silicification of the stromatolites and parts of their surrounding inter-reef facies by black and white chert (Text-fig. 3.6B). Oncoids and associated peloids also occur in a 5–21 cm bed, 80 m above the base of the Sailmhor Formation. The Sangomore Formation contains two horizons within which oncoidal and peloidal packstone is present. Between 37 and 39 m above formation base a 30 cm bed and other thin layers of oncoids are seen. The thickest bed contains oncoids which are discoidal and commonly 2 cm in diameter and 1 cm thick (Text-fig. 3.7A). Within the beds above this, oncoids are present but much smaller in size (2–4 mm). The second horizon containing oncoids occurs at the top of the Sangomore Formation, and comprises a tabular bed 20 cm thick.



Text-figure 3.7 Polished slabs displaying oncolites. **(A)** upper Sangomore Formation (38 m). **(B)** basal Balnakeil Formation.

The oncolites from the Durness Group range from 0.5 to 3 cm in diameter (macro-oncolite) are non-skeletal (spongiostromate) oncolites and are distinctly laminated around intraclasts. The surface of the oncolites is locally lobate but the majority are smooth. The laminations are dominantly uniform but there are some subordinate asymmetrical forms. Smaller nuclei tend to have larger cortices than large intraclasts which have a reduced and more asymmetrical cortex (Text-fig. 3.7). They can be classified as ‘type c’ oncolites (Logan *et al.* 1964), some laminae non-continuous, but all comprise micrite and sparite laminae, with a fenestral fabric. Oncoidal grainstones and wackestones are commonly found as inter-reef facies of columnar stromatolite bioherms and thrombolite bioherms/biostromes.

3.6 LEIOLITES FROM THE DURNESS GROUP

Leiolites occur within the Eilean Dubh Formation, but there is evidence to suggest that they result from destruction of the texture of a stromatolite precursor. Many of the stromatolites within the Eilean Dubh Formation show diffuse laminae and are commonly associated with evaporite pseudomorphs. This is supported by studies conducted by Planavsky & Ginsburg (2009) on Bahamian thrombolites. Vugs after crystallotopic gypsum occur in many of the leiolitic biostromes and bioherms from the Eilean Dubh Formation (Text-fig. 2.17E) and growth of a more disseminated fraction may have been responsible for the destruction of the texture. The leiolites can here be interpreted as biostromes of columnar and digitate stromatolites, and so are not discussed in detail.

Commonly the primary clotted fabric of the thrombolites has been accentuated by patchy recrystallisation and locally by dolomitisation. Leiolitic (cryptomicrobial forms) may occur as a result of:

- 1) Oxidation and bacterial decay of the formative microbial community to produce non laminated massive sediments (Gebelein 1969; Dravis 1983) or irregular voids that are subsequently infilled to form patches of detrital sediment or carbonate cement (Monty 1976).
- 2) Bioturbation (Neumann *et al.* 1970; Walter & Heys 1985; Planavsky & Ginsburg 2009).
- 3) Dehydration, desiccation, compaction and displacive growth of evaporites or other early diagenetic minerals (Park 1977; Planavsky & Ginsburg 2009).
- 4) Relatively late diagenetic processes, such as neomorphism, solution, stylolitisation, dolomitisation and silicification. (Howe 1966; Chafetz 1973, Semikhatov *et al.* 1979).

3.7 THROMBOLITES FROM THE DURNESS GROUP

Thrombolites from the Durness Group form tabular biostromes, and locally bioherms with a variety of morphologies. Where not obscured by recrystallisation, lower biostrome boundaries are developed on sharp, erosional surfaces, with up to several decimetres of relief. Assessing the biostromes' true dimensions is hampered by limited lateral exposure across the section. The thrombolites characteristically occur in large numbers at a given horizon forming a

biostrome, and biostromes of stacked thrombolite bodies have not been observed. The thrombolites may also be arranged in a stratiform (tabular, domed or mounded), subspherical, arborescent, cone shaped or vertical ellipsoid megastructure (Text-fig. 3.2). Biostromes of thick tabular thrombolites lacking conspicuous relief at the upper surface are common. These biostromes may be easily confused for burrow mottling. Unless laterally tracing of the “bed” reveals an edge to the bioherm or pocket of bedded carbonate filling the space between 2 thrombolites such beds are thus not resolvable into the individual constituent bodies.

Nearly all the thrombolites share the same microstructure of a grumulous fabric, dominated by dark spherical masses (see Turner *et al.* 2000) (Text-fig. 3.10H). This comprises individual, coalesced and multiple lobate bodies of non-ferroan calcite microspar, separated by irregular patches of massive micrite.

The exact origin of mesoclots in the thrombolites of the upper Durness Group is impossible to determine because they lack internal fabrics and external morphology that can be irrefutably tied to a biogenic, inorganic, or combined biogenic – inorganic origin. Recent work on modern thrombolites from the Bahamas by Planavsky & Ginsburg (2009) suggested that thrombolitic fabric is the result of taphonomic remodeling of a precursor fabric, caused by physical and metazoan disruption, penecontemporaneous micritisation, secondary cementation and localised carbonate dissolution.

3.7.1 Re-interpretation of the ‘leopard rock’

Previous studies

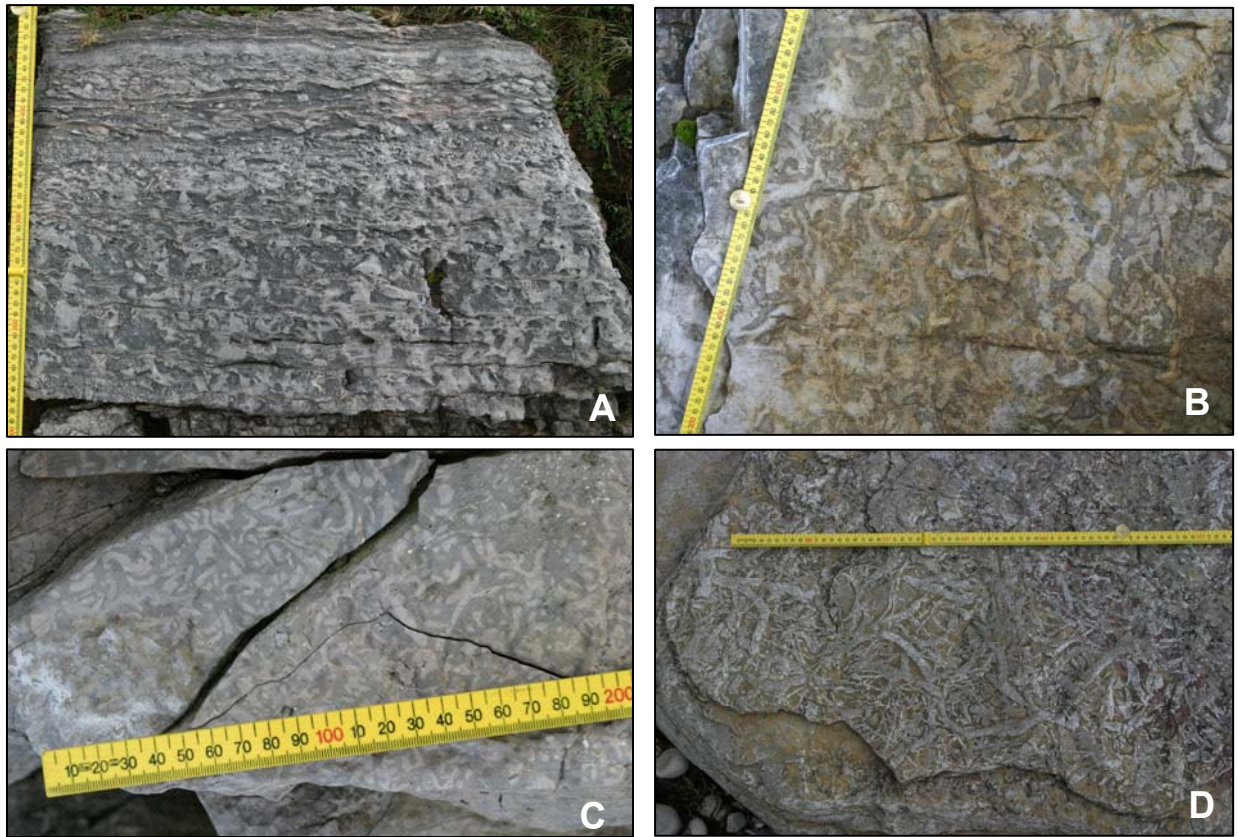
The leopard rock has been referred to in literature since the work of Peach & Horne (1884), and has been postulated to have been formed by variety of different processes. Peach & Horne (1884) described the leopard rock as ‘granular dolomites charged with dark worm-castings, set in a grey matrix’. Grabau (1916) in contrast interpreted the leopard rock to be a product of dolomitisation and Swett (1969) also argued against a biogenic origin, describing it as definitely not burrowing and probably two phases of dolomitisation. The leopard rock was subsequently interpreted by Wright (1985) as being the product of burrowing with a diagenetic overprint, and it was also interpreted to be the result of burrow-mottling by Wright & Knight (1995).

Description

The 'leopard rock' occurs throughout 114 m of the Salmhor Formation (lower Tremadocian), and comprises what are more correctly termed dark grey and light grey, mottled dolostones (Text-fig. 3.12A). They form beds up to 4 m thick, which are tabular in nature. The beds become paler towards the top of shallowing upwards parasequences, and the mottling, although present, becomes increasingly faint. The mottles comprise dark grey, dolomite patches up to 1 cm wide within a matrix of pale grey dolomite. Detailed structure is often difficult to distinguish due to coarse recrystallisation and the proportion of dark mottles varies greatly (with the size varying from a few millimetres to 3 cm in diameter).

Evidence for and against a burrow mottling interpretation

The burrows observed within the Durness Group are primarily of constant width (Text-fig. 3.12B, C), and comprise a pale burrow fill within a comparatively darker, more organic rich substrate. The burrow fill is commonly dolomitised or silicified, whilst the surrounding rock is not. Examples of burrow mottling are seen within the Croisaphuill Formation (Text-fig. 3.18A) and these differ markedly from the morphologies observed within the 'leopard rock'. The distribution of dolomite within the limestones is generally considered to be controlled by the original permeability, resulting in preferential dolomitisation of more permeable sediments commonly associated with the burrows (Rao 1990). The dolomite within the burrows comprises finely-crystalline, subhedral to euhedral crystals and is typical of dolomite formed syndepositionally under near-surface, low temperature conditions (Morrow 1978; Gregg & Shelton 1990). Within the upper Croisaphuill Formation, beds of burrow mottled carbonate have been coarsely dolomitised but are still represented by pale grey mottles within a darker substrate. In plan view beds of burrow mottling commonly display well developed networks of branching burrows (Text-fig. 3.8B). Better preserved burrows from the equivalent formation in western Newfoundland (Boat Harbour Formation) display the branching networks more clearly than those from the Croisaphuill Formation, which has been more diagenetically altered (Text-fig. 3.8D).



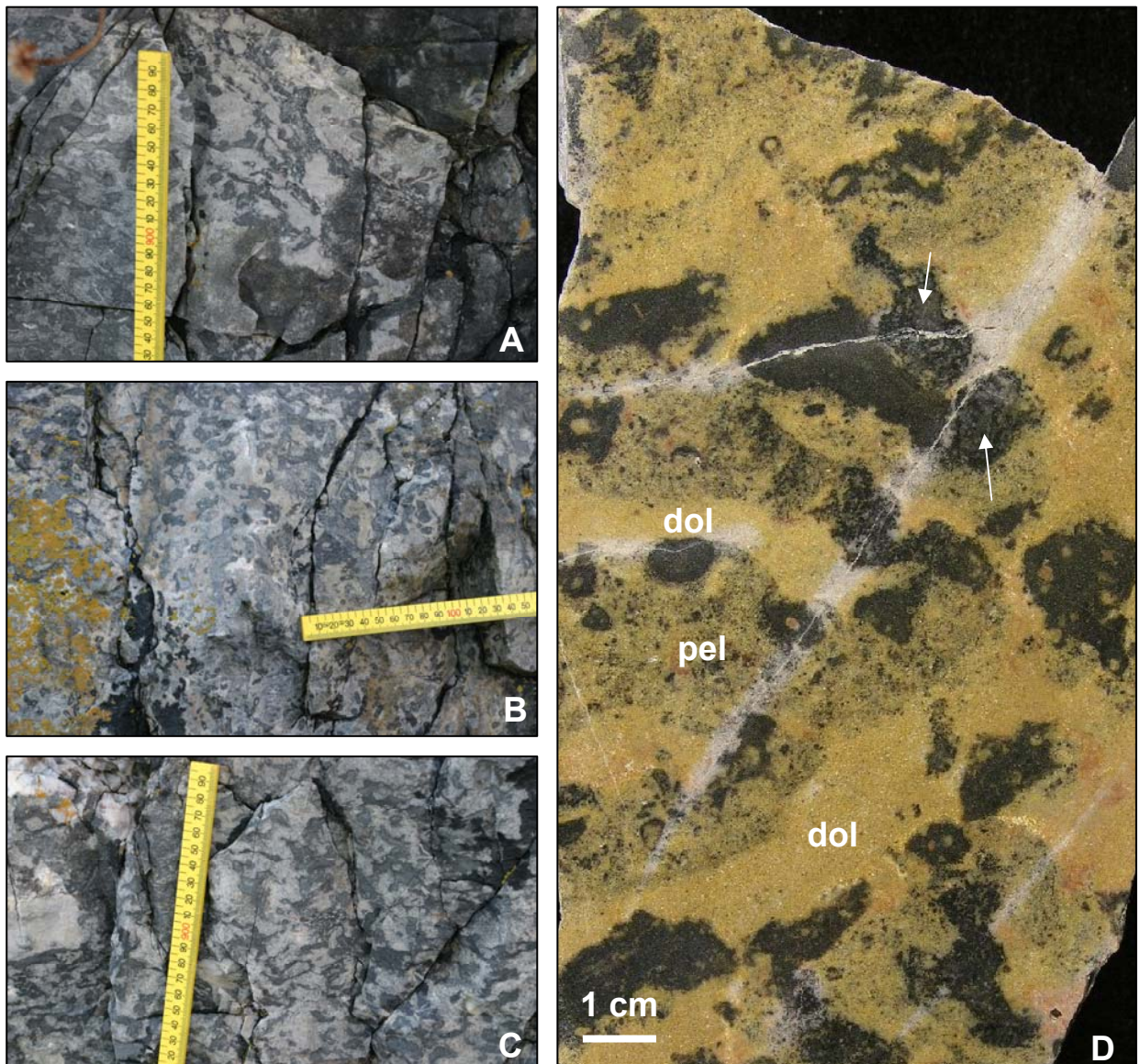
Text-figure 3.8 (A) selectively dolomitised burrows grading into ribbon carbonate heteroliths, Croisaphuill Formation. (B) bedding plane displaying light-grey, branching burrows, middle Balnakeil Formation. (C) simple branching burrows observed on a bedding plane, Ghrudaidh Formation. (D) burrow fill weathering out of a more lime rich lithology, Boat Harbour Formation, western Newfoundland.

Evidence suggesting a microbial origin

A more detailed study of the leopard rock has produced evidence to suggest that it represents beds of thrombolite boundstone, rather than bioturbation. The dark mottling, when not coarsely recrystallised, shows a clotted texture (interpreted as mesoclots) (Text-fig. 3.9D). The dolomite between the dark mottles is seen to comprise peloidal grainstone (Text-fig. 3.9D). In cross section the maceriae are horizontal to encephalitic (Text-fig 3.9). They range in shape from isolated to anastomosed, simple to polylobate masses. In plan view they are commonly meandroid to locally complexly meandroid.

If the ‘leopard rock’ is interpreted as thrombolitic in origin, then microbialites from the Sailmhor Formation are more abundant than previously assumed. Biostromes can be traced laterally for some 4.3 km to Leirinmore, where the parasequences match those from Balnakeil Bay in thickness and internal architecture. Assuming a burrowing origin for the

‘leopard rock’ microbialites (stromatolites) constitute some 16% of the 114 m thick Sailmhor Formation. A thrombolitic diagnosis dramatically changes the proportion of microbialites within the Sailmhor Formation to 70% of the succession and given the lateral consistency of the unit suggests that the microbialites were the most important contributors to sedimentation across a large area.



Text-figure 3.9 Photographs displaying microbialite features of the ‘leopard rock’. **(A)** irregular partly interconnected maceriae. **(B)** simple and lobate maceriae. **(C)** polylobate and anastomosed maceriae. **(D)** polished slab showing a close up view of individual maceriae. Dolomite recrystallisation (dol) has partly obscured the peloidal inter-maceria sediment (pel). Where visible the maceriae display a clotted texture (arrowed).

3.7.2 Domal and columnar thrombolite bioherms

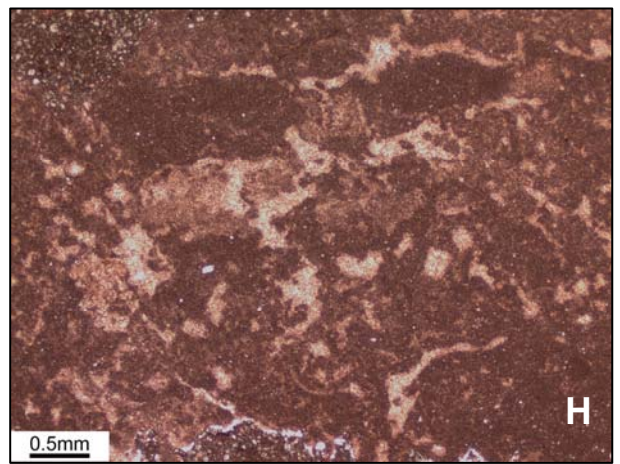
Domal thrombolite bioherms are observed within the middle Sangomore Formation and lower Balnakeil Formation (Text-fig. 3.10C, D). Columnar thrombolite bioherms represent a range of morphologies but commonly show little internal structure. Columnar bioherms are observed within the upper Sailmhor Formation at Smoo (Text-fig. 3.10B) and form within beds of 'leopard rock' texture. Turbinate examples are noted within the middle Sailmhor Formation and lower Balnakeil Formation and rare cone shaped bioherms are recorded from the middle Balnakeil Formation (Text-figs. 3.10E–G).

3.7.3 Stratiform thrombolites biostromes

Stratiform biostromes are the most common thrombolite morphology exhibited within the Durness Group. Biostromes of this type are composites of individual bioherms (Text-fig. 3.10A) that have often coalesced to form an extensive reef (mounded biostrome). They may be up to 4 m thick and occasionally have irregular lower boundaries but often have planar or slightly domal upper surfaces. A stratiform thrombolite biostrome is noted from the uppermost Eilean Dubh Formation (65 cm thick biostrome occurs 23 m below the formation top), but they are most common throughout the Sailmhor Formation, where they occur in almost every parasequence (the 'leopard rock'). Stratiform thrombolites also occur within the Sangomore Formation and parts of the lower Balnakeil Formation.

The mesostructure of the thrombolites comprises maceriae, which commonly exhibit an upward transition from prostrate and encephalitic forms at the base to predominantly pendant and occasionally radial maceriae towards the top of the biostrome (upper Sailmhor Formation at Leirinmore) (Text-fig. 3.10A, B). The prostrate maceriae at the base of the biostrome are small (1 cm) and round in cross section. They are overlain by encephalitic, commonly polylobate and anastomosed or coalesced maceriae. The radially arranged maceriae are predominantly unbranching, isolated and typically 2 cm in diameter. Inter-maceria material consists of peloidal grainstone and bioclastic wackestone/packstone.

Text-figure 3.10 Thrombolites from the Durness Group. **(A)** a tabular thrombolite biostrome from the upper Saimhor Formation, Smoo inlet. **(B)** columnar thrombolites from the upper Saimhor Formation at Smoo. **(C)** thrombolite bioherm within bioclastic wackestone facies in the upper Sangomore Formation, Balnakeil Bay. **(D)** domed surface to a stacked series of thrombolite bioherms, which together form a more extensive biostrome, lower Balnakeil Formation. **(E)** cone shaped columnar thrombolites from the middle Balnakeil Formation. **(F)** bulbous thrombolite bioherms from the basal Balnakeil Formation with a pale brown dolomite inter-reef facies. **(G)** thrombolite bioherm comprising radially arranged individual maceriae. **(H)** thin section micrograph displaying patchy nature of thrombolite mesoclos, comprising irregular areas of non-ferroan calcite spar and intervening clotted micrite from the upper Sangomore Formation. PPL.



3.8 MICROBIALITES AS ENVIRONMENTAL INDICATORS

3.8.1 Stromatolites

Water depth, energy and salinity

Measurements of sediment movement by Gebelein (1969) demonstrated that microbial mats were only likely to form in areas which experienced between 15 and 20 cm s⁻¹ surface current velocity. The thickness of the microbial mat increased as the rate of sediment movement decreased. Microbial domes only formed under 1–11 cm s⁻¹ surface current velocity. In very clear waters around Bermuda, microbial mats have been observed to depths of 50 m, but in general growth is most rapid in depths of less than 10 m (Gebelein 1976). The boundary between laminated sediment and un-laminated varies from place to place depending upon microbe and invertebrate activity within the sediment. At Andros Island microbial lamination dominates above the 50% flooding isograd, whilst on the Florida coast it is represented by the 25% flooding isograd (Gebelein 1976).

The precipitation of gypsum destroys all microbial structures in the upper 20–30 cm of the intertidal zone. This combined with metazoan grazing control in the lower intertidal and shallow subtidal areas limits the microbial flat in areas subject to these processes (Gebelein 1976). At Hamelin Pool, Shark Bay, Western Australia, the salinity is twice that of normal sea water and stromatolites thrive. In the less saline areas the sediment surface is grazed by gastropods. The deepest part of Hamelin Pool is 8–10 m, whilst the shelf water depth is <5 m (Hoffman 1976). Microbial mats are most prominent in the intertidal zone but also extend into the lower supratidal and shallow subtidal environments.

Mats colonise exposed crusts because they represent a more stable substrate, but once established the microbial mats resist turbulent conditions. Although the forms of stromatolite bioherms are dependant upon the physical environment, different types of lamination reflect different mat communities. Three types of mat are most commonly preserved: pustular, smooth, and colloform, although these are seldom preserved in the rock record. Headlands with water depth up to depths of 2 m below mean sea-level display columns up to 1 m in relief, and in places they coalesce to form biostromes. Bights give rise to stromatolites which are more prolate and show only 0.5 m relief. Elongation of the stromatolites is commonly perpendicular to the shore but they may also be arranged in rows parallel to the shore. Within the tidal pond environment digitate columnar stromatolites dominate. The internal structure

occurs beneath ovoid patches, less than 0.5 m in diameter, which are almost completely buried by sediment (Hoffman 1976).

In Shark Bay as a whole, microbial mats and stromatolites are limited in distribution to the intertidal zone where conditions are hypersaline, with salinities 56–65‰ (Logan 1961). Logan interpreted the subtidal bioherms to be a relict of Holocene sea-level rise. Later, Burne & James (1986) claimed that the subtidal zone was where much of the current growth occurred, and that the intertidal stromatolites were essentially stranded by sea-level fall. This question is difficult to answer and microbes have been found to be present on the surfaces of both the subtidal and the intertidal stromatolites, but their roles in accretion are not known.

Conditions needed for the development of microbial mats in the present day are a low to moderately smooth gradient 0.8–0.1 m/km, and restricted tidal influx, with a well defined tidal zonation (Logan *et al.* 1974). Mats at Hamelin Pool, Western Australia form in the supratidal (2 m above prevailing LWL) to the shallow subtidal zone (~4 m depth). In areas of less than 53‰ (metahaline) they are browsed and reduced to thin films. The hypersaline concentration is also important in penecontemporaneous lithification which acts to lower the aragonite precipitation threshold (Logan *et al.* 1974).

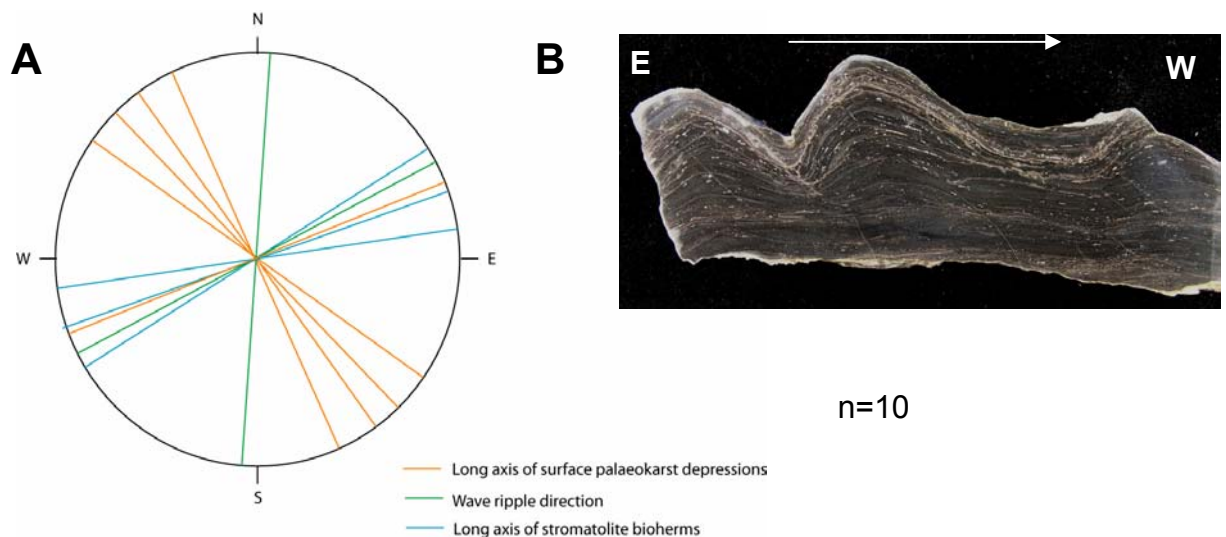
Growth rates

Rates of growth of microbial mats have been suggested to be the accretion of one layer per day (each lamina is approximately 1 mm). This would imply a growth rate of c. 36 cm/yr (Gebelein 1969). Stromatolite accretion rates for the Trucial Coast from buried sections dated to 2000–3000 yrs BP yielded accretion rates of 0.2 mm/yr whereas mats pre-desiccation and compaction yield much higher growth rates of 2.0–2.5 mm/yr (Park 1976, 1977). Growth of microbial mats and eventual formation of cryptomicrobial laminites and stromatolites requires protection from strongly erosive currents and the growth rates require further study before they can be applied to stromatolites from the rock record.

Current directions

A scarcity of bedding plane exposures limits the number of measurements of stromatolite elongation that can be taken. The degree of elongation and asymmetry of columns has been shown to be related to the direction of water flow and sediment transport (Logan *et al.* 1974; Hofmann 1973; Gebelein 1969; Semikhatov *et al.* 1979; Beukes & Lowe 1989). The degree

and nature of lateral linkage observed in some localities (Shark Bay and Bermuda) indicate that the degree of linkage between adjacent stromatolites is a function of sea-floor turbulence and sediment movement and also most likely of the proximity to adjacent growing build-ups (Semikhatov *et al.* 1979). Sedimentation will be greatest on the crest of a dome, therefore perpetuating the dome (Semikhatov *et al.* 1979). Stromatolites within the Durness Group show sediment transport from east to west (Text-fig. 3.11B) and elongated stromatolite bioherms from the Eilean Dubh Formation are aligned in an ENE–WSW orientation. The evidence from ripple cross lamination and elongated karst features suggests that the shore was aligned approximately north-south, and that the stromatolites formed parallel to the coast (Text-fig. 3.11A). With further speculation it can be suggested that wave activity was dominant over currents, which may have streamlined the stromatolites coast perpendicular.



Text-figure 3.11 (A) palaeocurrent data for the Durness Group displaying the long axes of stromatolite bioherms and other palaeocurrent indicators for comparison. (B) stromatolite biostrome from the Balnakeil Formation displaying asymmetry produced by a prevailing sediment transport direction (arrowed).

3.8.2 Thrombolites

Water depth, energy and salinity

Thrombolites in Lake Clifton, Western Australia grow in waters which are below seawater salinity for most of the year (15-35‰) but may occasionally range up to 40‰ (Moore & Burne 1994). In view of the grazing habits of much of the associated fauna it is reasonable to assume that thrombolites provide both a source of food as well as a refuge. The thrombolites are not attached to hard substrates but lie partly buried in the unconsolidated sediments. There

are 3 major types of thrombolite (i.e. tabular, domical and columnar/conical). The height of the thrombolites is limited by the maximum lake level and there is a correlation between depth and thrombolite height and shape, and also between height and energy (taller thrombolites occur in higher energy conditions where mud does not accumulate, whilst shorter, oblate or club shaped forms are recorded from lower energy settings (Moore & Burne 1994).

Thrombolites are interpreted to be a subtidal phenomenon (Pratt & James 1982; Aitken 1967; 1978). The conclusion is also drawn here that the thrombolites of the Durness Group are subtidal. Evidence supporting this view includes the common occurrence of thrombolites with a varied fauna of gastropods and cephalopods (indicating more open marine conditions).

Growth rates

A microbialite on a shell dated to 480 ± 80 years b.p. showed a relief of 90 cm (Dill *et al.* 1986). Feldmann & McKenzie (1998) recovered 15 cm high thrombolites growing on a 17th–19th century ballast stone. Serially dated examples of modern thrombolites show growth rates of 10 cm/100 years (Moore & Burne 1994), essentially half the growth rate of stromatolites. More recently obtained values for thrombolite growth rates indicate accumulation of ~ 0.33 mm/year for Bahamian examples (Planavsky & Ginsburg 2009).

3.9 DURNESS GROUP MICROBIALITES AND PALAEOENVIRONMENT

The sequence of Durness Group microbialites within each parasequence is interpreted to be ecological succession of benthic communities in response to sea-level fluctuations and shoaling sedimentation. The most common sequence in the upper Durness Group is one of decreasing synoptic relief from thrombolite to columnar stromatolite overlain by locally wavy and then planar stromatolites. Parasequences in the lower parts of the succession are relatively thin, dominated by intertidal facies and stratiform stromatolites with a low synoptic relief. Parasequences in the upper part of the Durness Group however are dominated by microbialites including subtidal thrombolite and stromatolite bioherms of relatively high synoptic relief. The interpreted microbial successions compares well to those observed in Hamelin Pool, Shark Bay, Western Australia, where columnar stromatolites are interpreted to have formed in a turbulent environment (Aitken 1967, Logan 1961).

A plot of the readings that have been obtained shows good correlation with measurements of ripple crest direction in associated grainstones and implies that the stromatolites were forming parallel to the shore. Some biohermal stromatolite beds in the sequence show weak asymmetric growth, similar to that reported by Hofmann (1973). The asymmetry indicates a supply of mud from the east (Text-fig. 3.11B).

Flat microbial laminites in the Durness Group are interpreted to have formed in the supratidal and uppermost intertidal zones of the tidal flats as evidenced by the commonly associated desiccation cracks, the uniformity of the lamination and the buckling and brecciation of the beds (tepees and flake breccias). Hemispheroidal stromatolites always occur beneath the laminites in the shallowing upward parasequences and most likely represent deposition within the intertidal zone. Below the stromatolites there is commonly 25–50 cm of massive or fenestral dolostone which may represent microbial mat that has suffered from the effects of burrowing or evaporate precipitation. It is likely that the mat was not lithified early enough to avoid destruction. A change upwards from microbial laminites to laterally linked hemispheroids in the St George Group of western Newfoundland (Pratt & James 1982) suggests transition from the supratidal to intertidal environment (deepening up), accompanied with an increase in scour, promoting the formation of domes. The reverse is true for much of the Durness Group.

The stromatolites within the Durness Group commonly show constant radius and no walls, indicating that the sedimentation rate was constant on both the mats and the surrounding substrate, resulting in the maintenance of a low synoptic relief. The columnar stromatolites probably formed when microbial mats experienced scour as a result of increased wave and storm activity, indicative of the lower intertidal to shallow subtidal environment.

Layers of domal stromatolites are characteristically persistent, and in one bed within the Eilean Dubh Formation can be traced for half a kilometre with no visible change. The lithological associations of the Durness Group stromatolites is indicative of very shallow water to intermittently emergent conditions, and the widespread early dolomitisation is also suggestive of hypersaline and/or emergent conditions. Feldmann & McKenzie (1997) and Aitken (1967) interpreted fossil thrombolites as having occurred in a subtidal environment under more or less normal marine conditions. This is supported by the diverse fauna often associated with them; the burrowing organisms that the mounds sometimes host, the flanking

beds never displaying mudcracks. Bioherms within parasequences show a change from thrombolites to stromatolites.

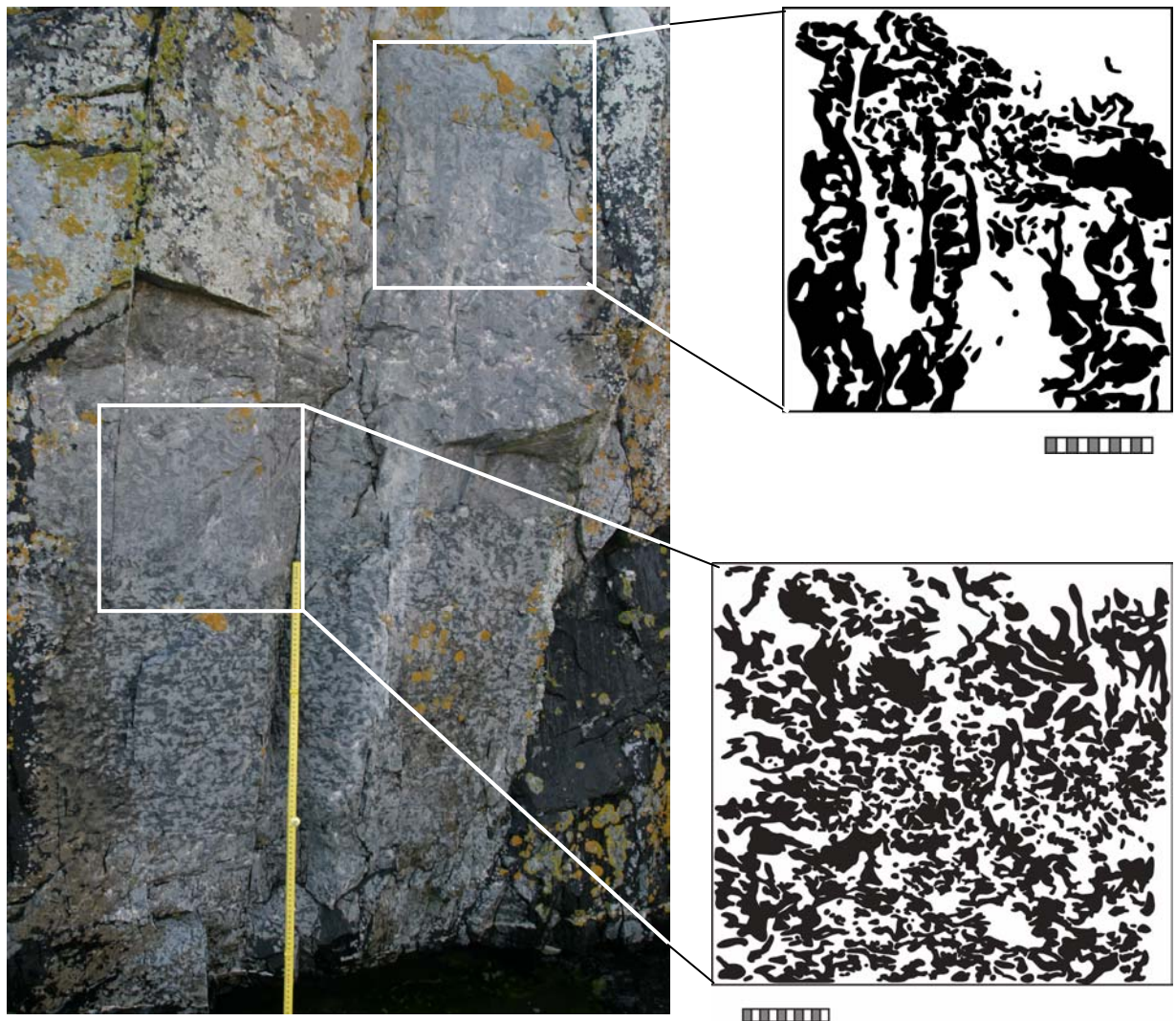
3.10 TEMPORAL TRENDS OF PALAEOENVIRONMENTAL CHANGE

3.10.1 Short term temporal trends

Microbialites form a significant part of parasequences within the Sailmhor Formation and the repetitive occurrence of microbialite successions and associated facies can give clues to the environments of deposition of each type of microbialite. The parasequences are dominantly of a shallowing upwards nature. The base is distinguished by a sharp deepening (marking a flooding surface). Typical microbialites from the base of the cycles comprise columnar stromatolites and oncoids (which are often silicified) (Text-fig. 3.6B). These stromatolites and oncoids are surrounded by bioclastic and peloidal grainstones, which form the inter-reef facies. Tabular thrombolite biostromes then overlie the stromatolites. They are up to 4 m in thickness and locally show the shapes of individual bioherms that comprise them, but mostly they exhibit a close network of maceriae (Text-fig. 3.10A). The thrombolites bed tops are normally planar and are overlain by hemispheroidal stromatolites bioherms which become progressively more planar up-sequence (Text-fig. 3.4A) and are commonly overlain by ripple laminated dolostone (Text-fig. 3.16).

The columnar stromatolites represent deposition after the initial flooding of the supratidal flats. Water depth increased as did turbulence, causing established microbial mats to be locally disrupted and encouraged the growth of columns. Fragments of the mat that were dislodged commonly become oncoids, following increased lamina accretion and constant agitation. The overlying thrombolites represent growth in a more settled subtidal regime. Local complete cephalopods and gastropods suggest not only a normal salinity, but also a sheltered environment, providing a refuge for some organisms. The initial colonising maceriae are primarily horizontal, and of a small size (Text-fig. 3.12). They increasingly become more upright and sometimes form columnar thrombolites bioherms (Text-fig. 3.12), but more often than not form a dense network of maceriae. The change in shape and orientation of the maceriae may be indicative of increasing accommodation space during deposition of the lower part of the parasequence. If this is the case, it suggests that many of the cycles may be more symmetrical than asymmetrical (asymmetry is commonly assumed

for parasequences due to the pronounced flooding at the base). It may also indicate an increase in wave energy as the thrombolites filled available accommodation space.



Text-figure 3.12 Thrombolite biostrome within a parasequence in the upper Sailmhor Formation, Smoo inlet. Tracings of the thrombolite shows a succession of flat lying maceriae overlain by upright maceriae representing columnar thrombolites (Photograph shows part of a 1 m rule for scale and the tracings display cm-scale bars).

There is no doubt that the overlying fine grained laminites, typified by hemispheroidal and subsequently planar stromatolites, represent progradation of intertidal flats over the subtidal thrombolites reefs. With increased sedimentation, accommodation space was reduced and supratidal flats also prograded. These supratidal flat deposits are then in turn overlain by the columnar stromatolites and dark grey dolostones of the succeeding parasequence.

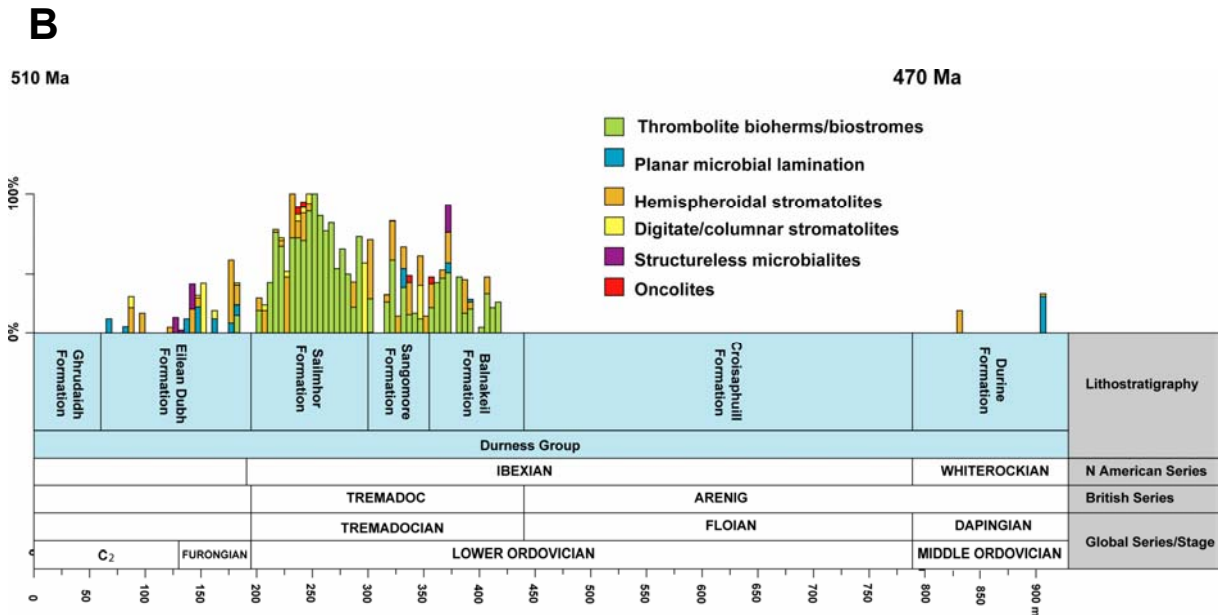
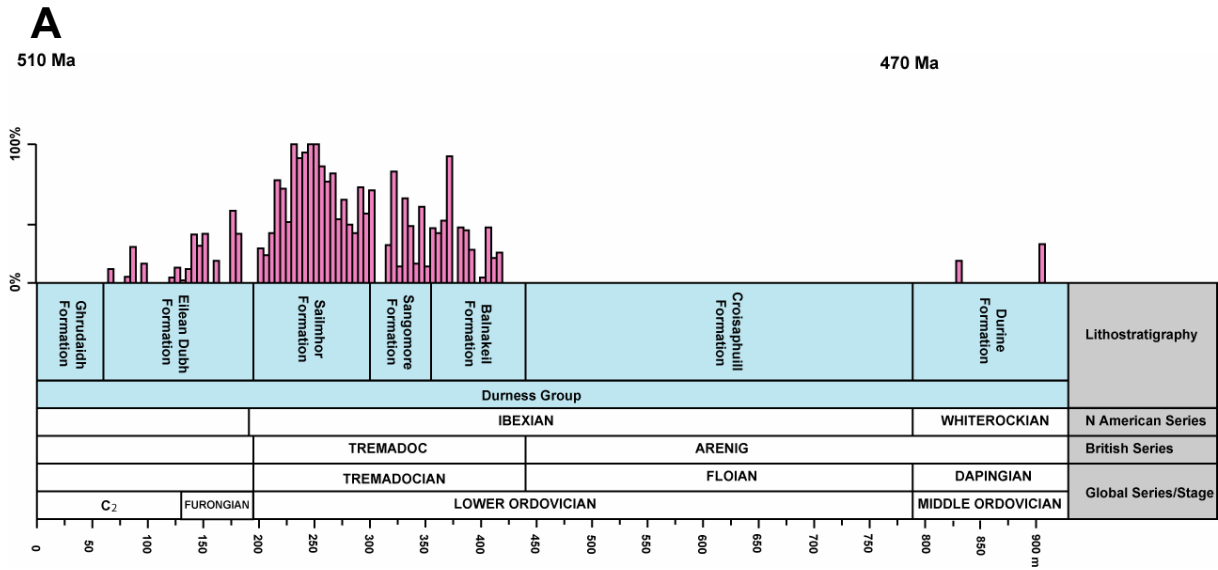
3.10.2 Long term temporal trends

Abundance data

In order to assess the abundance of microbialites a plot was constructed for the type section of the whole of the Durness Group. There have been few studies to quantify the abundance of microbialites through any Phanerozoic sections. Kiessling (2002) published abundance data which included the occurrences of microbialite reefs within separate sedimentary basins. This gives an approximate record of abundance but not at the resolution desirable for a meaningful study. Reef numbers used by Kiessling (2002) represent reef sites rather than bioherm abundance or volume (which is difficult to quantify). Kiessling grouped together age equivalent reefs from one area of more than 300 km² as a single occurrence.

In the current study, the 930 m logged section was divided into arbitrary units of 5 m thickness, for each of which the volumetric proportion of microbialites was worked out as a percentage of total sediment thickness per bin (Text-fig. 3.13). The percentage of microbialites within the studied section represents a minimum estimate, due to the difficulty of distinguishing planar stromatolites from parallel lamination. This stromatolite form has only been included where the identification is conclusive. The chart shows that microbialites constitute some 14% of the total rock record within the Durness Group. The abundance is not scattered randomly but shows a distinct trend through time. Microbialites are absent in the lowest formation (Ghrudaidh) and first appear in the Eilean Dubh Formation (11% of the formation thickness) (Text-fig. 3.13A). Abundance rapidly increases at the base of the Sailmhor Formation where microbialites locally constitute 100% of some intervals (with the revised interpretation of the leopard rock) and 70% of the formations' total thickness. Microbialite abundance is variable within the Sangomore and Balnakeil formations but shows an overall decline from 34% to 23%.

Microbialites are not recorded from the Croisaphuill Formation, but this may represent an absence of visible bioherms and biostromes rather than an absence of microbial influence in the sediments. Microbialites are abundant in the time equivalent unit (Catoche Formation) in western Newfoundland (Pratt & James 1982). The uppermost unit of the Durness Group, the Durine Formation contains occurrences of microbialites but they are not volumetrically important.



Text-figure 3.13 Plots of microbialite occurrences as a percentage of total rock thickness. **(A)** microbialite abundance through the Durness Group. **(B)** microbialite morphological diversity through the Durness Group.

Microbialites are recorded from the correlative Aguathuna Formation (western Newfoundland) but the abundance there is not recorded (Knight *et al.* 1991). The facies present in the Durine Formation would commonly contain abundant microbialites and it may be that the true proportion is underestimated in this study due to the coarse dolomitisation of much of the Durine Formation and the incomplete outcrop.

Diversity data

The diversity data for this section shows that planar stromatolites are most abundant within the Eilean Dubh Formation. Hemispheroidal stromatolites are distributed throughout the Durness Group, but form a volumetrically significant portion of the section through the Eilean Dubh, lower Sailmhor and Sangomore formations. The most marked change in microbialite community is the dominance of thrombolites within the Tremadocian (Sailmhor, Sangomore and Balnakeil formations). The proportion of thrombolites declines in the Sangomore and Balnakeil formations and is replaced by a more wide variety of microbialite forms (Text-fig. 3.13B).

Shapiro & Awramik (2000) successfully conducted microbialite morphostratigraphy on the Cambro-Ordovician rocks of the Great Basin, United States, and it has been utilised in pre-Phanerozoic strata for many years (Cloud & Semikhatov 1969). Shapiro & Awramik considered it helpful in peritidal environments where biostratigraphically useful fossils are scarce. However, if microbialite morphology reflects only environmental conditions it will therefore reflect changes in the sea-level or facies and is essentially a tool for lithostratigraphy/sequence stratigraphy (not biostratigraphy), but one which adds more support to a correlation. Riding (2000) suggested that microbialite morphology is influenced by a range of factors and that over time microbial communities may evolve, producing a chronologically unique form. Papineau *et al.* (2005), however, showed that there were some 28 species present in a microbial mat at Shark Bay, and Kennard (1994) suggested that the mesostructure of stromatolites and thrombolites was controlled by a complex interaction of biological and environmental factors whilst the megastructure was primarily controlled by environmental factors.

The common view is that stromatolite morphologies are determined by the types of bacteria present and/or the environment in which they grew (Beukes & Lowe 1989, Thurgate 1996, Immenhauser *et al.* 2005). In another study on recent stromatolites from Cenote Lake, SE Australia, Thurgate (1996) suggested that the stromatolites displayed high morphotype diversity due to the presence of different microbial communities. In contrast, Walter (1977) proposed that a balance of hydrodynamic level and luminosity served to determine stromatolite morphology. Stromatolite morphology has also been viewed as a cumulative effect of changing environmental conditions through time (McInnish *et al.* 2002). Hoffman (1976) also showed that the internal fabric was related to the constituent microbial mat, each

of which had a specific environmental setting. Smooth mat (lower intertidal zone), pustular mat (upper intertidal zone) and colloform mat (subtidal) were the main mat type comprising stromatolites within those environments. Knoll & Semikhatov (1998) have demonstrated a single mat community can give rise to several distinct lamination textures, depending upon relative timing of organic decay and carbonate production. If this is the case, changes in the diversity of microbialites may only indicate a change in environment, rather than an indication of the evolution of microbial communities through time. Use of diversity data assumes we know what a stromatolite morphotypes represents. There is broad agreement that morphology is affected by environment as well as biology. It is here considered that microbialite morphology is most indicative of base-level change. An increase in relative water depth also affects sedimentation rate, circulation, salinity and energy. If the microbial forms are ranked in order of interpreted water depth from shallowest to deepest, based on their repeated occurrence within specific parts of parasequences. They may be ordered as such, starting with the shallowest environments. Planar stromatolites commonly occur at the top of parasequences and are associated with aeolian quartz sand and evaporites. The planar stromatolites overly laterally linked low domes, which in turn overly larger hemispheroids and separated hemispheroids. This succession is repeated in many of the parasequences. The bases of the parasequences and almost always underling hemispheroidal stromatolites columnar stromatolites, oncoids and thrombolites are observed. The oncoids commonly surround the columnar stromatolites and are interpreted to have formed in a similar water depth.

3.11 THE RISE AND DEMISE OF CAMBRO-ORDOVICIAN MICROBIALITES

The changes shown in microbialite communities are not fully understood, but possible causes are discussed below. The apparent increase in abundance, diversity and importance of microbialites during the middle Cambrian and Lower Ordovician has been termed the 'Cambro-Ordovician microbialite resurgence' (Shapiro & Awramik 2006). Thrombolites are rare during the Sauk II sea-level cycle (see Chapter 5). During Sauk III, sea-level was higher, and thrombolites become the dominant reef type. The resurgence of microbialite reefs from the middle Cambrian to the Early Ordovician, represented a time more reminiscent of the Proterozoic, and spans some 40 million years. It occurs between the demise of early Cambrian

archaeocyathid reefs and the stromatoporoid–coral–receptaculitid reef development of the Middle Ordovician.

The Cambrian to Ordovician was a dynamic time in the Earth's history: major new metazoan taxa were radiating (Sepkoski 1992, 1997; Harper 2006), sea-level was generally rising (Vail *et al.* 1977; Haq & Schutter 2008), atmospheric CO₂ levels were at their Phanerozoic peak (Berner & Kothavala 2001) and greenhouse conditions prevailed (Crowley & Berner 2001) (Text-fig.3.14).

Microbialites are arguably at their most diverse during the Cambro-Ordovician, certainly in terms of disparity of form, with not only stromatolites and thrombolites occurring but also dendrolites (Riding 2000). There has been little attempt to comprehensively document stromatolite morphology during the Phanerozoic (Awramik & Sprinkle 1999). Abundance data published so far has been only qualitative and concern Precambrian stromatolites (Grotzinger 1990; Walter *et al.* 1992 and Schopf 1992).

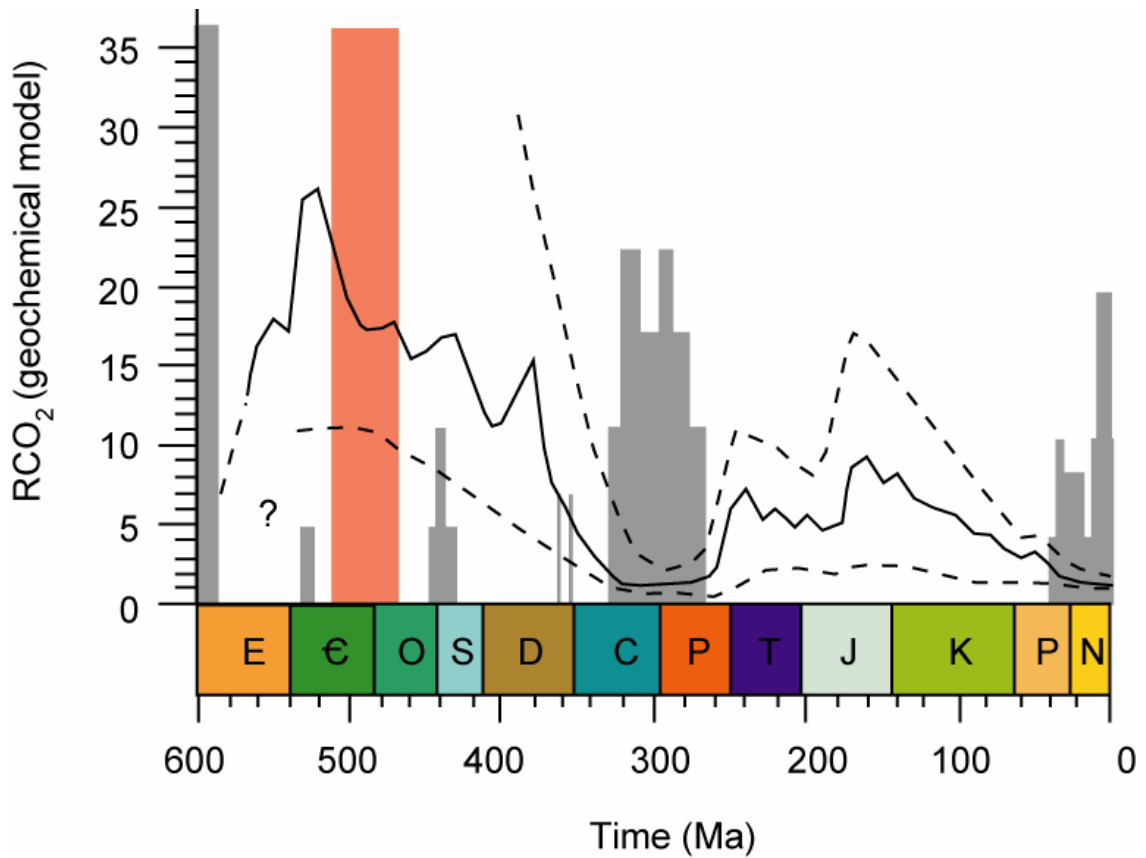
Although the decline on the graph (Text-fig. 3.13) largely reflects a change to facies in which microbialites are not common it does not necessarily indicate their 'extinction'. The facies within the Durine Formation would be expected to contain a significant number of microbialitic sediments, however there are surprising less abundant than expected. In comparison, in western Newfoundland thrombolites are uncommon in the Aguathuna Formation (equivalent of the Durine Formation), in contrast to the Catoche Formation (equivalent of the Croisaphuill Formation) (Pratt & James 1986).

Factors that may have influenced microbialite reef development include biotic evolution, plate movements, eustatic sea-level change, nutrient availability, palaeoclimate and shifts in sea-water chemistry (Rowland & Shapiro 2002). The 'disappearance of metazoans from reef communities during the mid Cambrian to Early Ordovician is as striking as.... the temporary replacement of mammals by dinosaurs in terrestrial communities during the Miocene' (Rowland & Shapiro 2002, p. 96).

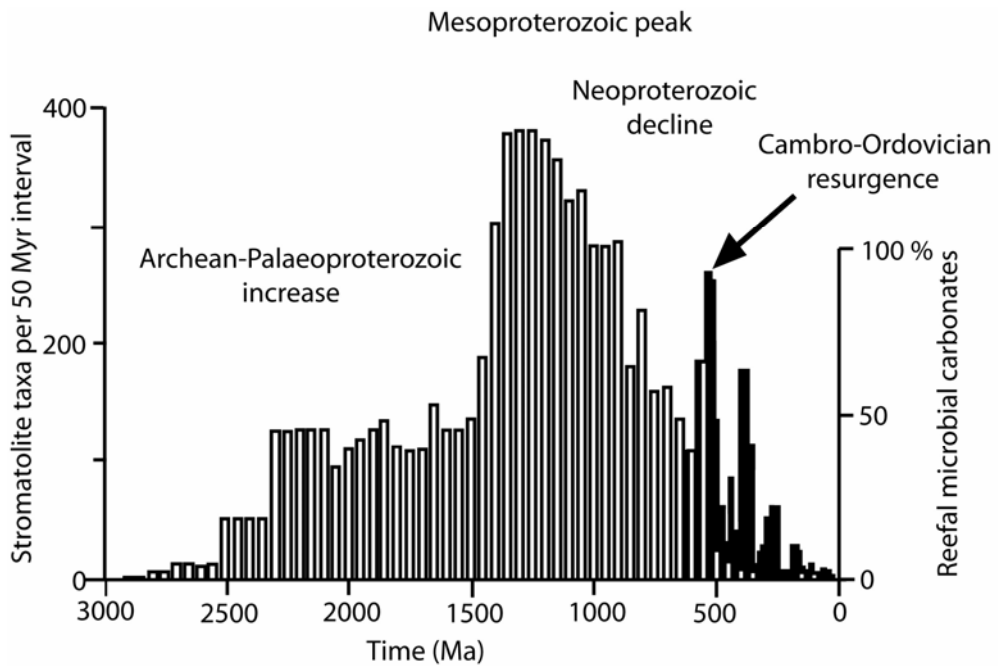
Awramik (1971) first compiled Proterozoic stromatolite diversity data and recorded an increase in diversity of columnar forms through the Proterozoic that culminated in a Neoproterozoic peak, followed by a sharp decline. Awramik (1971) attributed this decline to the diversification of metazoans. Walter & Heys (1985) plotted a different 'abundance' graph, which represented the recorded occurrences within each basin. The graphs of stromatolite abundance and diversity extend forward to c. 500 Ma but there has been comparatively little

work on abundance and diversity change through the Phanerozoic. Riding (2006) attempted to show trends by juxtaposing numbers of morphotype taxa from the Precambrian (Awramik & Sprinkle 1999) and relative abundance from the Phanerozoic (Kiessling 2002) (Text-fig. 3.15). Riding (2006) then compared this data with the metazoan diversity curves of Sepkoski (1992, 1997) to show that microbialites were increasing in abundance whilst metazoans were undergoing radiation, and that not all extinction events coincide with an increase in abundance of microbialites, as would be expected if their demise was primarily related to grazing, burrowing or competition. The comparison was made however between the Cambrian radiation of metazoans and the concurrent increase in microbialites as evidence to dismiss the link between the two. This does not disprove that metazoans played a major role in the subsequent decline during the Ordovician, as many groups were undergoing further radiation and new niches were being exploited, primarily by infauna (Harper 2006). This radiation (the 'Great Ordovician Biodiversification Event') heralded a tripling of marine diversity at a range of taxonomic levels and ecosystems similar to modern ones developed (Harper 2006). During this time there were increases in bioturbation and tiering below and above the sediment water interface. Hard substrate colonising communities and reefs evolved and there is no doubt that this radiation must have had an effect upon microbialite structure, if not abundance also. There are some extinction events after which microbialites increase in numbers, namely the end Ordovician extinction (Sheehan & Harris 2004) and the end Permian extinction (Schubert & Bottjer 1992).

The theory of competition by grazing animals is unlikely because thrombolites suffer the same decline experienced by stromatolites. Thrombolites were able to support a large community of metazoans, often with a high proportion of gastropods. Moore & Burne (1994) report that the thrombolites of Lake Clifton are both a source of food and a refuge for animals and that they support a diverse community of metazoans without much ill effect. The reason for the demise must lie with other causal factors but may still be related to the Ordovician radiation but in other ways than grazing pressure.



Text-figure 3.14 Graph showing interpreted Phanerozoic CO₂ levels. Ice ages are shown in grey and the studied time interval is marked by a red box (modified after Crowley & Berner 2001).



Text-figure 3.15 Graph showing stromatolite diversity and reefal microbialite abundance through time (modified after Riding 2006).

Awramik (1971) attributes the apparent decline in stromatolites abundance to the evolution of bottom deposit feeders and burrowing metazoans in the Late Precambrian. Garrett (1970) also suggested that the formation of microbial mats was prevented by grazing pressure.

Monty (1977) proposed that microbialites declined due to competition with newly evolving reef forming organisms. Riding (2005; 2006) disagreed with the view that the long term decline of stromatolites is due to substrate modification, predation or competition for space and suggests changes in ocean chemical state to be the cause (Riding 2005; 2006). Modern stromatolites are found in environments of high salinity or freshwater, although stromatolites do exist in less extreme conditions (Moore *et al.* 1984; Dill *et al.* 1986). However even in these environments sediment movement acts to restrict competitors.

Pratt (1982) suggested that the apparent decline of microbialites during the Ordovician may be masked by a dilution in the rock record by other metazoans and they are still volumetrically important and this seems plausible. By the Middle to Late Ordovician, reefs comprising algae, bryozoans, corals and stromatoporoids are reported (Webby 2002). During the Early Ordovician, microbialites are the dominant reef forming structures across the palaeocontinent of Laurentia, and are recorded from western Newfoundland, Virginia, west Texas, Colorado, Wisconsin, Missouri, Arctic Canada and Greenland (Webby 2002). They also are numerous in Argentina, the Siberian Platform, Kazakhstan, Kyrgyzstan, South China and Australia (Webby 2002). These localities are all interpreted to be on tropical or subtropically disposed continental platforms in a shelf to shelf slope setting. The Laurentian deposits formed on a passive cratonic margin where circulation was optimal and terrigenous influx was minimal with high sea-level giving rise to a widespread shallow epeiric sea (Webby 2002).

3.12 CONCLUSIONS

Despite the frequent obliteration of microbial fabric, relic features within the Durness build-ups allow insight into the origin of these forms. The microbialites from the Durness Group are morphologically varied and include a variety of domical, columnar and stratiform stromatolites and thrombolites, which have not previously been described.

The 'leopard rock' facies is re-interpreted as a thrombolite, therefore altering the significance of microbialites within the Durness Group and posing questions of similar textures from localities across Laurentia.

Diversity and abundance both show marked trends throughout the Durness Group, however the causal factors can only be known for sure with studies of other sections of this age and continued qualitative study of modern microbialites. Data from the Durness Group, suggest that a combination of factors may have lead to the initial rise and subsequent demise of microbial deposits during the Cambro-Ordovician of Laurentia.

There have been few studies to assess the quantity of microbialites during the Phanerozoic, it is only by the following method used here can we arrive at a more accurate record of abundance. The re-interpretation of facies from the Saimhor Formation suggests that we may have significantly underestimated the abundance of microbialites at this time, and they were the most abundant organisms on the Scottish Laurentian shelf, being responsible for much of the sedimentation. Microbialites may be the cause of the 'Great Ordovician Biodiversification Event' and it may also have caused their demise, circular arguments over cause and effect may be difficult to resolve.

Chapter 4

CONODONT BIOSTRATIGRAPHY OF THE DURNESS GROUP

4.1 INTRODUCTION

The conodont biostratigraphy of the upper four formations of the Durness Group is proposed in this chapter to constrain the sequence stratigraphical model proposed in Chapter 5. The Cambrian–Ordovician boundary was extensively sampled by Huselbee (1998) and only a brief review of this interval is necessary. Given its depositional context, the Durness Group is surprisingly sparse in macrofossils suitable for dating. Only four specimens of trilobites are known from the whole of the succession and of these, three were collected from the lower Croisaphuill Formation. The other fossils present include poorly preserved gastropods, cephalopods, brachiopods, rostroconchs and sponges (which are of limited use in biostratigraphy). It was therefore necessary to construct a rigid biostratigraphic framework for the succession, and preliminary samples collected by M. P. Smith indicated that conodonts were present in all formations above the top of the Eilean Dubh Formation. Systematic taxonomy is not provided for the species recorded in this study and will be the subject of a future publication.

4.2 SAMPLING AND PROCESSING METHODS

Fieldwork was completed over five field seasons. September 2003, May 2004, September 2004, September 2005 and May 2006. The samples were collected, bagged and labelled with an eight figure grid reference and height up a measured section. In total 55 stratigraphically constrained samples were collected from 11 different sections totalling 634 metres and supplemented by 17 spot samples from 3 transects. Transects through the Croisaphuill and Durine formations were the only source of samples until detailed mapping and logging allowed a composite section to be constructed and new samples to be collected and placed stratigraphically. Some of these transect samples contained conodont species not recorded in the main section and, although the stratigraphical constraint is weaker, they are referred to in this chapter and included in Appendix 2.

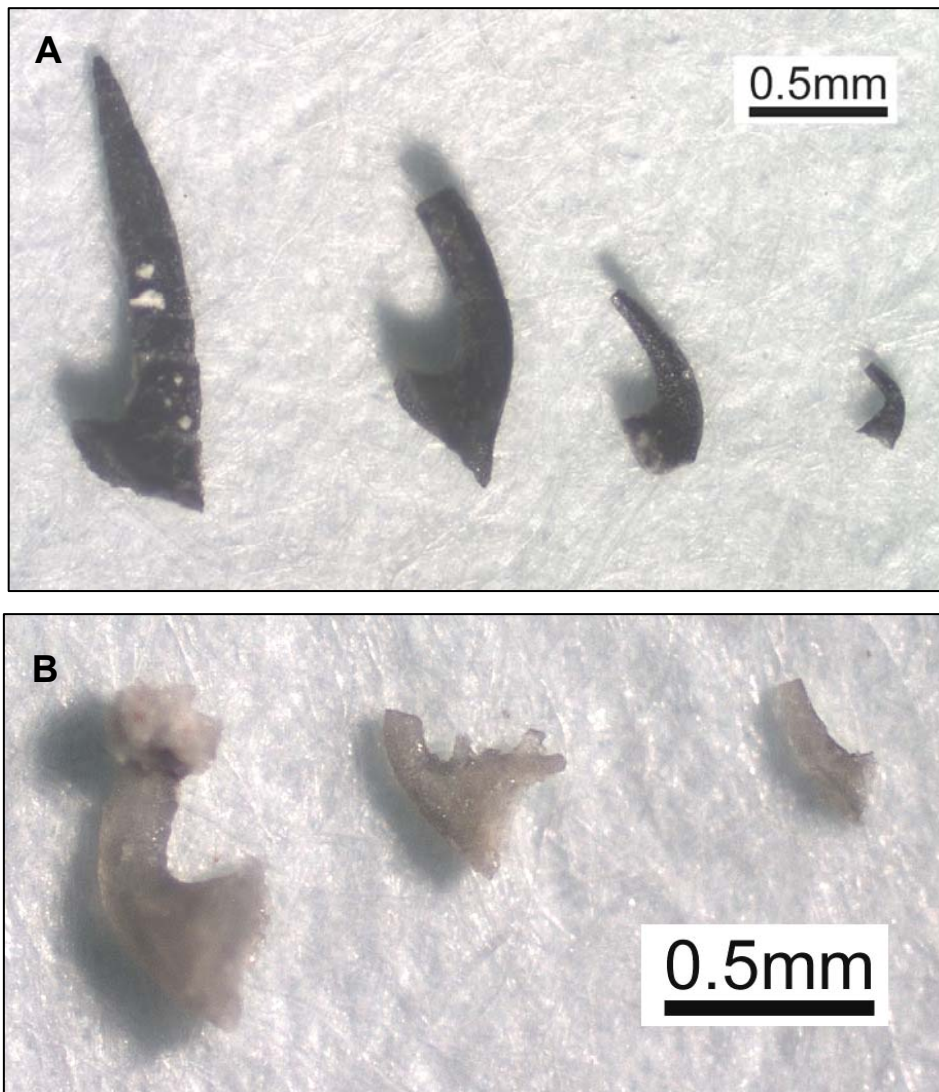
Samples of 3–5 kg were taken at approximately 10 m intervals along a composite section measured through the upper Durness Group in northwest Scotland. The sample weight

processed was based on reconnaissance samples (M. P. Smith *pers. comm.*) and work carried out by Huselbee (1998), which showed yields for some samples in the Salmhor Formation as low as 8 elements/kg.

In the current study, four kilograms of each sample were processed using standard techniques. Limestone samples were digested in buffered acetic acid following the method described by Jeppsson *et al.* (1999) and dolomite samples in a buffered solution of formic acid (Jeppsson & Anehus 1995). Some of the samples were buffered with precipitated calcium carbonate powder, whilst others towards the end of the project were buffered with crushed chalk. Acid solutions were changed every seven days and the residue wet sieved with a 1 mm and 63 μm mesh to produce the residues. The 1 mm fraction was fruitlessly scanned for silicified fossils and then returned back to the acid.

The concentration of conodonts from the fine fraction was accomplished by heavy-liquid separation in which the conodont elements (specific gravity of 2.84–3.10) were separated from the ‘light fraction’ using bromoform. The final extraction of conodonts from the sample was accomplished by handpicking under a Zeiss binocular microscope on a gridded picking tray. Picked conodonts were then transferred, using a damp paintbrush to a picking slide for identification. Difficulties maintaining the specific gravity of the bromoform at 2.85 which was necessary for the dolomite samples led to use of LST fastfloat (lithium heteropolytungstate) in the latter stages of the project. The method used was similar to that described for the use of SMT by Krukowski (1988). The Croisaphuill Formation was logged initially to a point believed to be the top, based upon previous literature. Following further examination of the area it was concluded that the thickness was much greater than previously thought and extra samples were taken in the upper half of the formation. Conodont abundances from the Durness Group range from barren samples to samples containing as many as 1231 elements recovered from 3789 g of dissolved rock (325 elements/kg) from the lower Croisaphuill Formation (17.9 m).

Most samples produced conodonts although yields and preservation varied widely depending upon facies and both thermal and hydrothermal alteration. The thermal alteration produced colour change (cf. Epstein *et al.* 1977; Rejebian *et al.* 1987), whereas alteration from fluids is manifested in mineral overgrowths on the elements. Conodont specimens locally show frosted surfaces suggesting incipient chemical corrosion, whilst many specimens show impressions of once adhering dolomite crystals (Plate 6), or display silica overgrowths.



Text-figure 4.1 Conodont colour within a range of different sized elements from the Durness Group. **(A)** black conodonts of CAI 5.5 from sample 2004-05 (Balnakeil Formation, Balnakeil Bay, Durness). **(B)** elements displaying grey colour (CAI 7) from 2003-38 (NC 2662 2006), Inchnadamph, Assynt.

Many specimens show incipient transverse fractures in transmitted light, others have been stretched and contorted by microfolds (the Durine Formation occupies the footwall immediately beneath the lowest thrust in the Moine thrust system). A large proportion of the specimens were more complete than previous studies, despite their preservation, largely due to very careful processing and gentle washing of the sieve. Due to the high CAI the elements are fragile and are easily broken after processing and care was taken to avoid this.

Conodont specimens from Durness show discolouration by thermal alteration, with colour alteration indices (CAI) of between 5 and 6 (Text-fig. 4.1). Conodonts recovered from Inchnadamph, Assynt have a CAI of 7 (Text-fig. 4.1) (Epstein *et al.* 1977). The absolute temperatures used for colour alteration were derived by Epstein *et al.* (1977) and Rejebian *et al.* (1987) in a classic series of papers in which unaltered conodont elements were experimentally heated to determine a colour based temperature scale (CAI 1–8). The scale extends from pale yellow (CAI 1) to dark brown and black (CAI 5), grey (CAI 6), white (CAI 7) and clear (CAI 8) (Epstein *et al.* 1977, Rejebian *et al.* 1987). The values from samples in the Durness area are consistent with regional low grade metamorphism to lower greenschist facies and suggesting minimum temperatures of greater than 300° C, whilst those from Assynt suggest higher-grade (550° C) hornblende hornfels facies (most likely due to proximity of an unknown igneous intrusion).

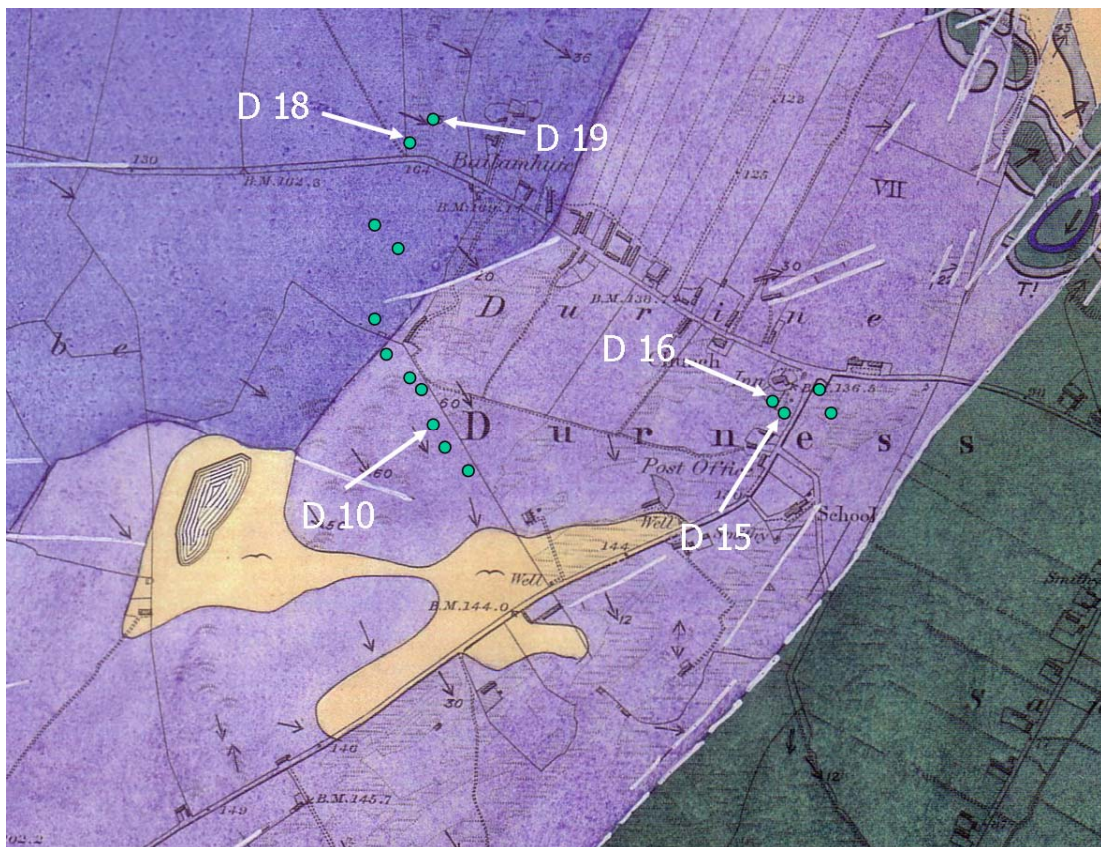
4.3 PREVIOUS RESEARCH

4.3.1 Early studies concerning the upper Durness Group

Conodonts were first discovered from the Durness Group by C. Downie and described by Higgins (1967), who examined 18 samples from the Durine Formation in and around Durness village. Only five samples were productive and of these two samples provided the majority of the specimens. In total, 16 form taxa were recorded, only selected species were figured as line drawings. When the sample locations are located on the geological map it can be seen that some were taken in the Croisaphuill Formation (Text-fig. 4.2) This has implications for previous dating of the upper part of the Durness Group. Despite noting that the Durness Group fauna showed close similarity with the Cambro-Ordovician of North America correlation was made with faunas from Sweden due to the lack of published reference sections in North America.

Higgins (1985) later recorded *Ulrichodina?* cf. *simplex* Ethington & Clark, *Protopanderodus gradatus* Serpagli, *Pteracontiodus cryptodens* (Mound), *Histiodela* sp. and *Drepanoistodus* sp. (which is here interpreted to be an element of *Ulrichodina abnormalis* (Branson & Mehl)) from the Durine Formation and correlated this with a mid-continent fauna attributable to the informal *Pteracontiodus cryptodens*–*Histiodela altifrons*–*Multioistodus auritus* interval of Ethington & Clark (1981).

Higgins (1971, 1985) also provided a discussion of three productive samples from the Croisaphuill Formation (at the base, 3 m and 20 m above the base). Conodonts from these samples included *Protopanderodus gradatus* Serpagli, ‘*Scolopodus*’ cf. *emarginatus* Barnes & Tuke, *Oistodus* sp. 6 Ethington & Clark (now included as an element of *Tropodus comptus*) and *Paltodus* aff. *sexplicatus* (Jones) *sensu* Abaimova, and was assigned to the informal *Aodus deltatus*–*Macerodus diana* interval of Ethington & Clark (1981).

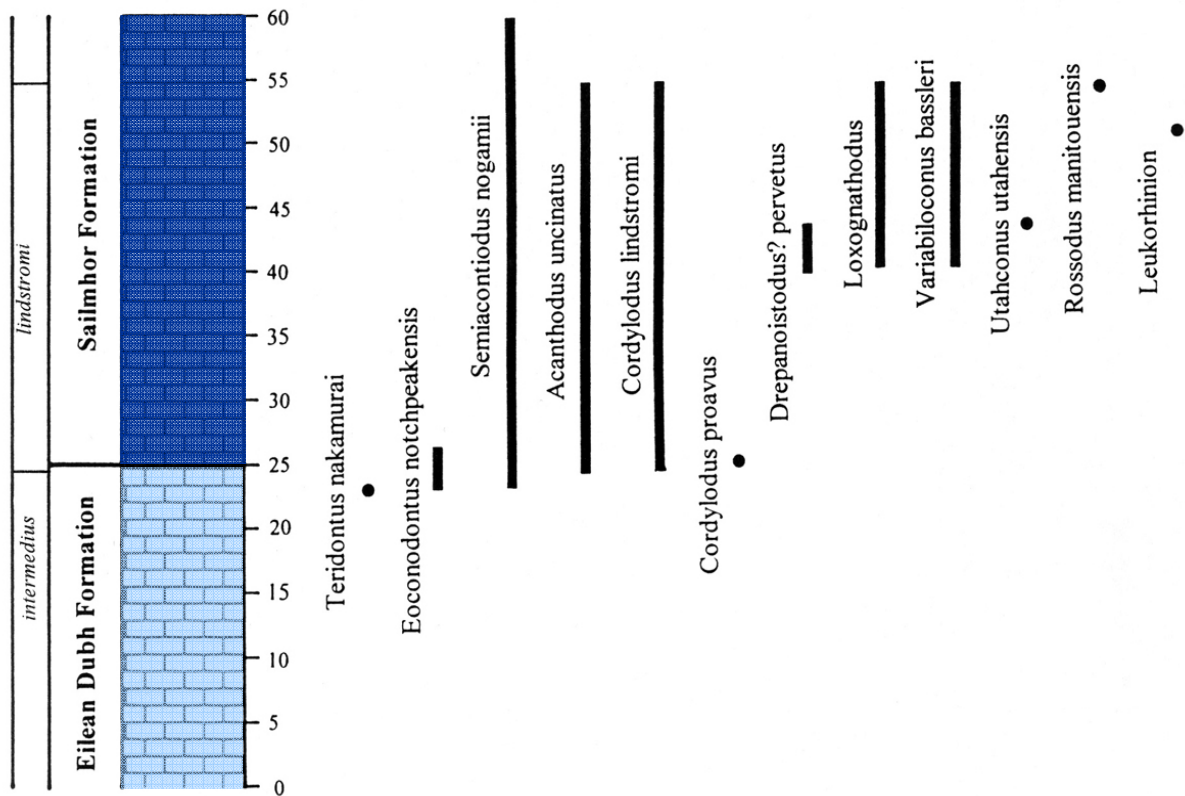


Text-figure 4.2 Higgins (1969) localities overlaid on the BGS 6 inch map, showing that some were collected from the upper Croisaphuill Formation rather than the Durine Formation as suggested in the publication. Productive samples are labelled.

4.3.2 The Cambrian–Ordovician boundary interval

Conodonts across the Cambrian–Ordovician boundary interval were studied by Huselbee (1998), who processed some 34 samples spanning the upper 25 m of the Eilean Dubh and lower 35 m of the Sailmhor formations. Although the conodont defining the base of the Ordovician (*Iapetognathus fluctivagus* Nicoll *et al.*) was not recovered, the following taxa

were recorded: *Eoconodontus notchpeakensis* (Miller), *Semiacontiodus nogamii* (Miller), *Rossodus manitouensis* Repetski & Ethington, *Teridontus nakamurai* (Nogami), *Utahconus utahensis* (Miller), *Variabiloconus bassleri* (Furnish), *Drepanoistodus? pervetus* Nowlan, *Cordylodus proavus* Miller, *Cordylodus lindstromi* Druce & Jones and *Acanthodus uncinatus* Furnish and new species of *Loxognathoides* and *Leukorhinion* (Text-fig. 4.3).



Text-figure 4.3 Range chart spanning the Cambrian–Ordovician boundary interval at the Eilean Dubh–Sailmhor formation boundary. The *manitouensis* Zone lies at the top of the studied section. The conodont zones spanning the Cambrian–Ordovician boundary interval have been revised, see text for discussion (after Huselbee 1998).

The lowest conodonts in the succession include *S. nogamii*, the long ranging *T. nakamurai* and the long ranging Cambrian conodont *E. notchpeakensis* (1.9 m below the top of the Eilean Dubh Formation). The LAD (last appearance datum) of *S. nogamii* is coincident with the base of the *C. angulatus* Zone in the standard reference section (Sweet & Tolbert 1997) and therefore the top of the *fluctivagus* Zone. In the Durness Group it is 1.6 m above the base of the Sailmhor Formation. Similarly, *Cordylodus proavus* has an LAD near the top

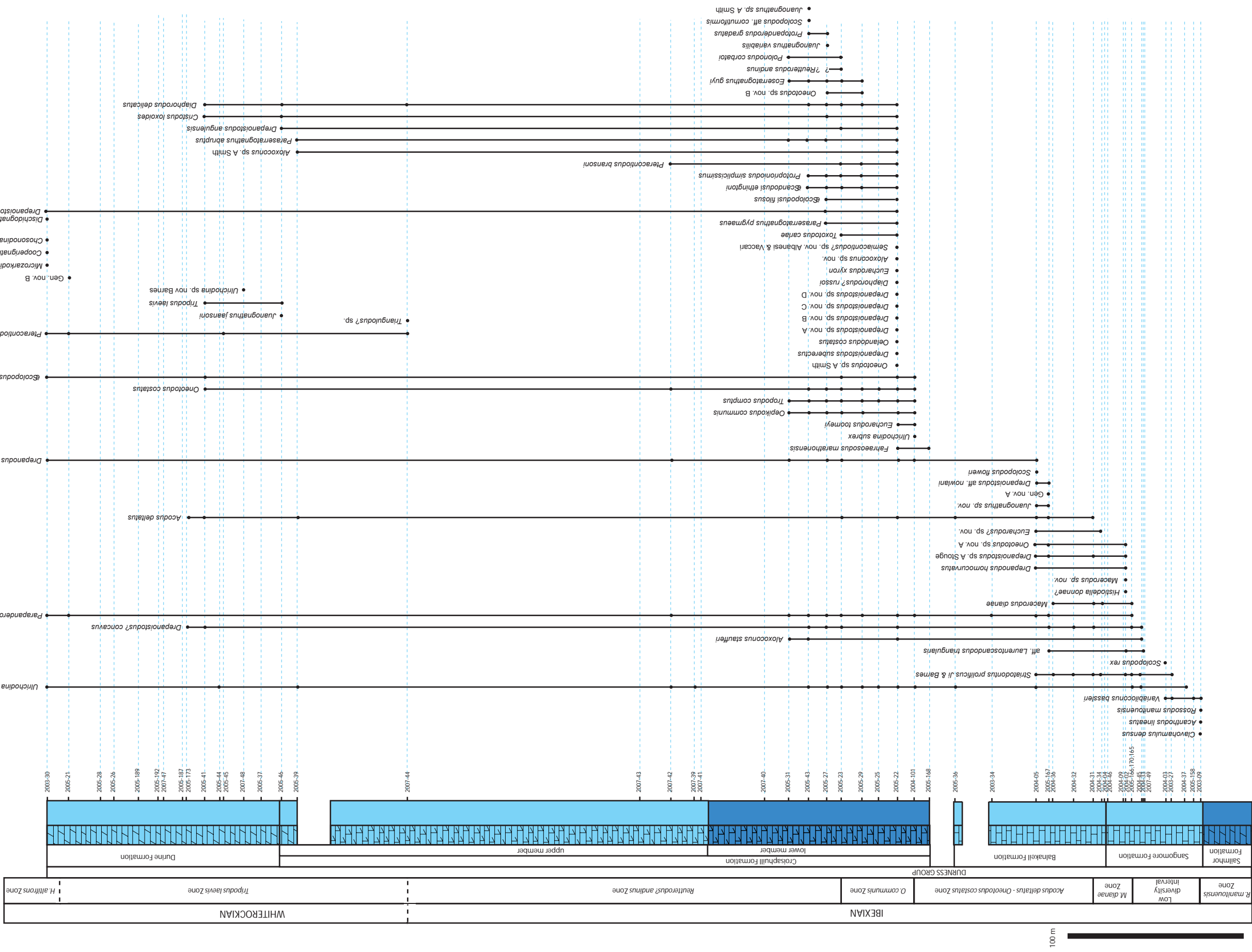
of the *I. fluctivagus* Zone (it is recorded from 0.3 m above the Sailmhor Formation base). This suggests that the base of the Ordovician lies below 1.6 m above the base of the Sailmhor Formation. The taxon *C. lindstromi* has an FAD (first appearance datum) 0.1 m below the top of the Eilean Dubh Formation indicating the base of the *lindstromi* Zone in Scotland (Text-fig. 4.3), but there are facies restrictions on conodont recovery from the upper Eilean Dubh Formation (supratidal dolomites, see Chapter 2) and the base of the zone is probably located at a horizon below the sample of Huselbee (1998). The boundary is c. 298 m above the base of the Durness Group.

4.4 CONODONT ZONATION

4.4.1 North American Midcontinent zones

The faunas recovered in this current study compare well with other Laurentian sections and therefore the zonal scheme of Sweet & Tolbert (1997) is applied (Text-fig. 4.4), rather than defining new zones as some authors have done (Ji & Barnes 1994). By correlation with species ranges in the composite standard section of Sweet & Tolbert (1997) the bases of the conodont zones can be placed with varying levels of resolution and confidence, even if the zonal taxon itself is absent.

The Ibexian Series is approximately correlative with the global Tremadocian and Floian stages of the Lower Ordovician (Text-fig. 1.9, 4.4), although the lower part is of late Cambrian (Furongian) age (Chapter 1). Sweet & Tolbert (1997) based their biostratigraphy on conodonts from the Ibexian type section within the Pogonip Group of Shingle Pass, Nevada and used graphical correlation to produce a composite standard section. In North American chronostratigraphy, the Ibexian is overlain by the Whiterockian Series (Ross & Ethington 1991, 1992).



Text-fig. 4.5 Chart displaying conodont species and their ranges within the upper Durness Group

The base of the Whiterockian Series is taken at the base of the *Tripodus laevis* Zone and thereby approximates to the boundary between the Lower and Middle Ordovician (Floian–Dapingian Stage boundary) in global stratigraphical terms (Text-fig. 1.9). The precise correlation of this boundary will be discussed in Section 4.4.8. A standard reference section has been constructed for the Whiterockian in central Nevada, (Ross & Ethington 1991, Sweet *et al.* 2005).

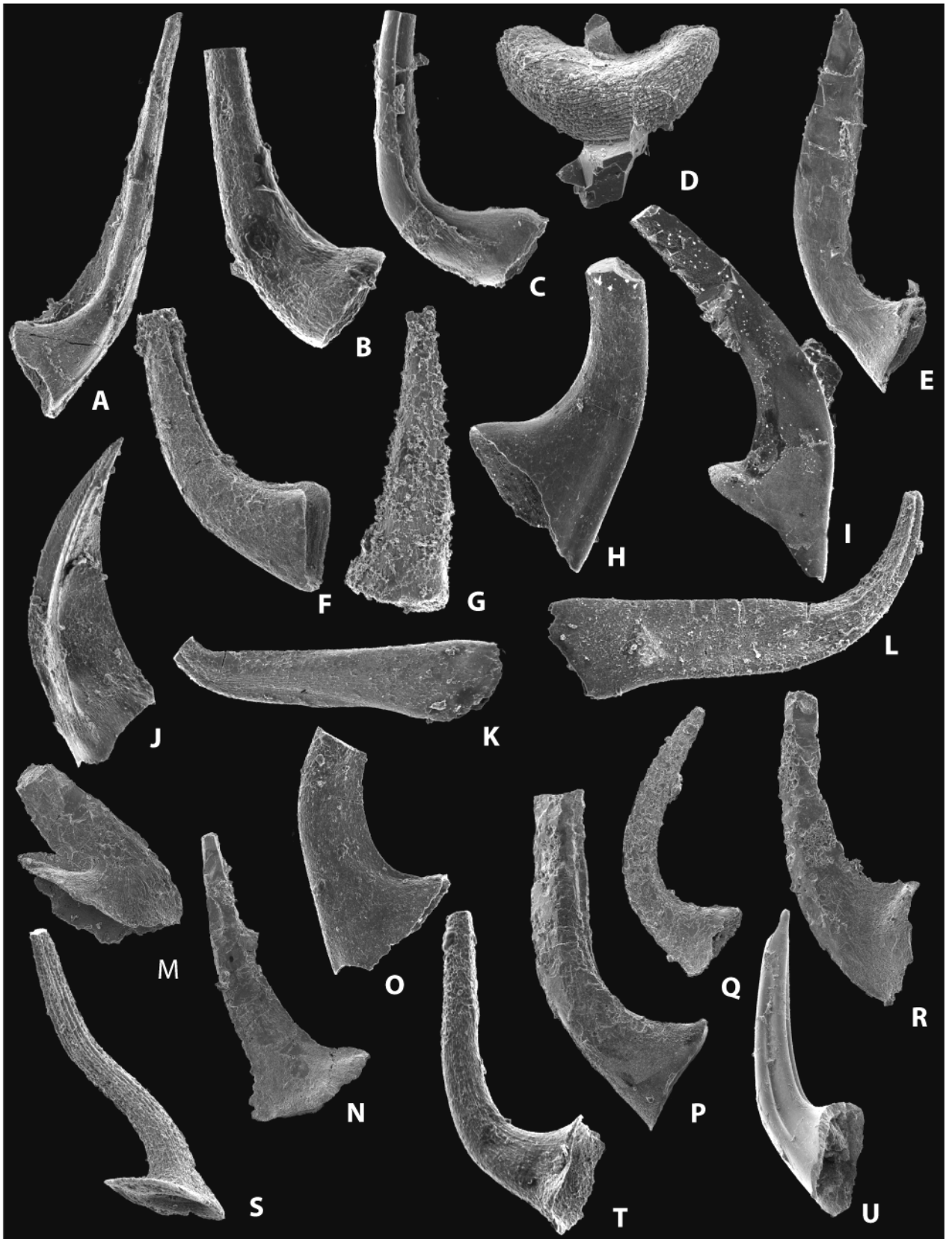
4.5 CONODONT BIOSTRATIGRAPHY OF THE DURNESS GROUP

A biostratigraphical zonation is applied to the Durness Group. The range chart for the species recorded is displayed (Text-Fig. 4.5) and selected conodonts are figured in Text-figs 4.6–4.10. An abundance table of the conodont elements (Text-table 4.1) provides the weight processed, sample height and constituent conodonts recovered. This study focuses on the lower Ibexian to Whiterockian zones (excluding the *I. fluctivagus* and *C. angulatus* zones; discussed earlier) and concerns strata from the base of the Sangomore Formation, through the Balnakeil and Croisaphuill formations and to the top of the Durine Formation (643 m).

4.5.1 *Rossodus manitouensis* Zone

This zone is approximately equivalent to the Fauna C interval of Ethington & Clark (1971) (Text-fig. 4.4) and can be recognised through some 80 m of strata in NW Scotland. The base is marked in the section studied by Huselbee (1998) by the lowest observed occurrence of the zonal species *Rossodus manitouensis* in a sample 35 m above the base of the Sailmhor Formation. The zone includes all of the remaining Sailmhor Formation. New samples from the lowest Sangomore Formation (1.45 m) yielded *Acanthodus lineatus* (Furnish), *V. bassleri*, *Clavohamulus densus* Furnish and *R. manitouensis?* (resembles *Rossodus longpinnatus* (Ji & Barnes)) (Text-figs 4.5E–E), all confirming an upper *manitouensis* Zone age (Sweet & Tolbert 1997) for the base of the Sangomore. This zonal assemblage can be recognised in many widespread localities in the Laurentian province and typically also includes ‘*Paltodus*’ *spurius* Ethington & Clark, *Loxodus bransoni* Furnish and *Polycostatus* spp. (faunas are detailed in Fåhræus & Nowlan 1978; Repetski & Ethington 1983; Landing *et al.* 1986 and Ji & Barnes 1994).

Text-figure 4.6 Conodonts from the Sangomore and Balnakeil formations and spanning the low upper *manitouensis* Zone, ‘Low diversity interval’, *dianae* Zone and *deltatus–costatus* Zone. **(A)** *Rossodus manitouensis* Repetski & Ethington; Sangomore Formation 01.45 m; x95. **(B)** *Variabiloconus bassleri* (Furnish); Sangomore Formation 01.45 m; x62. **(C)** *Variabiloconus bassleri* (Furnish) Sangomore Formation 01.45 m; x62. **(D)** *Clavohamulus densus* Furnish Sangomore Formation; 01.45 m; x112. **(E)** *Acanthodus lineatus* (Furnish) Sangomore Formation; 01.45 m; x62. **(F)** *Striatodontus prolificus* Ji & Barnes; Balnakeil Formation; 30.42 m; x85. **(G)** *Striatodontus prolificus* Ji & Barnes; Sangomore Formation; 44.0 m; x112. **(H)** *Laurentoscandodus triangularis* (Furnish); Sangomore Formation; 44.0 m; x95. **(I)** *Drepanodus* aff. *arcuatus* Pander; Sangomore Formation; 33.9 m; x150. **(J)** *Histiodellella donnae* Repetski; Sangomore Formation; 44.0 m; x112. **(K)** *Macerodus dianae* Fåhraeus & Nowlan; Balnakeil Formation; 30.42 m; x85. **(L)** *Macerodus dianae* Fåhraeus & Nowlan; Balnakeil Formation; 7.25 m; x95. **(M)** *Drepanoistodus* sp. A Stouge & Boyce; Balnakeil Formation; 39.82 m; x112. **(N)** *Drepanoistodus* sp. A Stouge & Boyce; Balnakeil Formation; 39.85 m; x150. **(O)** *Drepanoistodus concavus* (Branson & Mehl); Balnakeil Formation; 2.50 m; x62. **(P)** *Drepanodus homocurvatus* Lindström; Balnakeil Formation; 39.82 m; x95. **(Q)** *Drepanodus arcuatus* Pander; Balnakeil Formation; 39.82 m; x150. **(R)** *Drepanoistodus* aff. *nowlani* Ji & Barnes; Balnakeil Formation; 39.82 m; x95. **(S)** Gen. nov.; Balnakeil Formation; 30.42 m; x85. **(T)** ‘*Eucharodus*’ sp. nov.; Balnakeil Formation; 2.50 m; x85. **(U)** *Ulrichodina abnormalis* (Branson & Mehl); Balnakeil Formation top; x150.



4.5.2 'Low diversity interval'

The conodont samples between 5.4 and 40 m above the base of the Sangomore Formation have noticeably lower yields (typically <9 elements/kg) and contain a fauna less diverse than samples below or above. Only *V. bassleri* persists from the *manitouensis* Zone fauna but it disappears in samples above 21 m (Text-fig. 4.5). Other taxa recorded include *Scolopodus rex* Lindström, *Ulrichodina abnormalis* (Branson & Mehl), *Striatodontus prolificus* Ji & Barnes (Text-fig. 4.6F, 4.6G), aff. *Laurentoscandodus triangularis* (Furnish), *Drepanoistodus? concavus* (Branson & Mehl) and *Aloxoconus staufferi* Furnish. This low diversity and abundance interval is 39 m thick and may correspond to the informal 'low diversity interval' defined by sparse numbers and low diversity faunas recognised across much of North America (Ethington & Clark 1981). The interval has a range of 336–391 csu (composite standard units) in the composite reference section (Sweet & Tolbert 1997). *S. rex* is recorded from 21 m above the base of the Sangomore Formation. It is present across Laurentia and marks an important turnover in conodont faunas following a major extinction at the end of the *manitouensis* Zone (Ethington *et al.* 1987). The 'low diversity interval' equates to the lower Fauna D (Text-fig. 4.4). The faunal succession compares well with western Newfoundland, where samples from the uppermost Watts Bight Formation have barren or low diversity yields, with *V. bassleri* the only taxon present (Stouge & Boyce 1997).

4.5.3 *Macerodus diana* Zone

Some 40 cm above a sample yielding only two *S. prolificus* elements (2005-166) a sample (2005-170) records the FAD of *Macerodus diana* Fåhræus & Nowlan (Text-fig. 4.6K–L) from 40.9 m above the base of the Sangomore Formation. The base of the *diana* zone is placed at this sample and it has a total thickness of 21.25 m. The zone includes the upper 14.0 m of the Sangomore and the lowest 7.25 m of the Balnakeil Formation. Other taxa recorded from this zone include an element which may belong to *Histiodellla donnae* Repetski (J. E. Repetski *pers. comm.*) (Text-fig. 4.6J), *Eucharodus?* sp. nov. (Text-fig. 4.6T) *Oneotodus* sp. nov. A, *Macerodus* sp. nov., *Drepanodus homocurvatus* Lindström (Text-fig. 4.6P), *S. prolificus*, aff. *L. triangularis*, *D. concavus*, *Parapanderodus striatus* (Graves & Ellison) and *Drepanoistodus* sp. A Stouge. In the Durness Group, the range of *M. diana* extends beyond a sequence boundary interpreted to be a correlative of the Boat Harbour Disconformity in western Newfoundland (Chapter 5). In Newfoundland the strata beneath the sequence

boundary is of *dianae* Zone age (Ji & Barnes 1994, Stouge & Boyce 1997), and *M. dianae* has an FAD 16.5 m above the base of the Boat Harbour Formation and but this species and many others have their LAD at the disconformity. The occurrence of *M. dianae* above the sequence boundary in Scotland suggests either that the erosion was more long-lived in Newfoundland (thereby removing more strata) or that the range of *M. dianae* is not fully known. Sweet & Tolbert (1997) noted that further work is necessary before the range of *M. dianae* is fully known. In the composite standard section the *dianae* zone has a range of 391–471 csu.

4.5.4 *Acodus deltatus*/*Oneotodus costatus* Zone

Acodus deltatus has an FAD in the Durness Group 7.25 m above the base of the Balnakeil Formation. The zone is 88 m thick and includes the remaining Balnakeil Formation and the basal beds of the Croisaphuill Formation (Text-fig. 4.5). The zone has also provided *Parapanderodus striatus* (Graves & Ellison) and *Juanognathus* sp. nov. (co-specific with *Juanognathus* sp. A, *sensu* Stouge 1982), aff. *L. triangularis*, *S. prolificus*, *D. concavus*, *M. dianae*, *D. homocurvatus*, *Drepanoistodus* sp. A Stouge, *Oneotodus* sp. A and a new genus (Text-fig. 4.6S).

In western Newfoundland, *S. floweri* is recorded with *M. dianae* 16.5 m above the base of the Boat Harbour Formation, *D. nowlani* and *M. dianae* at 29 m and *Juanognathus?* sp. A Stouge are recorded at 75 m above the formation base. All of these taxa do not extend beyond the Boat Harbour Disconformity (Stouge 1982; Stouge & Boyce 1997). The occurrence of these within the *deltatus*–*costatus* Zone in Scotland suggests that the lower part of the zone is missing in Newfoundland. In the composite standard section the zone has a range of 471–660 csu and *S. floweri* has an FAD of 477 csu.

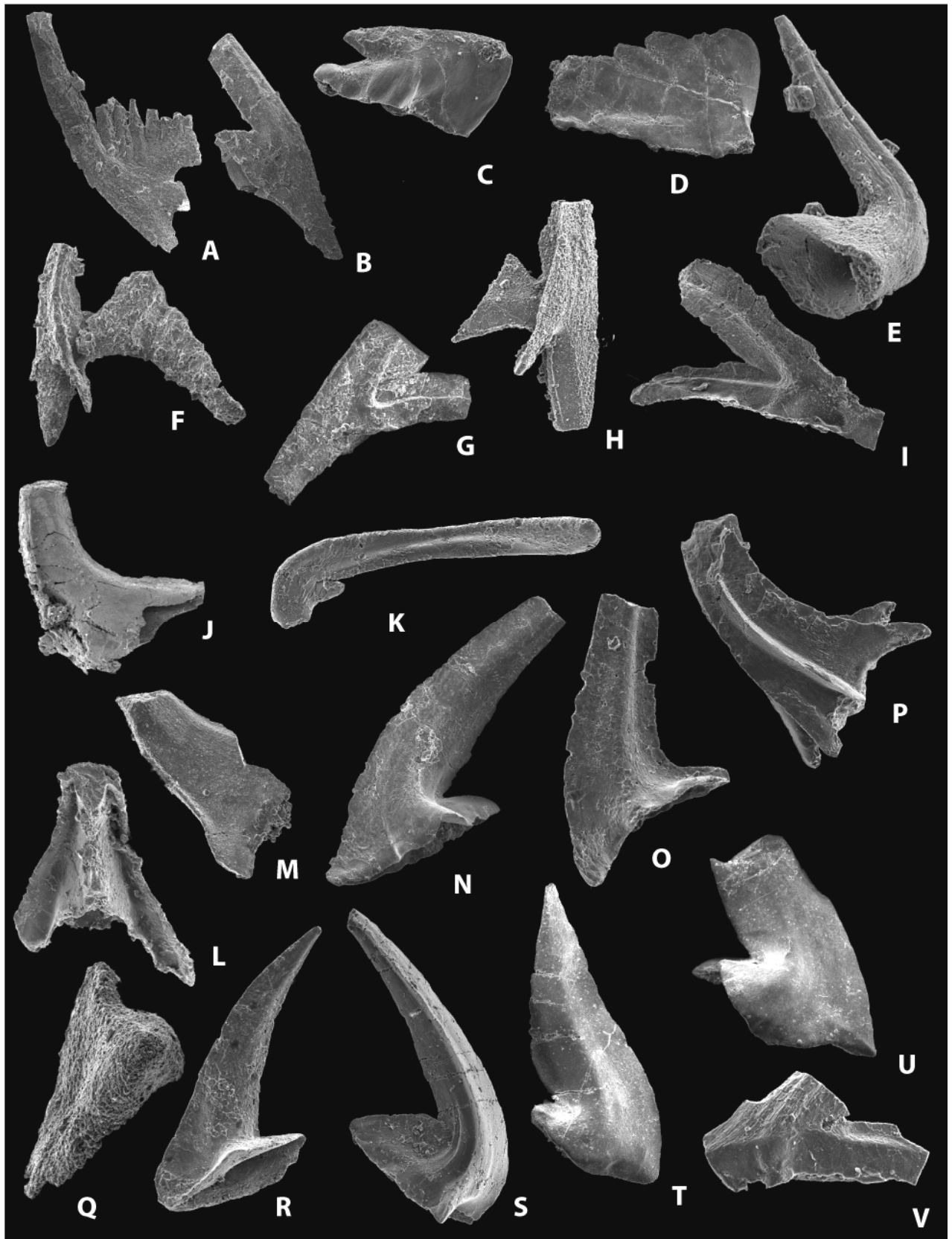
The base of the Floian and the top of the Tremadocian Stage is marked by the FAD of the graptolite *Tetragraptus approximatus* Nicholson (Text-fig. 4.4). If the position of this boundary lies at the base of the *A. deltatus*–*O. costatus* Zone, as suggested by Harris *et al.* 1995 (Text-fig. 4.4), the stage boundary would lie within the lower but not lowest part of the Balnakeil Formation (c. 380 m above the base of the Durness Group and approximately 200 m above the base of the Ordovician). Webby *et al.* (2004) however correlated the Tremadocian–Floian Boundary with the uppermost *deltatus*–*costatus* Zone. In the Durness Group this would correspond to a height of c. 435 m above the base of the group and a position just below the Croisaphuill Formation. The presence of *Acodus deltatus* Lindström

within sections in Sweden was suggested to be coeval with the occurrence of *A. deltatus* in North America by Sweet & Tolbert (1997), however, correlation of the Laurentian faunas and those of Scandinavia is difficult as they share very few taxa in common. Correlation of the GSSP for the base of the Floian Stage with either Scotland or the Ibexian reference section is problematic (Bergström *et al.* 2004).

4.5.5 *Oepikodus communis* Zone

The base of the *Oepikodus communis* Zone is marked by the FAD of *O. communis* (Ethington & Clark) (Text-fig. 4.7A, B), 8.5 m above the base of the Croisaphuill Formation. The zone is 41.5 m thick within the Durness Group (Text-fig. 4.5). It represents peak diversity and the base corresponds to the maximum flooding event of the whole succession (Chapter 5). Based upon the recovery of *O. communis*, the Croisaphuill Formation is significantly younger than the *Acodus deltatus*/*Macerodus diana* interval age suggested by Higgins (1985). Many of the species recorded from the Durness Group have their FADs at or within a sample 9.4 m above the base of the zone. Excluding long ranging taxa, species recovered include, *Ulrichodina subrex* (Ji & Barnes) (Text-fig. 4.9A), *Eucharodus toomeyi* (Ethington & Clark) (Text-figs 4.9D, E), ‘*Scandodus*’ *ethingtoni* Smith (Text-fig. 4.7R), *Oelandodus* cf. *O. costatus* van Wamel (Text-fig. 4.7V), *Toxotodus carlae* (Repetski) (Text-fig. 4.8T), *Protoprioniodus simplicissimus* McTavish (Text-figs 4.7F–H), ‘*Scolopodus*’ *filosus* Ethington & Clark (Text-fig. 4.9K), *Tropodus comptus* (Branson & Mehl) (Text-fig. 4.7N–P), *Oneotodus* sp. A *sensu* Smith (1991) (Text-fig. 4.8Q), *Oneotodus* sp. B (this study), *Fahraeosodus marathonenis* (Bradshaw) *Drepanoistodus suberectus* and several new species of *Drepanoistodus* (Text-figs 4.8F, H, I, L). The base of the *communis* Zone also represents the FAD of a group of form species which may represent parts of a single species apparatus – *Paraserratognathus abruptus* (Repetski), *Paraserratognathus pygmaeus* (Ji & Barnes) *Eoserratognathus guyi* (Smith) (Text-figs 4.8M, N, O, R, S). This taxon will require further taxonomic work however, as *E. guyi* is not recorded from sections containing *P. abruptus* (J. E. Repetski *pers. comm.*).

Text-figure 4.7 Conodonts from the Croisaphuill Formation (*communis* Zone and the *andinus* Zone). **(A)** *Oepikodus communis* (Ethington & Clark); spot sample 2003-10; x80. **(B)** *Oepikodus communis* (Ethington & Clark); spot sample 2003-10; x80. **(C)** *Cristodus loxoides* Repetski; 17.9 m; x73. **(D)** *Cristodus loxoides* Repetski; 17.9 m; x43. **(E)** aff. *Semiacontiodus* sp. Albanesi & Vaccari; 17.9 m; x117. **(F)** *Protoprioniodus simplicissimus* McTavish; 50 m; x88. **(G)** *Protoprioniodus simplicissimus* McTavish; 50 m; x88. **(H)** *Protoprioniodus simplicissimus* McTavish; 58.55; x66. **(I)** *Protoprioniodus simplicissimus* McTavish; 17.9 m; x117. **(J)** *Diaphorodus delicatus* (Branson & Mehl); 297 m; x66. **(K)** ‘*Oistodus*’ *ectyphus* Smith; spot sample mid Croisaphuill Formation 2004-01; x88. **(L)** *Pteracontiodus cryptodens* (Mound); 297 m; x88. **(M)** *Triangulodus?* sp.; 297 m; x88. **(N)** *Tropodus comptus* (Branson & Mehl); 17.9 m; x60. **(O)** *Tropodus comptus* (Branson & Mehl); 17.9 m; x80. **(P)** *Tropodus comptus* (Branson & Mehl); 17.9 m; x80. **(Q)** *Polonodus corbatoi* (Serpagli); 78.9 m; x117. **(R)** ‘*Scandodus*’ *ethingtoni* Smith; 17.9 m; x60. **(S)** aff. *Oistodus lanceolatus* Pander; 2003-05; x60. **(T)** *Pteracontiodus bransoni* (Ethington & Clark); 38.25 m; x32. **(U)** *Pteracontiodus bransoni* (Ethington & Clark); 38.25 m; x32. **(V)** *Oelandodus* cf. *O. costatus* van Wamel; 17.9 m; x117.



Text-figure 4.8 Conodonts from the Croisaphuill Formation (*communis* Zone and *andinus* Zone). **(A)** *Drepanoistodus* sp.; 17.9 m; x40. **(B)** *Drepanodus arcuatus* Pander; 17.9 m; x60. **(C)** *Drepanoistodus angulensis* (Harris); 17.9 m; x110. **(D)** *Drepanoistodus angulensis* (Harris); spot sample mid Croisaphuill Formation 2004-01; x97. **(E)** *Drepanodus* sp.; spot sample 2003-10; x73. **(F)** *Drepanoistodus* sp. nov. A; 17.9 m; x60. **(G)** *Drepanoistodus* sp.; 17.9 m; x60. **(H)** *Drepanoistodus* sp. nov. B; 17.9 m; x60. **(I)** *Drepanoistodus* sp. nov. C; 17.9 m; x110. **(J)** *Drepanoistodus* aff. *forceps* (Lindström); 17.9 m; x121. **(K)** *Acodus* sp. cf. *A. deltatus* Lindström; 50 m; x88. **(L)** *Drepanoistodus* sp. nov. D; 17.9 m; x88. **(M)** *Paraserratognathus pygmaeus* (Ji & Barnes); 17.9 m; x110. **(N)** *Paraserratognathus abruptus* (Repetski); 17.9 m; x121. **(O)** *Paraserratognathus abruptus* (Repetski); 17.9 m; x66. **(P)** *Oneotodus costatus* Ethington & Brand; 17.9 m; x66. **(Q)** *Oneotodus* sp. A Smith; lower Croisaphuill Formation from a spot sample (2003-10); x60. **(R)** *Eoserratognathus guyi* (Smith); 2003-10 spot sample, lower Croisaphuill Formation; x102. **(S)** *Paraserratognathus abruptus* (Repetski); spot sample 2003-10; x88. **(T)** *Toxotodus carlae* (Repetski); 17.9 m; x121. **(U)** *Protopanderodus gradatus* Serpagli; 58.55 m; x121. **(V)** *Aloxoconus* sp. nov. (Scolopodiform C of Ethington & Clark); 17.9 m; x110. **(W)** *Aloxoconus staufferi* (Furnish); 17.9 m; x66.





Text-figure 4.9 Conodonts from the Croisaphuill Formation and their height above formation base when from a measured section; **(A)** *Ulrichodina subrex* (Ji & Barnes); 8.5 m; x43. **(B)** ‘*Ulrichodina*’ sp. nov.; spot sample, mid formation (2004-01); x80. **(C)** *Ulrichodina abnormalis* (Branson & Mehl); 17.9 m; x60. **(D)** *Eucharodus toomeyi* (Ethington & Clark); 8.5 m; x80. **(E)** *Eucharodus toomeyi* (Ethington & Clark); 17.9 m; x88. **(F)** *Eucharodus* cf. *toomeyi* (Ethington & Clark) 17.9 m x88. **(G)** *Eucharodus xyron* (Repetski); 17.9 m; x117. **(H)** *Parapanderodus striatus* (Graves & Ellison); spot sample (2003-10) lower part of formation; x60. **(I)** *Ulrichodina abnormalis* (Branson & Mehl); 17.9 m; x80. **(J)** *Parapanderodus striatus?* (Graves & Ellison) spot sample (2004-01); x88. **(K)** ‘*Scolopodus*’ *filosus* Ethington & Clark; 58.55 m; x80. **(L)** *Parapanderodus striatus* (Graves & Ellison); 17.9 m; x88. **(M)** *Parapanderodus striatus* (Graves & Ellison); 17.9 m, x117. **(N)** ‘*Scolopodus*’ *emarginatus* Barnes & Tuke; 17.9 m; x117. **(O)** ‘*Scolopodus*’ *emarginatus* Barnes & Tuke; 17.9 m; x117.

The long ranging taxa *U. abnormalis* (Text-fig 4.9C, I), *P. striatus* (Text-fig.4.9H, L, M) , *A. deltatus* (Text-fig. 4.8K), *D. concavus* and *D. arcuatus* persist through the zone, whilst others have their FAD near the *communis* Zone and include; *Oneotodus costatus* (Ethington & Brand) (Text-fig. 4.8P), ‘*Scolopodus*’ *emarginatus* Barnes & Tuke (Text-fig. 4.9O), *Drepanoistodus* aff. *forceps* (Lindström) (Text-fig. 4.8J), *Aloxoconus* sp. A Smith, *Drepanoistodus angulensis* (Harris) (Text-figs 4.8C, D), *Cristodus loxoides* Repetski (Text-figs 4.7C, D), *Pteracontiodus bransoni* (Ethington & Clark) (Text-figs 4.7T, U) and *Diaphorodus delicatus* (Branson & Mehl).

Although *Aloxoconus staufferi* (Furnish) (Text-fig. 4.8W) represents part of an unknown apparatus, it is not placed in the reconstructed apparatus of *Ulrichodina abnormalis*, as suggested by Ji & Barnes (1994) and the reconstruction of Landing & Westrop (2006) is followed (incorporating the form species *Eucharodus parallelus*, *Ulrichodina abnormalis* and *Colaptoconus quadruplicatus*. A new species of *Aloxoconus* was also recovered from 17.9 m above the Base of the Croisaphuill Formation (Text-fig. 4.8V) and an identical species was figured as scolopodiform C by Ethington & Clark (1981).

The element resembling a species named as *Scolopodus subrex* Ji & Barnes is tentatively assigned to *Ulrichodina*, due to the erect nature and the folded basal cavity margin, although it is only represented by a single specimen (Text-fig. 4.9A), so the apparatus cannot yet be confirmed. The *communis* Zone has a composite standard range of 660 –758 csu (Sweet & Tolbert 1997). In western Newfoundland within 3 m of the top of the Boat Harbour Formation *Oepikodus communis* and *E. guyi* first appear, whilst *T. comptus* and *Oneotodus costatus* become abundant. In the lower Catoche Formation, conodonts become increasingly abundant and the fauna becomes more diverse. The conodonts *C. loxoides* and *Protoprioniodus* sp. A (*sensu* Stouge 1982), then *T. carlae* and finally *B. extensus*, *P. corbatoi* and *R. andinus* have their first appearances successively higher in the Catoche Formation (Stouge & Boyce 1997). This mirrors the succession observed in the Durness Group (Text-fig. 4.5).

4.5.6 ?*Reutterodus andinus* Zone

The FAD of ?*Reutterodus andinus* Serpagli occurs at 50 m above the base of the Croisaphuill Formation (Text-fig. 4.5). The zone is 223 m thick within the Durness group and includes much of the formation (including 77 m of the lower member and 170 m of the upper

member). The conodonts *Polonodus corbatoi* (Serpagli) (Text-fig. 4.7Q), *Juanognathus variabilis* Serpagli, *Protopanderodus gradatus* Serpagli (Text-fig. 4.8U), *Scolopodus* aff. *cornutiformis* Branson & Mehl and *Juanognathus* sp. A *sensu* Smith (1991) all have their FAD within the lower parts of the *andinus* Zone (Text-fig. 4.5) and characterise the fauna of this zone.

Other conodonts recovered include; *U. abnormalis*, *D. concavus*, *P. striatus*, *A. deltatus*, *D. arcuatus*, *O. costatus*, *S. emarginatus*, *D. aff. forceps*, *Aloxoconus* sp. A *sensu* Smith (1991), *P. abruptus*, *D. angulensis*, *C. loxoides* and *D. delicatus* all persist through the zone. *A. staufferi*, *O. communis*, *T. comptus*, *P. pygmaeus*, *S. filusus*, *S. ethingtoni*, and *P. simplicissimus* extend from the underlying *communis* Zone but have their LADs within the lower parts of the zone (Text-fig. 4.5).

Spot samples from the Croisaphuill Formation have yielded ‘*Oistodus*’ *ectyphus* (Smith) (Text-fig. 4.7K) and *Bergstroemognathus extensus* confirming the presence of the *andinus* Zone within the middle of the Croisaphuill Formation. Only six elements of this species occur in samples from the Durness Group. *?Reutterodus andinus* is also recorded from sections in Greenland but only two specimens were recovered (Smith 1991) and is clearly a rare taxon in this part of the Laurentian carbonate system. In the Ibexian composite standard section, the *andinus* Zone has a range of 758–928 csu (Sweet & Tolbert 1997).

4.5.7 *Tripodus laevis* Zone

The base of the *laevis* Zone and the base of the Whiterockian Series is tentatively placed at single occurrence of *Pteracontiodus cryptodens* (Mound) 297 m above the base of the Croisaphuill Formation (Text-fig. 4.7L). *Tripodus laevis* (Bradshaw) has recently been re-named *Tripodus combsi* (Bradshaw) by Sweet *et al.* (2005). The zone is less than 185 m thick and extends through much of the upper member of the Croisaphuill Formation and most of the Durine Formation. Conodont species recorded from this zone include many long ranging taxa, some of which have their LAD within the zone (Text-fig. 4.5). *Tripodus laevis* is recorded from a sample 10 cm below the Croisaphuill–Durine formation boundary and also from 43 m above the base of the Durine Formation (Text-fig. 4.10N). A new species of Ulrichodina (Text-fig. 4.10K) (similar to *Ulrichodina* sp. nov. Barnes) is recorded from 20.7 m above the base of the Durine Formation

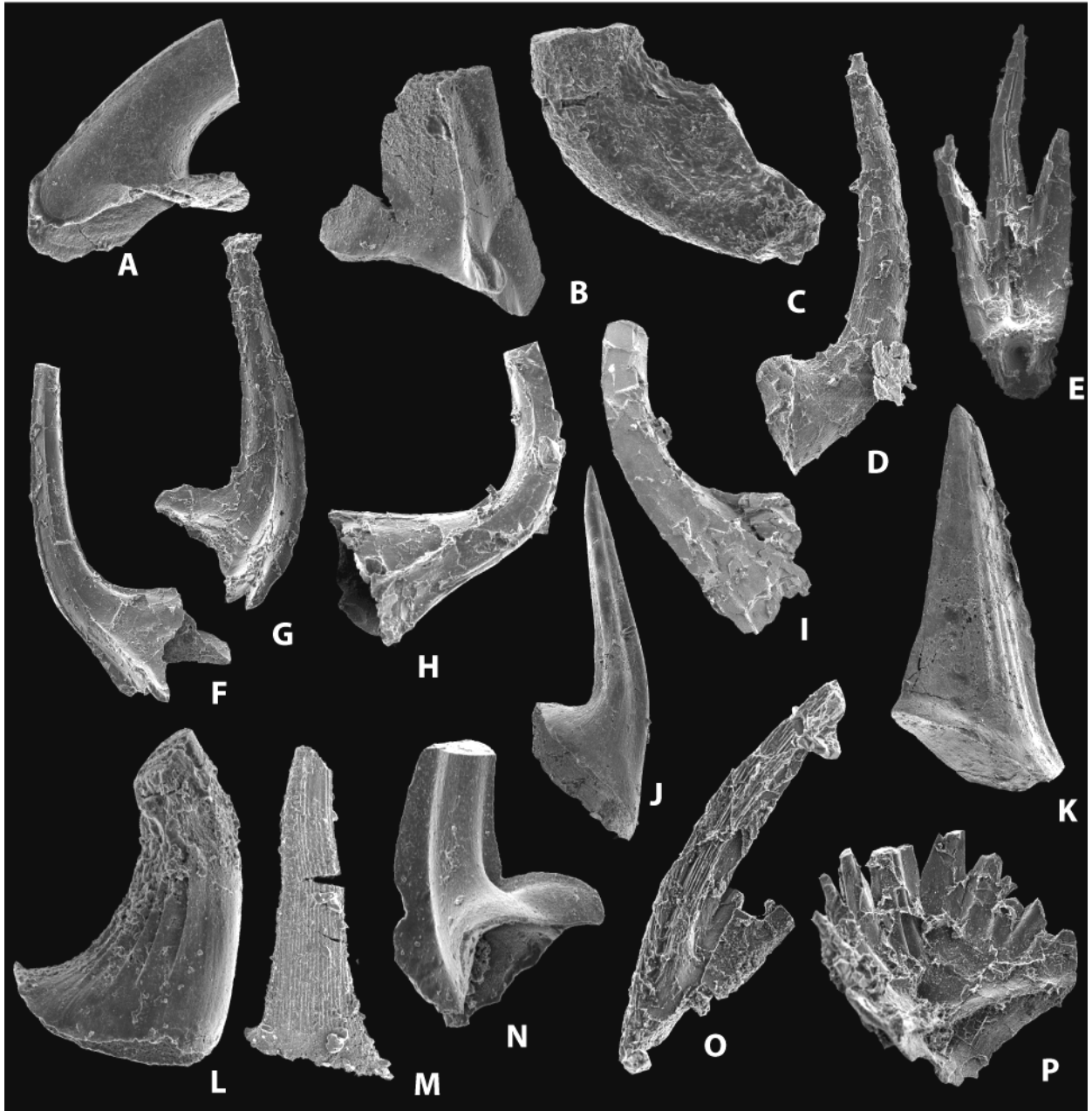
The biostratigraphical resolution of this zone and the overlying *H. altifrons* Zone is hampered by the increasingly poor preservation of elements up-section, the discontinuous nature of the sections and the increased number of barren samples. In the standard reference section *P. cryptodens* has a range of 965–1161 csu and the *laevis* Zone 928–1006, so the use of this species as the base of the zone is approximate.

The base of the Middle Ordovician is placed at the FAD of *Baltoniodus? triangularis* (Text-figs 1.9, 4.4) in the Huanghuachang section GSSP, Yichang, China (Wang *et al.* 2005). The base of the *B. triangularis*–*M. flabellum* Zone in the GSSP section was correlated by Wang *et al.* (2005) with the base of the *T. laevis*–*M. flabellum* interval in the North American Whiterockian and Ibexian sections (Ethington & Clark 1981; Ross & Ethington 1992) (i.e. the *T. laevis* Zone of Sweet & Tolbert 1997) and correlates with the base of the *T. laevis* Zone in the upper San Juan Formation, Argentina (Albanesi *et al.* 2003) based upon the underlying diagnostic taxa of *Oepikodus evae* Zone age. Wang *et al.* (2005) documented a worldwide lowstand event preceding the FAD of *B. triangularis*. This may correspond to the shallowing observed at the base of the upper member of the Croisaphuill Formation (Chapter 5). The Lower–Middle Ordovician boundary and the boundary between the Floian and Dapingian stages is placed 297 m above the base of the Croisaphuill Formation (73 m above the base of the Durness Group) and thus the Lower Ordovician is c. 540 m thick.

4.5.8 *Histiodelia altifrons* Zone

A spot sample (2003-30) at the top of the Durine Formation, as close to the Moine Thrust as possible, yielded *Pteracontiodus cryptodens*, (Text-figs 4.10F–I) *Chosonodina rigbyi* and *Dischidognathus* sp. nov. Ethington & Clark (1981).

Higgins (1969) recorded a number of form taxa from the upper Durine at Durness and unpublished collections (J. E. Repetski) from the same position as Higgins' localities (D15 and 16) (Text-fig. 4.2) contain *Jumudontus gananda*, *Cooperignathus aranda*, *C. rigbyi*, *Dischidognathus* sp. nov. *Diaphorodus delicatus*–*Pteracontiodus cryptodens*, *Pteracontiodus cryptodens*, *Scolopodus paracornutiformis*, *Oistodus scalenocarinatus*, *Histodelia altifrons*, *Baltoniodus minutus?*, *Drepanodus arcuatus*, *Parapanderodus striatus*, *Drepanodus concavus*, *Drepanoistodus* spp., *Drepanoistodus* cf. *angulensis*, *Ulrichodina abnormalis* and '*Scolopodus*' *emarginatus* (J. E. Repetski *pers comm.*). (Text-fig. 4.11).



Text-figure 4.10 Selected conodonts species from the Durine Formation including stratigraphic height. **(A)** *Drepanoistodus?* sp.; 42.9 m; x100. **(B)** *Diaphorodus?* sp.; 42.9 m; x100. **(C)** *Reutterodus?* sp.; 42.9 m; x100. **(D)** *Ulrichodina abnormalis* (Branson & Mehl) spot sample (2003-10) top Durine Formation; x110. **(E)** *Dischidognathus* sp. nov.; spot sample (2003-30), top of formation; x110. **(F)** *Pteracontiodus cryptodens* (Mound); spot sample (2004-06) lower Durine Formation; x110. **(G)** *Pteracontiodus cryptodens* (Mound); spot sample (2003-08); top of formation; x110. **(H)** *Pteracontiodus cryptodens* (Mound); Durine Formation top; x110. **(I)** *Pteracontiodus cryptodens* (Mound); 32.2 m; x110. **(J)** aff. '*Oistodus*' *akpatokensis* Barnes in Workum *et al.*; spot sample (2004-06), lower Durine Formation x55. **(K)** *Ulrichodina* n. sp. Barnes; 20.7 m; x50. **(L)** *Oneotodus costatus* Ethington & Brand; 42.9 m x130. **(M)** Gen. nov. B; 120.45 m; x143. **(N)** *Tripodus laevis?* Bradshaw; 42.9 m; x143. **(O)** Prioniodontid M element; spot sample (2003-08) top of formation; x143. **(P)** *Chosonodina rigbyi* Ethington & Clark spot sample (2003-30) top of formation: x143.

Text-figure 4.11 Conodonts from the uppermost Durine Formation (*altifrons* Zone) SEM images kindly supplied by J. Repetski, USGS. Specimens were processed from Higgins' localities D-15 and D-16. **(A)** *Pteracontiodus cryptodens* (Mound); D-16; x100. **(B)** *Pteracontiodus cryptodens* (Mound); D-16; x50. **(C)** *Pteracontiodus cryptodens* (Mound); D-16; x90. **(D)** *Oistodus scalenocarinatus* Mound, D-15; x100. **(E)** '*Scolopodus*' sp.; D-15; x100. **(F)** *Parapanderodus striatus* (Graves & Ellison); D-15; x81. **(G)** *Parapanderodus striatus* (Graves & Ellison); D-15; x100. **(H)** *Histiodella altifrons* Harris; D-16; x100. **(I)** *Histiodella altifrons* Harris; D-16; x100. **(J)** *Histiodella altifrons* Harris; D-16; x100. **(K)** *Ulrichodina abnormalis* (Branson & Mehl); D-16; x110. **(L)** *Jumudontus gananda* Cooper; D-16; x100. **(M)** *Jumudontus gananda* Cooper; D-15; x100. **(N)** *Jumudontus gananda* Cooper; D-15; x90. **(O)** *Baltoniodus minutus* McTavish; D-16; x100. **(P)** *Cooperignathus aranda* (Cooper); D-15; x100. **(Q)** *Cooperignathus aranda* (Cooper); D-15; x90. **(R)** *Drepanoistodus? concavus* (Branson & Mehl); D-15; x50. **(S)** *Drepanoistodus angulensis* (Harris); D-16; x55. **(T)** *Drepanoistodus* aff. *forceps* (Lindström); D-15; x200. **(U)** '*Scolopodus*' *emarginatus* Barnes & Tuke; D-15; x50. **(V)** *Drepanodus arcuatus* Pander; D-16; x100. **(W)** *Diaphorodus delicatus* (aff. *P. cryptodens*) (Branson & Mehl); D-15; x160. **(X)** *Diaphorodus delicatus* (aff. *P. cryptodens*) (Branson & Mehl); D-15; x240. **(Y)** *Dischidognathus* sp. nov.; D-16 x100.



The thickness of the zone is not known, but the spot samples containing *H. altifrons* come from near the top of the Durine Formation and Higgins estimated his samples to be within 20 m of the top (Text-fig. 4.10, 4.11).

The age of the top of the Durine Formation and the top of preserved carbonates in the Durness Group was for many years assumed to be latest Arenig and probably early Llanvirn (Higgins 1967). This view accepted by Whittington (1972) although they were cautious based upon the uncertainty of the stratigraphical locations of Higgins' samples. The age of the top of the Durness Group was more precisely referred to the *Pteracontiodus cryptodens*–*Histiodelia altifrons*–*Multioistodus auritus* interval of Ethington & Clark (1981) by Bergström (1985) who collected the samples of J. E. Repetski.

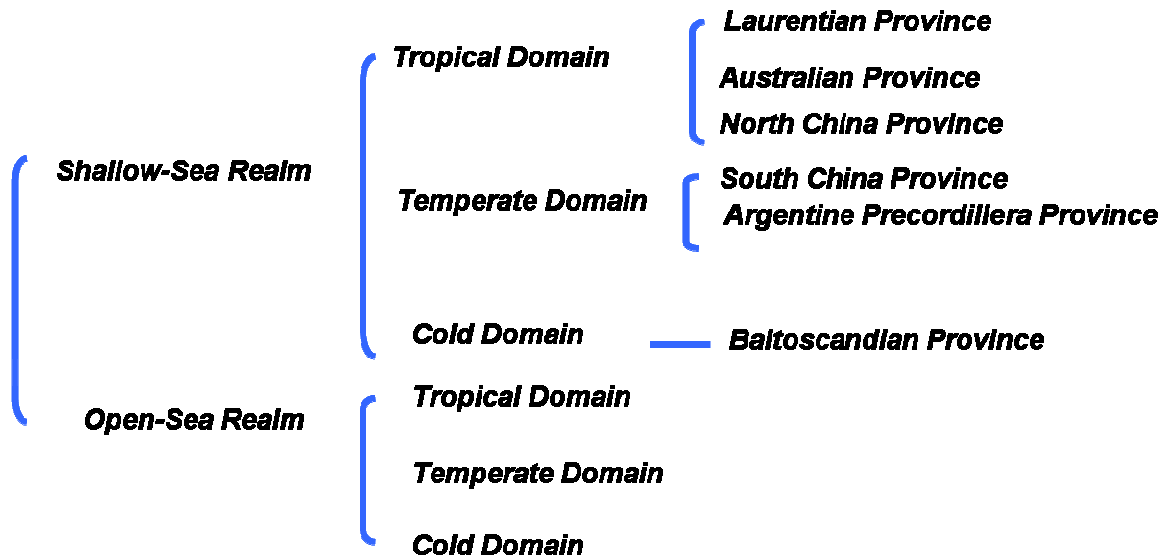
Samples from this study and a re-examination of those of J.E. Repetski confirm that the top of the Durine Formation is of lower *altifrons* Zone age, (lower Whiterockian) and therefore lower Dapingian, (Middle Ordovician) in age and c. 470.5 Ma. (Gradstein *et al.* 2004)

4.6 PALAEOBIOGEOGRAPHY

4.6.1 Extent of the Tropical Domain

From their origin in the late Cambrian, euconodonts are cosmopolitan in their palaeogeographical distribution, but this soon resulted in a strongly developed global provincialism by the Floian Stage (Lower Ordovician). The long-established view of this provincialism comprises two provinces: a high latitude, cold water North Atlantic Province (NATP), and a low latitude North American Midcontinent Province (NAMP) (Sweet *et al.* 1959). This was seen to be an over simplification, as new faunas were recovered from Australia, Argentina and China which had a close affinity with the NAMP (Zhen & Percival 2003). Recent work has also established the retention of cosmopolitanism in deep, cold water conodont faunas within Ordovician oceans. Zhen & Percival (2003) proposed a new model using modern ocean biogeographical methods (Text-fig. 4.12). They grouped conodont faunas into Tropical, Temperate and Cold Domains (part of the Shallow-Sea Realm). Faunas from the Cold Domain comprise the Baltoscandian Province and a Temperate Domain is represented by the South China Province and the Argentine Precordillera Province, which share taxa with both the Cold and Tropical domains. The Tropical Domain includes the

Laurentian, Australian and North China Provinces (Zhen & Percival 2003). The Laurentian Province represents the distribution of shallow, warm water faunas inhabiting shelf regions fringing Laurentia, which was within tropical zones throughout much of the Ordovician.



Text-figure 4.12 Ordovician conodont realms, domains and provinces recognised (after Zhen & Percival 2003).

In the British Isles, the only other coeval conodont faunas have been recorded from the Dounans Limestone, within the Highlands Border Complex, Scotland (Ethington & Austin 1991). The fauna comprises the typical tropical domain species *Jumudontus gananda* Cooper, *Parapanderodus striatus* (Graves & Ellison) and *Eucharodus parallelus* (Branson & Mehl) (now *Ulrichodina abnormalis* (Branson & Mehl)), with the cold domain, Baltoscandian province conodont *Periodon flabellum* (Lindström). However only 48 elements were recovered from 71 kilograms of limestone and all available limestone was removed from the area during quarrying. The low yields precluded its use in this study, but it shares fauna also recovered from the Durness Group. The position of this terrane is still not known, but it must have had connections with the Laurentian margin.

In terms of species composition, the most similar faunas to those from the Durness Group are, perhaps predictably, those from western Newfoundland (Pohler 1994, Johnston & Barnes 2000, Ji & Barnes 1994, Stouge 1982, Stouge & Boyce 1983) and Greenland (Smith 1991).

4.6.2 A multivariate statistical analysis of Laurentian faunas at the time of maximum flooding

A cluster analysis of a representative conodont zone was conducted to assess the degree to which faunas across the palaeocontinent of Laurentia are endemic. Few studies have sought to analyse localities along the margin of Laurentia and have treated faunas as endemic. Species lists were collated from published sources and compared to the fauna recorded from the Durness Group.

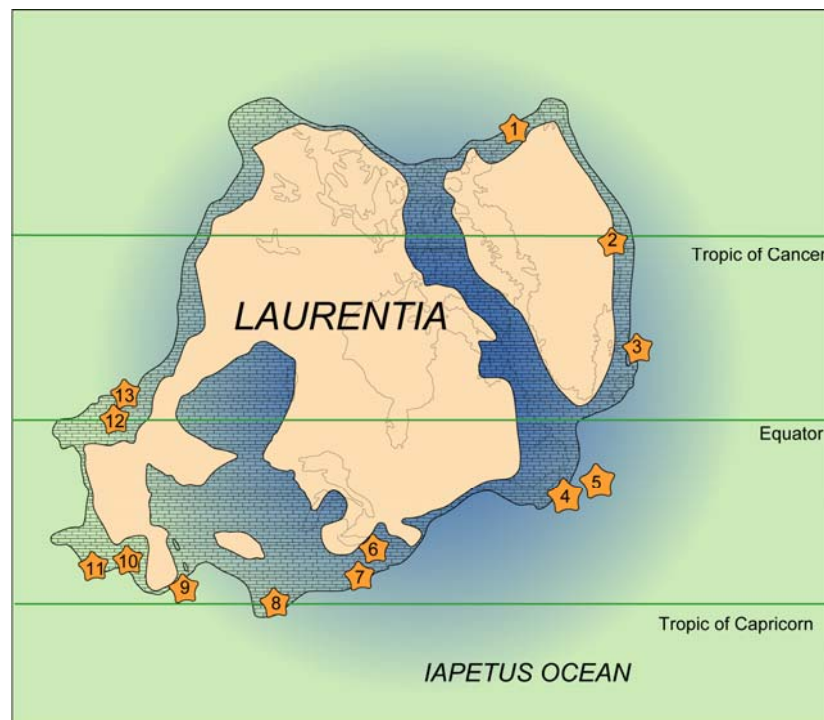
	LOCALITY	PUBLICATION
1	eastern North Greenland	Smith (1991)
2	East Greenland	Smith (1991)
3	northwest Scotland	this study
4	western Newfoundland	Ji & Barnes (1994), Stouge (1982)
5	western Newfoundland (slope)	Pohler (1994), Stouge & Bagnoli (1988)
6	New York	Landing & Westrop (2006)
7	New Jersey	Karklins <i>et al.</i> (1989)
8	Georgia	Repetski (1992)
9	Mississippi	Alberstadt & Repetski (1989)
10	Texas	Repetski (1982)
11	Mexico	Stewart <i>et al.</i> (1999)
12	Utah	Ethington & Clark (1981)
13	Nevada	Sweet & Tolbert (1997)

Text-table 4.2 Localities included in the cluster analyses and the principle publications used to compile the species lists given in Text-table 4.3.

The similarity was assessed using PAST (Hammer *et al.* 2001). The palaeobiogeography of species is based on three simple principles: 1) that not all taxa live everywhere, 2) that taxa are not randomly distributed, 3) that some taxa tend to occur together, whilst others do not (Zhen & Percival 2003).. The interval used is the *communis* Zone (479–475 Ma), which has a range of 660–758 csu in the Ibexian composite standard section. Only conodonts from this zone were included, to minimise introducing artificial

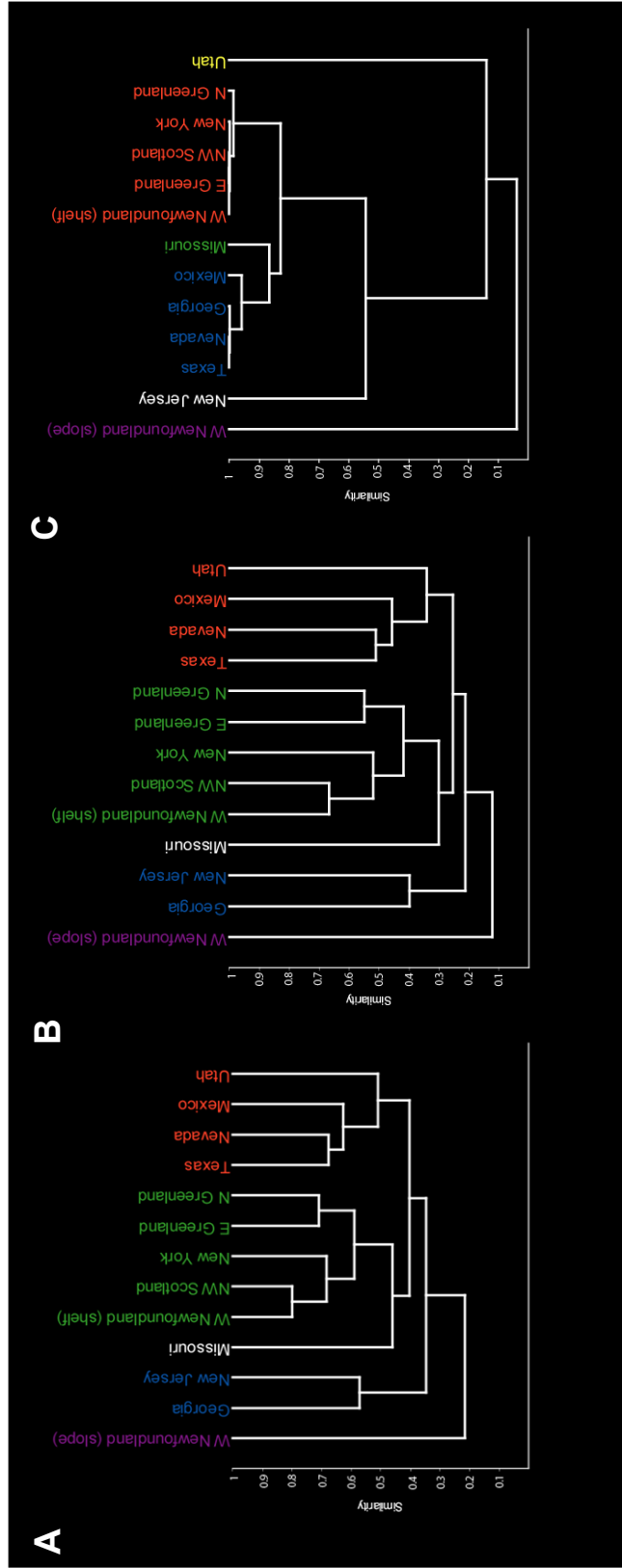
disparity. The zone is well documented, and several large monographs have been published on faunas of this age (Smith 1991; Ji & Barnes 1994; Repetski 1982; Ethington & Clark 1981).

The base of the zone marks an important flooding event and period of substantial faunal turnover. During this time diversity was high and shallow marine facies were extensive across Laurentia. Faunas from Greenland, NW Scotland, western Newfoundland, New York, New Jersey, Georgia, Mississippi, Texas, Mexico, Utah and Nevada (Text-fig. 4.13, Text-table 4.2), incorporating a total of 92 taxa (Text-table 4.3).



Text-figure 4.13 Palaeogeographical map of Laurentia, displaying the distribution of Ordovician strata and the localities included in this study. The numbers refer to publications listed in Text-table 4.2. Basemap is modified after Dzik (1983).

Potential sources of error include the misdating of samples by authors, taxonomic misidentification, palaeogeographical mislocation of small continental fragments, preservational bias, publishing bias, use of form taxa (which would change estimates of diversity), the presence of overly rare taxa (which over-emphasise patterns of endemism due to non-recovery) and the possible diachroneity of taxa.



Text-figure 4.14 (A) Dendrogram displaying data using paired linkage and Dice coefficient. (B) Dendrogram displaying data using paired linkage and Jaccard coefficient. (C) Dendrogram using paired linkage and Raup-Crick coefficient. All plots were constructed using PAST.

These were minimised as much as possible, by basing the study upon figured specimens rather than species lists. It was possible to view some collections to confirm unanimity of conodont identification. The data was analysed using PAST (Hammer *et al.* 2001) on the basis of presence/absence data. Cluster analysis organises the objects in a two-dimensional dendrogram by forcing the data into discrete groups. Thirteen localities were compared one to one with respect to their individual faunas. Cosmopolitan taxa were removed from the analysis to reduce the effect that those taxa would influence on the overall clustering (Rasmussen 1998, Zhen & Percival 2003).

The dendrograms were plotted using the Dice (Sorensen), Jaccard and Raup-Crick coefficients with paired linkages. These were chosen due to the binary nature of the data and are commonly used in palaeobiogeographical studies. A description of each coefficient used can be found in Harper (1999).

All the dendrograms show a clustering of New York, western Newfoundland, Greenland and NW Scotland with a high similarity value (Text-fig. 4.13). The deep water fauna from western Newfoundland plots separately from all other localities. Texas, Mexico and Nevada are always linked. Utah is present within the same cluster when Dice and Jaccard coefficients are used (Text-fig. 4.13). Interpretation of conodont biogeography is also heavily dependant on an understanding of the mode of life of the conodont animals. Spatial distribution of conodonts was very much dependant upon palaeoecological factors and it is important to consider biofacies before identifying faunal provinces (Bergstöm 1985). The localities in Scotland, East Greenland and western Newfoundland at this point in time experienced deposition of widespread burrow mottled facies (Croisaphuill, Cape Weber and Catoche formations) and these are all interpreted to represent a similar palaeo-water depth (Fortey 1984, Smith & Rasmussen 2008). It is not certain how this facies compares to those from other sites included in the study and a slightly different facies may have resulted in a different fauna. Some attempts have been made to set standard criteria for defining biogeographical units and the definitions of Kauffman (1973) are used here (Text-table 4.4). This approach has not generally been embraced and despite preference for a well ordered hierarchical system with equally weighted divisions, nature rarely conforms to this. According to Campbell & Valentine (1977), there is still a use in quantifying the amount of endemic taxa upon which subdivisions are based. Sites from East Laurentia comprise 14% endemic taxa of

the 92 included in the analyses and would therefore warrant classification as a separate subprovince according to Kauffman (1973).

BIOGEOGRAPHIC UNIT	% ENDEMIC SPECIES
Realm	>75%
Region	50 - 75%
Province	25 - 50%
Subprovince	10 - 25%
Endemic Centre	5 - 10%

Text-table 4.4 Percentage contribution of endemic species within a hierarchical classification of biogeographical units. (after Kauffman 1973).

4.7 CONCLUSIONS

The conodonts zonation of the North American mid-continent (Sweet & Tolbert 1997) can be recognised within the upper five formations of the Durness Group. The Cambrian–Ordovician boundary and the base of the Tremadocian Series lie at the flooding event marked by the Eilean Dubh–Sailmhor formation boundary (298 m above the base of the Durness Group), although the conodont defining the base of the Ordovician has not been recovered. The base of the Floian Stage (the second stage of the Lower Ordovician) lies within the *A. deltatus* – *O. costatus* Zone and thereby at a horizon within the Balnakeil Formation, most likely at a level within 10s metres below the Croisaphuill Formation. This indicates that the boundary lies 730 m above the base of the Durness Group and that the Lower Ordovician has a thickness of c. 540 m

The base of the Whiterockian (Middle Ordovician) lies within the upper member of the Croisaphuill Formation, but is probably more correctly placed in lithostratigraphical terms at the boundary between the upper and lower members and is equivalent of the Floian–Dapingian stage boundary. The age of the youngest preserved carbonates within the Durness Group is within the *H. altifrons* Zone (Ross-Hintze zone M; early Whiterockian; late but not latest Arenig; c. 470.5 Ma). The cluster analysis and the quantity of endemic taxa from sites across East Laurentia suggest that the subdivision of the Laurentian Province into two separate subprovinces is applicable (Text-Table 4.4) (Kauffman 1973). The conodont faunas from NW Scotland represent part of an East Laurentian Subprovince, which includes Greenland, western Newfoundland and New York. This is separate from a South Laurentian Subprovince.

Chapter 5

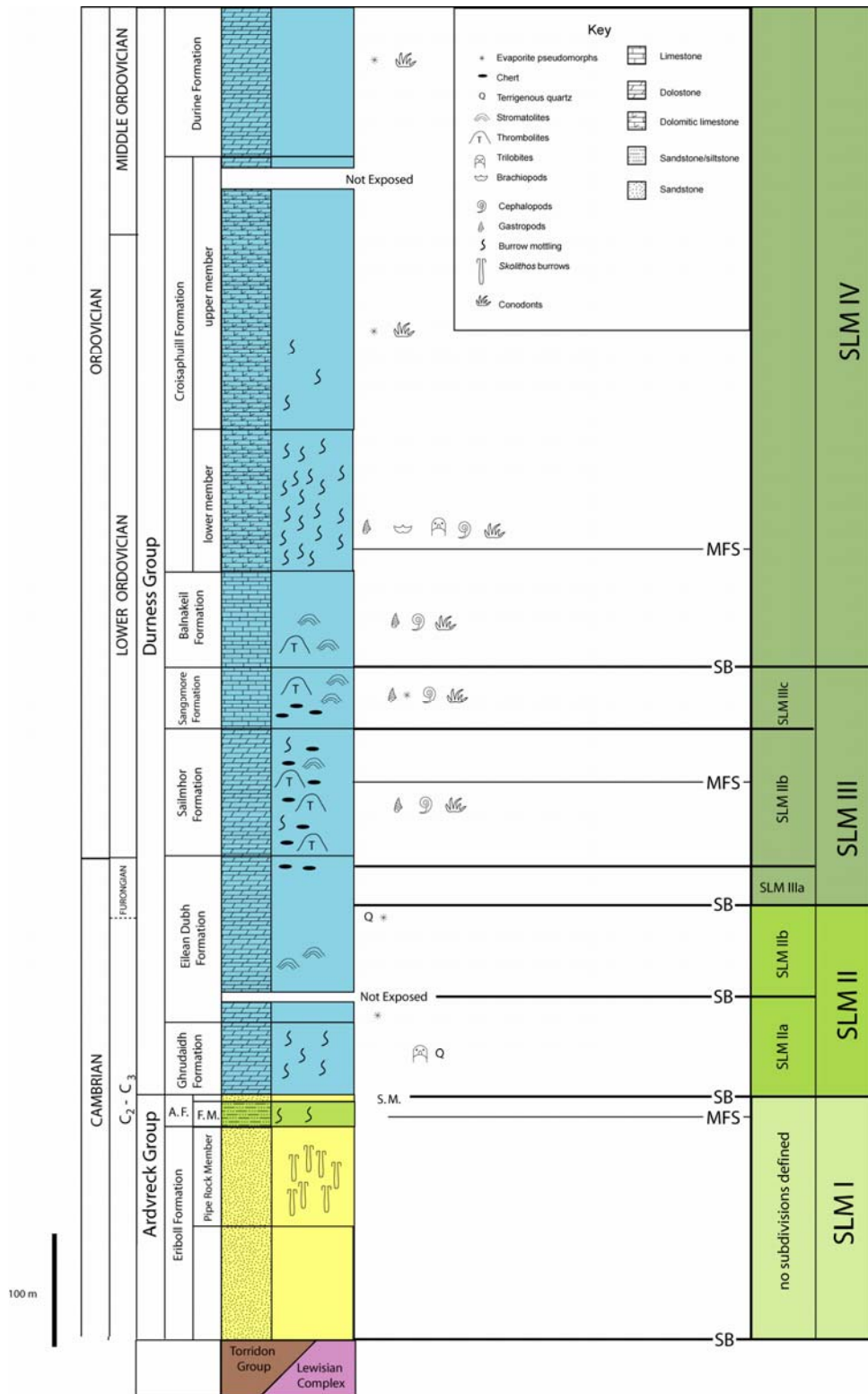
SEQUENCE STRATIGRAPHY OF THE SCOTTISH LAURENTIAN MARGIN AND RECOGNITION OF THE SAUK MEGASEQUENCE

5.1 INTRODUCTION

Shallow marine rocks of Cambrian and Ordovician age were deposited widely along the continental margin of Laurentia, and rocks of this age in northwest Scotland represent a fragment of a once extensive cratonic margin. In Scotland, as elsewhere along the contiguous Lower Palaeozoic palaeo-margin, these strata can be divided into a lower siliciclastic unit, and an overlying carbonate succession (Swett & Smit 1972a, b; Smith & Rasmussen 2008). The lower unit (Ardvreck Group) predominantly comprises cross bedded subarkoses, quartz arenites, and rippled dolomitic siltstones, with subordinate thin crinoidal grainstones, whilst the overlying unit, the Durness Group comprises dolomites/stones, limestones and dolomitic limestones, with cherts and minor evaporite pseudomorphs (Chapter 2) (Text-fig. 5.1).

In NW Scotland, Cambro-Ordovician rocks crop out in a narrow belt along the Caledonian foreland and within the Moine Thrust zone, stretching some 180 km from Loch Eriboll in the north, south-westwards to Skye (Text-fig. 1.3), forming an almost continuous belt which is rarely more than 10 km in width. The best exposed and preserved section is the readily accessible coastal exposure at the type section of Balnakeil Bay, Durness. This section along with nearby inland exposures provides the main data used in this study (Text-fig. 1.5). Supplementary sections were also examined at An-t Sròn, Stronchrubie, Skiag Bridge, Ardvreck Castle, Ullapool and Strath Suardal (Text-figs. 1.3, 1.4, 1.6).

The succession in northwest Scotland forms part of an autochthonous sequence (Hebridean terrane), which can be correlated with the external Humber zone of the northern Appalachian orogen in western Newfoundland (Williams 1979). The equivalent rocks in Newfoundland differ from those in Scotland by also preserving the outer detrital belt (allochthonous Cow Head and Curling groups), which represent represent ramp-margin and slope deposits (James & Stevens 1986). The margin and slope deposits preserve the lowstand systems tracts (LSTs; see later explanation of terminology), which were deposited when the shelf experienced a fall in sea-level.



Text-figure 5.1 Simplified sedimentary log showing the principal occurrences of fossil remains, the lithostratigraphy, chronostratigraphy, and the position of the SLM (Scottish Laurentian Margin) Megasequence, its subdivisions, sequence boundaries (SB) and maximum flooding surfaces (MFS). The An t-Sròn Formation is indicated by A.F., the Fucoid Member by F.M. and the Salterella Grit Member by S.M.

The Cambro-Ordovician sediments in northwest Scotland are believed to represent deposition on a palaeo-southeast facing, low latitude and passively subsiding cratonic margin (Text-fig. 1.2). During this time Laurentia moved very little and Scotland was situated around 25° S (Cocks & Torsvik 2006). The rocks overlie a planar unconformity which truncates the underlying Archaean and Palaeoproterozoic Lewisian Complex and the Neoproterozoic Torridon Group sandstones.

Scotland's Laurentian passive margin formed following the break up of the supercontinent Rodinia and initiation of the Iapetus Ocean following rift–drift transition at 600–580 Ma (Torsvik *et al.* 1996). Recent studies suggest that the rifting was a two stage process forming the Iapetus Ocean between west Gondwana and Laurentia at 570 Ma, followed by continued rifting between 540–535 Ma, when the Laurentian passive margin *sensu stricto* formed (Cawood *et al.* 2001).

The southern Laurentian palaeo-margin consists of a series of promontories and re-entrants (Lavoie *et al.* 2003), with Scotland situated on a promontory that marks a significant inflexion in the continental margin (Thomas 1977; Soper 1994) (Text-fig. 1.2B). These palaeogeographical features suggest that the original shape of the Iapetus margin reflects the interplay of rifting and oceanic transform faults (Williams & Max 1980; Soper 1994; Lavoie *et al.* 2003). The northwest Scottish Cambro-Ordovician succession lies at the transition between the Newfoundland and Greenland margins and its history is important to understanding early Palaeozoic global palaeogeography and tectonics (Dalziel & Soper 2001).

Large scale sedimentary sequences are recognised in the Palaeozoic rocks of North America (Sloss 1963). On the craton, the Sauk sequence, the oldest sequence, begins with lower to upper Cambrian strata and rests unconformably upon Precambrian-age basement. The Sauk sequence is subdivided into three smaller scale transgressive–regressive cycles (second- and third-order) on the basis of lithostratigraphy and trilobite biostratigraphy (Palmer 1981), each cycle separated by eustatic lowering of sea-level. The Sauk III Supersequence was later subdivided and a fourth cycle (Sauk IV) recognised in the upper part in sections across Laurentia (Golonka & Kiessling 2002). However, the correlation of this upper sequence has been problematic due to the diachronous nature of the sequence boundary. Following sequence stratigraphical revision, Sloss's sequences were termed 'megasequences' (first-order) and the subdivisions 'supersequences' (second-order), largely based upon the thickness, extent and duration. The Sauk Megasequence is of Early Cambrian to Dapingian

(early Middle Ordovician) in age (although different authors have defined the boundary at different events) and it is interpreted to reflect deposition following progressive flooding of the Laurentian Craton during prolonged sea-level rise. The Sauk Megasequence rests unconformably upon Precambrian rocks and is separated from the overlying Tippecanoe Megasequence by a widespread unconformity. A number of third-order cycles have been recognised both from the Cambrian ('Grand Cycles') and from the Ordovician parts of the Sauk, although the causes and correlative potential of these sequences remains problematic.

In NW Scotland, the Sauk Megasequence includes the Ardvreck and Durness Groups. The Sauk –Tippecanoe boundary is not observed in the section due to truncation by the Moine Thrust zone, but thick dolostones at the top of the Durness Group suggest that the Scottish shelf was shallowing similar to western Newfoundland, where the sequence boundary is well developed.

Although the sequence stratigraphical subdivisions of the Scottish Cambro-Ordovician compare well with other sections along the Laurentian margin, a separate classification will be applied to maintain objectivity prior to correlation with the Sauk. The Ardvreck and Durness groups represent a thick, first-order sequence of major cratonic transgression and regression (the Scottish Laurentian Margin (SLM) Megasequence). In northwest Scotland, the SLM Megasequence represents c. 1130 m of strata and can be divided into four constituent second-order supersequences (SLM I–IV), which are each several hundred metres in thickness and are separated by distinctive sequence boundaries, or sequence boundary zones (Text-fig. 5.1). Two of these supersequences (SLM II and SLM III) contain recognisable third-order sequences, which are separated by evidence of shallowing.

Stratigraphical breaks that have been suggested to occur within the succession (e.g. Grabau 1916, Poulsen 1951 and Palmer *et al.* 1980) but recent work (this study and Nicholas *et al.* 1994) suggest that they are not of the duration or in the same stratigraphic position proposed by the former publications. Macrofaunas are rare within much of the Ardvreck and Durness groups and this led to the assumption of parts of the succession being absent. The age of the sequence boundaries and systems tracts has been dated using conodont biostratigraphy in this study to produce a higher resolution framework (Chapter 4).

5.2 TERMINOLOGY

The fundamental unit of sequence stratigraphy is the sequence; ‘a conformable succession of genetically related strata bounded by unconformities and their correlative conformities’ (Mitchum 1977). A sequence can be subdivided into systems tracts, which are defined by their position within a sequence, and by the stacking patterns of parasequences and parasequence sets (Van Wagoner *et al.* 1988).

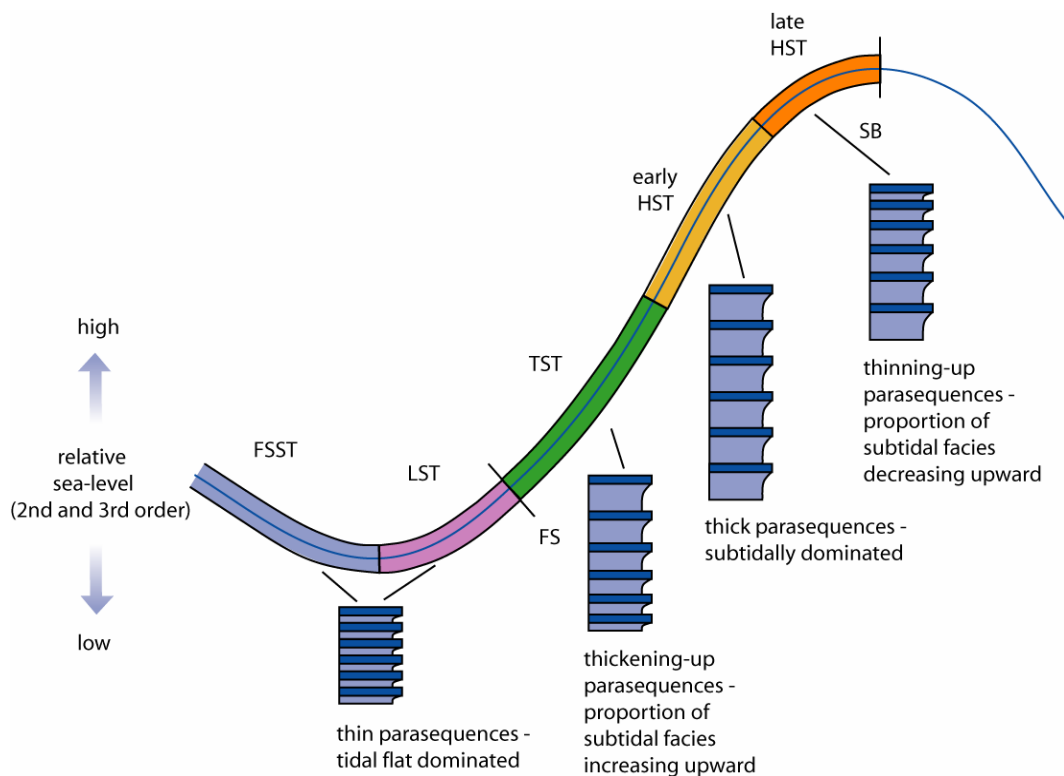
A parasequence represents a conformable succession of genetically related beds or bed-sets, bounded by marine-flooding surfaces and their correlative surfaces (Van Wagoner 1985). Marine-flooding surfaces separate younger from older strata, across which there is evidence of an abrupt increase in water depth and the surfaces are commonly associated with minor submarine erosion and non-deposition. Parasequences may be grouped together to form a parasequence set; this is a succession of genetically related parasequences, which form a distinctive stacking pattern, and may represent either progradational, retrogradational or aggradational depositional trends (Van Wagoner 1985; Goodwin & Anderson 1985).

The building blocks of sequence stratigraphy are the systems tracts. These are primarily recognised by their bounding surfaces and the nature of the constituent parasequence sets. There are a number of different systems tracts that have been recognised. Commonly occurring at the base of shelf-deposited successions, the transgressive systems tract (TST) represents increasing accommodation space, during relative sea-level rise (Text-fig. 5.2). It is separated from the highstand systems tract (HST) by the maximum flooding surface (MFS) (Text-fig. 5.2). As the rate of sea-level rise begins to slow, accommodation space is filled and an HST is deposited. Deposition during falling relative sea-level may form a falling stage systems tract (FSST) and also a lowstand systems tract (LST), however sediment is usually removed from, or by-passes the shelf and these are therefore commonly missing in section, and only deposited basinward of the shelf-break. With a subsequent rise in sea-level, a transgressive-, or flooding surface (FS) is sometimes preserved, separating the LST from the overlying TST and marking the first significant marine flooding across the shelf. A sequence boundary (SB) separates the HST from the FSST (Text-fig. 5.2), but on the shelf, generally lies between the HST and the succeeding TST. Where a sequence boundary cannot be recognised, a sequence boundary zone (SBZ) is defined where possible and the MFS is commonly recognisable in sections as a maximum flooding zone (MFZ) (*sensu* Glumac & Walker 2000).

In an attempt to classify the variety of thicknesses and duration of cycles, Vail *et al.* (1977) assigned a hierarchy to them. First-order eustatic cycles (50 My or more) represent continental flooding cycles, defined on the basis of major times of encroachment and restriction of sediments on a craton (Vail *et al.* 1991). Second-order cycles (5–50 My) are the combination of long-term changes in the subsidence rates, coupled with long-term changes in eustasy. They are characterised by transgressive–regressive facies cycles. Third-order cycles are the combination of short-term changes in eustatic sea-level and the accommodation space created by subsidence (0.5–5 myr). They are generally depositional sequences composed of systems-tracts. Fourth- to fifth-order cycles (<0.01–0.5 myr) result from the interaction of high-frequency eustatic changes and accommodation space created by subsidence (Van Wagoner *et al.* 1990). The stratigraphical signatures of these cycles are simple sequences and parasequences (Vail *et al.* 1991). Theoretically fifth-order cycles are superimposed on longer-term fourth order and third-order cycles to form a composite eustatic sea-level curve. Schlager (2004, 2005) has proposed that cycles may be fractal and are therefore subdivisions of convenience, thus it may be largely irrelevant to try and separate 2nd and 3rd order cycles (Hardenbol *et al.* 1998). Because of this 4th and 5th order cycles may take the form of standard sequences or parasequences and larger cycles may exhibit the form of parasequences (separated by marine flooding surfaces).

5.3 METRE-SCALE, SHALLOWING-UPWARD PARASEQUENCES WITHIN THE DURNES GROUP

Shallow marine sediments are commonly arranged into regular upward coarsening units with an upwards shallowing facies succession (regressive trend) (James 1984). These equate to the ‘punctuated aggradational cycles’ (PACs) described by Goodwin & Anderson (1985). The shallowing upward facies are separated by much thinner units (represented by a hardground or omission surface) representing upward deepening. Cycles within siliciclastic rocks were termed parasequences by Van Wagoner *et al.* (1990), who defined them as ‘relatively conformable successions of genetically related beds or bedsets bounded by marine flooding surfaces’. The bases of parasequences are defined by the marine flooding surface; hence they are less easily distinguished in settings where changes in water depth go unrecorded, such as deeper oceanic environments (Emery & Myers 1996).



Text-figure 5.2 Idealised stacking patterns of shallow marine carbonate parasequences on a carbonate platform top. The curve shows a long term (e.g. third-order) relative sea-level cycle and the logs show the thickness and composition (subtidal vs. intertidal) of the higher frequency cycles or parasequences within each systems tract (Bosence & Wilson 2003).

The 100 parasequences recognised within the Durness Group, consist of subtidal dolostones or limestones that commonly shallow upward into peritidal, parallel-laminated dolostones, exhibiting evidence of subaerial exposure. The mean thickness of parasequences within the Durness Group is 2.62 m, and they range from 0.4–8 m, but the majority are 1–3 m in thickness. The time over which 83 of the parasequences formed (from the Cambrian–Ordovician boundary to the base of the *Oepikodus communis* Zone) is estimated as 11 million years (Gradstein *et al.* 2004), which would indicate an average cycle duration of approximately 130,000 years, largely assuming that each parasequence represents the same amount of time, that entire parasequences have not been removed by erosion, and assuming there is no loss of section at the faults present. Both the thickness and individual facies composition of parasequences within the Durness Group varies greatly and, as would be expected, the proportions of subtidal to peritidal facies differ through the section. Based on

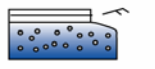
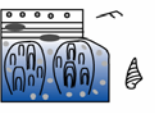
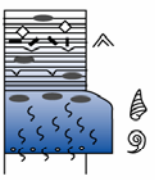
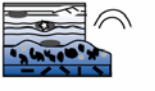
the variable proportion of subtidal to peritidal facies, they can be divided into two classes: peritidally and subtidally dominated parasequences. The division is based solely on the relative proportion of the two, but few parasequences are recorded that contain equal proportions.

5.3.1 Subtidally dominated parasequences

These parasequences consist of an upward shallowing succession of subtidal and then peritidal facies, with the thickness of the subtidal portion accounting for >51% of the total cycle. They can be grouped according to the subtidal facies present into stromatactoid, columnar/digitate stromatolite bioherm and ooidal grainstone based parasequences (Text-fig. 5.3). The basal facies indicates the position upon the carbonate platform at which sedimentation recommenced and the upper part of parasequences has the potential to be removed by erosion prior to deposition of the succeeding parasequences. The parasequence boundaries range from sharp to gradational, with internal facies boundaries commonly being gradational. They range in thickness from a few tens of centimetres (ooidal grainstone parasequences) to 6 m, although most are in the order of 1–3 m thick. At times of normal salinity, a macro- and micro-fauna, including nautiloids, gastropods and conodonts is observed and bioturbation is locally common. The environment of deposition of these parasequences is interpreted to have been seaward of the tidal-flats, with water depths interpreted to be moderately shallow (10–20 m at the most) (Sarg 1988).

5.3.2 Peritidally dominated parasequences

These cycles have relatively thick peritidal portions, equal to or thicker than the subtidal facies. They frequently have a thin (<10 cm) transgressive lag deposit at their bases containing intraclasts, peloids and/or terrigenous quartz grains. The main constituents are microbialites, tidal flat laminites (mechanical and microbial), ooidal grainstones, wavy laminated peloidal wackestones and quartz-rich dolostones. Peritidally dominated cycles typically include quartz sand and evidence for subaerial exposure near the cycle caps, such as desiccation cracks, karstified tops, fenestrae, small scale tepee structures, silicified evaporite pseudomorphs and intraclast mudflake breccias. The parasequence boundaries are marked by

Subtidal Parasequences		<p>Stromatactoid Parasequences</p> <p>The parasequences vary from 2 to 4 m and the internal composition of facies is relatively consistent. The base usually consists of a darkening-upward succession of laminated, stromatactoid, bioturbated carbonate, or columnar stromatolites preserved in chert and surrounded by ooids, peloids, intraclasts and occasional oncoids. In almost all cases, thrombolites overly these facies although dolomitisation sometimes makes their separation from burrow mottling difficult. They generally form biostromes or bioherms up to 4 m in height. Stromatolites and parallel lamination in the upper part of the parasequence indicates intertidal conditions but probably not supratidal, as evidence of exposure is generally lacking. Stromatactoid parasequences are common throughout the Sailmhor Formation.</p>	<p>Key</p> <ul style="list-style-type: none">  Gastropod  Cephalopod  Chert  Stromatactoid texture  Vug/fenestrae  Parallel lamination  Ripple lamination  Desiccation cracks  Teepee structure  Burrows  Evaporite pseudomorphs  Microbial lamination  Hemispheroidal stromatolite  Columnar stromatolite  Thrombolite  Detrital quartz  Intraclasts  Ooids  Peloids
		<p>Ooidal Grainstone Parasequences</p> <p>Ooidal grainstone based parasequences are relatively rare in the Durness Group, although this may be partly of preservational bias, as ooidal grainstone is frequently coarsely dolomitised. They are always less than a metre and are most common in the upper Sailmhor and lower Sangomore formations.</p>	
		<p>Columnar/digitate Stromatolite Bioherm Parasequences</p> <p>Only a few of these cycles occur, and are most common in the upper Sangomore Formation. Their thickness ranges from 1-2 m and occasionally a succession of stromatolite morphologies is present. Fossils are present but scarce and include an impoverished fauna of planispiral gastropods.</p>	
Peritidal Parasequences		<p>Peloidal Grainstone Parasequences</p> <p>Peritidal parasequences which consist of a basal bed of peloidal grainstone are present in the Sangomore, Balnakeil and upper Croisaphuill formations. They are generally less than 3 metres in thickness and burrow mottling commonly grades into ripple lamination with increased shallowing.</p>	
		<p>Bioturbated Wackestone Parasequences</p> <p>Peritidal parasequences which are characterised by a basal burrow-mottled bed/s are present within the Sangomore Formation and the upper Croisaphuill Formation. They frequently show evidence for supratidal conditions in the form of teepees, desiccation cracks, spar filled fenestrae and intraclast breccias. Burrowing is sometimes observed to penetrate into the parasequence below.</p>	
		<p>Thrombolite Parasequences</p> <p>Thrombolite based parasequences are common within the middle Sangomore Formation and lower Balnakeil Formation. The thrombolites are often thin and consist of biostromes. Evaporite pseudomorphs of anhydrite are occasionally present.</p>	
		<p>Columnar Stromatolite Biostrome Parasequences</p> <p>These parasequences are characterised by bioherms of columnar stromatolites. These may or may not rest upon a structureless microbialite. Although the bioherms are generally not thick, they may have a wavelength of several metres. Teepees, evaporites and ripple lamination occur in the peritidal part. The parasequences often have karst at their tops and eolian derived quartz occurs throughout. They only occur within the middle Eilean Dubh Formation.</p>	

Text-figure 5.3 Diagrammatic representation of identifiable parasequence subdivisions within the Durness Group. A stylised log is shown for each highlighting the characteristic facies. The types of parasequences are named after the basal facies as the upper parts of the parasequence may not be preserved.

a sharp change in facies. Internal facies boundaries are gradational. Four subtypes are characterised by the basal facies type: peloidal grainstone, bioturbated wackestone, thrombolite and columnar stromatolite biostrome parasequences (Text-fig. 5.3).

The Eilean Dubh Formation at Balnakeil Bay [NC 376 688] (Text-fig. 1.5) shows some shallowing-up parasequences, particularly at sequence boundary zones. These are bounded by surfaces exhibiting evidence of erosion, suggesting a lowering of sea level, or filling of accommodation space. Along Balnakeil Bay, parasequences are well developed within the Sailmhor, Sangomore and Balnakeil formations, which contain 36, 18 and 21 complete parasequences respectively. The upper part of the Balnakeil Formation contains parasequences that become increasingly subtidal and thicker (or parasequence boundaries become less distinguishable). This implies rapid aggradation due to an increase in accommodation space, resulting from base level rise. Within the lower Croisaphuill formation there is very little evidence for cyclicity and thick beds of burrow mottled subtidal facies are present. Within the upper half of the Croisaphuill Formation cycles start to become more prominent. The upper part of the Croisaphuill Formation (145–208 m above the base) comprises 27 parasequences, which are primarily subtidally dominated, although there are 3 peloidal grainstone-based peritidal parasequences. The latter comprise a basal unit (primarily dark grey peloidal grainstone up to 20 cm) overlain by burrow mottled dolomitic limestone and are commonly capped by fine grained pale-grey parallel laminated dolostone. Outcrop is patchy and very faulted. Parasequences can be distinguished in the lower part of the Durine Formation, however outcrop is not good enough to include any cycles within the Fischer plot.

5.3.3 Origin of metre-scale parasequences

The facies succession and thickness of a sequence depend mainly on three parameters; sediment accumulation rate, subsidence rate, and the rate of eustatic sea-level change (Strasser 1991). Sediments build up to sea level (or to the level of wave and storm reworking) and, in doing so, pass from subtidal to intertidal facies. If the sediment supply continues, progradation of facies will occur. There has been much discussion in the literature as to the mechanism of formation of high-frequency, shallowing upward parasequences which are commonly observed in many Laurentian sections of this age, but it has not yet been satisfactorily explained how high-frequency cycles in relative sea-level can occur during a time interpreted to represent global greenhouse conditions (Miller *et al.* 2005). Wilkinson

(1982) incorporated proposed mechanisms for carbonate shallowing upward parasequences into two end-member models, an allocyclic model (supported by Anderson *et al.* 1984; Grotzinger 1986; Read *et al.* 1986) and an autocyclic model (Ginsburg 1971; Matti & McKee 1976; Mossop 1979; Wong & Oldershaw 1980). The autocyclic model is here considered the most compelling as it does not require eustatic sea level fluctuation during a period in time when there is little evidence for extensive polar ice-caps.

5.3.4 Allocyclic model

Eustatic oscillations were considered to be the causal factors of shallowing upward cycles by Fischer (1964), Goodwin & Anderson (1985) and Koerschner & Read (1989), and these eustatic oscillations have been attributed to be products of higher frequency precession and obliquity Milankovitch rhythms (Koerschner & Read 1989). Wright (1992) suggested that a climatic control during greenhouse conditions is likely and that the amplitudes of climatically induced cycles are small. Falls in sea-level may have been small and slow enough to be outpaced by subsidence, thereby creating minor amounts of accommodation space readily filled by peritidal cycles, since the rises were slow enough to be outpaced by carbonate production. Climate modelling of warm periods of earth history suggest that the interiors of mid- to high latitude continents may have had subfreezing temperatures and that no global climate is truly “equable” (Sloan & Barron 1990). Even though there is little evidence for major large-scale continental glaciers existing during the Late Cambrian, diamictites and striated cobbles have been reported in lower Tremadocian strata of Argentina and Bolivia (Erdtmann & Miller 1981), and carbon isotope records show fluctuations in the Earth’s climate.

Spectral analysis, which may identify possible Milankovitch control is particularly difficult for shallow platform carbonates of Early Palaeozoic age for a number of reasons (Osleger & Read 1991).

- 1) Peaks on the power spectra difficult to calibrate due to inaccuracies in the timescale.
- 2) Missed beats are a common phenomenon (Hardie 1986; Hardie *et al.* 1986; Koerschner & Read 1989; Goldhammer *et al.* 1990).
- 3) Peritidal successions are a poor proxy for time as much of the time is taken up by non-deposition (Read *et al.* 1986, 1991).

Hardie *et al.* (1991) conducted a series scan on a section in the southern Appalachians that was used previously by Koerschner & Read (1989) to suggest Milankovitch cyclicity. They used maximum entropy spectral analysis (MESA) and failed to identify any statistically significant frequencies, indicating a random succession of cycles. Using 2-D modelling, they suggested that shallow marine platforms and shelves are not depositional environments conducive to preserving Milankovitch signals, because of the inevitability of progradation and therefore the diachronous nature of the cycles. Spectral analysis was not conducted on the Durness Group carbonates because the succession preserved is dominantly peritidal, displays numerous erosive surfaces and the lower part of the Durness Group yields no biostratigraphically useful fossils and additionally due the relatively large amount of faulting in the section.

Unrelated to eustasy, climatically induced cycles of rainfall and desertification may have affected runoff and therefore carbonate productivity. Tectonic cycles or 'jerky subsidence' has been proposed (Hardie *et al.* 1986) as a control on shallowing upwards cycles. This could explain cycles that are entirely subtidal, but would be fairly localised and could not explain the lateral persistence in some sections (James *et al.* 1989 and Grotzinger 1986). Tectonism of this type is also largely restricted to active settings, not passive continental margins. Intraplate stress, as suggested by Cloetingh (1986) is thought too slow (0.01–0.1 m/ky) and is non-periodic (Osleger & Read 1991).

5.3.5 Autocyclic model

Autogenic controls on cyclicity have been proposed by Ginsburg (1971) and Wilkinson (1982). In the classic model proposed by Ginsburg, sediment produced in open marine environments moves shoreward, eventually causing progradation. With increased progradation, the sediment source area decreases in size, production slows and accumulation is eventually outpaced by subsidence. Once water depth increases, a new source area is created. Matti & McKee (1976) and Mossop (1979) also suggest that parasequences form during progradation of the shoreline.

Pratt & James (1986) proposed an alternative model involving the local vertical accretion of facies by laterally prograding tidal flats surrounding islands. They observed rapid lateral facies changes in some outcrops, when correlating closely spaced sections. The stratigraphical array of facies appeared too irregular to be simplified into widespread, laterally

continuous, shallowing upward parasequences. Removal of some beds during burial pressure dissolution may make this phenomenon more apparent than real, and recent work shows that locally, some tidal-flat caps may be traced laterally over areas of 255 km² (James *et al.* 1989). In Cambro-Ordovician rocks on the Mingan Islands, Quebec, Desrochers (1988) was able to trace individual metre-scale cycles over 20 km with only minor changes in thickness and facies. Production of parasequences by tidal island progradation may only be the case in mid-platform settings, and thus inapplicable to inner-platform carbonates according to James *et al.* 1989. Grotzinger (1986) showed that lower Proterozoic sediments from the Rocknest Formation, North West Territories, Canada displayed 1–15 m thick cycles that could be traced >100 km across, and 200 km parallel to depositional strike.

Subsidence rates on passive margins have been argued to be too low to drown platform sediments in a reasonable period of time (20–40 mm/ka, Pitman (1978); 50–100 mm/ka, Grotzinger (1986)). Koerschner & Read (1989) also argued against progradational autocyclicality because of the long lag times of over 20,000 years before deposition can begin, but this is entirely consistent with the average age of cycles 44–130 thousand years (Hardie *et al.* 1991), assuming no sea level change.

Autocyclic processes are inherent in a peritidal system. The resulting sequences can be laterally consistent over the length of the system (Strasser 1991). However there are many examples where they cannot be traced laterally (Pratt & James 1986 and Cloyd *et al.* 1990). Waters *et al.* (1989) interpreted the grainstone facies at the bases of the fining-upward sequences as representing the deposits of laterally migrating tidal channels, with channel fills representing abandoned channels and the microbial laminites representing overbank deposits. Waters *et al.* (1989) recognised lateral accretion bedding in half of the described parasequences, with grainstone and conglomerates at the base of parasequences represent channel lags of reworked overbank deposits within the Middle and Upper Cambrian Waterfowl Formation, Alberta.

Beach ridges, migrating channels, crevasse-splays and levees are important components of modern tidal flats on Andros Island and the Arabian Gulf (Hardie 1977; Shinn, 1983; Wright 1984 and Hardie 1986). However, such elements are only rarely interpreted from ancient carbonate tidal flat deposits (Friedman & Braun 1975; Loucks & Anderson 1980; Sellwood 1986 and Waters *et al.* 1989). Cloyd *et al.* (1990) gave an alternative interpretation of the fining-upward cycles as crevasse-splay and levee deposits (i.e. overbank

deposition) of migrating tidal channels analogous to fluvial overbank sequences. Evidence for tidal creek deposition in the Durness Group is suggested by fining upward sediment from a basal lag, moderate and variable flow conditions, cracked mud drapes that occur throughout some of the sequence, lack of fauna, dispersion in palaeocurrent directions and the thickness corresponding to the depth of most modern creeks (Hardie 1977).

Strasser (1991) considered cycles showing a continued facies evolution to be the result of autocyclic processes, while those showing, widespread subaerial erosion and facies overprinting are the result of allocyclic processes. Cessation of shoaling can also be autogenic, where shoals may migrate out of the principal transport path, meaning that cycles do not fill available accommodation space (Cowan & James 1996).

5.3.6 Parasequence sets and accommodation curve

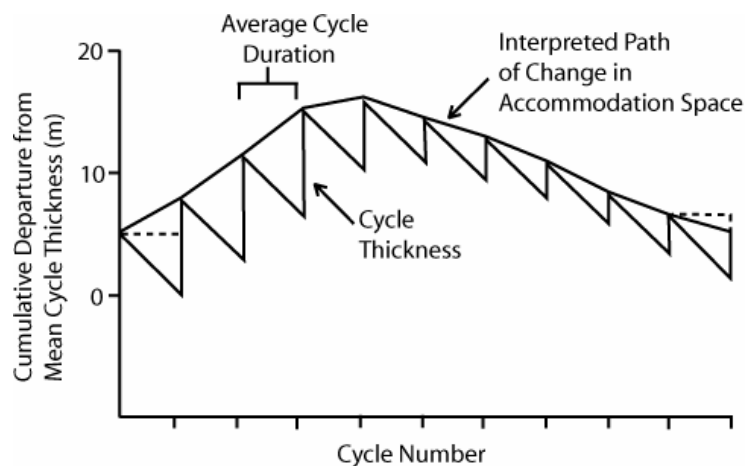
Large parts of the Durness Group are dominated by parasequences, and 100 complete parasequences can be recognised. Parasequences can be grouped into parasequence sets, which are genetically related parasequences forming a distinctive pattern, bounded by major marine-flooding surfaces and their correlative conformities and of progradational, aggradational or retrogradational nature (Van Wagoner *et al.* 1990). In some cases one or both boundaries of a parasequence set will be a sequence boundary (Emery & Myers 1996). The terms ‘parasequence set’ and ‘systems tract’ are not always synonymous (Posamentier & James 1993) and in areas of high subsidence and sediment input, more than one parasequence set can exist in a systems tract.

The Durness Group sequences and systems tracts are recognised by parasequence stacking patterns, the nature of the upper boundaries and the form of the accommodation plot. These sequences are categorised as second- and third-order sequences; in part based on the time span of the strata and the presence of metre-scale cycles (fourth- and fifth-order) in each sequence. Throughout much of the Durness Group, recognisable lowstand systems tracts (LST) and falling stage systems tracts (FSST) are absent. Sequence boundaries are usually represented by a zone, referred to as the sequence boundary zone (SBZ). Upward-thickening, subtidally dominated parasequences are characteristic of the TST. Aggradational sets of thick, subtidally dominated parasequences represent the early highstand systems tract (HST). This is overlain by upward-thinning, increasingly peritidally dominated parasequences representing the late HST. Together, these systems tracts represent a single sequence, as expressed in the

inner ramp/platform setting of the Scottish Laurentian succession. The late HST in Fischer plots appears as a long negative slope on the plot due to increasingly thinner than average parasequences (Read & Goldhammer 1988, Koerschner & Read 1989 and Goldhammer *et al.* 1987, 1990).

Fischer plots (Fischer 1964) are graphs of cumulative derivation of parasequence thickness from the average value (Text-fig. 5.4). They were first constructed for the Triassic “Lofer cyclothems” of the Austrian Alps, but have been widely used since their conception for other cyclic successions. There has been much debate concerning the over-interpretation of Fischer plots (Hardie *et al.* 1991; Drummond & Wilkinson 1993; Sadler 1994 and Boss & Rasmussen 1995). The plots are not reliable representations of past fluctuations of eustatic sea-level as previously suggested by Read & Goldhammer (1988), Osleger & Read (1991, 1993), Osleger (1991), Montañez & Osleger (1993) and Koerschner & Read (1989). Despite this, a Fischer plot still serves as a useful graphic representation of deviation from the average cycle thickness through the section (Text-fig. 5.5). It has been recommended (Sadler *et al.* 1993) that Fischer plots contain a minimum of 50 cycles for the curve to be statistically significant. For the Durness Group plot, no constant was subtracted from cycle thickness to correct for subsidence or a correction for compaction because the plots are used to show broad changes in cycle variation and it is believed that they do not represent a true representation of sea-level change. If Fischer plots are to be used as sea-level curves, it requires acceptance of multiple assumptions for example; the constant duration of each cycle, constant subsidence, stratigraphical completeness, and the decompacted parasequence thickness being a reasonable proxy for accommodation space (Boss & Rasmussen 1995).

To construct the Fischer plot for the Durness Group (Text-fig. 5.5), outcrop sections along the coast at Balnakeil Bay (Text-fig. 1.5) and An t-Sròn (Text-fig. 1.4) were logged to produce a detailed composite section of 935 m thickness. Additional short sections at Loch Borralie and at Leirinmore were logged to supplement information (see Appendix 1 for locality details). The analysis concentrated on detailed lithofacies analysis, and the thickness of parasequences was measured at cm-scale. The facies analysis is based partly upon the interpretation of relict facies observed within the dolomite and preserved within chert. A Fischer plot was constructed for the parts of the succession (using FISCHERPLOTS, Husinec *et al.* 2008) that were cyclic. The section was long enough to make a statistically significant Fisher plot (Sadler *et al.* 1993).

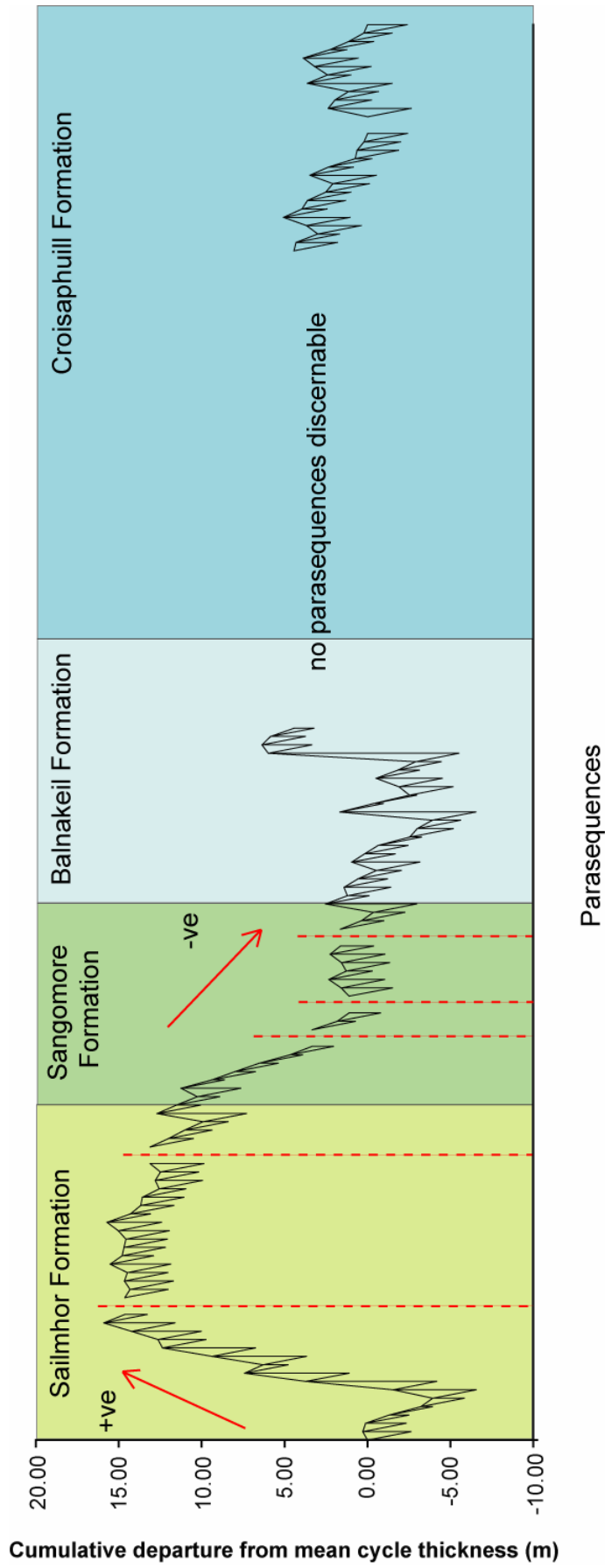


Text-figure 5.4 Diagram showing the parts of a Fischer plot. The graph represents cumulative departure from the mean cycle thickness through the succession (after Drummond & Wilkinson 1993).

Missing strata, such as covered units and faults are represented by a gap in the Fischer plot, with no vertical change, as are successions containing no distinguishable parasequences such as the Ghrudaidh and Eilean Dubh formations and the basal Croisaphuill and Durine formations.

Because of the apparent non-cyclical nature of parts of the succession, and possible subjectivity in recognising shallowing-upward trends (see Wilkinson *et al.* 1996), subdivision of these intervals was not attempted. The Ghrudaidh Formation and lower Eilean Dubh Formation contain some parasequences but they are not common enough to be used in the Fischer plot. Parasequences could not be defined within the Durine Formation due to patchy outcrop, although an alternation of peritidal and subtidal facies indicates clearly that they are present.

On the Fischer plot, subtidally dominated cycles are commonly thicker than average and so occur as steep positive slopes (e.g. the lower Sailmhor Formation). By contrast peritidally dominated cycles are thinner than average and occur as shallow (negative) slopes stacked together. Following the suggestions of Read & Goldhammer (1988), the positive slope of the Fischer plot in the lower Sailmhor Formation records the TST, with cycles increasing in thickness and increasing proportions of subtidal facies. In the lower Sailmhor Formation the parasequences show this pattern and form a retrogradational parasequence set.



Text-figure 5.5 Fisher plot for the Durness Group. Only parts of the succession containing well developed parasequences were used. Positive and negative slopes of the plot are marked. (constructed using FISHERPLOTS (Husinec *et al.* 2008)).

The deviation maximum of the plot, within the middle Sailmhor Formation, equates to the MFS (Vail 1987) or, more commonly, when observed in outcrop, the maximum flooding zone (MFZ).

The early HST in the Sailmhor Formation contains aggradational parasequences and as relative sea-level rose, progradation slowed and this is reflected in the parasequence sets. Cycles within the upper Sailmhor and Sangomore formations that plot on the falling limb of the Fischer plot constitute the late HST, culminating in a sequence boundary. The late HST is characterised by cycles that progressively thin upward, are relatively restricted and contain the most early dolomite. The sequence boundaries at the Sailmhor–Sangomore, and Sangomore–Balnakeil formation boundaries are marked by a high proportion of peritidal facies within parasequences. A subsequent TST is recorded in the Balnakeil Formation. The lower Balnakeil Formation shows an aggrading parasequence set, which may indicate that carbonate production was able to ‘keep up’ with sea-level rise. Within the Croisaphuill Formation, a thick sequence of subtidal lithofacies was deposited through which it is difficult to distinguish parasequences. This unit represents a non-cyclic, early HST. The upper part of the Croisaphuill Formation, where cyclicity becomes apparent represents the late HST.

5.4 SLM I SUPERSEQUENCE

The SLM I Supersequence in Scotland is represented by approximately 215 m of strata of the Eriboll and An t-Sròn formations (Ardvreck Group) (BGS 2007; McKie 1993; Park *et al.* 2002). The basal sequence boundary is represented by an angular unconformity upon Archaean gneiss and Neoproterozoic Torridon Group sandstones (both relationships are observed at a double unconformity in the Assynt area). Relative sea-level rise is recorded within the Basal Quartzite and Pipe Rock Member, with maximum transgression representing deposition of the Furoid Member (An t-Sròn Formation). A thin quartz arenite unit (*Salterella* Grit Member) at the top of the An t-Sròn Formation marks a relative shallowing of sea-level and a return to deposition of facies similar to those of the Pipe Rock Member. The sequence boundary at the top of SLM I separates the predominantly siliciclastic Ardvreck Group from the predominantly carbonate Durness Group (SLM II–III).

The age of the transgression at the base of the Sauk Megasequence in Scotland is not known, and the lowest occurrences of body fossils in the section are those of *Salterella* and *Olenellus* within the Furoid Member. Peach *et al.* (1907) also reported the presence of

Salterella within the Pipe Rock Member and isolated *Skolithos* in the upper part of the Basal Quartzite Member suggest that the base of the succession is most likely to not be older than the base of C₂ (middle Lower Cambrian), although further study is needed.

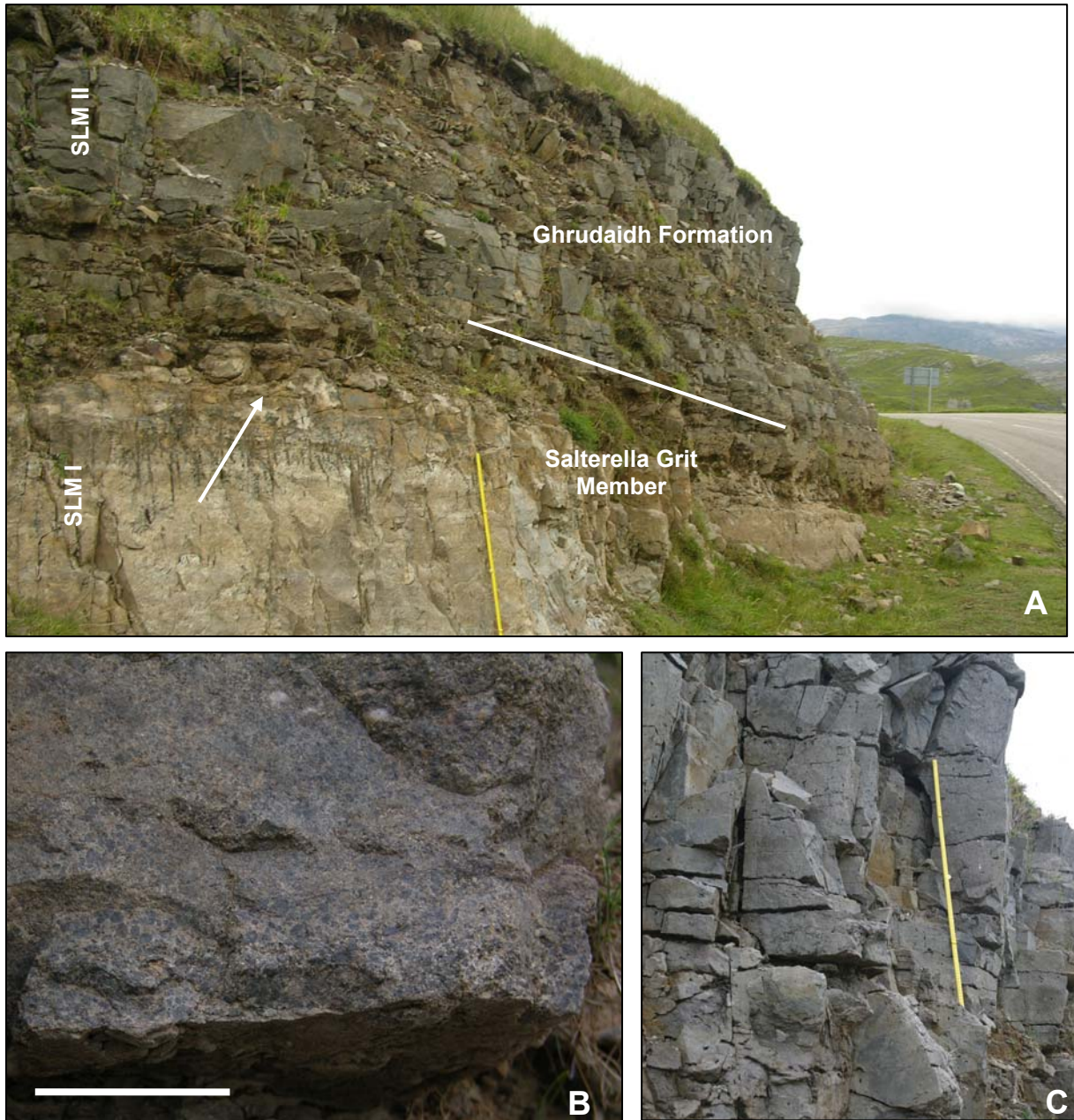
The Basal Quartzite Member consists of tidal channel fill and shore-face sandstones representing a tidal shelf depositional environment (McKie 1990a). Palaeocurrent data are unimodal and broadly southeast (McKie 1993). The overlying Pipe Rock Member represents a comparatively more offshore, but not necessarily much deeper depositional environment. Sedimentation rate may have been lower allowing colonisation of bedforms by the organisms that generated *Skolithos*.

The Furoid Member represents the culmination of sea-level rise (late HST) (Text-fig. 5.1) within SLM I, and represents a condensed section of storm-deposited siltstones and sandstones. Hummocky cross stratification is observed at Skiag Bridge [NC 2360 2420]. Glauconite is most common at the base of the member, but occurs throughout. The most common facies comprise wave-rippled silts, mudstone and echinoderm grainstone (McKie & Donovan 1992). Palaeocurrents show a north to north-easterly mode, whilst those from wave ripples show northwest/southeast and northeast and southwest modes (McKie 1990b). Shallowing at the top of the SLM I subsequence in Scotland is represented by the uppermost Furoid and *Salterella* Grit members (An t-Sròn Formation). The presence of *Olenellus* and *Salterella* suggest that the Furoid and *Salterella* Grit members are of middle *Bonnia–Olenellus* Zone in age (upper Lower Cambrian) (Fritz & Yochelson 1988).

Facies within the *Salterella* Grit Member include laminated mudstone, cross-bedded, planar laminated quartz arenites, burrowed (abundant *Skolithos*) and fossiliferous quartzarenites representing marine dunes and sandwaves. Palaeocurrent directions have south, north, and southwestward trends (McKie 1990c). The quartz arenites of the *Salterella* Grit Member are overlain by brown, rubbly-weathering, dolomitic sandstone or a dark grey dolomitic siltstone, marking the base of the Ghrudaidh Formation (Durness Group) and the start of carbonate-dominated deposition (Text-fig. 5.6A). The basal beds of the Ghrudaidh Formation contain dispersed quartz sand and silt, and thin beds of dolomitic sandstone are present containing small, well-rounded mudstone clasts (Text-fig. 5.6B). Bioturbated dolostones typify the Ghrudaidh Formation thereafter, and vugs containing dolomite spar or gypsum are common (Text-fig. 5.6C).

5.5 SLM I–II Boundary

The Salterella Grit Member has been suggested to be equivalent to the Hawke Bay Formation of western Newfoundland (McKie 1990a, c; McKie 1993; Wright & Knight 1995).



Text-figure 5.6 (A) the SLM I–II sequence boundary at the top of the Salterella Grit Member, Ardvreck, Assynt [NC 2373 2405]. Cyclic pale and dark beds within the upper part of the member are punctuated by *Skolithos* burrows (marked by arrow). A thin bed of rubbly weathering dolomitic sandstone, represents flooding above the sequence boundary. Scale is 1 metre. **(B)** small rounded mud-flake clasts occurring at the base of a dolomitic sandstone within the lowest 2 meters of the Ghrudaidh Formation. Scale is 5 cm. **(C)** burrow mottled lead-grey dolomites, with spar-filled vugs, 3 meters above the sequence boundary.

The Hawke Bay Formation comprises terrigenous clastic rocks and minor carbonates. The sandstones of the Hawke Bay Formation in Newfoundland are interpreted to be the product of a lowstand event 'Hawke Bay event' (Palmer & James 1980) which marks the Sauk I–II boundary. This event has subsequently been recognised across many parts of Laurentia. Trilobites within the Hawke Bay Formation range in age from the upper part of the *Bonnia–Olenellus* Zone of the upper Lower Cambrian to the *Bathyriscus–Elrathina* Zone of the late Middle Cambrian (Knight 1977; Knight & Boyce 1987). Although the upper part of the formation is dominated by thick, massive quartz arenites, in eastern sections (Knight & Boyce 1987; Knight 1991) the siliciclastic sediments are finer grained and more thinly bedded, forming cyclical units with oolitic and stromatolitic limestones (Bridge Cove Member; Knight & Boyce 1987). Trilobites constrain the unit as mid-Middle Cambrian (*Plagiura* to *Ehmaniella* zones; Knight & Boyce 1987).

The basal age of both the Salterella Grit Member and the Hawke Bay Formation is comparable, suggesting that they record the same sequence stratigraphical event, but there is a disparity in the age of the upper parts. The top of the Hawke Bay Formation is younger than equivalent sandstones in Scotland. A single specimen of *Olenellus* aff. *reticulatus* Peach has been recorded from the basal few metres of the overlying Ghrudaidh Formation (Huselbee & Thomas, 1998) suggesting that the Salterella Grit Member lies entirely within the *Bonnia–Olenellus* Zone and casting some doubt on correlation of this sequence boundary with the Hawke Bay Event.

5.6 SLM II SUPERSEQUENCE

SLM II sediments in Scotland are 158 m thick. They can be further subdivided into two higher order depositional sequences, which are interpreted to be equivalent to the basal two Cambrian Grand Cycles (third-order) recognised elsewhere along the Laurentian margin (Chow & James 1987). The two cycles are, respectively, 83 m thick (Ghrudaidh and lowest Eilean Dubh formations; SLM IIa) and 75 m thick (lower–middle Eilean Dubh Formation; SLM IIb). They are separated by a regressive event at the Ghrudaidh–Eilean Dubh formation boundary, which is characterised by pale grey supratidal dolomites (Text-fig. 5.7A) containing evaporite pseudomorphs (Text-fig. 5.7B) and thin evaporite dissolution breccias (Text-fig. 5.7C, D) (Chapter 2). The base of SLM II is marked by continued sea-level rise/flooding at the base of the Ghrudaidh Formation, and the upper boundary occurs within

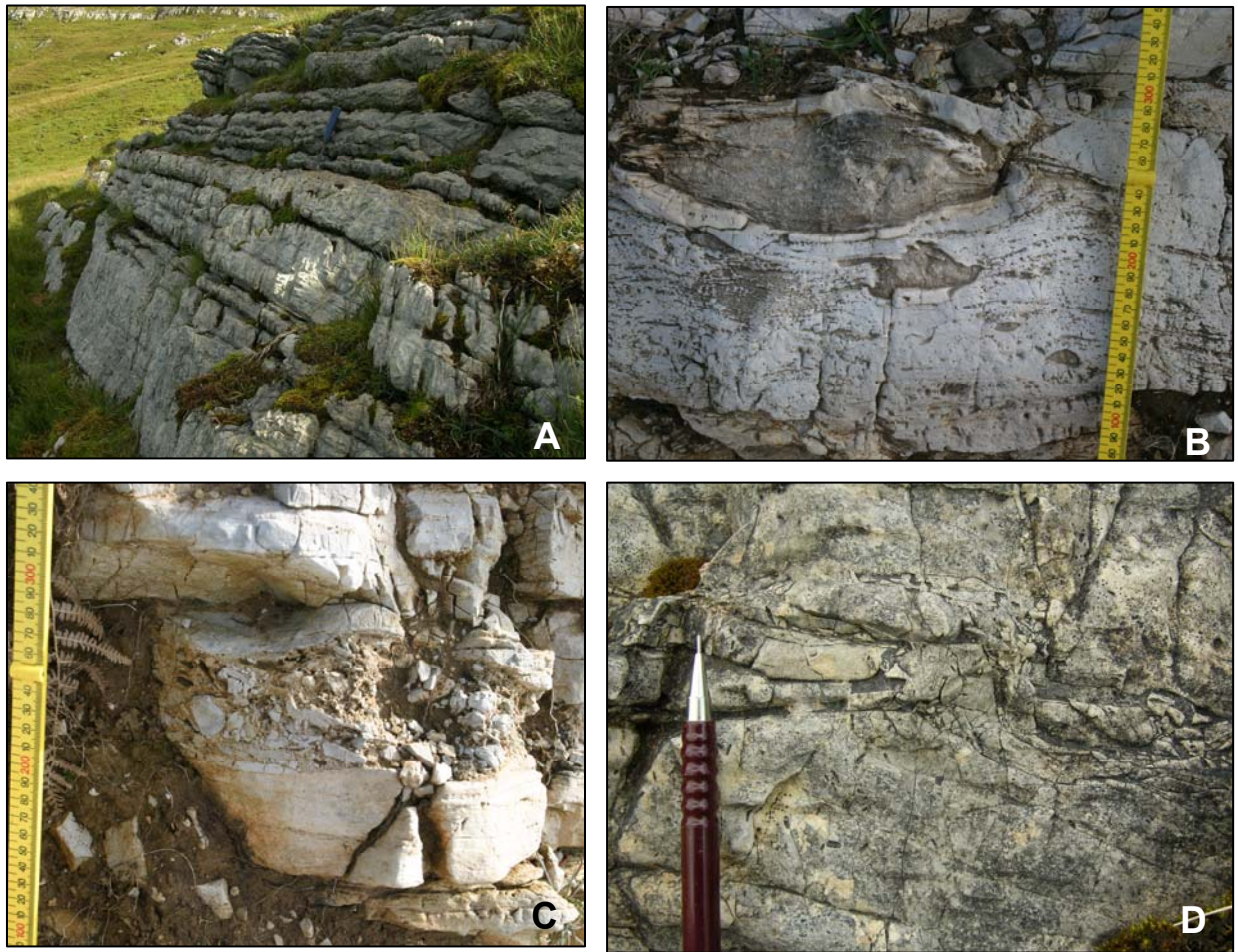
the middle Eilean Dubh Formation, where it is marked by metre-scale parasequences containing terrigenous quartz sand and exhibiting evidence for subaerial exposure.

5.6.1 SLM IIa Sequence

The predominantly carbonate Ghrudaidh Formation conformably overlies the Salterella Grit Member (An t-Sròn Formation) and its base is marked by a locally developed c. 2 m thick, laminated siltstone. The Ghrudaidh Formation, which is approximately 65 m thick consists of dark grey, burrow mottled dolostones, rare ooidal grainstones and bioclastic wackestones. These carbonate facies record shallow subtidal deposition, but they commonly contain vugs filled with evaporite pseudomorphs. The occurrence of silicified ooid beds suggests that ooidal grainstone may once have been a larger constituent of the facies that has subsequently been destroyed by dolomitisation.

The Ghrudaidh Formation marks a significant change in the nature of the shelf. Siliciclastic sand becomes scarcer up-section, and carbonate sedimentation rapidly becomes predominant, with burrow-mottled, subtidal dolostones and local ooidal grainstones. This sequence is separated from the overlying SLM IIb Sequence by a previously unrecognised regressive event at the top of the Ghrudaidh Formation (seen at An t-Sròn, Ardvreck and Stronchrubie). At An t-Sròn [NC 4396 5798] and Ardvreck, 12 m and 18 m respectively of supratidal fine-grained, cream-weathering dolostones are exposed beneath a thrust fault (Text-fig. 5.7A). The dolostones contain evidence of former evaporites, including crystallotopic lath-shaped vugs, commonly filled with calcite, and large nodules of spar, both interpreted to reflect crystalline and nodular gypsum/anhydrite (Text-fig. 5.7B) (Chapter 2).

The occurrences of breccias suggest that more extensive beds of evaporite once occurred. The succession of facies represents the top of a transgressive–regressive sequence (83 m thick), comprising the entire Ghrudaidh Formation and basal part of the Eilean Dubh Formation. Systems tracts were difficult to distinguish within this cycle due to the lack of discernable shallowing upward parasequences.



Text-figure 5.7 (A) thinly bedded, cyclic pale gray and mid-gray dolomites at the base of the Eilean Dubh Formation (SLM IIa–IIb sequence boundary), Ardvreck, Assynt [NC 2448 2335]. They represent a marked shallowing above the predominantly burrow mottled Ghrudaidh Formation. Evaporite pseudomorphs and dissolution breccias are common. (B) large lens shaped nodule of calcite spar, and small calcite filled fenestrae. The calcite is interpreted to be a replacement of or anhydrite. (C) evaporite dissolution breccia, characterized by a flat base and irregular upper boundary, lower Eilean Dubh Formation, An t-Sròn, Loch Eriboll [NC 4396 5798]. (D) fitted dissolution breccia with calcite spar infilling space between clasts, Ardvreck, Assynt.

Much of the Ghrudaidh Formation represents the TST, with the beds containing evaporite pseudomorphs potentially representing a late HST at the top of the sequence. A covered interval in all sections studied may hide the transition interval of the sequence.

5.6.2 SLM IIb Sequence

The logged thickness (132 m) of the Eilean Dubh Formation represents a minimum thickness, as the lowest beds are not exposed at Balnakeil Bay where the most complete section occurs,

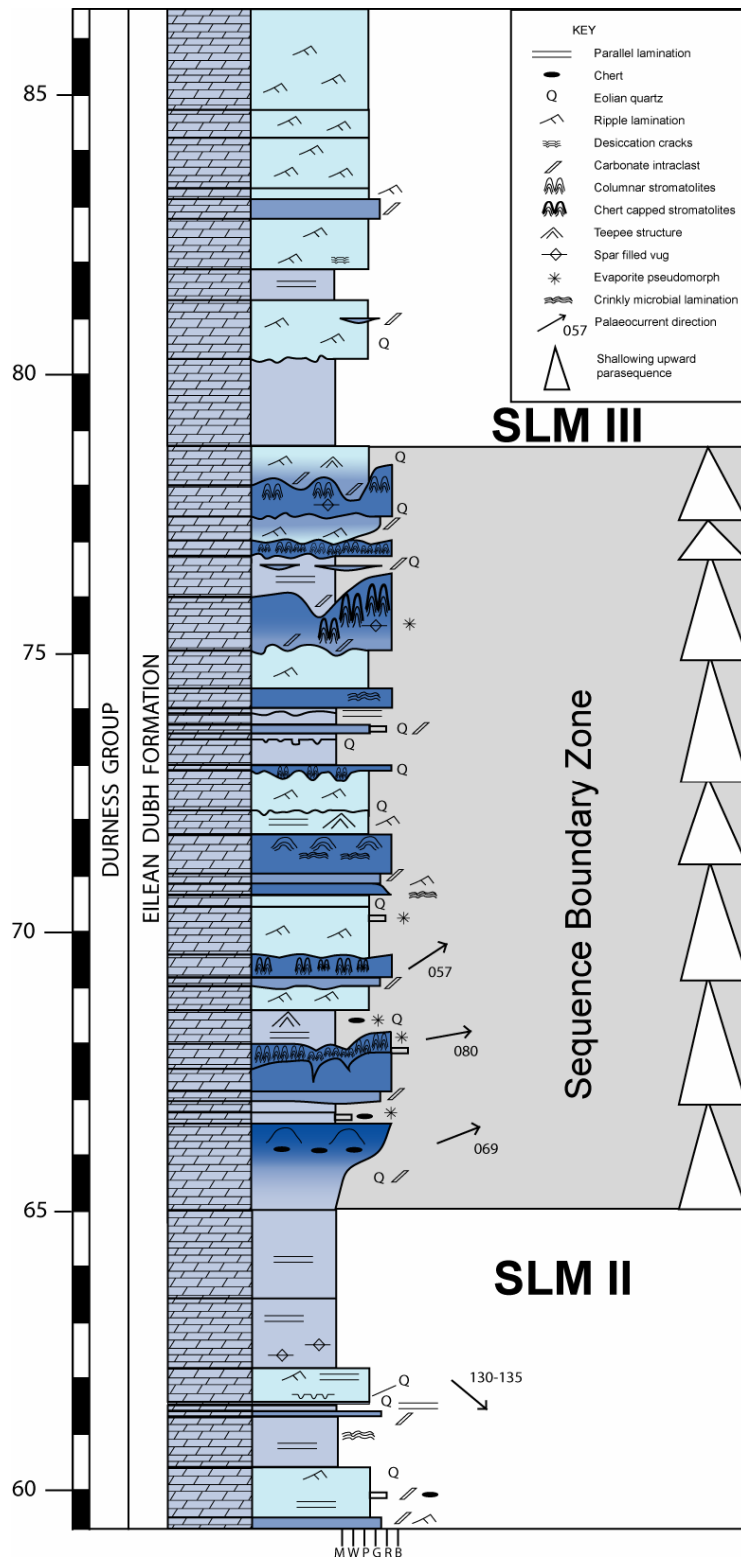
and the transgressive systems tract sediments are most likely missing. The exposed thickness of the combined TST and HST is 67 m, but may be significantly thicker. The TST comprises stromatactoid dolostones and dolostones exhibiting spar-filled vugs, plus local intraclast breccias, minor terrigenous quartz and stromatolites are locally abundant. The HST of the sequence (middle Eilean Dubh Formation) is dominated by ripple- and flaser-laminated fine-grained dolostone, interbedded with mudflake breccias and rare beds of quartz sand, representing deposition on an aggrading tidal flat.

5.7 SLM II–III BOUNDARY

Within the Durness Group, siliciclastic material represents a minor constituent of the succession and siliciclastic deposition during the Cambrian Eilean Dubh Formation resulted in thin beds interspersed within the dolostone sequence. At several horizons however, quartz sand creates a distinctive marker, interpreted to be the boundary of SLM II and SLM III. Although quartz sand beds make up only a small percentage of this 10 m thick boundary interval, it occurs in almost every bed (Text-fig. 5.8) and caps many of the metre-scale parasequences, where it occurs as sand lenses and stringers, and in-fills the hollows of irregular, scalloped and karstified tops to the cycles (Text-fig. 5.9E). The sequence boundary zone is also marked by abundant mud-flake breccias, teepee structures and evaporite pseudomorphs of both gypsum/anhydrite (Text-fig. 5.9A, B, C) and local halite. The SLM II–III sequence boundary is arbitrarily taken at the top of the most developed karst surface.

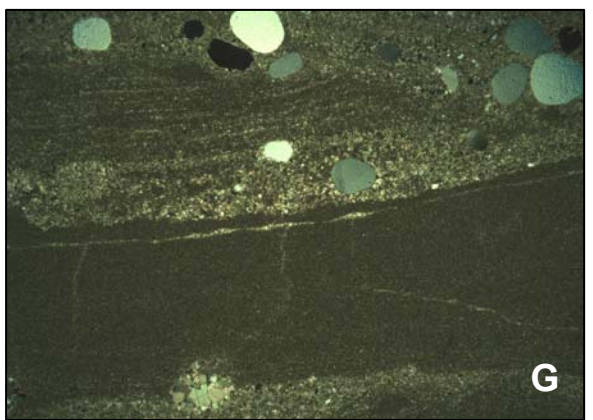
The highly spherical millet-seed quartz within the Eilean Dubh Formation appear to have come from an aeolian environment (Text-fig. 5.9G), and it is possible they may have formed the distal fingers of a siliciclastic wedge, similar to those described by Mount (1985) and Batten Hender & Dix (2006). This may suggest a significant prolonged shallowing event during which the shoreline was given time to prograde.

The Sauk II–III boundary interval in North America coincides with a large positive carbon-isotope excursion (SPICE) (Saltzman *et al.* 1998, 2004; Glumac & Walker 1998). The boundary is dated by trilobites to the Laurentian mid-Steptoean Stage (*Dunderbergia* trilobite zone, equivalent to a middle Pabian Stage and lower Furongian Series age) and coincides with maximum regression on the North American craton (Palmer 1981).



Text-figure 5.8 Sedimentary log of the interval spanning the SLM II – III boundary. No particular sequence boundary can be recognised so a sequence boundary zone is marked, Balnakeil Bay.

Text-figure 5.9 Features observed at the SLM II–III boundary. **(A)** evaporite pseudomorphs in the form of crystal vugs within a columnar stromatolite biostrome. **(B)** quartz nodules with irregular cauliflower margins after anhydrite nodules. **(C)** large cavities filled with gypsum, possibly related to cave formation beneath karstic surfaces. **(D)** tepee structure. **(E)** scalloped margin to a karstic surface at the top of a parasequence. The hollow contains an in-fill of carbonate clasts and millet seed quartz sand. **(F)** intraclastic rudstone with a matrix comprising millet seed quartz grains. **(G)** thin section photomicrograph of small scale desiccation cracks and millet seed quartz grains in a ripple laminated dolostone.



The regression was marked by an influx of quartz sand across carbonate platforms and resulted in a distinctive sequence boundary that is recognised in northern Utah (Saltzman *et al.* 2004), western Newfoundland (Westrop 1992; Chow & James 1987; James *et al.* 1989; Cowan & James 1993, Saltzman *et al.* 2004), central Iowa and eastern Tennessee (Glumac & Walker 1998). In coeval platform margin deposits, such as the Cow Head Group, western Newfoundland, the regression is recognised as a quartzose calcarenite sediment apron, deposited during a period of arrested shallow water sedimentation, aeolian sand bypassing, and margin progradation (James & Stevens 1986, James *et al.* 1989). Slope and shelf-margin facies in eastern New York and Vermont contain periplatform breccias, and re-sedimented and locally channelised quartz sands (Read 1989) which may represent the LST.

Although little direct evidence for subaerial exposure and erosion exists at the Sauk II–III boundary in the upper Mississippi Valley, Runkel *et al.* (1998) used outcrop and subsurface biostratigraphically constrained facies relationships across a wide area to estimate that the shoreline regressed by about 300 km from western Wisconsin to central Iowa by the late *Dunderbergia* Zone. This corresponds to a mid-Steptoean sea-level fall of at most a few tens of metres, on the basis of an inferred shelf gradient of approximately 0.1 m/km (Runkel *et al.* 1998). There is good evidence for the interpretation of the Sauk II–III boundary as a major continental-scale regressive event (Saltzman *et al.* 2004). Saltzman *et al.* did not decide on a likely cause of the sea-level fall but Sial *et al.* 2008 suggested that the event represented climatic oscillation rather than glaciation.

5.8 Cambrian Grand Cycles and correlation with the Durness Group (SLM IIa, IIb & IIIa)

Transgressive–regressive cycles occurring within the Cambrian Sauk Megasequences have been recognised across much of Laurentia, where they are termed ‘Grand Cycles’ (Aitken 1966). Described first by Aitken (1966) in the Cambrian of the Canadian Rockies, and later recorded across much of the Laurentian shelf sequence (Stitt 1977; King & Chafetz 1983; Chow & James 1987; James *et al.* 1989; Koerschner & Read 1989; Read 1989). Grand Cycles are roughly equivalent to third order depositional sequences (Osleger & Read 1993). They typically are 90–600 m in thickness, consist of a lower unit of fine grained terrigenous mudstone and limestone, which passes upwards into predominantly limestone and dolomitic-limestone and include two or more trilobite zones.

Cambrian Grand Cycles have been recognised within the succession in western Newfoundland, although both their sedimentology and thickness are different to those that have been recognised elsewhere (Chow & James 1987). They were interpreted as deposits of muddy tidal-flats ('shaley' half-cycle) and ooid shoal complexes (upper carbonate half-cycle) in an outer platform setting (Chow & James 1987). No such cycles occur in the Durness Group in Scotland and without biostratigraphical data for much of this part of the Durness Group; it is difficult to accurately correlate with the sequences in Newfoundland and elsewhere in North America. Third-order sequences within the Cambrian part of the Durness Group include SLM IIa, b and SLM IIIa (Text-fig. 5.1)

The origin of Cambrian Grand Cycles, like that of other third-order sequences, has most commonly been attributed to eustatic sea-level fluctuations (Read *et al.* 1986; Bond *et al.* 1988, 1989; Koerschner & Read 1989; Osleger & Read 1991, 1993). Other controls on Grand Cycle formation that have been suggested include tectonism (Palmer 1981), changes in sediment supply related to climatic changes (Chow & James 1987; Cowan & James 1993), changes in the rate of sea-level rise (Palmer & Halley 1979; Mount & Rowland 1981; Chow & James 1987), combinations of changes in the rate of subsidence and rate of sedimentation (Hardie 1989; Kozar *et al.* 1990; Srinivasan & Walker 1993) and a combination of platform exposure, 'lag time' and thermal subsidence (Rankey *et al.* 1994; Srinivasan & Walker 1993). Rankey *et al.* (1994) suggested that aggradation and progradation controlled the internal facies makeup of the cycles, with each cycle being initiated by non-thermal or 'jerky' subsidence, possibly coupled with eustasy.

5.9 SLM III SUPERSEQUENCE

The SLM III Supersequence in Scotland is 214 m thick, and consists of the upper Eilean Dubh (46 m), Sailmhor (113 m) and Sangomore (55 m) formations. The lower sequence boundary (SB) coincides with the quartz sand-rich interval at the top of the middle Eilean Dubh Formation. Three smaller scale (third-order) sequences are recognised within SLM III, each separated by regressive events. The lowest rests above the SLM II–III boundary, is 28 m thick and its upper boundary is marked by a breccia bed in the uppermost part of the Eilean Dubh Formation. The second (SLM IIIb) sequence (131 m) is represented by the uppermost Eilean Dubh and all of the Sailmhor Formation. Its base is marked by the breccia (18 m below the top of the Eilean Dubh Formation) and its upper boundary by beds of dolomite sand and

chert intraclast breccias at the Sailmhor–Sangomore formation boundary. The third sequence, SLM IIIc is 55 m thick and entirely comprises the Sangomore Formation. The upper boundary of the sequence coincides with the contact with the overlying Balnakeil Formation.

5.9.1 SLM IIIa Sequence

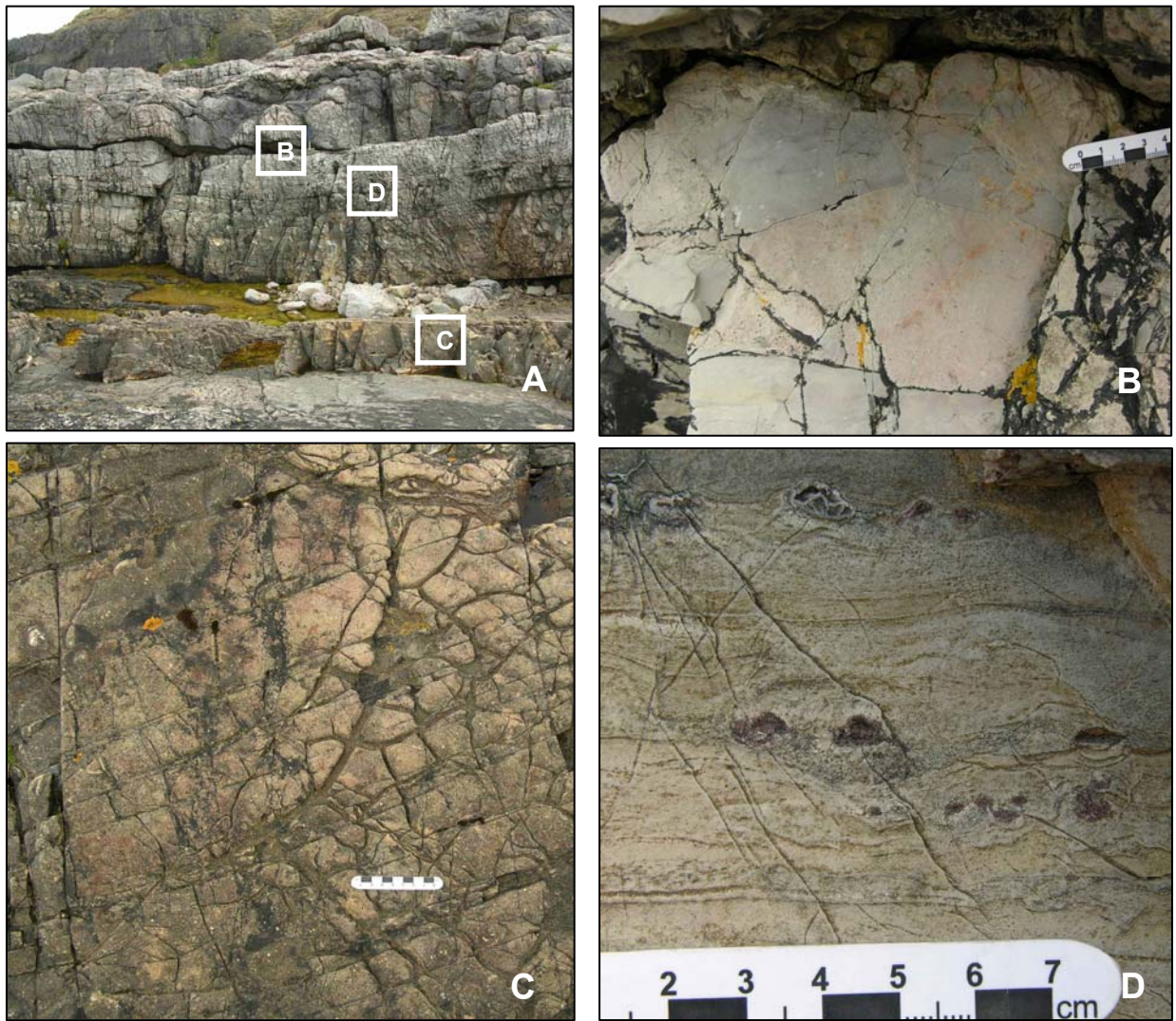
The SLM IIIa sequence consists of columnar stromatolitic biostromes, which are overlain by a succession of ripple- and flaser-laminated dolostones. The sequence rests disconformably upon the SLM II–III boundary. The upper boundary coincides with a 6–10 cm breccia that lies within 1.78 m of shallow intertidal and supratidal carbonates c.28 m above the SLM II–III subsequence boundary zone and 18 m below the Eilean Dubh–Sailmhor formation boundary (Text-fig. 5.10).

The cream weathering conglomerate/breccia contains angular, mid-grey carbonate clasts up to 7x5 cm (Text-fig 5.10B) including fragments of stromatolite. The breccia is clast-supported, has a bimodal matrix of terrigenous and dolomite silt, and is rich in granule grade material (Text-fig 5.10B). The granules comprise well-rounded to angular chert of several different colours, small dark carbonate clasts, well-rounded millet seed quartz up to 2 mm in diameter and local K-feldspars. Quartz filled vugs (presumably after evaporites) occur beneath the breccia in a 1.3 m thick bed of ripple laminated dolostone, displaying convolution within the top 30 cm (Text-fig. 5.10D). Beneath this dolostone there is a brown-weathering 40 cm thick, dolomitic siltstone showing extensive desiccation cracks (Text-fig. 5.10C).

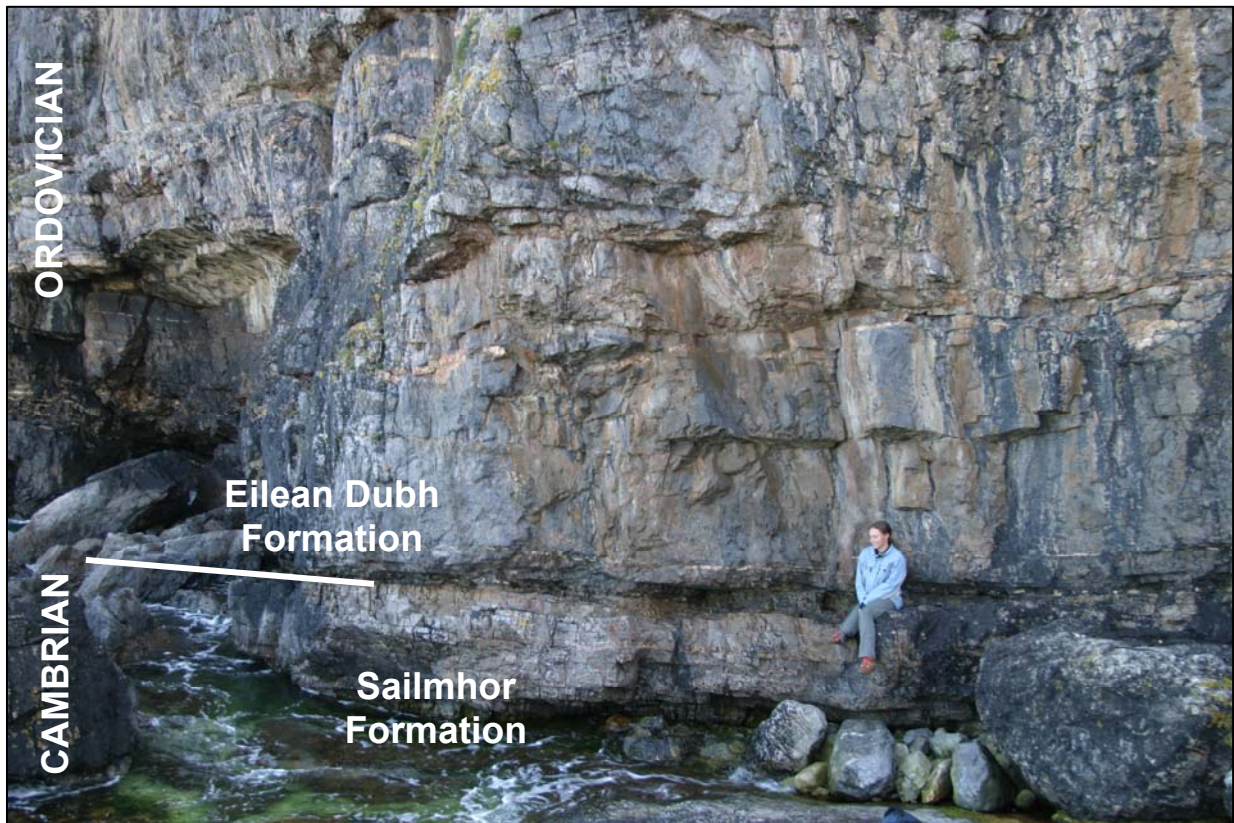
5.9.2 SLM IIIb Sequence

The SLM IIIb sequence comprises the uppermost Eilean Dubh Formation and the conformably overlying Sailmhor Formation (Text-fig. 5.11). Although the zonal conodont species *Iapetognathus fluctivagus* Nicoll *et al.* has not been recovered, the basal bed of the Sailmhor Formation has yielded *Cordylodus lindstromi* Druce and Jones, suggesting that the Cambrian–Ordovician boundary lies not far below this (Chapter 4) and that the sequence likely begins in the latest Cambrian.

Below the formation boundary the uppermost Eilean Dubh Formation consists predominantly of beds of ooidal grainstone but includes a bed of hemispheroidal stromatolites with ooidal grainstone immediately above the lower sequence boundary, suggesting a slightly deeper depositional environment represents the base of the sequence (Text-fig. 5.10A).



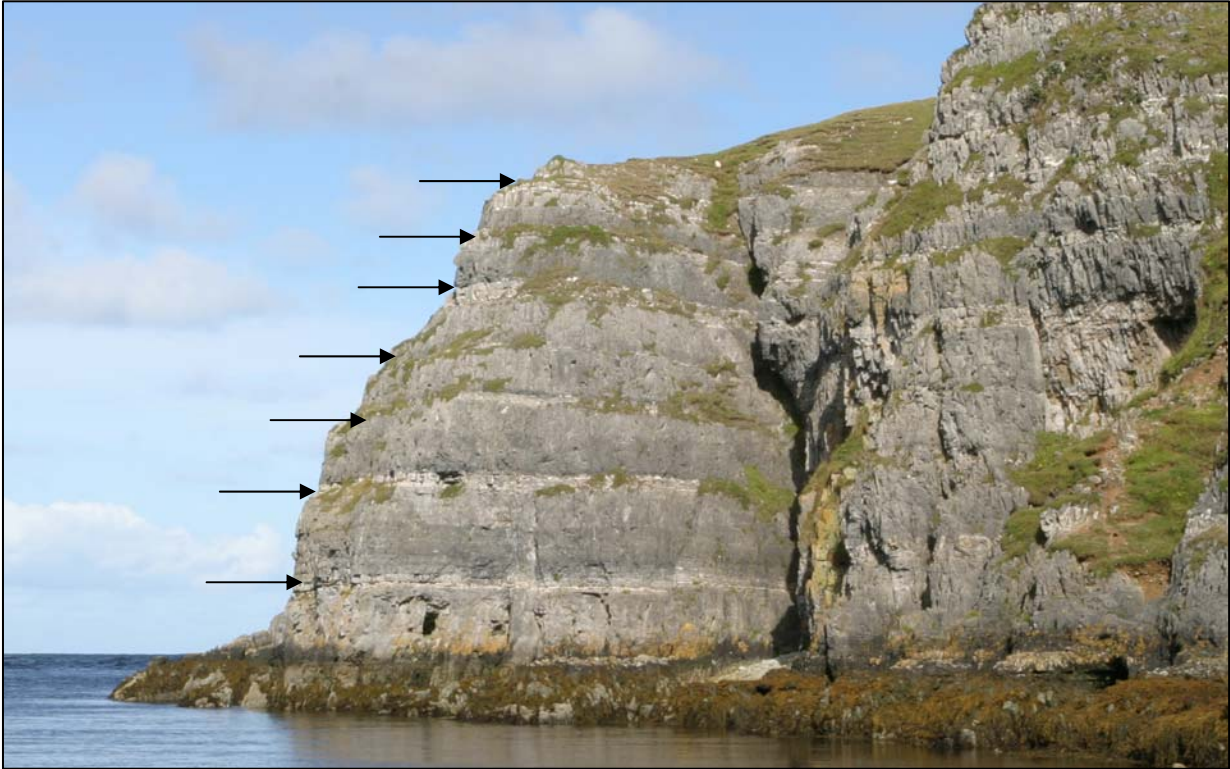
Text-figure 5.10 Sequence boundary between SLM IIIa and SLM IIIb 18 m below the top of the Eilean Dubh Formation, Balnakeil Bay, Durness. **(A)** overview of the sequence boundary, the position of each photograph is shown. The uppermost bed visible represents flooding above the sequence boundary, and growth of stromatolite bioherms, surrounded by ooidal grainstone. Hammer for scale. **(B)** 6 cm thick breccia containing carbonate intraclasts and chert granules **(C)** desiccation cracked top of siliciclastic silt bed marked C in figure A. **(D)** small spar filled vugs after evaporites, surrounded by contorted laminations. Overlain by small scale tepees and breccia. (position of the bed is marked in A).



Text-figure 5.11 Marine flooding at the Eilean Dubh–Sailmhor formation boundary [NC 3783 6877], 18 m above the base of the SLM IIIb Sequence at Balnakeil Bay, Durness. The Cambrian–Ordovician boundary lies not far below the formation boundary. Pale grey intertidal and supratidal dolomites are sharply overlain by dark gray, chert rich, subtidal dolomites of the Sailmhor Formation.

At the boundary, the Sailmhor Formation marks a sharp transition to chert rich, dark grey, subtidal dolostones, with abundant thrombolites. The distinctively cyclic lower part of the Sailmhor Formation represents the TST, exhibiting both increasing subtidal facies dominance and cycle thickness upwards. The parasequences that reach up to 6 m thick commonly have a very thin peritidal caps, and display little evidence of subaerial exposure. Columnar stromatolites are locally observed to colonise the parasequence boundaries, representing an increase in accommodation space following inundation of the tidal flats (Chapter 3).

A large coast perpendicular fault and a precipitous, cliff fringed inlet obscure the MFZ. The cycles thicken up to the fault but become thinner than average thereafter, suggesting that the transition is displaced at this locality and the upper part of the formation represents the HST. During the early HST, base-level was highest and the creation of accommodation space was greater than sediment supply.



Text-figure 5.12 The upper Sailmhor Formation (SLM IIIb) at Smoo Inlet [NC 422 675] showing well developed parasequences that become thinner towards the top of the cliff. The boundary with the Sangomore Formation lies a few metres above the observed section. The dark grey base of each parasequence is marked by an arrow.

Thick microbial reefs/mounds filled the available accommodation space and were capped by very thin peritidal tops to the parasequences. The cycles are less asymmetrical than below and commonly display a 10–50 cm thick dark massive base, which darkens upwards. This is then overlain by peloidal grainstones and thrombolites. The MFZ of this sequence represents the most subtidally dominated part of the entire SLM III Megasequence and corresponds to the Tremadocian maximum flooding discussed later.

5.9.3 SLM IIIc sequence

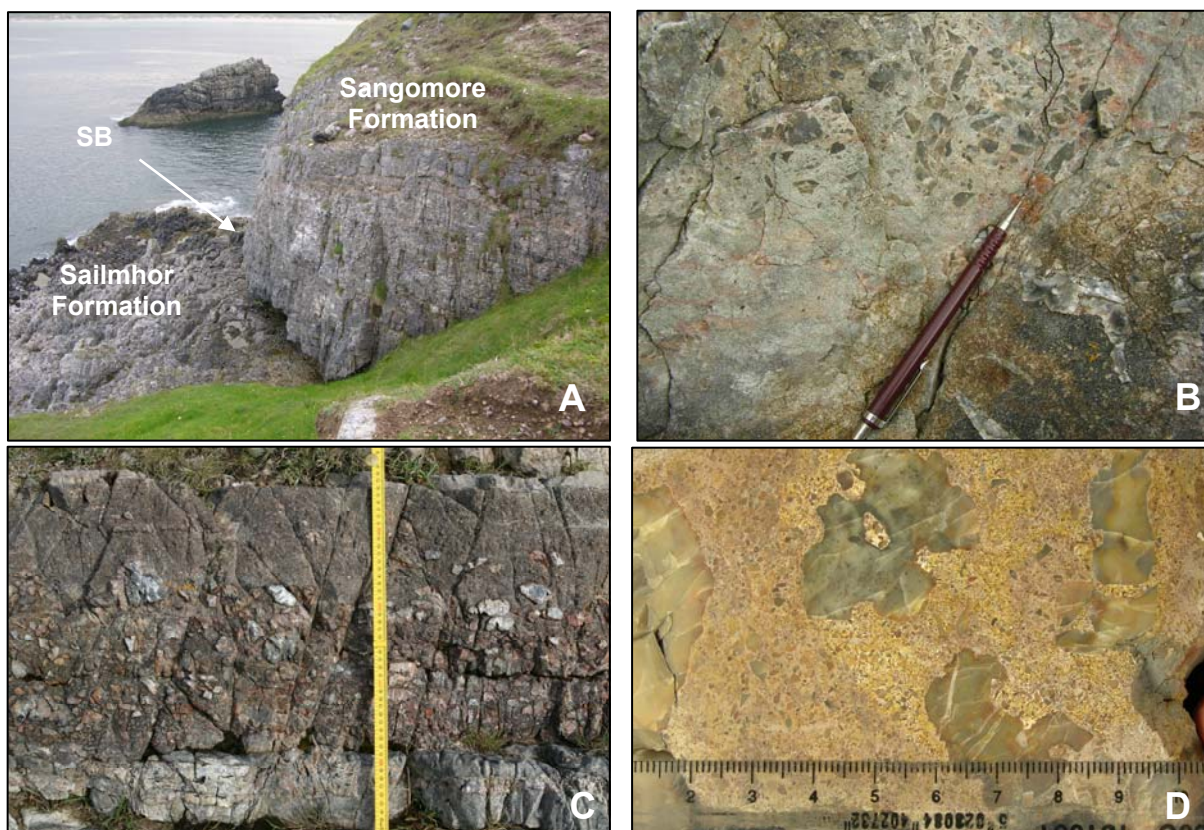
The SLM IIIc subsequence is 55 m thick and corresponds to deposition of the Sangomore Formation. The formation is represented by a series of parasequences containing thrombolite and stromatolites, peloidal and ooidal grainstones, and the formation marks the point at which limestones first appear within the succession.

The sequence boundary between the 2nd and 3rd SLM III subsequences coincides with the Sailmhor–Sangomore formation contact although it is represented by a zone of chert-rich

breccias observed below and above the boundary. The formation boundary is observed at a wave-cut notch at the base of the cliff along Balnakeil Bay (Text-fig. 5.13A) and can be traced to Leirinmore, 4.5 km to the east and also along the Kyle of Durness, 2.5 km to the south west. The boundary coincides with a 45 cm thick bed of coarse grained, dolomite sand that has a slightly undulating and the thickness varies from 30 cm to 45 cm. This is overlain by a 1.2 m thick thrombolite bed, which in turn is overlain by 1.3 m of fine grained dolostone with cherts and hemispheroidal stromatolite bioherms. These are overlain by a 2 m thick chert which preserves dolomite sand and succeeding parasequences contain chert breccias. The uppermost Sailmhor Formation contains a 2.5 m thick bed of chert, which may have been the source of the re-worked chert clasts in the basal beds of the Sangomore Formation (Text-fig. 5.13B–D).

The basal sequence boundary lies at the top of the *manitouensis* Zone and taxa indicative of this zone (*Clavohamulus densus*, *Acanthodus lineatus* and *Rossodus manitouensis*) have their last appearance 1.45 m above the base of the formation. The sequence therefore spans the ‘Low Diversity Interval’ and much of the *dianae* Zone. The SLM II. The upper sequence boundary coincides with a 20 cm thick bed of distinctive oncoidal pebbles at the top of the Sangomore Formation (Text-fig. 5.14, 5.15D, E). Pebbles are up to 3 cm in diameter and consist of sub-angular, laminated and massive, fine grained dolostone with local chert. The pebbles commonly display pale rims, indicating weathering. In the upper half of the bed pebbles form the cortices of symmetrical oncoids up to 2 cm in diameter, and the oncoids float in a matrix of ooidal grainstone. Angular carbonate breccias occur above this bed, infilling the hollows of karstic surfaces, which mark the tops of parasequences (Text-fig. 5.15B, C), and chert breccias also occur, with angular chert clasts within a sucrosic dolomite matrix (Text-fig. 5.15B). This boundary is tentatively correlated with the Boat Harbour disconformity based upon the *dianae* Zone fauna preceding the surface in both Scotland and western Newfoundland (Chapter 4). It is necessary to be cautious however as the presence of *M. dianae* above the boundary in Scotland and its absence in Newfoundland may indicate that the Scottish sequence boundary is older.

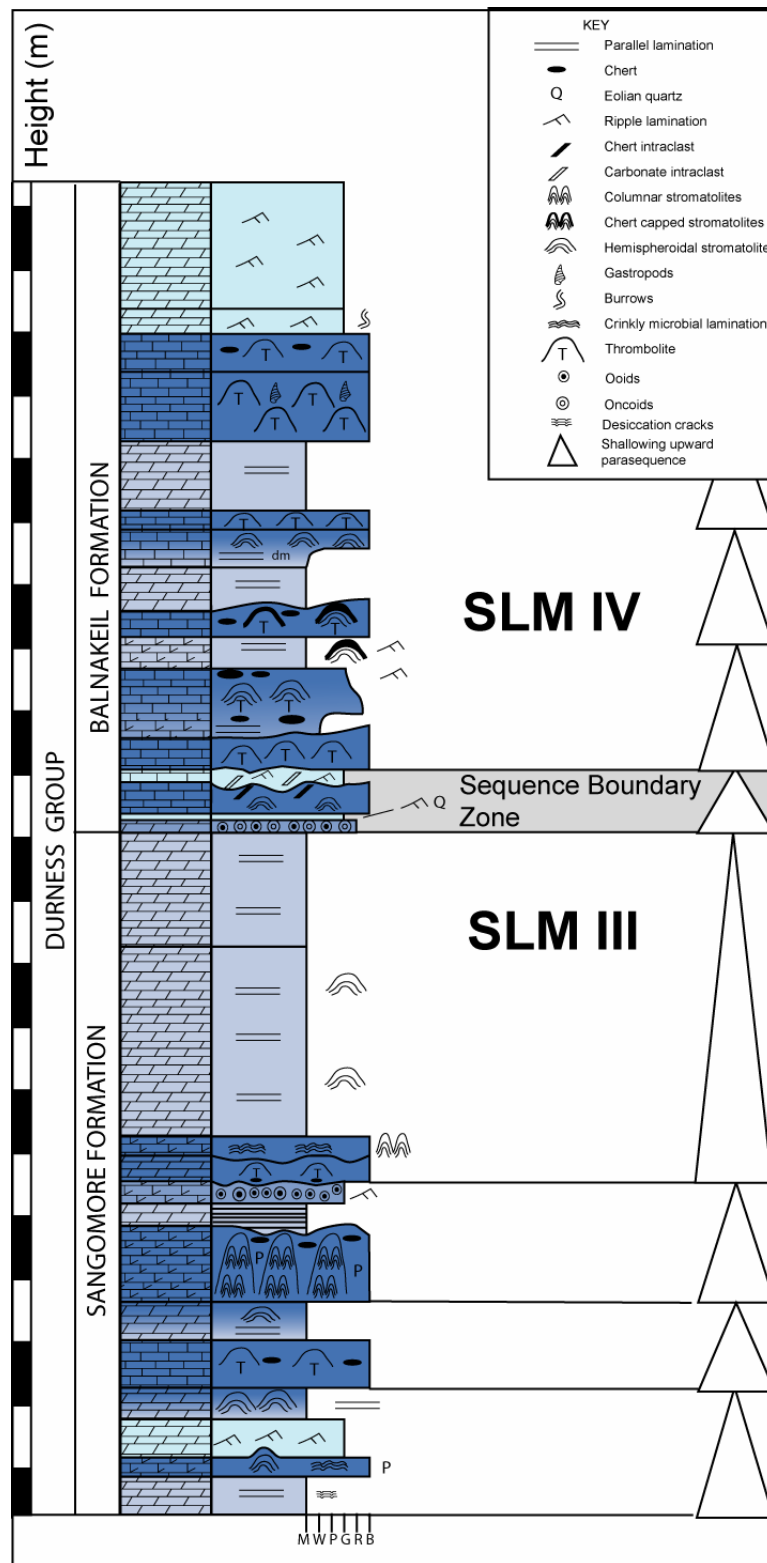
In western Newfoundland, the Boat Harbour disconformity lies 17–52 m below the top of the Boat Harbour Formation (Knight *et al.* 2008) and marks the boundary between the two ‘megacycles’ within the Ordovician part of the Sauk Megasequence (Knight 1978; Knight & James 1987; Boyce 1989; Knight 1991; Knight *et al.* 2007, 2008).



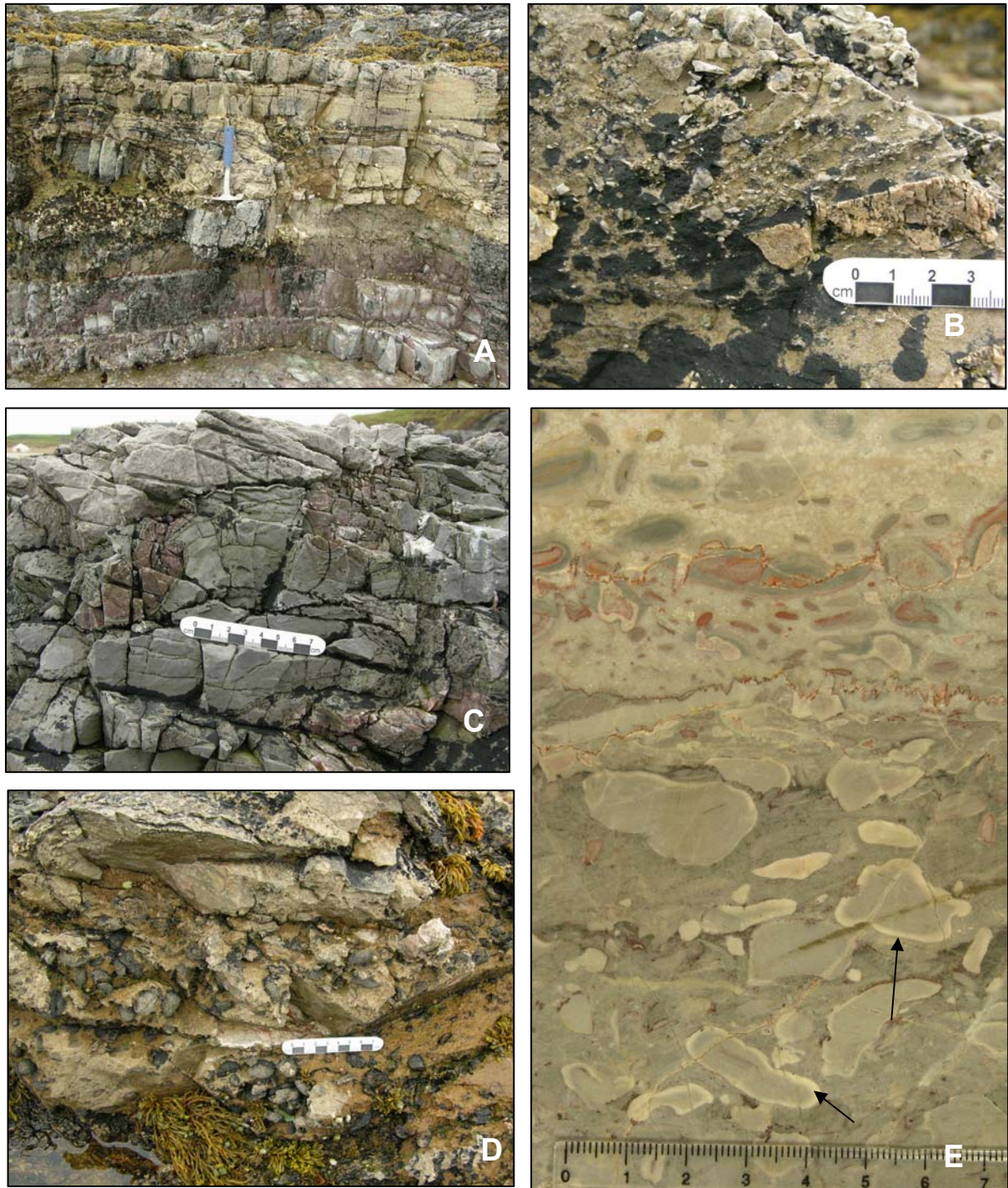
Text-figure 5.13 The SLM IIIb–c sequence boundary at the Sailmhor–Sangomore formation boundary [NC 3835 6886]. **(A)** photograph of cliff at Balnakeil Bay exposing the contact between the Sailmhor Formation and the overlying Sangomore Formation. The cliff is approximately 7 m high. The orange cherts towards the top of the cliff are breccias which rest upon a thick chert bed. **(B)** matrix supported reworked chert intraclasts in the upper Sailmhor Formation, Balnakeil Bay. **(C)** a 35 cm thick bed composed entirely of angular chert intraclasts. The bed occurs a few metres above the base of the Sangomore Formation, Kyle of Durness. **(D)** polished slab showing the variation in chert clast size, shape and colour. Scale bar in cm. Specimen comes from the same bed as pictured in image C.

In the northern part of western Newfoundland, a pebble bed marked by small-scale karren, a veneer of intraformational quartz pebbles, cherts and quartz sand forms the surface. Below the disconformity surface a bioturbated limestone is dolomitised for a few tens of centimetres and contains spherical bodies of crystalline dolostone. At Port au Choix, the sequence boundary truncates a stromatolite with silicification below and local pockets of breccia above (Knight 1991). Karst occurs at the top of the three parasequences spanning the disconformity on the Port au Port Peninsula (Knight *et al.* 2007, 2008). The disconformity

also marks a change in trilobite and conodont faunas (Boyce 1989; Ji & Barnes 1994; Boyce & Stouge 1997).



Text-figure 5.14 Sedimentary log spanning the SLM III – IV sequence boundary. The sequence boundary zone is shaded.



Text-figure 5.15 (A) photograph of the SLM III–IV sequence boundary. A 20 cm oncolite rests beneath the hammer, and is overlain by hemispheroidal stromatolite bioherms, which are in-turn overlain by chert and dolomite breccias and small-scale karst, Sangomore–Balnakeil formation boundary, Balnakeil Bay, [NC 3887 6876]. (B) angular fractured chert clasts overlain by cross bedded dolomite intraclasts. (C) erosional karst surface which truncates chert nodules. (D) oncolites weathering out on a bedding plane. (E) pebble and oncolite bed with ooids towards the top. Pebbles in the lower part of the bed display distinctive weathered rinds (arrowed). This bed marks the Sangomore–Balnakeil formation boundary, scale bar in cm.

The Boat Harbour disconformity bears a close resemblance to the SLM III–IV boundary (Text-fig. 5.14) and both occur at approximately the same age (*Macerodus diana*e Zone). Parasequences in both regions exhibit karst at the upper surfaces. Silicification occurs below the sequence boundary in both western Newfoundland and Scotland, and a carbonate and chert breccia and pebble bed above. The absence of *M. diana*e above the Boat Harbour disconformity may reflect a more prolonged period of erosion in western Newfoundland compared to NW Scotland (see Chapter 4). There is a possibility that the sequence boundary in Scotland correlates with a one at a lower position within the Boat Harbour Formation, which is entirely within the *M. diana*e Zone (I. Knight *pers. comm.*).

Knight *et al.* (1991) appear to imply that the Boat Harbour disconformity may be related to tectonism and changing ocean geometry associated with convergent plate dynamics. The sequence boundary coincides with a proposed glacio-eustatic regressive event at the end of the Tremadocian (Fortey 1984), and this event, regardless of causal factors has been observed across much of the Lower Ordovician platform of east North America (Barnes 1984; Knight & James 1987; James *et al.* 1989; Read 1989; Knight *et al.* 1991).

5.10 SLM IV SUPERSEQUENCE

The SLM IV Supersequence is the thickest within the Durness Group and represents some 558 m of strata. It includes the Balnakeil (86 m), Croisaphuill (340 m) and Durine (132 m) formations. The supersequence records a significant period of coastal onlap in the lower Croisaphuill Formation, followed by a progressive shallowing of facies thereafter. Above the Sangomore–Balnakeil sequence boundary, peritidal, shallowing-upward cycles typify the lower Balnakeil Formation. The parasequences comprise peloidal and bioclastic wackestone with thrombolites overlain by microbial and mechanical tidal-flat laminites with a variety of stromatolite bioherms. Higher in the formation, ribbon carbonates become dominant as the peritidal constituent and burrow-mottling is commonly seen to be gradational up into ribbon beds/with this facies (Chapter 2). The parasequences become thicker and difficult to recognise as they lack the pale peritidal caps and represent an aggrading mosaic of subtidal and lower intertidal flat facies. This most likely reflects carbonate production keeping up with base-level rise and the Balnakeil Formation represents the SLM IV TST deposited as accommodation space increased with marine onlap of the Scottish platform during the upper Tremadocian.

The overlying Croisaphuill Formation (350 m) consists of an informal lower member, 135 m thick of monotonous, burrow-mottled, dolomitic limestones, and an informal upper member, comprising 215 m of shallowing-upward parasequences. The maximum flooding zone is recorded towards the base of the lower member and is represented by an aggrading sequence of thickly bedded, burrow-mottled, dolomitic limestones (26 m above the formation base) (Text-fig. 5.16A). Conodont species from this horizon (Chapter 4) are consistent with a position low in the *O. communis* Zone (basal Floian stage). Macrofossils are recovered from the Croisaphuill Formation at Durness and from the correlative the Ben Suardal Formation, on Skye (Fortey 1992; Curry & Williams 1984). Chert is common at this level and may be due to a concentration of sponge spicules or radiolarians, marking the inflexion point on the sea-level curve. The absence of well-developed parasequences at this point in the succession indicates fairly rapid aggradation due to an increase in accommodation space. As base-level rise slowed, fossil remains may have been concentrated and the decreased rate of deposition may have led to more colonisation by sponges (some of the large cherts still preserve the remains of *Calathium* spp.), or concentration of radiolarians, which in turn, may have contributed to the abundance of chert. The overlying rocks show aggrading thick beds of burrow-mottled dolomitic limestone with rare bioclastic and peloidal wackestones.

The upper 215 m of the Croisaphuill Formation represents the late HST. Sediments show a progressive shallowing and a filling of available accommodation space. Cyclicity consisting of m-scale, shallowing upwards parasequences (Text-fig. 5.5) becomes apparent and the parasequences are commonly capped by peritidal laminites (Text-fig. 5.16B), locally containing evaporite pseudomorphs and increasing amounts of dolomite within beds. The uppermost part of the Croisaphuill Formation is not well exposed however, preventing detailed sequence stratigraphical analysis.

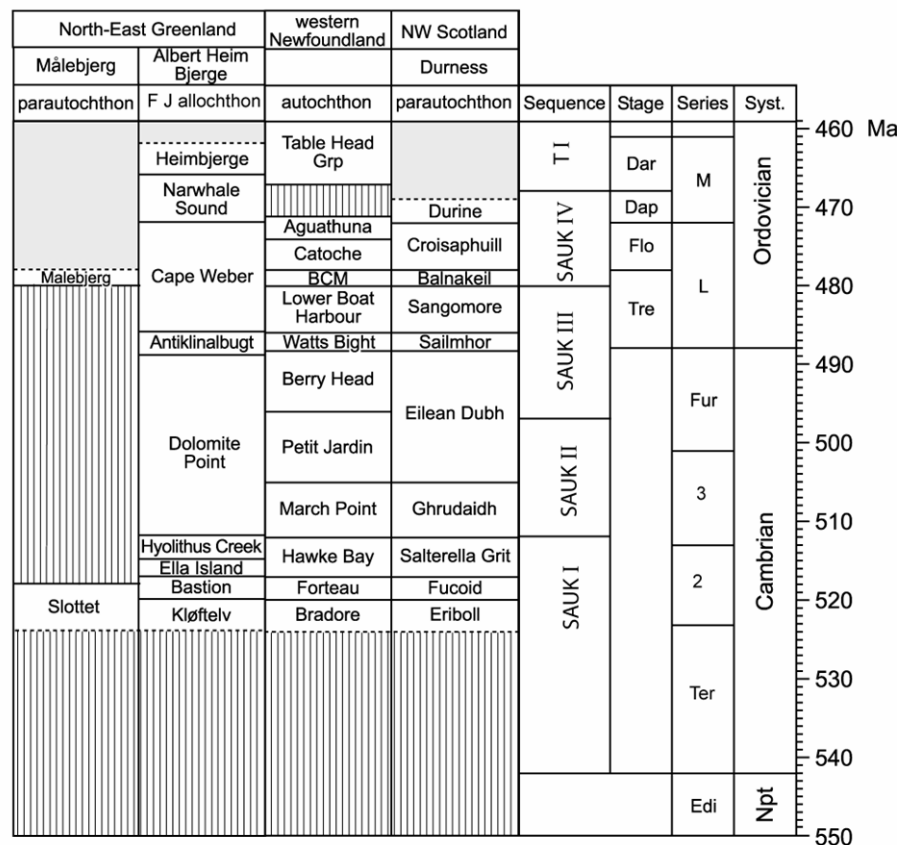
The overlying Durine Formation (132 m) predominantly comprises fine-grained, grey dolostones with parallel lamination and subordinate limestones. Evaporite pseudomorphs, preserved as chert nodules are present. Burrow-mottling is not present in the upper half of the formation, suggesting that the Durine Formation represents an even more restricted environmental setting than the upper Croisaphuill Formation.



Text-figure 5.16 (A) maximum flooding of SLM III within the lower part of the Croisaphuill Formation, thick beds of burrow mottled dolomitic limestone with abundant fossiliferous cherts, Loch Borrallie, Durness **(B)** view south from Balnakeil Craft Village of the 'upper member' within the Croisaphuill Formation, showing thick parasequences of dark grey dolostone and light-gray dolomitic limestone (arrowed), indicating shallowing of relative sea-level (dry stone wall for scale).

In western Newfoundland, a lower and upper ‘megacycle’ can be recognised (Knight & James 1987). The upper megacycle corresponds in chronostratigraphical terms approximately to the Arenig Series of Avalonia and the upper Ibexian and lower Whiterockian Series of Laurentia.

In Scotland, rocks of the Balnakeil, Croisaphuill and Durine formations (SLM IV) are believed to be equivalent of the upper Tremadocian to lowest Dapingian (i.e. Arenig/Ibexian) ‘megacycle’ described on the western Newfoundland platform by Knight & James (1987) and which is known to span the *A. deltatus*–*O. costatus* Zone to the early Whiterockian Mid-continent faunas 1 and 2 (Knight *et al.* 1991). In Scotland however, the megacycle ranges in age from the *M. diana*e Zone (Ibexian, Early Ordovician 485 Ma) to the *H. altifrons* Zone (Lower Whiterockian, early Middle Ordovician c. 470.5 Ma). It therefore spans approximately 15 million years. This cycle represents the upper sequence within the originally undivided Sauk III (Sauk IV of Golonka & Kiessling 2002), and its maximum flooding is the expression of a globally recognised Floian transgression (Fortey 1984).



Text-figure 5.17 Correlation of the Cambro-Ordovician of northwest Scotland with sections in western Newfoundland and North-east Greenland. The Sauk III is not subdivided (modified after Smith and Rasmussen 2008).

In Newfoundland, the megacycle comprises the Barbace Cove Member (upper part of the Boat Harbour Formation), Catoche and Aguathuna formations (Text-fig. 5.17). Onlap was extensive during this cycle, which represents the sea-level highstand in the Early Ordovician (Barnes 1984), and perhaps the Phanerozoic. Burrow-mottled facies, similar to those of the Croisaphuill and the Catoche formations, coupled with large thrombolite mound complexes are more widespread than at any other time in the Lower Ordovician as also seen in the Romaine, Beauharnois and Naylor Ledge formations in Ontario and Quebec (Desrochers 1988, Knight *et al.* 1991, 1995, Bernstein 1992, Salad Hersi *et al.* 2003), and into North-East Greenland (Cape Weber Formation; Smith & Rasmussen 2008). All these units record similar transgressive- to highstand marine events suggesting the platform was extensive and covered by an epeiric sea (James *et al.* 1989). Additional evidence for maximum flooding at the time of deposition of the Catoche and Croisaphuill formations is preserved in Newfoundland in the off-shelf, deepwater Cow Head Group. Slope sediments equivalent to the subtidal Catoche Formation are dominated by dark shales, with condensed graptolite zones: silica replaces many ribbon limestone layers, phosphate pebbles are common in conglomerates (James & Stevens 1986).

5.11 THE END OF THE SLM MEGASEQUENCE IN SCOTLAND

The termination of the SLM sequence and the onset of the Tippecanoe sequence are recognised across much of North America by a major lowering of relative sea-level at the end of the Lower Ordovician. Opinions vary as to the most suitable event to serve as the boundary. Finney *et al.* (2007) place the boundary just below the base of the Middle Ordovician, where the earliest evidence of sea-level fall is observed. This boundary would equate to the boundary between the lower and upper members of the Croisaphuill Formation. Other authors (Derby *et al.* 1991) place the sequence boundary at a higher level in the uppermost part of the *Histiodella holodentata* Zone and corresponding to the peak of regression. In contrast with either of these views, Landing & Westrop (2006) extended the Sauk up as far as the base of the transgressive facies at or near the base of the Upper Ordovician. The view that the boundary should be placed at the Floian sequence boundary is maintained here. Although first implied by Sloss (1963), the lowering of sea-level across this sequence boundary was identified by Vail *et al.* (1977), on the basis of coastal onlap curves for North America. The fluctuations in the onlap curve of Vail *et al.* were interpreted to be

global eustatic events and the well documented interregional sub-Tippecanoe sequence boundary is assumed, in part, or in total, to be the product of eustatic lowering of sea-level (Sloss 1964, 1984). Approximate rates of 2–3 m/my for the drop in depth of the shelf break at the time when the Sauk–Tippecanoe unconformity developed have been suggested by Worsley *et al.* (1984). Sea-level drawdown is observable throughout much of North America and the Siberian platform, and coincides with geochemical trends related to plate tectonics (Worsley *et al.* 1984), which resulted in a regionally recognised sequence boundary (Barnes *et al.* 1996). The Sauk–Tippecanoe sequence boundary is marked in Quebec and Ontario by the Beekmantown Group–Chazy group boundary (Bernstein 1992).

The unconformity lacks synchronicity within parts of North America such as eastern Canada and between paleocontinents and this may imply a tectonic influence (Knight *et al.* 1991). In the southern Appalachians, the Knox Unconformity is thought to mark the transition from a passive to a convergent plate boundary (Mussman & Read 1986) and reflect passage of the carbonate platform across a structural forebulge (Chapple 1973; Jacobi 1981; Rowley & Kidd 1981; Shanmugam & Lash 1982; Quinlan & Beaumont 1984; Bradley 1989).

A synthesis of stratigraphy, facies and chronostratigraphy led Knight *et al.* (1991) to suggest that the major eustatic event leading to the Sauk–Tippecanoe sequence boundary was enhanced at the continental margin by the inception of the Taconic foreland basin and that the shallowing event and the restricted peritidal sedimentation resulted from the impending Taconic overthrust loading of the margin and migration of a peripheral bulge across the shelf (Jacobi 1981; Quinlan & Beaumont 1984). This would have effectively interrupted margin subsidence causing abrupt shallowing of this part of the Laurentian margin (represented in western Newfoundland by the Costa Bay Member of the Catoche Formation). Because the outer part of the passive margin was uplifted as the bulge impinged on the shelf edge, oceanic circulation was restricted in the inner shelf, encouraging the widespread deposition of very shallow, restricted peritidal carbonates of the Aguathuna Formation and the Grand Ile Member at Mingan Islands (Knight *et al.* 1995). Regional erosion during the uplift associated with the Taconic Orogeny probably lasted 1 to 3 my and locally removed as much as 50 m of stratigraphy on topographic highs (Knight *et al.* 1991).

Knight *et al.* (1991) concluded that tectonism was the driving force in all these areas, partly based on the diachroneity of the event suggesting collision on the continental margin (Bradley 1989). The shallowing upward transition from the Catoche to the Aguathuna

formation is a rapid to abrupt event throughout the Newfoundland platform. It is interpreted that there was a slowing, and perhaps a cessation of platform subsidence as imminent convergence of the continental margin terminated thermal subsidence. Similar peritidal sediments occur in the top of the Romaine Formation on the Mingan Islands, Quebec (Desrochers 1988) and in the top of the Beekmantown Group in the St Lawrence Lowlands (Bernstein 1992; Salad Hersi *et al.* 2003).

Hatcher & Repetski (2007) contested the idea that the Taconic orogeny led to erosion marking the Sauk–Tipppecanoe sequence boundary, noting that the unconformity reaches as far as Nevada and California, as well as occurring on other continental blocks (e.g. Siberia, SE Asia, and S Baltica). They instead attribute the boundary to represent a global eustatic event.

There is thus evidence to support the theory of a tectonic influence, but the presence of a synchronous eustatic event at this time is suggested by widespread correlation of the Sauk–Tipppecanoe boundary. The succession in Scotland offers little to discriminate between these theories, but it is believed that the shallowing observed in the upper Croisaphuill and Durine formations is likely to be the product of both tectonic collision and a eustatic sea-level fall. In Scotland, the Durine Formation extends up into the Whiterockian (Chapter 4) but there is no evidence of the Sauk–Tipppecanoe sequence boundary. The interpreted influence of the Taconic orogeny in Scotland relies on identification of the cause/s of the similar shallowing event observed in Newfoundland.

The Grampian orogenic phase in Scotland is considered to be related to the collision of an ocean arc (possibly the Ballantrae arc) with Laurentia (Dewey & Mange 1999; Soper *et al.* 1999). The Humberian Phase in western Newfoundland and the Taconic Phase in the mainland Maritimes and New England are also related to arc-continent collisions and are regarded as direct lateral equivalents of the Grampian Phase (McKerrow *et al.* 2000). Scotland and Ireland occupied a Laurentian position along strike of the Taconic orogenic belt (Dalziel 1997 and Mac Niocaill *et al.* 1997), suggesting that the tectonostratigraphical evolution of both regions should be similar (Prave *et al.* 2000 and Oliver 1998).

The Durness Group is truncated by a thrust fault in the type area, where the youngest sediments are preserved. An age for the youngest carbonates present is indicated by a conodont fauna comprising *Histiodellella altifrons* Harris, *Chosonodina rigbyi* Ethington & Clark, *Cooperignathus aranda* (Cooper), *Jumudontus gananda* Cooper, *Dischidognathus* sp.

and *Pteracontiodus cryptodens* (Mound) (Chapter 4). This fauna is age diagnostic of the lower part of the *altifrons* Zone (middle Dapingian Stage, Middle Ordovician), and indicates an age of 470.5 Ma (Gradstein *et al.* 2004). Many of the dates for orogenesis during the Grampian phase coincide with this date, possibly suggesting a cause for the shallowing observed through the upper Croisaphuill and Durine formations. In Connemara, orogeny was caused by collision of the Loch Nafoeey arc with Laurentia. Synorogenic gabbros (Currywongaun and Cashel) are dated at 474.5 ± 1.0 and 470.1 ± 1.4 Ma respectively, and a post-tectonic granite has been dated at 462.5 ± 1.2 Ma (Friedrich *et al.* 1999). Soper *et al.* (1999) hypothesised that synorogenic deposits succeeded the Durness Group carbonates not far above their structural truncation.

Metamorphic and radiometric age data synthesised from across the Laurentian segments of the northern Appalachian and northwestern Ireland Taconic–Caledonian orogen further substantiate that orogenesis consisted of several short-lived (c. 10–20 Ma) deformational episodes confined to the Ordovician to lowermost Silurian (485–440 Ma).

These dates are consistent with the possibility that collision may have affected the change in sedimentation in the upper Croisaphuill Formation, but unfortunately the Ordovician rocks in northwest Scotland are truncated by Scandian thrusting (Moine Thrust) associated with the collision of Baltica. A minimum date of 430 ± 4 Ma for the thrust emplacement is derived from the synorogenic Borrolan Complex (van Breemen *et al.* 1979).

5.12 CONCLUSIONS AND RELATIVE SEA-LEVEL HISTORY

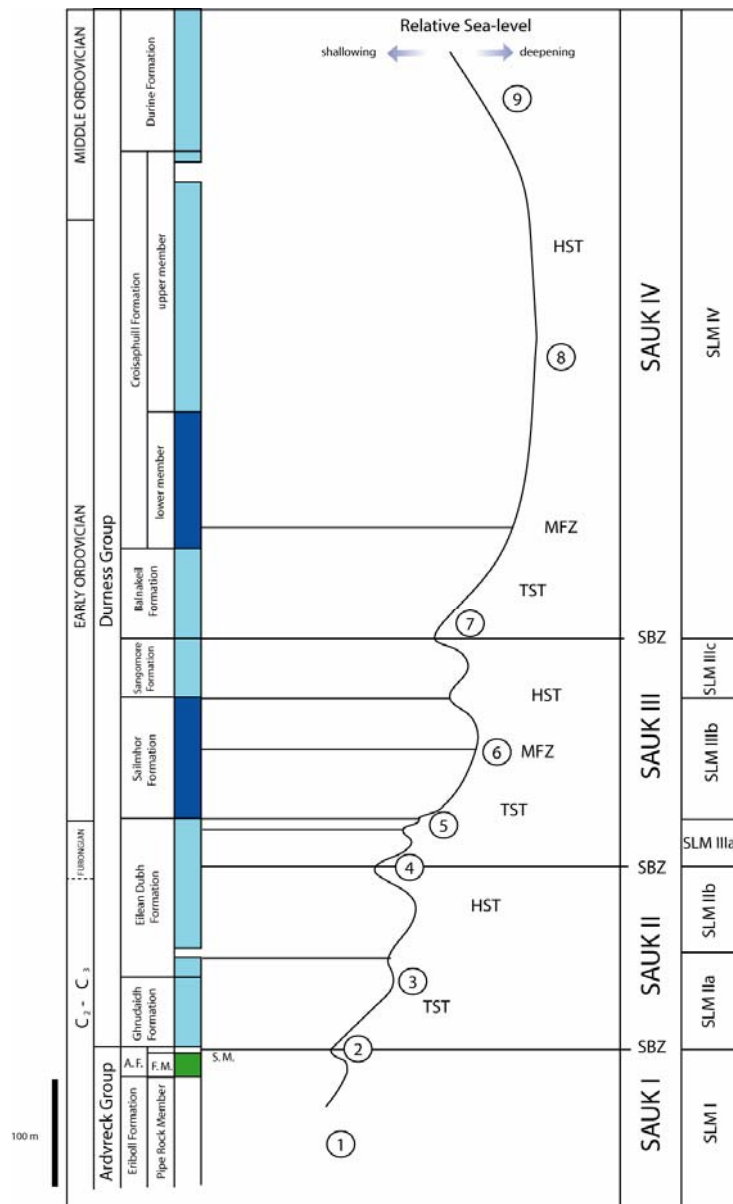
The SLM sequence can be correlated almost one for one with the Sauk sequence recognised across Laurentia (Text-fig. 5.18). The sequence stratigraphical evolution of the Scottish sector of the Laurentian passive margin can be separated into three temporal divisions that correspond to three phases in the evolution of the continental platform in Scotland: (1) Early to Middle Cambrian (pre-platform shelf); (2) Middle to Late Cambrian (high energy shelf) and (3) Early to Middle Ordovician (wider low energy platform).

Pre-platform shelf

1) The Cambrian is interpreted to be a time of major sea-level rise following rifting (Matthews & Cowie 1979). In Laurentia, this caused the onset of the Sauk Megasequence and the Sauk I Supersequence. In Scotland, deposition of siliciclastic sediments (Eriboll

Formation) occurred during, and after rift-drift transition. This was followed by progressive relative sea-level rise during deposition of the Fucoïd Member.

2) Sea level fall at the top of the Sauk I subsequence produced the Salterella Grit Member, and subsequent development of a carbonate shelf occurred (SLM II & early SLM III). Conditions on the shelf were commonly restricted, evaporites were common and ooids and flake breccias are noted along with a paucity of fauna. The Newfoundland shelf interpreted to be less than 200 km wide at this time (Knight *et al.* 1995).



Text-figure 5.18 Relative sea-level curve for the Durness Group, showing the systems tracts present and correlation between the SLM and the Sauk subdivisions. The numbers refer to the main points discussed in the conclusions.

High-energy shelf

3) A repetitive succession of aggrading subtidal (lagoonal?) burrow mottled dolostone passes upwards into shallower facies at the Ghrudaidh–Eilean Dubh formation boundary. This marks a significant sequence boundary within the Sauk II, and resulting progradation of supratidal and locally of sabkha facies across the area (Chapter 2). This event can be recognized from Assynt to Eriboll in the North of the study region.

4) Aggrading intertidal flat facies of the middle Eilean Dubh Formation represent deposition of a transgressive and early highstand systems tract prior to pronounced shallowing of facies at a sequence boundary within the middle Eilean Dubh Formation. This sequence boundary is marked by karstic surfaces, sabkha facies and deposition of quartz sand. It may be correlative to the Sauk II –II boundary recognized across much of Laurentia.

5) A pronounced but presumably minor sequence boundary is observed 18 m below the top of the Eilean Dubh Formation. The boundary with the overlying Sailmhor Formation marks a flooding event, coinciding with the Cambrian–Ordovician boundary.

Wider, low-energy platform

6) Relative sea level continued to rise throughout the Sailmhor Formation (Text-fig. 5.18), with the Tremadocian aged MFS recorded by thick parasequences, dominated by subtidal burrow mottled and thrombolitic facies.

7) An oncolitic pebble bed at the Sangomore –Balnakeil formation boundary is similar in nature and age to the Boat Harbour disconformity in western Newfoundland and is taken to represent the Sauk III–IV sequence boundary within the Durness Group.

8) The Floian aged maximum flooding is marked by a thick succession of burrow mottled dolomitic limestones represented by the Croisaphuill Formation. The base of an informal upper member represents the inflection of the relative sea-level curve and the onset of shallower peritidal facies prior to the Lower –Middle Ordovician boundary.

9) Continued shallowing of facies and an introduction of supratidal and locally evaporate pseudomorph bearing dolomites indicate relative sea level continued to fall until the top of the preserved Durness Group. The tectonically truncated upper boundary has removed any evidence of the Sauk–Tippecanoe sequence boundary that may have been present in NW Scotland.

It has been shown that the Sauk Megasequence is well developed in Scotland and that all three transgressive-regressive constituents can be recognised. Further correlation with other Laurentian sections may begin to elucidate the causes of the Sauk subsequences.

In the Cambrian part of the Durness Group, smaller sequences within the Sauk I – III subsequences may correlate with grand cycles recorded along the Appalachians although their thickness is different and the constituent facies differ significantly. Within the Ordovician strata, Sauk IIIb and c can be correlated with the lower megacycle observed in western Newfoundland. Sauk IIId can be correlated with the upper megacycle.

New biostratigraphical data for the top of the Durness Group indicate that the uppermost age coincides or precedes radiometric dates for the onset of the Taconic orogeny and the possibility of this as a cause of the shallowing within the upper parts of the succession is proposed.

Chapter 6 SUMMARY OF CONCLUSIONS

The Durness Group represents a succession of Cambrian to Ordovician aged carbonate and subordinate siliciclastic facies, which were deposited in a tropical setting on the passively subsiding Laurentian cratonic margin. The rocks crop out in several areas of northwest Scotland, but are restricted to the Hebridean terrane, which lies to the west of the Moine Thrust zone. The outcrop extends from Loch Eriboll in the north, to Skye in the south.

The Durness Group can be divided into seven different lithostratigraphical formations which are recognised along the outcrop belt. The constituent formations are best observed in the area around Durness and it was these that were examined during this study. In the type area of Durness, measured sections suggest that the carbonates have a minimum thickness of 920 m, but the succession may be thicker if strata are concealed by the numerous faults observed. The revised thickness of the Durness Group differs significantly from some published estimates.

The sedimentary rocks of the Durness Group were deposited in a range of shallow marine environments and are represented by sixteen recognisable lithofacies. These lithofacies are broadly restricted to three facies associations, indicating sabkha facies (supratidal), peritidal (dominantly intertidal) and shallow subtidal depositional settings.

Evaporite facies recorded at sequence boundaries suggest that a once more extensive coastal sabkha developed on the Laurentian margin during this time, but the tendency for active deposition to be restricted to the intertidal zone means that this facies now represents a rare constituent of successions along the margin.

Fenestral carbonates, oolites, evaporate pseudomorphs, stromatolites and finely-laminated dolomites displaying desiccation cracks and teepees all confirm deposition within a supratidal to shallow subtidal setting. More open marine conditions developed during maximum flooding events within the Sailmhor and Croisaphuill formations. During this time monotonous burrowed carbonate mud dominated deposition within the section. Locally a marine fauna comprising sponges, cephalopods, common gastropods, rostroconchs and brachiopods recorded. Trilobites are a rare part of this fauna in comparison to western Newfoundland, but their scarcity is most likely due to preservational bias, as they are observed frequently in thin section. Facies deposited under shallow subtidal to shelf settings

also include peloidal and bioclastic wackestones, oncoidal packstones, thrombolites and stromatolite mudstones.

Microbialites from the Durness Group are diverse in their morphology and display changes in both this diversity of form and in their abundance throughout the succession. The abundance of the microbialites within the Durness Group mirrors that seen elsewhere across Laurentia at this time and is part of a Cambro-Ordovician microbialite resurgence, recognised globally. The causes of the rise and demise are not currently known. The ‘leopard rock’ texture observed within the Sailmhor Formation is here interpreted as a thrombolite, thus greatly changing the abundance and therefore the significance of microbialite facies within this succession.

A revised conodont based age of the top of the Durness Group suggests that it lies within the lower part of the *altifrons* Zone and corresponds to a lower Dapingian (lower Middle Ordovician and early Whiterockian) age. Conodont faunas from the Durness Group compare well with those from western Newfoundland, New York State and East Greenland and a multivariate statistical analysis of faunas from the communis zone suggest that these localities can be classified as a separate, East Laurentian Subprovince, when compared to other sections from the North American midcontinent. The causal factors of this observed endemism are not known at this time but may result from latitudinal restriction of species, as no known barrier to obstruct migration along the Laurentian margin during this time is currently known.

The Cambrian and Ordovician of the Ardvreck and Durness groups correspond to a ‘first-order’ depositional sequence representing major cratonic transgression and regression (the Scottish Laurentian Margin (SLM) Megasequence). This comprises c. 1130 m of strata, and can be divided into four constituent second-order supersequences (SLM I–IV), separated by distinctive sequence boundaries or sequence boundary zones. New conodont data indicate that the two maximum flooding events recognised within the Durness Group, within the middle Sailmhor and lower Croisaphuill formations correspond to the middle *manitouensis* Zone (Tremadocian Stage) and the lower *communis* Zone (Floian Stage) respectively.

The sequence stratigraphical model and conodont biostratigraphy provide a framework for the Durness Group against which other Laurentian margin sections, and allows the sea-level history and lithostratigraphy to be placed in a global chronostratigraphical context. The SLM Megasequence and its subdivisions documented from Scotland compares well with the

Sauk Megasequence recognised across much of North America and the subdivisions of SLM I and II may represent the equivalents of the third order Cambrian Grand Cycles. Without age data for the Cambrian part of the succession this cannot be confirmed.

REFERENCES

- AITKEN, J.D. 1966. Middle Cambrian to Middle Ordovician cyclic sedimentation, southern Rocky Mountains of Alberta, Canada. *Bulletin of Canadian Petroleum Geology*, **14**, 405–441.
- AITKEN, J.D. 1967. Classification and environmental significance of cryptalgal limestones and dolomites, with illustrations from the Cambrian and Ordovician of southwestern Alberta. *Journal of Sedimentary Petrology*, **37**, 1163–1178.
- AITKEN, J.D. 1978. Revised models for depositional grand cycles, Cambrian of the southern Rocky Mountains, Canada. *Bulletin of Canadian Petroleum Geology*, **26**, 515–542.
- AITKEN, J.D. & NARBONNE, G.M. 1989. Two occurrences of Precambrian thrombolites from the Mackenzie Mountains, northwestern Canada. *PALAIOS*, **4**, 384–388.
- ALBANESI, G.L., CARRERA, M.G., CANAS, F.L. & SALTZMAN, M. 2003. The Niguivil section, Precordillera of San Juan, Argentina, proposed GSSP for the Lower/Middle Ordovician boundary. In: ALBANESI, G.L., BERESI, M.S. & PERALTA, S.H. (eds). *Ordovician from Andes*. INSUGEO, Serie Correlación Geológica, **17**, 33–40.
- AL-FARRAJ, A. 2005. An evolutionary model for sabkha development on the north coast of the UAE. *Journal of Arid Environments*, **63**, 740–755.
- ALLISON, I. & RUSSELL, M.J. 1985 Anhydrite discovered in the Furoid Beds of northwest Scotland. *Journal of Sedimentary Petrology*, **55**, 917–918.
- ALLWOOD, A.C., WALTER, M.R., KAMBER, B.S., MARSHALL, C.P. & BURCH, I.W. 2006. Stromatolite reef from the Early Archaean era of Australia. *Nature*, **441**, 714–718.
- ALSHARHAN, A.S. & KENDALL, C.G.ST.C. 1994. Depositional setting of the Upper Jurassic Hith Anhydrite of the Arabian Gulf an analogue to Holocene evaporites of the United Arab Emirates and Lake Macleod of Western Australia. *AAPG Bulletin*, **78**, 1075–1096.
- ALSHARHAN, A.S. & KENDALL, C.G.ST.C. 2003. Holocene coastal carbonates and evaporites of the southern Arabian Gulf and their ancient analogues. *Earth-Science Reviews*, **61**, 191–243.
- AMTHOR, J.E., GROTZINGER, J.P., SCHRÖDER, S., BOWRING, S.A., RAMEZANI, J., MARTIN, M.W. & MATTER, A. 2003. Extinction of *Cloudina* and *Namacalathus* at the Precambrian-Cambrian boundary in Oman. *Geology*, **31**, 431–434.
- ANDERSON, E.J., GOODWIN, P.W. & SOBIESKI, T.H. 1984. Comment and Reply on "Episodic accumulation and the origin of formation boundaries in the Helderberg Group of New York State": REPLY *Geology*, **12**, 573–574.
- ARBEY, F. 1980. Les formes de la silice et l'identification des évaporites dans les formations silicifiées. *Bulletin des Centres de Recherches Exploration –Production Elf-Aquitaine*, **4**, 309–365.

- ARMELLA, C. 1994. Thrombolitic-stromatolitic cycles of the Cambro-Ordovician boundary sequence, Precordillera Oriental basin, western Argentina. *In: BERTRAND-SARFATI, J. & MONTY, C. (eds.) Phanerozoic Stromatolites II*, Kluwer Academic Publishers 101–129.
- ASSERETO, R.L.A. & KENDALL, C.G.St.C. 1971. Megapolygons in Landinian limestones of Triassic of southern Alps: evidence of deformation by penecontemporaneous desiccation and cementation. *Journal of Sedimentary Petrology*, **41**, 715–23.
- ASSERETO, R.L.A. & KENDALL, C.G.St.C. 1977. Nature, origin and classification of peritidal tepee structures and related breccias. *Sedimentology*, **24**, 153–210.
- AWRAMIK, S.M. 1971. Precambrian columnar stromatolites diversity: reflection of metazoan appearance. *Science*, **174**, 825–826.
- AWRAMIK, S.M. & SPRINKLE, J. 1999. Proterozoic stromatolites: the first marine evolutionary biota. *Historical Biology*, **13**, 241–253.
- BABCOCK, L.E. & PENG, S. 2007. Cambrian chronostratigraphy: current state and future plans. *Palaeogeography, Palaeoclimatology, Palaeoecology*, **254**, 62–66.
- BABCOCK, L.E., ROBINSON, R.A., REES, M.N., PENG, S. & SALTZMAN, M. R. 2007. The Global boundary Stratotype Section and Point (GSSP) of the Drumian Stage (Cambrian) in the Drum Mountains, Utah, USA. *Episodes*, **30**, 85–95.
- BALL, M.M. 1967. Carbonate sand bodies of Florida and the Bahamas. *Journal of Sedimentary Petrology*, **37**, 556–591.
- BARNES, C.R. 1984. Early Ordovician eustatic events in Canada. *In: BRUTON, D.L. (ed.) Aspects of the Ordovician System*. Palaeontological Contributions from the University of Oslo, **295**, 51–64.
- BARNES, C.R., FORTEY, R.A. & WILLIAMS, S.H. 1996. The Pattern of Global Bio-Events during the Ordovician Period. *In: WALLISER, O.H. (ed.) Global Events and Event Stratigraphy in the Phanerozoic*, Springer Verlag. 139–172.
- BATHURST, R.G.C. 1982. Genesis of stromatactis cavities between submarine crusts in Palaeozoic carbonate mud buildups. *Journal of the Geological Society, London*, **139**, 165–181.
- BATTEN HENDER, K.L. & DIX, G.R. 2006. Facies, geometry and geological significance of Late Ordovician (early Caradocian) coral bioherms: Lourdes Formation, western Newfoundland. *Sedimentology*, **53**, 1361.
- BERGSTRÖM, S.M. 1985. Facies and its control upon the conodont faunas. *In: HIGGINS, A.C. & AUSTIN, R.L. (eds) A Stratigraphical Index of Conodonts*. British Micropalaeontological Society Series, Ellis Horwood Ltd., Chichester. 49–53.
- BERGSTRÖM, S.M., LÖFGREN, A & MALETZ, J. 2004. The GSSP of the Second (Upper) Stage of the Lower Ordovician Series: Diasbrottet at Hunneberg, Province of Västergötland, southwestern Sweden. *Episodes*, **27**, 265–272.

- BERGSTRÖM, S.M., FINNEY, S.C., CHEN, X., GOLDMAN, D. & LESLIE, S.A. 2006. Three new Ordovician global stage names. *Lethaia*, **39**, 287–288.
- BERNER, R.A. & KOTHAVALA, Z. 2001. GEOCARB III: A revised model of atmospheric CO₂ over Phanerozoic time. *American Journal of Science*, **301**, 182–204.
- BERNSTEIN, L. 1992. A revised lithostratigraphy of the Lower–Middle Ordovician Beekmantown Group, St. Lawrence Lowlands, Quebec and Ontario. *Canadian Journal of Earth Sciences*, **29**, 2677–2694.
- BEUKES, N.J. & LOWE, D.R. 1989. Environmental control on diverse stromatolites morphologies in the 3000 Myr Pongola Supergroup, South Africa. *Sedimentology*, **36**, 383–397.
- BOND, G.C., KOMINZ, M.A. & GROTZINGER, J.P. 1988. Cambro-Ordovician eustasy: evidence from geophysical modelling of subsidence in Cordilleran and Appalachian passive margins. *In*: KLEINSPEHN, K.L., & PAOLA, C. (eds). *New Perspectives in Basin Analysis*. Springer-Verlag, New York, 129–160.
- BOND, G.C., KOMINZ, M.A., STECKLER, M.S. & GROTZINGER, J.P. 1989. Role of thermal subsidence, flexure, and eustasy in the evolution of early Paleozoic passive-margin carbonate platforms. *In*: CREVELLO, P.D., WILSON, J.L. & Read, J.F. (eds). *Controls on Carbonate Platform and Basin Development*. Society of Economic Paleontologists and Mineralogists, Special Publication, **44**, p. 39-61.
- BOSENCE, D.W.J. & WILSON, R.C.L. 2003. Sequence stratigraphy of carbonate depositional systems. *In*: COE, A.L., BOSENCE, D.W.J. & CHURCH, K.D. (eds) *The Sedimentary Record of Sea-level Change*. Open University, Cambridge University Press, 234–256.
- BOSS, S.K. & RASMUSSEN, K.A. 1995. Misuse of Fischer plots as sea-level curves. *Geology*, **23**, 221–224.
- BOURQUE, P.A. & GIGNAC, H. 1983. Sponge-constructed stromatactis mud mounds, Silurian of Gaspé, Quebec. *Journal of Sedimentary Research*, **53**, 521–532.
- BOYCE, W.D. 1989. Early Ordovician trilobite faunas of the Boat Harbour and Catoche formations (St. George Group) in the Boat Harbour - Cape Norman area, Great Northern Peninsula, western Newfoundland. *Newfoundland Department of Mines and Energy, Geological Survey Branch Report*, **89-3**, 1–169.
- BOYCE, W.D. & STOUGE, S. 1997. Trilobite and conodont biostratigraphy of the St. George Group at Eddies Cove West, western Newfoundland. *Newfoundland Department of Mines and Energy, Geological Survey, Report*, **97-1**, 183–200.
- BRADLEY, D.C. 1989. Taconic plate kinematics as revealed by foredeep stratigraphy, Appalachian Orogeny. *Tectonics*, **8**, 1037–1049.
- BRAGA, J.C., MARTIN, J.M. & RIDING, R. 1995. Controls on microbial dome fabric development along a carbonate-siliciclastic shelf-basin transect, Miocene, SE Spain. *PALAIOS*, **10**, 347–361.
- BRASIER, M., COWIE, J. & TAYLOR, M. 1994. Decision on the Precambrian–Cambrian boundary stratotype. *Episodes*, **17**, 3–8.

- BRITISH GEOLOGICAL SURVEY, 2002. Loch Eriboll. Sheet 114W. Bedrock, 1:50 000 Geology Series, (Keyworth, Nottingham: British Geological Survey).
- BRITISH GEOLOGICAL SURVEY. 2007. Assynt. Scotland Special Sheet S101. Bedrock. 1:50 000 Geology Series, (Keyworth, Nottingham: British Geological Survey).
- BURNE, R.V. & JAMES, N.P. 1986. Subtidal origin of club-shaped stromatolites, Hamelin Pool. *Canberra, 12th International Sedimentological Congress, Abstracts*, 49–50.
- BURNE, R.V. & MOORE, L.S. 1987. Microbialites; organosedimentary deposits of benthic microbial communities. *PALAIOS*, **2**, 241–254.
- BURRI, P., DU DRESNAY, R. & WAGNER, C.W. 1973. Teepee and associated diagenetic features in intertidal carbonate sands. *Sedimentary Geology*, **9**, 221–228.
- BUTLER, G.P., HARRIS, P.M. & KENDALL, C.G.ST.C., 1982. Recent evaporites from Abu Dhabi coastal flats. In: HANDFORD, C.R. ROBERT, G.L. & GRAHAM, R.D. (eds), *Depositional and Diagenetic Spectra of Evaporites (core workshop no. 3.)*, SEPM, Tulsa, Oklahoma.
- CAMPBELL, C.A. & VALENTINE, J.W. 1977. Comparability of modern and ancient faunal provinces. *Palaeobiology*, **3** 49–57.
- CAROZZI, A.V. & GERBER, M.S. 1978. Synsedimentary chert breccia: A Mississippian tempestite. *Journal of Sedimentary Petrology*, **48**, 705–708.
- CAWOOD, P.A., MCCAUSLAND, P.J.A. & DUNNING, G.R. 2001. Opening Iapetus: Constraints from the Laurentian margin in Newfoundland. *Geological Society of America Bulletin*, **113**, 443–453.
- CAWOOD, P.A., NEMCHIN, A.A., STRACHAN, R., PRAVE, T. & KRABBENDAM, M. 2007. Sedimentary basin and detrital zircon record along East Laurentia and Baltica during assembly and breakup of Rodinia. *Journal of the Geological Society*, **164**, 257–275.
- CHAFETZ, H.S. 1973. Morphological evolution of Cambrian algal mounds in response to a change in depositional environment. *Journal of Sedimentary Petrology*, **43**, 435–446.
- CHAFETZ, H.S. & ZHANG, J. 1998. Authigenic euhedral megaquartz crystals in a Quaternary dolomite. *Journal of Sedimentary Research*, **68**, 994–1000.
- CHAPPLE, W.M. 1973. Mechanics of thin-skinned fold and thrust belts. *Geological Society of America Bulletin*, **89**, 1189–1198.
- CHOQUETTE, P.W. & JAMES, N.P. 1988. Introduction. In: N. P. JAMES & CHOQUETTE, P. W. (eds) *Paleokarst*, Springer-Verlag, New York. 1–21.
- CHOW, N. & JAMES, N.P. 1987. Cambrian grand cycles; a northern Appalachian perspective. *Geological Society of America Bulletin*, **98**, 418–429.

- CHOW, N. & JAMES, N.P. 1992. Synsedimentary diagenesis of Cambrian peritidal carbonates; evidence from hardgrounds and surface paleokarst in the Port au Port Group, western Newfoundland. *Bulletin of Canadian Petroleum Geology*, **40**, 115–127.
- CHOWNS, T.M. & ELKINS, J.E. 1974. The origin of quartz geodes and cauliflower cherts through the silicification of anhydrite nodules. *Journal of Sedimentary Petrology*, **44**, 885–903.
- CLOETINGH, S. 1986. Intraplate stresses: a new tectonic mechanism for regional sea-level variations. *Geology*, **14**, 617–620.
- CLOUD, P.E. & SEMIKHATOV, M.A. 1969. Proterozoic stromatolites zonation. *American Journal of Science*, **267**, 1017–1061.
- CLOYD, K.C., DEMICCO, R.V. & SPENSER, R.J. 1990. Tidal channel, levee, and crevasse-splay deposits from a Cambrian tidal channel system: a new mechanism to produce shallowing-upward sequences. *Journal of Sedimentary Petrology*, **60**, 73–83.
- COCKS, L.R.M. & TORSVIK, T.H. 2006. European geography in a global context from the Vendian to the end of the Palaeozoic. In: GEE, D.G. & STEPHENSON, R.A. (eds). *European Lithosphere Dynamics*. Geological Society, London, Memoirs, **32**, 83–95.
- CODY R.D. 1976. Growth and early diagenetic changes in artificial gypsum crystals grown within bentonite muds and gels. *Geological Society of America Bulletin*, **87**, 1163–1168.
- COOPER, R.A., NOWLAN, G.S. & WILLIAMS, S.H. 2001. Global Stratotype Section and Point for the base of the Ordovician System. *Episodes*, **24**, 19–28.
- CORON, C.R. & TEXTORIS, D.A. 1974. Non-calcareous algae in Silurian carbonate mud mound, Indiana. *Journal of Sedimentary Research*, **44**, 1248–1250.
- COWAN, C.A. & JAMES, N.P. 1993. The interactions of sea-level change, terrigenous sediment influx and carbonate productivity as controls of Upper Cambrian Grand Cycles of western Newfoundland, Canada. *Geological Society of America Bulletin*, **105**, 1576–1590.
- COWAN, C.A. & JAMES, N.P. 1996. Autogenic dynamics in carbonate sedimentation: metre-scale, shallowing upward cycles, Upper Cambrian, western Newfoundland, Canada. *American Journal of Science*, **296**, 1175–1207.
- COWIE, J.W. 1974. The Cambrian of Spitsbergen and Scotland. In: Holland, C.H. (ed.). *Cambrian of the British Isles, Norden and Spitsbergen. Lower Palaeozoic Rocks of the World, 2*. John Wiley & Sons, London. 123–155.
- COWIE, J.W. & MCNAMARA, K.J. 1978. *Olenellus* (Trilobita) from the Lower Cambrian strata of north-west Scotland. *Palaeontology*, **21**, 615–634.
- COWIE, J.W., RUSHTON, A.W.A. & STUBBLEFIELD, C.J. 1972. *A correlation of Cambrian rocks in the British Isles*. Geological Society of London Special Report, **2**, 42 pp.
- CROWLEY, T.J. & BERNER, R.A. 2001. CO₂ and climate change. *Science*, **292**, 870–872.

- CURRAN, H.A. & WHITE, B. 1991. Trace fossils of shallow subtidal to dunal ichnofacies in Bahamian Quaternary carbonates. *PALAIOS*, **6**, 498–510.
- CURRY, G.B. & WILLIAMS, A. 1984. Lower Ordovician brachiopods from the Ben Suardal Limestone Formation (Durness Group) of Skye, western Scotland. *Transactions of the Royal Society of Edinburgh: Earth Sciences*, **75**, 301–310.
- DALRYMPLE, R. W., NARBONNE, G. M., SMITH, L. 1985. Eolian action and the distribution of Cambrian shales in North America. *Geology*, **13**, 607–610.
- DALZIEL, I.W.D. 1997. Neoproterozoic-Paleozoic geography and tectonics: review, hypothesis, environmental speculation. *Geological Society of America Bulletin*, **190**, 16–42.
- DALZIEL, I.W.D. & SOPER, N.J. 2001. Neoproterozoic Extension on the Scottish Promontory of Laurentia: Paleogeographic and Tectonic Implications. *Journal of Geology*, **109**, 299–317.
- DAVIES, G.R. 1970. Algal-laminated sediments, Gladstone Embayment, Shark Bay, Western Australia. In: LOGAN, B.W. DAVIES, G.R. READ, J.F. & CEBULSKI, D.E (eds) *Carbonate Sedimentation and Environments, Shark Bay, Western Australia*. AAPG. Memoir, Tulsa, **13**, 169–205.
- DEMICCO, R.V. 1983. Wavy and lenticular-bedded carbonate ribbon rocks of the Upper Cambrian Conococheague Limestone, central Appalachians. *Journal of Sedimentary Research*, **53**, 1121–1132.
- DEMICCO, R.V. 1985. Platform and off-platform carbonates of the Upper Cambrian of western Maryland, USA. *Sedimentology*, **32**, 1–22.
- DERBY, J.R., BAUER, J.A., CREATH, W.B., DRESBACH, R.I, ETHINGTON, R.L., LOCH, J.D., STITT, J.S., MCHARGUE, T.R., MILLER, J.F., MILLER, M.A., REPETSKI, J.E., SWEET, W.C., TAYLOR, J.F. & WILLIAMS, M. 1991. Biostratigraphy of the Timbered Hills, Arbuckle, and Simpson Groups, Cambrian and Ordovician, Oklahoma: a review of correlation tools and techniques available to the explorationist. In: JOHNSON, K. (ed) *Late Cambrian–Ordovician geology of the southern midcontinent*. Oklahoma Geological Survey Circular, **92**, 15–41.
- DESROCHERS, A. 1988. Stratigraphie de l’Ordovicien de la region de l’archipel de Mingan. *Ministère de l’Énergie et des Ressources du Québec*, **MM87-01**.
- DEWEY, J. & MANGE, M. 1999. Petrography of Ordovician and Silurian sediments in the western Ireland Caledonides: tracers of a short-lived Ordovician continent-arc collision orogeny and the evolution of the Laurentian Appalachian-Caledonian margin. In: MACNIOCAILL, C. & RYAN, P.D. (eds). *Continental Tectonics*. Geological Society, London, Special Publication, **164**, 55–107.
- DILL, R.F., SHINN, E.A., JONES, A.T., KELLY, K. & STEINEN, R.P. 1986. Giant subtidal stromatolites forming in normal salinity waters. *Nature*, **324**, 55–58.
- DOWNIE, C. 1982. Lower Cambrian acritarchs from Scotland, Norway, Greenland and Canada. *Transactions of the Royal Society of Edinburgh: Earth Sciences*, **72**, (for 1981), 257–285.

- DRAVIS, J.J. 1983. Hardened subtidal stromatolites, Bahamas. *Science*, **219**, 385–386.
- DRUMMOND, C.N. & WILKINSON, B.H. 1993. On the use of thickness/subsidence diagrams as records of long-term sealevel change during accumulation of cyclic carbonate sequences. *Journal of Geology*, **101**, 687–702.
- DUNHAM, R.J. 1962. Classification of carbonate rocks according to depositional texture. In: HAM, W.E. (ed.) *Classification of carbonate rocks: a Symposium*. American Association of Petroleum Geologists Memoir. 1, Tulsa, 108–121.
- DUPONT, E. 1881. Sur l'origine des calcaires Dévoniens de la Belgique. *Bulletin de l'Academie Royale des Sciences de Belgique, 3rd Series*, **2**, 264–280.
- DZIK, J. 1983. Relationships between Ordovician Baltic and North American Midcontinent conodont faunas. *Fossil and Strata*, **15**, 59–85.
- EGGLESTON, J.R. & DEAN, W.E. 1976. Freshwater stromatolitic bioherms in Green Lake, New York. In: WALTER, M.R. (ed.) *Stromatolites*. Elsevier, Amsterdam 479–488.
- EMBRY, A.F. & KLOVAN, J.E. 1971. A Late Devonian reef tract on north eastern Banks Island, Northwest Territories. *Bulletin of the Canadian Petroleum Geologists*, **19**, 730–781.
- EMERY, D. & MYERS, K. J. (eds) 1996. *Sequence Stratigraphy*. Oxford: Blackwell Science. 297 pp.
- EPSTEIN, A.G., EPSTEIN, J.B. & HARRIS, L.D. 1977. Conodont color alteration – an index to organic metamorphism. *U.S. Geological Survey, Professional Paper*, **995**, 1–27.
- ERDTMANN, B.D. & MILLER, J.F. 1981. Eustatic control of lithofacies and biofacies near the base of the Tremadocian. In: TAYLOR, M.E. (ed.). *Short Papers for the Second International Symposium on the Cambrian system*. U.S. Geological Survey Open-File Report, **81-773**, 78–81.
- ETHINGTON, R.L. & AUSTIN, R.L. 1991. Conodonts of the Dounans Limestone, Highland Border Complex, Scotland. *Journal of Micropalaeontology*, **10**, 51–56.
- ETHINGTON, R.L. & CLARK, D.L. 1971. Lower Ordovician conodonts in North America. *Geological Society of America, Memoir*, **127**, 63–82.
- ETHINGTON, R.L. & CLARK, D.L. 1981. Lower and Middle Ordovician conodonts from the Ibex area, western Millard County, Utah. *Brigham Young University Geology Studies*, **28**: 155 pp.
- ETHINGTON, R.L. ENGEL, K.M. & ELLIOT, K.L. 1987. An abrupt change in conodont faunas in the Lower. *Brigham Young University Geology Studies*, **28**: 155 pp.
- EVAMY, B.D. 1973. The precipitation of aragonite and its alteration to calcite on the Trucial Coast of the Persian Gulf. In: PURSER, B.H. (ed.) *The Persian Gulf*, Springer-Verlag, Berlin, pp. 329–342.
- EVANS, G., SCHMIDT, V., BUSH, P. AND NELSON, H. 1969. Stratigraphy and geologic history of the sabkha, Abu Dhabi, Persian Gulf. *Sedimentology*, **12**, 145–159.

- FÄHRÆUS, L.N. & NOWLAN, G.S. 1978. Franconian (Late Cambrian) to early Champlanian (Middle Ordovician) conodonts from the Cow Head Group, western Newfoundland. *Journal of Paleontology*, **52**, 444–471.
- FELDMANN, M. & MCKENZIE, J.A. 1997. Messinian stromatolite-thrombolite associations, Santa Pola, SE Spain: an analogue for the Palaeozoic? *Sedimentology*, **44**, 893–914.
- FELDMANN, M. & MCKENZIE, J.A. 1998. Stromatolite-thrombolite associations in a modern environment, Lee Stocking Island, Bahamas. *PALAIOS*, **13**, 201–212.
- FINNEY, S.C., ETHINGTON, R.L. & REPETSKI, J.E. 2007. The boundary between the Sauk and Tippecanoe Sloss Sequences of North America. *Acta Palaeontologica Sinica*, **46**, (suppl.), 128–134.
- FISCHER, A.G. 1964. The Lofer cyclothems of the Alpine Triassic. In: D.F. Merriam, Editor, Symposium on Cyclic Sedimentation. *Kansas Geological Survey Bulletin*, **169**, 107–146.
- FISCHER, A.G., & SARNTHEIN, M. 1988. Airborne silts and dune-derived sands in the Permian of the Delaware basin. *Journal of Sedimentary Petrology*, **58**, 637–643.
- FLÜGEL, E. 2004. *Microfacies of Carbonate Rocks: Analysis, Interpretation and Application*. Springer. 976 pp.
- FOLK, R.L. & PITTMAN, J.S. 1971. Length-slow chalcedony: a new testament for vanished evaporites. *Journal of Sedimentary Petrology*, **41**, 1045–1048.
- FOORD, A.H. 1887. On the genus *Piloceras*, Salter, as elucidated by examples lately discovered in North America and in Scotland. *Geological Magazine, New Series*, **4**, 541–546.
- FOORD, A.H. 1888. *Catalogue of the Fossil Cephalopods in the British Museum (Natural History), Part 1*. Trustees of the British Museum (Natural History) London. 344 pp.
- FORTEY, R.A. 1979. Early Ordovician trilobites from the Catoche Formation (St. George Group), western Newfoundland. *Bulletin of the Geological Survey of Canada*, **321**, 61–114.
- FORTEY, R. A. 1984. Global earlier Ordovician transgressions and regressions and their biological implications, In: BRUTON, D.L. (ed.). *Aspects of the Ordovician System*. Palaeontological Contributions from the University of Oslo, **295**, 37–50.
- FORTEY, R.A. 1992. Ordovician trilobites from the Durness Group, north-west Scotland and their palaeobiogeography. *Scottish Journal of Geology*, **28**, 115–121.
- FRIEDMAN, G.M. & BRAUN, M. 1975. Shoaling and tidal deposits that accumulated marginal to the proto-Atlantic Ocean, p. 307–314 In: GINSBURG, R.N. (ed.). *Tidal deposits: A casebook of recent examples and fossil counterparts*. Springer-Verlag, New York-Heidelberg-Berlin, 428 pp.
- FRIEDMAN, G.M. & SHUKLA, V. 1980. Significance of authigenic quartz euhedra after sulfates; example from the Lockport Formation (Middle Silurian) of New York. *Journal of Sedimentary Research*, **50**, 1299–1304.

- FRIEDRICH, A.M., HODGES, K.V., BOWRING, S.A. & MARTIN, M.W. 1999. Geochronological constraints on the magmatic, metamorphic and thermal evolution of the Connemara Caledonides, western Ireland. *Journal of the Geological Society, London*, **156**, 1217–1230.
- FRITZ, W.H. & YOCHELSON, E.L. 1988. The status of *Salterella* as a Lower Cambrian index fossil. *Canadian Journal of Earth Sciences*, **25**, 403–416.
- GAO, G-Q & LAND, L. S. 1991. Nodular chert from the Arbuckle Group, Slick Hills, SW Oklahoma: a combined field, petrographic and isotopic study. *Sedimentology*, **38**, 857–870.
- GARRETT, P. 1970. Phanerozoic stromatolites: noncompetitive ecologic restriction by grazing and burrowing animals. *Science*, **169**, 171–173.
- GEBELEIN, C.D. 1969. Distribution, morphology, and accretion rate of recent subtidal algal stromatolites, Bermuda. *Journal of Sedimentary Petrology*, **39**, 49–69.
- GEBELEIN, C.D. 1976. Open marine subtidal and intertidal stromatolites (Florida, the Bahamas and Bermuda). In: Walter, M.R. (ed.) *Stromatolites*. Elsevier Scientific Publishing Company, Amsterdam. Developments in Sedimentology, **20**, 381–388.
- GEESLIN, J.H. & CHAFETZ, H.S. 1982. Ordovician Aleman ribbon cherts; an example of silicification prior to carbonate lithification. *Journal of Sedimentary Research*, **52**, 1283–1293.
- GEHLING, J.G., JENSEN, S., DROSER, M.L., MYROW, P.M. & NARBONNE, G.M. 2001. Burrowing below the basal Cambrian GSSP, Fortune Head, Newfoundland. *Geological Magazine*, **138**, 213–218.
- GERDES, G. & KRUMBEIN, W.E. 1994. Peritidal potential stromatolites – a synopsis. In BERTRAND-SARFATI, J. & MONTY, C. (eds) *Phanerozoic Stromatolites II*, Kluwer Academic Publishers 101–129.
- GINGRAS, M.K., PEMBERTON, S.G., MUEHLENBACHS, K., AND MACHEL, H. 2004. Conceptual models for burrow-related, selective dolomitization with textural and isotopic evidence from the Tyndall Stone, Canada. *Geobiology*, **2**, 21–30.
- GINSBURG, R.N. 1971. Landward movement of carbonate mud: new model for regressive cycles in carbonate. *American Association of Petroleum Geologists Bulletin*, **55**, 340.
- GINSBURG, R.N. & HARDIE, L.A. 1975. Tidal and storm deposits, northeastern Andros Island, Bahamas. In: GINSBURG, R.N. (ed.) *Tidal Deposits, a Casebook of Recent examples and Fossil Counterparts*. Springer-Verlag. 428 pp.
- GINSBURG, R.N., HARDIE, L.A., BRICKER, O.P., GARRETT, P. & WANLESS, H.R. 1977. Exposure index: a quantitative approach to defining position within the tidal zone. In: Hardie, L.A. (ed.) *Sedimentation on the Modern Carbonate Tidal Flats of Northwest Andros Island, Bahamas*. The Johns Hopkins University Studies in Geology No. **22**, The Johns Hopkins University Press, Baltimore. 7–11.

- GLUMAC, B. & WALKER, K.R. 1998. A Late Cambrian positive carbon-isotope excursion in the southern Appalachians: Relation to biostratigraphy, sequence stratigraphy, environments of deposition, and diagenesis. *Journal of Sedimentary Research*, **68**, 1212–1222.
- GLUMAC, B. & WALKER, K.R. 2000. Carbonate deposition and sequence stratigraphy of the terminal Cambrian grand cycle in the southern Appalachians. *Journal of Sedimentary Research*, **70**, 952–963.
- GOLDHAMMER, R.K., DUNN, P.A. & HARDIE, L.A. 1987. High frequency glacio-eustatic sea level oscillations with Milankovitch characteristics recorded in Middle Triassic platform carbonates in northern Italy. *American Journal of Science*, **287**, 853–892.
- GOLDHAMMER, R.K., DUNN, P.A. & HARDIE, L.A., 1990. Depositional cycles, composite sea level changes, cycle stacking patterns, and the hierarchy of stratigraphic forcing: examples from platform carbonates of the Alpine Triassic. *Geological Society of America Bulletin*, **102**, 535–562.
- GOLONKA, J. & KIESSLING, W. 2002. Phanerozoic time scale and definition of time slices. In: KIESSLING, W., FLÜGEL, E. & GOLONKA, J. (eds). *Phanerozoic Reef Patterns*. SEPM Special Publication. **72**, 11–20.
- GOODWIN, P.W. & ANDERSON, E.J. 1985. Punctuated aggradational cycles: a general model of stratigraphic accumulation. *Journal of Geology*, **71**, 515–534.
- GRABAU, A.W. 1916. Comparison of American and European Lower Ordovician formations. *Geological Society of America Bulletin*, **27**, 555–622.
- GRADSTEIN, F.M., OGG, J.G. & SMITH, A.G. 2004. *A Geologic Time Scale 2004*. Cambridge University Press. Cambridge. 589 pp.
- GREGG, J.M. & SHELTON, K., 1990. Dolomitization and dolomite neomorphism in the back-reef facies of the Bonnetterre and Davis Formations (Cambrian), southeastern Missouri. *Journal of Sedimentary Petrology*, **60**, 549–562.
- GREY, K. 1989. Handbook for the study of stromatolites and associated structures. *Stromatolite Newsletter*, **14**, 82–171.
- GROTZINGER, J.P. 1986. Cyclicity and paleoenvironmental dynamics of an early Proterozoic carbonate platform, Rocknest Formation, Wopmay Orogen, N.W.T., Canada. *Geological Society of America Bulletin*, **97**, 1208–1231.
- GROTZINGER, J.P. 1990. Geochemical model for Proterozoic stromatolite decline. *American Journal of Science*, **290-A**, 80–103.
- HALLEY, R.B. 1976. Textural variation within Great Salt Lake algal mounds. In WALTER, M. R. (ed.) *Stromatolites*. Elsevier, Amsterdam 433–445.
- HAMMER, Ø., HARPER, D.A.T. & RYAN, P.D. 2001. PAST: Palaeontological Statistics Software Package for education and data analysis. *Palaeontologica Electronica*, **4**, 1–9.

- HANDFORD, R., LOUCKS, R.G., & DAVIES, G.R. 1982. Depositional and diagenetic spectra of evaporates. *Society of Economic Paleontologists and Mineralogists, Core Workshop*, **3**, 395 pp.
- HARDENBOL, J., THIERRY, J. FARLEY, M.B. JACQUIN, T., GRACIANSKY, P.C. de & VAIL, P.R. 1998. Mesozoic and Cenozoic sequence chronostratigraphic framework of European basins. *In: GRACIANSKY, P.C. de, HARDENBOL, J., JACQUIN, T. & VAIL, P.R. (eds) Mesozoic and Cenozoic Sequence Stratigraphy of European Basins*. SEPM Special Publication, **60**, 3–13.
- HARDIE, L.A. (ed.) 1977. *Sedimentation on the Modern Carbonate Tidal Flats of Northwest Andros Island, Bahamas*. The Johns Hopkins University Studies in Geology No. **22**, The Johns Hopkins University Press, Baltimore, 202 pp.
- HARDIE, L.A. 1986 Tidal flats. *In: HARDIE, L.A. & SHINN, E.A. (eds). Carbonate Depositional Environments, Modern and Ancient*. Colorado School of Mines Quarterly, **81**, 1–74.
- HARDIE, L.A., 1989, Cyclic platform carbonates in the Cambro-Ordovician of the central Appalachians. *In: WALKER, K.R., READ, J.F. & HARDIE, L.A. (eds). Cambro-Ordovician banks and siliciclastic basins of the United States Appalachians*. Field Trip Guidebook T161 for the 28th International Geological Congress. Washington, D.C. American Geophysical Union. 51–78.
- HARDIE, L.A, BOSELLINI, A. & GOLDHAMMER, R.K. 1986. Repeated subaerial exposure of subtidal carbonate platforms, Triassic, northern Italy: evidence for high frequency sea level oscillations on a 104 year scale. *Paleoceanography*, **1**, 447–457.
- HARDIE, L.A., DUNN, P.A. & GOLDHAMMER, R.K., 1991. Field and modelling studies of Cambrian carbonate cycles, Virginia Appalachians — Discussion. *Journal of Sedimentary Petrology*, **61**, 636–646.
- HARPER, D.A.T. (ed.) 1999. *Numerical Palaeobiology—Computer Based Modelling and Analysis of Fossils and their Distributions*. John Wiley & Sons.
- HARPER, D.A.T. 2006. The Ordovician Biodiversification: setting an agenda for marine life. *Palaeogeography, Palaeoclimatology, Palaeoecology*, **232**, 148–166.
- HARRIS, A.G., DUMOULIN, J.A., REPETSKI, J.E. & CARTER, C. 1995 Correlation of Ordovician rocks of northern Alaska, p. 21–26. *In: COPPER, J.D., DROSER, M. & FINNEY, S.C. (eds) Ordovician Odyssey: Short Papers for the Seventh International Symposium on the Ordovician System*. SEPM Pacific Section, Fullerton, California, 77 pp.
- HATCHER, R.D., Jr. & REPETSKI, J.E. 2007. The post-Knox unconformity: Product of global, not regional processes. *Geological Society of America Abstracts with Programs*, **39**, 8.
- HAQ, B.U. & SCHUTTER, S.R. 2008. A chronology of Paleozoic sea-level changes. *Science*, **322**, 64–68.
- HECKEL, P.H. 1972 Possible inorganic origin for stromatactis in calcilitite mounds in the Tully Limestone, Devonian of New York. *Journal of Sedimentary Research*, **42**, 7–18.

- HERRINGSHAW, L.G. & RAINE, R.J. 2007. The earliest turrelpadid: a machaeridian from the Lower Ordovician of the Northwest Highlands. *Scottish Journal of Geology*, **43**, 97–100.
- HIGGINS, A.C. 1967. The age of the Durine Member of the Durness Limestone Formation at Durness. *Scottish Journal of Geology*, **3**, 382–388.
- HIGGINS, A.C. 1971. Conodont faunas from the Croisaphuil and Durine members of the Durness Limestone. *Proceedings of the Geological Society, London*, **121**, 297.
- HIGGINS, A.C. 1985. Conodonts of the Cambrian and Ordovician Systems from the British Isles. In: HIGGINS, A.C. & AUSTIN, R.L. (eds) *A Stratigraphical Index of Conodonts*. British Micropalaeontological Society Series, Ellis Horwood Ltd., Chichester. 43–44.
- HIGGINS, A.K., LESLIE, A.G. & SMITH, M.P. 2001. Neoproterozoic–Lower Palaeozoic stratigraphical relationships in the marginal thin-skinned thrust belt of the East Greenland Caledonides: comparisons with the foreland in Scotland. *Geological Magazine*, **138**, 143–160.
- HINE, A.C. 1977. Lily Bank, Bahamas; history of an active oolite sand shoal. *Journal of Sedimentary Research*, **47**, 1554–1581.
- HINDE, G.J. 1889. On *Archaeocyathus* Billings, and on other genera, allied to or associated with it, from the Cambrian strata of North America, Spain, Sardinia, and Scotland. *Quarterly Journal of the Geological Society*, **45**, 125–148.
- HLADIL, J. 2005. The formation of stromatolite-type fenestral structures during the sedimentation of experimental slurries – a possible clue to a 120-year-old puzzle about stromatolites. *Bulletin of Geosciences*, **80**, 193–211.
- HOFFMAN, P. 1976. Stromatolite morphogenesis in Shark Bay, Western Australia. In: WALTER, M.R. (ed.) *Stromatolites*. Elsevier, Amsterdam, 261–271.
- HOFMANN, H.J. 1969. Attributes of stromatolites. *Geological Survey of Canada, Paper*, **69-39**, 1–59.
- HOFMANN, H.J. 1973. Stromatolites: characteristics and utility *Earth Science Reviews* **9**, 339–373.
- HOLDROYD, J.D. 1994. *The structure and stratigraphy of the Suardal area, Isle of Skye, north-west Scotland: an investigation of Tertiary deformation in the Skye Volcanic Complex*. Unpublished PhD Thesis, University of Manchester.
- HOWE, W.B. 1966. Digitate algal stromatolites structures from the Cambrian and Ordovician of Missouri. *Journal of Paleontology*, **40**, 64–77.
- HUSELBEE, M.Y. 1998. *Late Cambrian to earliest Ordovician (Ibexian) conodont evolution and biogeography of Greenland and northwest Scotland*. Unpublished PhD Thesis, University of Birmingham.
- HUSELBEE, M.Y. & THOMAS, A.T. 1998. *Olenellus* and conodonts from the Durness Group, NW Scotland, and the correlation of the Durness succession. *Scottish Journal of Geology*, **34**, 83–88.

- HUSINEC, A., BASCH, D., ROSE, B. & READ, J.F. 2008. FISCHERPLOTS: An Excel spreadsheet for computing Fischer plots of accommodation change in cyclic carbonate successions in both the time and depth domains. *Computers & Geosciences*, **34**, 269–277.
- IMMENHAUSER, A., HILLGÄRTNER, H., VAN BENTUM, E. 2005. Microbial-foraminiferal episodes in the Early Aptian of the southern Tethyan margin: ecological significance and possible relation to oceanic anoxic event 1a. *Sedimentology*, **52**, 77–99.
- JACOBI, R.D. 1981. Peripheral bulge– a causal mechanism for the Lower/Middle Ordovician unconformity along the western margin of the northern Appalachians. *Earth and Planetary Science Letters*, **56**, 245–251.
- JAMES, N.P. 1984. Shallowing-upwards sequences in carbonates. In: WALKER, R.G. (ed.) *Facies Models*, 2nd edn, pp. 213–228. Geoscience Canada Reprint Series **1**.
- JAMES, N.P. & STEVENS, R.K. 1986. Stratigraphy and correlation of the Cambro-Ordovician Cow Head Group, western Newfoundland. *Geological Survey of Canada Bulletin*, **366**, 1–143.
- JAMES, N.P., STEVENS, R.K., BARNES, C.R. & KNIGHT, I. 1989. Evolution of a lower Paleozoic continental-margin carbonate platform, northern Canadian Appalachians. In: CREVELLO, P.D., WILSON, J.L. & READ, J.F. (eds). *Controls on Carbonate Platform and Basin Development*. Society of Economic Paleontologists and Mineralogists Special Publication, **44**, 123–146.
- JEPPSSON, L. & ANEHUS, R. 1995. A buffered formic acid technique for conodont extraction. *Journal of Paleontology*, **69**, 790–794.
- JEPPSSON, L., ANEHUS, R. & FREDHOLM, D. 1999. The optimal acetate buffered acetic acid technique for extracting phosphatic fossils. *Journal of Paleontology*, **73**, 964–972.
- JI, Z. & BARNES, C.R. 1994. Lower Ordovician conodonts of the St. George Group, Port au Port Peninsula, western Newfoundland, Canada. *Palaeontographica Canadiana*, **11**, 1–149.
- JOHNSTON, D.I. & BARNES, C.R. 2000. Early and Middle Ordovician (Arenig) conodonts from St Pauls Inlet and Martin Point, Cow Head Group, western Newfoundland, Canada 2: systematic paleontology. *Geologica et Palaeontologica*, **34**, 11–87.
- KAH, L.C. & GROTZINGER, J.P. 1992. Early Proterozoic (1.9 Ga) thrombolites of the Rocknest Formation, Northwest Territories. *PALAIOS*, **7**, 305–315.
- KALLOWSKY, E. 1908. Oolith und stromatolith im norddeutschen Buntsandstein. *Zeitschrift der Deutschen geologischen Gesellschaft*. **60**, 68–125.
- KARKLINS, O.L., REPETSKI, J.E. & KETNER, K.B. 1989. Maps showing ages and thermal maturation values of conodonts from the Goshute-Toano Range, Elko County, Nevada. *Miscellaneous Field Studies Map*, **MF-2065**. U.S. Geological Survey.
- KAUFFMAN, E.G. 1973. Cretaceous bivalvia In: HALLAM, A. (ed.) *Atlas of Palaeobiogeography*. Elsevier, New York, 353–383.

- KENDALL, C.G.ST.C. 1984. Evaporites. In: Walker, R.G. (ed.) *Facies Models*, Second Edition, Geoscience Canada Reprint Series, 259–296.
- KENDALL, C.G.ST.C & SKIPWITH, P.A.D'E. 1968. Recent algal mats of a Persian Gulf lagoon. *Journal Sedimentary Petrology*, **38**, 1040–1058.
- KENDALL, C.G.ST.C., & SKIPWITH, P.A.D'E. 1969. Holocene shallow water carbonate and evaporite sediments of Khor Al Bazam, Abu Dhabi, Southwest Persian Gulf. *American Association of Petroleum Geologists Bulletin*, **53**, 841–869.
- KENDALL, C.G.ST.C. & WARREN, J. 1987. A review of the origin and setting of tepees and their associated fabrics. *Sedimentology*, **34**, 1007–1027.
- KENNARD, J. 1981. The Arrinhrunga Formation, Georgina Basin, central Australia. *Bureau of Mineral Resources, Australia. Bulletin*, **211**, 61 pp.
- KENNARD, J.M. 1994. Thrombolites and stromatolites within shale-carbonate cycles, Middle-Late Cambrian Shannon Formation, Amadeus Basin, central Australia. In: BERTRAND-SARFATI, J. & MONTY, C. (eds) *Phanerozoic Stromatolites II*, Kluwer Academic Publishers 443–471.
- KENNARD, J.M. & JAMES, N.P. 1986. Thrombolites and stromatolites: two distinct types of microbial structures. *PALAIOS*, **1**, 492–503.
- KIESSLING, W. 2002. Secular variations in the Phanerozoic reef ecosystem. In: KIESSLING, W., FLÜGEL, E. & GOLONKA, J. (eds) *Phanerozoic Reef Patterns*. SEPM Special Publication, **72**, 625–690.
- KING, D.T.JR. & CHAFETZ, H.S. 1983. Tidal-flat to shallow-shelf deposits in the Cap Mountain Limestone Member of the Riley Formation Upper Cambrian of central Texas. *Journal of Sedimentary Petrology*, **53**, 261–273.
- KINSMAN, D.J.J. 1964. The recent carbonate sediments near Halat el Bahrani, Trucial Coast, Persian Gulf. In: STRAATEN, L. M. J. U. VAN (ed.), *Deltaic and Shallow Marine Deposits*, Developments in Sedimentology, **1**, Elsevier, Amsterdam, pp. 185–192.
- KNIGHT, I. 1977. The Cambro-Ordovician platformal rocks of the Northern Peninsula, Newfoundland. *Newfoundland Department of Mines and Energy, Mineral Development Division Report*, **77-6**, 27.
- KNIGHT, I. 1978. Platformal sediments on the Great Northern Peninsula; stratigraphic studies and geological mapping of the North St. Barbe District. *Report of Activities for 1977, Newfoundland Department of Mines and Energy, Mineral Development Division Report*, **78-1**, 140–150.
- KNIGHT, I. 1991. Geology of Cambro-Ordovician rocks in the Port Saunders (NTS 12I/11), Castors River (NTS 12I/15), St. John Island (NTS 12I/14) and Torrent River (NTS 12I/10) map areas. *Newfoundland Department of Mines and Energy, Geological Survey Branch, Report*, **91-4**, 138 pp.
- KNIGHT, I., AZMY, K., BOYCE, W.D & LAVOIE, D. 2008. Tremadocian carbonate rocks of the lower St. George Group, Port au Port Peninsula, western Newfoundland: lithostratigraphic setting of diagenetic, isotopic and

- geochemistry studies. *Current Research Newfoundland and Labrador Department of Natural Resources, Geological Survey Report*, **08-01**, 115–149.
- KNIGHT, I., AZMY, K., GREENE, M. & LAVOIE, D. 2007. Lithostratigraphic setting of diagenetic, isotopic, and geochemistry studies of Ibexian and Whiterockian carbonates of the St. George and Table Head Groups in western Newfoundland. *Current Research. Newfoundland and Labrador Department of Natural Resources, Geological Survey Report*, **07-1**, 55–84.
- KNIGHT, I. & BOYCE, W.D. 1987. Lower to Middle Cambrian terrigenous-carbonate rocks of Chimney Arm, Canada Bay: lithostratigraphy, preliminary biostratigraphy and regional significance. *Current research, Newfoundland and Labrador Mineral Development Division, Report*, **87-1**, 359–365.
- KNIGHT, I. & JAMES, N.P. 1987. Stratigraphy of the Lower Ordovician St. George Group, western Newfoundland: the interaction between eustasy and tectonics. *Canadian Journal of Earth Science*, **24**, 1927–1951.
- KNIGHT, I., JAMES, N.P. & LANE, T.E. 1991. The Ordovician St. George unconformity, northern Appalachians: the relationship of plate convergence at the St. Lawrence Promontory to the Sauk/Tippecanoe sequence boundary. *Geological Society of America Bulletin*, **103**, 1200–1225.
- KNIGHT, I., JAMES, N.P. & WILLIAMS, H. 1995. Cambrian–Ordovician carbonate sequence (Humber Zone). In: WILLIAMS, H. (ed.). *Geology of Canada, 6, Geology of the Appalachian–Caledonian Orogen in Canada and Greenland*. 67–87. Geological Survey of Canada, Ottawa.
- KNOLL, A.H. & SEMIKHATOV, M.A. 1998. The genesis and time distribution of two distinctive Proterozoic stromatolite microstructures. *PALAIOS*, **13**, 408–422.
- KOERSCHNER, W.F., III & READ, J.F. 1989. Field and modelling studies of Cambrian carbonate cycles, Virginia Appalachians. *Journal of Sedimentary Petrology*, **59**, 654–687.
- KOZAR, M.G., WEBER, L.J. & WALKER, K.R. 1990. Field and modelling studies of Cambrian carbonate cycles, Virginia Appalachians—Discussion. *Journal of Sedimentary Petrology*, **60**, 790–794.
- KRUMBEIN, W. E. 1983. Stromatolites; the challenge of a term in space and time. *Precambrian Research*, **20**, 493–531.
- KRYLOV, I.N. 1976. Approaches to the classification of stromatolites. In: WALTER, M.R. (ed.) *Stromatolites*. Elsevier, Amsterdam, 31–43.
- KRUKOWSKI, S.T. 1988. Sodium metatungstate: a new heavy-mineral separation medium for the extraction of conodonts from insoluble residues. *Journal of Paleontology*, **62**, 314–316.
- LANDING, E. 1994. Precambrian-Cambrian boundary global stratotype ratified and a new perspective of Cambrian time. *Geology*, **22**, 496–498.
- LANDING, E., BARNES, C.R. & STEVENS, R.K. 1986. Tempo of earliest Ordovician graptolite faunal succession: conodont based correlations from the Tremadocian of Quebec. *Canadian Journal of Earth Sciences*, **23**, 1928–1949.

- LANDING, E. & WESTROP, S.R. 2006. Lower Ordovician faunas, stratigraphy, and sea-level history of the middle Beekmantown Group, northeastern New York. *Journal of Paleontology*, **80**, 958–980.
- LANDING, E., PENG, S., BABCOCK, L.E., GEYER, G. & MOCZYDLOWSKA-VIDAL, M. 2007. Global standard names for the lowermost Cambrian series and stage. *Episodes*, **30**, 287–289.
- LAPWORTH, C. 1879. On the tripartite classification of the Lower Paleozoic: *Geological Magazine*, **26**, 1–15.
- LAPWORTH, C. 1883. The secret of the Highlands. *Geological Magazine*. Decade 2: **10**, 120–128.
- LAVOIE, D., BURDEN, E. & LEBEL, D. 2003. Stratigraphic framework for the Cambrian–Ordovician rift and passive margin successions from southern Quebec to western Newfoundland. *Canadian Journal of Earth Sciences*, **40**, 177–205.
- LIEBERMAN, B.S. 2001. Phylogenetic analysis of the Olenellina Walcott, 1890 (Trilobita, Cambrian). *Journal of Paleontology*, **75**, 96–115.
- LOGAN, B.W. 1961. *Cryptozoon* and associate stromatolites from the Recent of Shark Bay, Western Australia. *Journal of Geology*, **69**, 517–533.
- LOGAN, B. W., HOFFMAN, P. & GEBELEIN, C.D. 1974. Algal mats, cryptalgal fabrics, and structures, Hamelin Pool, Western Australia. In: LOGAN, B.W., READ, J.F., HAGAN, G.M. HOFFMAN, P., BROWN, R.G., WOODS, P.J. & GEBELEIN, C.D. (eds) *Evolution and Diagenesis of Quaternary Carbonate Sequences, Shark Bay, Western Australia*. AAPG Memoir, **22**, Tulsa, 140–194.
- LOGAN, B.W., REZAK, R. & GINSBURG, R.N. 1964. Classification and environmental significance of algal stromatolites. *Journal of Geology*, **72**, 68–83.
- LOGAN, B.S. & SEMENIUK, V. 1976. Dynamic metamorphism; Processes and products in Devonian carbonate rocks, Canning Basin, Western Australia. *Geological Society of Australia Special Publication*, **6**. 138 pp.
- LOREAU, J.P. & PURSER, B.H. 1973. Distribution and ultrastructure of Holocene ooids in the Persian Gulf. In: PURSER, B.H. (ed.) *The Persian Gulf*. Springer-Verlag, New York, pp. 279–328.
- LOUCKS, R.G. & ANDERSON, J.L. 1980. Depositional facies and porosity development in Lower Ordovician Ellenburger dolomite, Puckett Field, Pecos County, Texas. In: HALLEY, R.B. & LOUCKS, R.G. (eds). *Carbonate reservoir rocks*. Society for Sedimentary Geology Core Workshop, **1**, 1–31.
- LUCIA, F.J. 1961. Dedolomitization in the Tansill (Permian) Formation: *Geological Society of America Bulletin*, **72**, 1107–1110.
- MACCULLOCH, J. 1814. Remarks on several parts of Scotland which exhibit quartz rock, and on the nature and connections of this rock in general. *Transactions of the Geological Society of London*, **2**, 450–487.
- MAC NIOCAILL, C., VAN DER PLUIJM, B.A. & VAN DER VOO, R. 1997. Ordovician paleogeography and the evolution of the Iapetus Ocean. *Geology*, **25**, 159–162.
- MAIKLEM, W.R., BEBOUT, D.G. & GLAISTER, R.P. 1969. Classification of anhydrite; a practical approach. *Bulletin of Canadian Petroleum Geology*, **17**, 194–233.

- MARSHALL, J.F. & DAVIES, P.J. 1975. High-magnesium calcite ooids from the Great Barrier Reef. *Journal of Sedimentary Petrology*, **45**, 285–291.
- MATTHEWS, S.C. & COWIE, J.W. 1979. Early Cambrian transgression. *Journal of the Geological Society, London*, **136**, 133–135.
- MATTI, J.C. & MCKEE, E.D. 1976. Stable eustasy, regional subsidence and a carbonate factory: self-regulating model for onlap-offlap cycles in shallow water carbonate sequences. *Geological Society of America Abstracts with Programs*, **8**, 1000–1001.
- MCINNISH, M.B., BARTLEY, J.K. & KAH, L. 2002. Environmental change recorded by stromatolites morphology: quantitative approaches. *Abstracts with Programmes—Geological Society of America*, **34**, 14–15.
- MCKERROW, W.S., MAC NIOCAILL, C. & DEWEY, J.F. 2000. The Caledonian Orogeny redefined. *Journal of the Geological Society, London*, **157**, 1149–1154.
- MCKIE, T. 1990a. Tidal and storm influenced sedimentation from a Cambrian transgressive passive margin sequence. *Journal of the Geological Society, London*, **147**, 785–794.
- MCKIE, T. 1990b. A model for marine shelf storm deposition in the Lower Cambrian fucoid beds of Northwest Scotland. *Geological Magazine*, **127**, 45–53.
- MCKIE, T. 1990c. Tidal sandbank evolution in the Lower Cambrian Salterella Grit. *Scottish Journal of Geology*, **26**, 77–88.
- MCKIE, T. 1993. Relative sea-level changes and the development of a Cambrian transgression. *Geological Magazine*, **130**, 245–256.
- MCKIE, T. & DONOVAN, S.K. 1992. Lower Cambrian echinoderm ossicles from the Fucoid Beds, northwest Scotland. *Scottish Journal of Geology*, **28**, 49–53.
- MCWHAIE, J.R.H. 1953. The Carboniferous breccias of Billefjorden, Vestspitsbergen *Geological Magazine*, **90**, 287–298.
- MIDDLETON, G.V. 1961. Evaporite solution breccias from the Mississippian of southwest Montana. *Journal of Sedimentary Petrology*, **31**, 189–195.
- MILLER, K.G., KOMINZ, M.A., BROWNING, J.V., WRIGHT, J.D., MOUNTAIN, G.S., KATZ, M.E., SUGARMAN, P.J., CRAMER, B.S., CHRISTIE-BLICK, N. & PEKAR, S.F. 2005. The Phanerozoic Record of Global Sea-Level Change. *Science*, **310**, 1293–1298.
- MILLIKEN, K. 1979. The silicified evaporite syndrome – two aspects of silicification history of former evaporite nodules from southern Kentucky and northern Tennessee. *Journal of Sedimentary Petrology*, **49**, 245–256.
- MITCHUM, R.M. JR. 1977. Seismic stratigraphy and global changes of sea level, Part 11 Glossary of terms used in seismic stratigraphy. In: CLAYTON, C.E. (ed.) *Seismic Stratigraphy—Application to Hydrocarbon Exploration*, AAPG Memoir, **26**, 205–212.

- MOLYNEUX, S.G. 2006. A palynological investigation of samples from the Lower Cambrian, NW Highlands, Scotland. *British Geological Survey Internal Report*, **IR/06/134**. 22 pp.
- MONTY, C.L.V. 1976. The origin and development of cryptalgal fabrics. *In*: WALTER, M.R. (ed.), *Stromatolites*, Elsevier, Amsterdam, 193–249.
- MONTY, C.L.V. 1977. Evolving concepts on the nature and the geological significance of stromatolites: a review. *In*: Flügel, E. (ed.) *Fossil algae, Recent Results and Developments*. Springer, Berlin 15–35.
- MONTY, C.L.V., BOSENCE, D., BRIDGES, P. & PRATT, B. 1995. (eds) *Carbonate mud mounds, their origin and evolution*. Special Publication of the International Association of Sedimentologists **23**, pp 537.
- MOORE, L.S., & BURNE, R.V. 1994. The modern thrombolites of Lake Clifton, Western Australia, pp. 3–19. *In*: BERTRAND-SARFATI, J. & MONTY, C. (eds) *Phanerozoic Stromatolites II*. Kluwer Academic Publishers, Dordrecht.
- MOORE, L., KNOTT, B. & STANLEY, M. 1984. The stromatolites of Lake Clifton, Western Australia. *Search*, **14**, 309–314.
- MONTAÑEZ, I.P. & OSLEGER, D.A. 1993. Parasequence stacking patterns, third-order accommodation events and sequence stratigraphy of Middle to Upper Cambrian platform carbonates, Bonanza King Formation, southern Great Basin, Chapter 12. *In*: LOUCKS, R.G. & SARG, F.R., (eds). *Carbonate Sequence Stratigraphy: Recent Developments and Applications*. AAPG Memoir, **57**, 305–326.
- MORROW, D.W. 1978. Dolomitization of lower Paleozoic burrow-fillings. *Journal of Sedimentary Research*, **48**, 295–305.
- MORROW D.W. 1982 Dolomites - Chemistry and precipitation. *Geoscience Canada*, **9**, 5–13.
- MOSHIER, S.O. 1986. Carbonate platform sedimentology, Upper Cambrian Richland Formation, Lebanon Valley, Pennsylvania. *Journal of Sedimentary Petrology*, **56**, 204–216.
- MOSSOP, G.D. 1979. The evaporites of the Ordovician Baumann Fiord Formation, Ellesmere Island, Arctic Canada. *Geological Survey of Canada Bulletin*, **298**, 52 pp.
- MOUNT, J. 1985. Mixed siliciclastic and carbonate sediments: a proposed first-order textural and compositional classification. *Sedimentology*, **32**, 435–442.
- MOUNT, J.F. & KIDDER, D. 1993. Combined flow origin of edgewise intraclast conglomerates: Sellick Hill Formation (Lower Cambrian), South Australia. *Sedimentology*, **40**, 315–329.
- MOUNT, J.F. & ROWLAND, S.M. 1981. Grand Cycle A (Lower Cambrian) of the southern Great Basin: A product of differential rates of relative sea-level rise. *In*: Taylor, M.E. (ed.). *Short Papers for the Second International Symposium on the Cambrian System*. U.S. Geological Survey, Open-File Report **81-743**, 143–146.
- MUSSMAN, W.J. & READ, J.F. 1986. Sedimentology and development of a passive- to convergent-margin unconformity: Middle Ordovician Knox unconformity, Virginia Appalachians. *Geological Society of America Bulletin*, **97**, 282–295.

- NEUMANN, A.C., GEBELEIN, C.D. & SCOFFIN, T.P. 1970. The composition, structure and erodability of subtidal mats, Abaco, Bahamas. *Journal of Sedimentary Research*, **40**, 274–297.
- NICHOLAS, C.J. 1994. New stratigraphical constraints on the Durness Group of NW Scotland. *Scottish Journal of Geology*, **30**, 73–85.
- OGG, G. 2008. International Stratigraphic Chart. International Commission on Stratigraphy. (www.stratigraphy.org).
- OLDROYD, D.R. 1990. *The Highlands Controversy: Constructing Geological Knowledge through Fieldwork in Nineteenth-Century Britain*. University of Chicago Press. 448 pp.
- OLIVER, G.J.H. 1998. Reconstruction of the Grampian orogeny in Britain. *Acta Universitatis Carolinae-Geologica*, **42**, p. 312–313.
- OSLEGER, D. 1991. Subtidal carbonate cycles: Implications for allocyclic vs. autocyclic controls. *Geology*, **19**, 917–920.
- OSLEGER, D. & READ, J.F. 1991. Relation of eustasy to stacking patterns of meter-scale carbonate cycles, Late Cambrian, USA. *Journal of Sedimentary Petrology*, **61**, 1225–1252.
- OSLEGER, D. & READ, J.F. 1993. Comparative analysis of methods used to define eustatic variations in outcrop; Late Cambrian. *American Journal of Science*, **293**, 157–216.
- PALMER, A.R. 1981. Subdivision of the Sauk sequence. *U.S. Geological Survey Open-file Report*, **81-743**, 160–162.
- PALMER A.R., & HALLEY, R.B. 1979. Physical stratigraphy and trilobite biostratigraphy of the Carrara Formation (Lower and Middle Cambrian) in the southern Great Basin. *U.S. Geological Survey Professional Paper*, **1047**, 1–131.
- PALMER, A.R. & JAMES, N.P. 1980. The Hawke Bay event: a circum-Iapetus regression near the Lower–Middle Cambrian boundary. In: WONES, D.R. (ed.). *The Caledonides in the U.S.A.* Virginia Polytechnic Institute and State University Memoir, **2**, 15–18.
- PALMER, T.J., MCKERROW, W.S. & COWIE, J.W. 1980. Sedimentological evidence for a stratigraphical break in the Durness Group. *Nature*, **287**, 720–722.
- PAPINEAU, D., WALKER, J.J., MOJZSIS, S.J. & PACE, N.R. 2005. Composition and structure of microbial communities from stromatolites of Hamelin Pool in Shark Bay, Western Australia. *Applied and Environmental Microbiology*, **71**, 4822–4832.
- PARK, R.G., STEWART, A.D. & WRIGHT, D.T. 2002. The Hebridean terrane. In: TREWIN, N.H. (ed.). *The Geology of Scotland*. Geological Society, London, 45–80.
- PARK, R.K. 1976. Note on the significance of lamination in stromatolites. *Sedimentology*, **23**, 379–393.
- PARK, R.K. 1977. The preservation potential of some recent stromatolites. *Sedimentology*, **24**, 485–506.
- PATTERSON, R.J. & KINSMAN, D.J.J. 1981. Hydrologic framework of a sabkha along Arabian Gulf. *American Association of Petroleum Geologists Bulletin*, **65**, 1457–1475.

- PEACH, B.N. 1894. Additions to the fauna of the *Olenellus* Zone of the north-west Highlands. *Quarterly Journal of the Geological Society*, **50**, 661–676.
- PEACH, B.N. 1913. The relation between the Cambrian faunas of Scotland and North America. *Report of the British Association for the Advancement of Science*. For 1912, Dundee, Section C. 448–459.
- PEACH, B.N. & HORNE, J. 1884. Report on the geology of the north-west of Sutherland. *Nature*, **31**, 31–35.
- PEACH, B.N. & HORNE, J. 1892. The *Olenellus* Zone in the North-west Highlands of Scotland. *Quarterly Journal of the Geological Society of London*, **48**, 227–242.
- PEACH, B.N. & HORNE, J. 1930. *Chapters on the Geology of Scotland*. Oxford University Press, London. 234pp.
- PEACH, B.N., HORNE, J., GUNN, W., CLOUGH, C.T., HINXMAN, L.W. & TEALL, J.J.H. 1907. *The geological structure of the north-west Highlands of Scotland*. Memoirs of the Geological Survey of Great Britain. 668 pp.
- PEACH, C.W. 1855. Notice of the discovery of fossils in the limestone of Durness, in the county of Sutherland. *Edinburgh New Philosophical Journal*, **2**, 197–198.
- PENG, S., BABCOCK, L.E., ROBINSON, R.A., LIN, H., REES, M.N. & SALTZMAN, M.R. 2004. Global Standard Stratotype-section and Point (GSSP) of the Furongian Series and Pabian Stage (Cambrian). *Lethaia*, **37**, 365–379.
- PHEMISTER, J. 1948. Scotland: the Northern Highlands. Geological Survey and Museum, HMSO, Edinburgh. 2nd edition, 94 pp.
- PITMAN, W.C. 1978. The relationship between eustasy and stratigraphic sequences of passive margins. *Geological Society of America Bulletin*, **89**, 1389–1403.
- PLANAVSKY, N. & GINSBURG, R.N. 2009. Taphonomy of modern Bahamian microbialites. *PALAIOS*, **24**, 5–17.
- POHLER, S.M.L. 1994. Conodont biofacies of Lower to lower Middle Ordovician megaconglomerates, Cow Head Group, western Newfoundland. *Geological Survey of Canada, Bulletin* **459**, 1–71.
- POSAMENTIER, H.W. & JAMES, D.P. 1993. An overview of sequence-stratigraphic concepts: uses and abuses. In: POSAMENTIER, H.W., SUMMERHAYES, C.P., HAQ, B.U. & ALLEN, G.P. (eds). *Sequence stratigraphy and facies associations*. Blackwell, Oxford, p. 3-18.
- POULSEN, C. 1951. The position of East Greenland Cambro-Ordovician in the palaeogeography of the North Atlantic region. *Meddelelser fra Dansk Geologisk Forening*, **12**, 161–162.
- PRATT, B.R. 1982. Stromatolite decline—a reconsideration. *Geology*, **10**, 512–515.
- PRATT, B.R. & JAMES, N.P. 1982. Cryptalgal-metazoan bioherms of Early Ordovician age in the St. George Group, western Newfoundland. *Sedimentology*, **29**, 543–569.
- PRATT, B.R. & JAMES, N.P. 1986. The St. George Group (Lower Ordovician) of western Newfoundland: tidal flat island model for carbonate sedimentation in shallow epeiric seas. *Sedimentology*, **33**, 313–343.

- PRAVE, R., KESSLER, L.G., II, MALO, M., BLOECHL, W.V. & RIVA, J. 2000. Ordovician arc collision and foredeep evolution in the Gaspé Peninsula, Québec: the Taconic Orogeny in Canada and its bearing on the Grampian Orogeny in Scotland. *Journal of the Geological Society*, **157**, 393–400.
- PREISS, W.V. 1976. Basic field and laboratory methods for the study of stromatolites. In: WALTER, M.R. (ed.) *Stromatolites*. Elsevier, Amsterdam. 5–13.
- PURSER, B.H. (ed.) 1973. *The Persian Gulf*. Springer-Verlag, Berlin, 471 pp.
- QUINLAN, G.M. & BEAUMONT, C. 1984. Appalachian thrusting, lithospheric flexure, and the Paleozoic stratigraphy of the Eastern Interior of North America. *Canadian Journal of Earth Sciences*, **21**, 973–996.
- RADKE, B.M., & MATHIS, R.L. 1980. On the formation and occurrence of saddle dolomite. *Journal of Sedimentary Petrology*, **50**, 1149–1168.
- RANKEY, E.C., WALKER, K.R. & SRINIVASAN, K. 1994. Gradual establishment of Iapetan "passive" margin sedimentation: stratigraphic consequences of Cambrian episodic tectonism and eustasy, southern Appalachians. *Journal of Sedimentary Research*, **B64**, 298–310.
- RAO, C.P. 1990. Marine to mixing zone dolomitization in peritidal carbonates: the Gordon Group (Ordovician), Mole Creek, Tasmania, Australia. *Carbonates and Evaporites*, **5**, 153–178.
- RASMUSSEN, J.A. 1998. A reinterpretation of the conodont Atlantic Realm in the late Early Ordovician (early Llanvirn). *Palaeontologica Polonica*, **58**, 67–77.
- READ, J.F. 1989. Controls on evolution of Cambrian–Ordovician passive margin, U.S. Appalachians. In: CREVELLO, P.D., WILSON, J.L. & READ, J.F. (eds). *Controls on Carbonate Platform and Basin Development*. Society of Economic Paleontologists and Mineralogists Special Publication, **44**, 147–165.
- READ, J.F. & GOLDHAMMER, R.K. 1988. Use of Fischer plots to define third-order sea-level curves in peritidal carbonates, Ordovician, Appalachians. *Geology*, **16**, 895–899.
- READ, J.F., GROTZINGER, J.P., BOVA, J.A. & KOERSCHNER, W.F. 1986. Models for generation of carbonate cycles. *Geology*, **14**, 107–110.
- READ, J.F., KOERSCHNER, W.F., OSLEGER, D.A., BOLLINGER, G.A. & CORUH, C. 1991. Field and modelling studies of Cambrian carbonate cycles, Virginia Appalachians — Reply. *Journal of Sedimentary Petrology*, **61**, 636–646.
- REITNER, J. & NEUWEILER, F. 1995. Mud mounds: a polygenetic spectrum of fine-grained carbonate buildups. *Facies*, **32**, 1–70.
- REJEBIAN, V.A., HARRIS, A.G. & HUEBNER, J.S. 1987. Conodont color and textural alteration: an index to regional metamorphism and hydrothermal alteration. *Geological Society of America Bulletin*, **99**, 471–479.
- REPETSKI, J.E. 1982. Conodonts from El Paso group (Lower Ordovician) of westernmost Texas and southern New Mexico. *New Mexico Bureau of Mines and Mineral Resources Memoir*, **40**, 121pp.

- REPETSKI, J. E. 1992. Knox Group and basal Stones River Group conodonts from near Graysville, Catoosa County, Georgia. In: CHOWNS, T.M., AND O'CONNOR, B.J. (eds) *Cambro-Ordovician strata in northwest Georgia and southeast Tennessee; the Knox Group and the Sequatchie Formation*. 39–46. Georgia Geological Society. Field trip, Dalton, Ga.
- REPETSKI, J. E. & ETHINGTON, R.L. 1983. *Rossodus manitouensis* (Conodonta), a new Early Ordovician index fossil. *Journal of Paleontology*, **57**, 289–301.
- RIDING, R. 1991. Classification of microbial carbonates In RIDING, R. (ed.) *Calcareous Algae and Stromatolites*. Springer-Verlag, Berlin 21–51.
- RIDING, R. 2000. Microbial carbonates: the geological record of calcified bacterial–algal mats and biofilms. *Sedimentology*, **47** (Suppl. 1), 179–214.
- RIDING, R. 2002. Structure and composition of organic reefs and carbonate mud mounds: concepts and categories. *Earth Science Reviews*, **58**, 163–231.
- RIDING, R. 2005. Phanerozoic reefal microbial carbonate abundance: comparisons with metazoan diversity, mass extinction events, and seawater saturation state. *Revista Española de Micropaleontología*, **37**, 23–39.
- RIDING, R. 2006. Microbial carbonate abundance compared with fluctuations in metazoan diversity over geological time. *Sedimentary Geology*, **185**, 229–238.
- ROBERTSON, T., SIMPSON, J.B. & ANDERSON, J.G.C. 1949. The Limestones of Scotland. *Memoirs of the Geological Survey, Special Reports on the Mineral Resources of Great Britain*, **35**, 221 pp.
- ROHR, D.M., BOYCE, W.D., KNIGHT, I. & MEASURES, E.A. 2008. The rostroconch mollusc *Euchasma* Billings, 1865 from the Lower Ordovician Catoche Formation, western Newfoundland. *Newfoundland and Labrador Department of Natural Resources Geological Survey, Report*, **08-1**, 79–91.
- ROSS, R.J., JR., ETHINGTON, R.L. 1991. Stratotype of Ordovician Whiterock Series, with an appendix on graptolite correlation of the topmost Ibexian by C.E Mitchell. *PALAIOS*, **6**, 156–173.
- ROSS, R.J., JR. & ETHINGTON, R.L. 1992. North American Whiterock Series suited for global correlation. In: Webby, B.D. & Laurie, J.R. *Global perspectives on Ordovician Geology*. Balkema, Rotterdam. 135–152.
- ROSS, R.J., JAANUSSON, V. & FRIEDMAN, I. 1975. Lithology and origin. of Middle Ordovician calcareous mud mound at Meiklejohn. Peak, southern Nevada. *US Geological Survey, Professional Paper*, **871**, 45 pp.
- ROWLAND, S.M. & SHAPIRO, R.S. 2002. Reef patterns and environmental influences in the Cambrian and earliest Ordovician. In: KIESSLING, W., FLÜGEL, E. & GOLONKA, J. (eds) *Phanerozoic Reef Patterns*. SEPM Special Publication, **72**, 95–128.
- ROWLEY, D.B. & KIDD, W.S.F. 1981. Stratigraphic relationships and detrital composition of the Medial Ordovician flysch of western New England: Implications for the tectonic evolution of the Taconic orogeny. *Journal of Geology*, **89**, 199–218.

- RUNKEL, A.C., MCKAY, R.M. & PALMER, A.R. 1998. Origin of a clastic cratonic sheet sandstone: Stratigraphy across the Sauk II-Sauk III boundary in the Upper Mississippi Valley. *Geological Society of America Bulletin*, **110**, 188–210.
- RUSHTON, A.W.A. 2000. NW Scotland: Hebridean Terrane. In: FORTEY, R.A., HARPER, D.A.T., INGHAM, J.K., OWEN, A.W., PARKES, M.A., RUSHTON, A.W.A. & WOODCOCK, N.H. *A Revised Correlation of Ordovician rocks in the British Isles*. The Geological Society, Special Report. **24**, 50–51.
- SADLER, P.M., 1994. The expected duration of upward-shallowing peritidal carbonate cycles and their terminal hiatuses. *Geological Society of America Bulletin*, **106**, 791–802.
- SADLER, P.M., OSLEGER, D.A. & MONTAÑEZ, I.P. 1993. On the labelling, length and objective basis of Fischer plots. *Journal of Sedimentary Petrology*, **63**, 360–368.
- SALAD HERSI, O., LAVOIE, D. & NOWLAN, G.S. 2003. Sedimentologic and biostratigraphic reappraisal of the Beekmantown Group of the Montreal area, southwestern Quebec: implications for the depositional evolution of the Lower–Middle Ordovician Laurentian margin of eastern Canada. *Canadian Journal of Earth Sciences*, **40**, 149–176.
- SALTER, J.W. 1859. Fossils of the Durness Limestone. *Quarterly Journal of the Geological Society*, **15**, 374–381.
- SALTZMAN, M.R., COWAN, C.A. RUNKEL, A.C., RUNNEGAR, B., STEWART, M.C. & PALMER, A.R. 2004. The Late Cambrian Spice ($\delta^{13}\text{C}$) Event and the Sauk II-Sauk III Regression: New Evidence from Laurentian Basins in Utah, Iowa, and Newfoundland. *Journal of Sedimentary Research*, **74**, 366–377.
- SALTZMAN, M.R., RUNNEGAR, B. & LOHMANN, K.C. 1998. Carbon isotope stratigraphy of Upper Cambrian (Steptoean Stage) sequences of the eastern Great Basin; record of a global oceanographic event. *Geological Society of America Bulletin*, **110**, 285–297.
- SARG, J.F. 1988. Carbonate sequence stratigraphy. In: WILGUS, C.K., HASTINGS, B.S. KENDALL, C.G., POSAMENTIER, H.W., ROSS, C.A. & VAN WAGONER, J.C. (eds.). *Sea-Level Changes: An Integrated Approach*. Special Publication Society of Economic Paleontologists and Mineralogists, **42**, 155–181.
- SCHLAGER, W. 2004. Fractal nature of stratigraphic sequences. *Geology*, **32**, 185–188.
- SCHLAGER, W. 2005. *Carbonate Sedimentology and Sequence Stratigraphy*. *SEPM Concepts in Sedimentology and Paleontology Series*, 8, 200pp.
- SCHOPF, J.W. 1992. Patterns of Proterozoic microfossil diversity: an initial, tentative, analysis. In: SCHOPF, J.W. & KLEIN, C. (eds.), *The Proterozoic Biosphere; a Multidisciplinary Study*. Cambridge University Press, Cambridge, 529–552.
- SCHUBERT, J.K. & BOTTJER, D.J. 1992. Early Triassic stromatolites as post-mass extinction disaster forms. *Geology*, **20**, 83–886.
- SCHWARZACHER, W. 1961. Petrology and structure of some lower Carboniferous reefs in northwestern Ireland. *AAPG Bulletin*, **45**, 1481–1503.

- SELLWOOD, B., 1986. Shallow-marine carbonate environments. *In*: READING, H.A. (ed.). *Sedimentary environments and facies*. Blackwell, Oxford 482 pp.
- SEMIKHATOV, M.A., GEBELEIN, C.D., CLOUD, P., AWRAMIK, S.M. & BENMORE, W.C. 1979. Stromatolite morphogenesis—progress and problems. *Canadian Journal of Earth Sciences*, **16**, 992–1015.
- SEPKOSKI, J.J.JR. 1982. Flat-pebble conglomerates, storm deposits and the Cambrian bottom fauna. *In*: EINSELE, G. & SEILACHER, A. (eds) *Cyclic and Event Stratification*. Springer-Verlag, Berlin. pp. 371–385.
- SEPKOSKI, J.J.JR. 1992. Proterozoic–Early Cambrian diversification of metazoans and metaphytes. *In*: SCHOPF, J.W. & KLEIN, C. (eds), *The Proterozoic Biosphere; a Multidisciplinary Study*. Cambridge University Press, Cambridge, 553–561.
- SEPKOSKI, J.J.JR. 1997. Biodiversity; past, present, and future. *Journal of Paleontology*, **71**, 533–539.
- SHANMUGAM, G. & LASH, G.G. 1982. Analogous tectonic evolution of the Ordovician foredeep, southern and central Appalachians. *Geology*, **10**, 562–566.
- SHAPIRO, R.S. 2000. A comment on the systematic confusion of thrombolites. *PALAIOS*, **15**, 166–169.
- SHAPIRO, R.S. & AWRAMIK, S.M. 2000. Microbialite morphostratigraphy as a tool for correlating Late Cambrian–Early Ordovician sequences. *The Journal of Geology*, **108**, 171–180.
- SHAPIRO, R.S. & AWRAMIK, S.M. 2006. *Favomaceria cooperi* new group and form: a widely dispersed, time restricted thrombolites. *Journal of Paleontology*, **80**, 411–422.
- SHEEHAN, P.M. AND HARRIS, M.T. 2004. Microbialite resurgence after the Late Ordovician extinction. *Nature*, **430**, 75–78.
- SHINN, E.A. 1968. Practical significance of birdseye structures in carbonate rocks. *Journal of Sedimentary Research*, **38**, 215–223.
- SHINN, E.A. 1983. Tidal flat environment. *In*: SCHOLLE, P.A., BEBOUT, D.G. & MOORE, C.H. (eds) *Carbonate Depositional Environments*. AAPG Memoir, **33**. pp. 171–210.
- SHINN, E.A. 1986. Modern carbonate tidal flats: their diagnostic features. *In*: HARDIE, L.A. & SHINN, E.A. (eds) *Carbonate depositional environments. Modern and ancient. Part 3: Tidal flats*. Colorado School of Mines Quarterly, **81/1**, 17–36.
- SIAL, A.N., PERALTA, S., FERREIRA, V.P., TOSELLI, A.J., ACEÑOLAZA, F.G., PARADA, M.A., GAUCHER, C., ALONSO, R.N. & PIMENTEL, M.M. 2008. Cambrian carbonate sequences of the Argentine Precordillera and the Steptoean C-Isotope positive excursion (SPICE). *Gondwana Research*, **13**, 437–452.
- SIEDLECKA, A. 1972. Length-slow chalcedony and relicts of sulphates—evidence of evaporitic environments in the Upper Carboniferous and Permian beds of Bear Island, Svalbard. *Journal of Sedimentary Petrology*, **42**, 812–816.

- SIEDLECKA, A. 1976. Silicified Precambrian evaporite nodules from northern Norway: a preliminary report. *Sedimentary Geology*, **16**, 161–175.
- SLOAN, L.C. & BARRON, E.J. 1990. Equable climates during Earth history. *Geology*, **18**, 489–492.
- SLOSS, L.L. 1963. Sequences in the cratonic interior of North America. *Geological Society of America Bulletin*, **74**, 93–114.
- SLOSS, L.L. 1964. Tectonic cycles of the North American Craton. *Kansas Geological Survey Bulletin*, **169**, 449–460.
- SLOSS, L.L. 1984. Comparative anatomy of cratonic unconformities. In: MCNEE, J.S. (ed.). *Interregional Unconformities and Hydrocarbon Accumulation. American Association of Petroleum Geologists Memoir*, **36**, 7–36.
- SMITH, M.P. 1991. Early Ordovician conodonts of East and North Greenland. *Meddelelser om Grønland Geoscience*, **26**, 81 pp.
- SMITH, M.P. & RASMUSSEN, J.A. 2008. Cambrian–Silurian development of the Laurentian margin of the Iapetus Ocean in Greenland and related areas. In: HIGGINS, A.K., GILOTTI, J.A. & SMITH, M.P. (eds). *The Greenland Caledonides: evolution of the northeast margin of Laurentia*. Geological Society of America Memoir, **202**, 137–167.
- SOPER, N.J. 1994. Was Scotland a Vendian RRR junction? *Journal of the Geological Society*, **151**, 579.
- SOPER, N.J., RYAN, P.D & DEWEY, J.F. 1999. Age of the Grampian orogeny in Scotland and Ireland. *Journal of the Geological Society*, **156**, 1231–1236.
- SRINIVASAN, K. & WALKER, K.R. 1993. Sequence stratigraphy of an intrashelf basin carbonate ramp to rimmed platform transition; Maryville Limestone (Middle Cambrian), Southern Appalachians. *Geological Society of America Bulletin*, **105**, 883–896.
- STANTON, R.J. 1966. The solution brecciation process. *Geological Society of America Bulletin*, **77**, 843–847.
- STEINHOFF, I. & STROHMENGER, C. 1996. Zechstein 2 Carbonate platform subfacies and grain-type distribution (Upper Permian, Northwest Germany). *Facies*, **35**, 105–132.
- STEWART, J.H., POOLE, F.G. HARRIS, A.G., REPETSKI, J.E., WARDLAW, B.R., MAMET, B.L., & MORALES-RAMIREZ, J.M. 1999. Neoproterozoic (?) to Pennsylvanian inner-shelf miogeoclinal strata in Sierra Agua Verde, Sonora, Mexico. *Revista Mexicana de Ciencias Geológicas*, **16**, 35–62.
- STITT, J.H. 1977. Late Cambrian and earliest Ordovician trilobites, Wichita Mountains area, Oklahoma. *Oklahoma Geological Survey Bulletin*, **124**, 1–79.
- STOUGE, S.S. 1982. Preliminary conodont biostratigraphy and correlation of Lower to Middle Ordovician carbonates of the St George Group, Great Northern Peninsula, Newfoundland. *Government of Newfoundland and Labrador, Department of Mines and Energy, Report*, **82-3**, 59 pp.
- STOUGE, S.S. & BAGNOLI, G. 1988. Early Ordovician conodonts from Cow Head Peninsula, western Newfoundland. *Paleontographica Italica*, **75**, 89–179.

- STOUGE, S.S. & BOYCE, W.D. 1983. Fossils of northwestern Newfoundland and southeastern Labrador: conodonts and trilobites. *Government of Newfoundland and Labrador, Department of Mines and Energy, Report*, **83-3**, 55 pp.
- STOUGE, S.S. & BOYCE, W.D. 1997. Trilobite and conodonts biostratigraphy of the St. George Group, Eddies Cove West area, western Newfoundland. *Current Research (1997) Newfoundland Department of Mines and Energy, Geological Survey, Report*, **97-1**, 183–200.
- STRASSER, A. 1991. Lagoonal-peritidal sequences in carbonate environments: autocyclic and allocyclic processes. In: EINSELE, G., RICKEN, W. & SEILACHER, A. (eds). *Cycles and Events in Stratigraphy*, Springer-Verlag, Berlin, Heidelberg, New York. 709–721.
- SWEET, W.C. & TOLBERT, C.M. 1997. An Ibexian (Lower Ordovician) reference section in the southern Egan Range, Nevada, for a conodont-based chronology. *U.S. Geological Survey Professional Paper*, **1579-B**, 53–84.
- SWEET, W.C., ETHINGTON, R.L. & HARRIS, A.G. 2005. A conodont-based standard reference section in central Nevada for the lower Middle Ordovician Whiterockian Series. *Bulletins of American Palaeontology*, **369**, 35–52.
- SWEET, W.C., TURCO, C.A., WARNER, E. & WILKIE, L.C. 1959. The American Upper Ordovician Standard. I. Eden Conodonts from the Cincinnati region of Ohio and Kentucky. *Journal of Paleontology*, **33**, 357–370.
- SWENNEN, R., VIAENE, W. & CORNELISSEN, C. 1990. Petrography and geochemistry of the Belle Roche breccia (lower Viséan, Belgium): evidence for brecciation by evaporite dissolution. *Sedimentology*, **37**, 859–878.
- SWETT, K. 1965. Dolomitization, silicification and calcitization patterns in Cambro-Ordovician oolites from northwest Scotland. *Journal of Sedimentary Petrology*, **35**, 928–938.
- SWETT, K. 1969. Interpretation of depositional and diagenetic history of Cambrian-Ordovician succession of northwest Scotland. In: KAY, M. (ed.), *North Atlantic – Geology and continental drift*, Memoir, American Association of Petroleum Geologists, **12**, 630–646.
- SWETT, K. 1981. Cambro-Ordovician strata in Ny Friesland, Spitsbergen and their palaeotectonic significance. *Geological Magazine*, **118**, 225–250.
- SWETT, K., KLEIN, G.DEV. & SMIT, D.E. 1971. A Cambrian tidal sand body. The Eriboll Sandstone of northwest Scotland: an ancient–recent analog. *Journal of Geology*, **79**, 400–415.
- SWETT, K. & SMIT, D.E. 1972a. Paleogeography and depositional environments of the Cambro-Ordovician shallow-marine facies of the North Atlantic *Geological Society of America Bulletin*, **83**, 3223–3248.
- SWETT, K. & SMIT, D.E. 1972b. Cambro-Ordovician shelf sedimentation of western Newfoundland, northwest Scotland and central East Greenland. 24th IGC, section 6, 33–41.
- TAYLOR, A.M., GOLDRING, R. & GOWLAND, S. 2003. Analysis and application of ichnofabric. *Earth Science Reviews*, **60**, 227–259.
- TEBBUTT, G.E., CONLEY, C.D. & BOYD, D.W. 1965. Lithogenesis of a distinctive carbonate rock fabric. *Rocky Mountain Geology*, **4**, 1–13.

- TEXTORIS, D.A. & CAROZZI, A.V. 1964. Petrography and evolution of Niagaran (Silurian) reefs, Indiana. *AAPG Bulletin*, **48**, 397–426.
- THOMAS, W.A. 1977. Evolution of Appalachian-Ouachita salients and recesses from reentrants and promontories in the continental margin. *American Journal of Science*, **277**, 1233–1278.
- THURGATE, M.E. 1996. The stromatolites of the Cenote Lakes of the lower south east of South Australia. *Helictite*, **34**, 17–25.
- TSIEN, H.H. 1985. Origin of Stromatactis - a replacement of colonial microbial accretions. In: TOOMEY, D.F. & NITECKI, M.H. (eds) *Paleoalgology: contemporary research and applications*, Springer Verlag, 274–289.
- TORSVIK, T.H., SMETHURST, M.A., MEERT, J.G., VAN DER VOO, R., MCKERROW, W.S., BRASIER, M.D., STURT, B.A. & WALDERHAUG, H.J. 1996. Continental break-up and collision in the Neoproterozoic and Palaeozoic: A tale of Baltica and Laurentia. *Earth Science Reviews*, **40**, 229–258.
- TUCKER, M.E. 1976a. Quartz replaced anhydrite nodules ('Bristol Diamonds') from the Triassic of the Bristol District. *Geological Magazine*, **113**, 569–574.
- TUCKER, M.E. 1976b. Replaced evaporites from the late Precambrian of Finnmark, Arctic Norway. *Sedimentary Geology*, **16**, 193–204.
- TUCKER, M.E. & WRIGHT, V.P. 1990. *Carbonate Sedimentology*. Blackwell Scientific Publications, Oxford. 482 pp.
- TUDHOPE, A.W. & SCOFFIN, T.P. 1984. The effects of *Callianasa* bioturbation on the preservation of carbonate grains in Davies Reef lagoon, Great Barrier Reef, Australia. *Journal Sedimentary Petrology*, **54**, 1091–1096.
- TURNER, E.C., JAMES, N.P. & NARBONNE, G.M. 2000. Taphonomic control on microstructure in early Neoproterozoic reefal stromatolites and thrombolites. *PALAIOS*, **15**, 87–111.
- ULMER-SCHOLLE, D.S. & SCHOLLE, P.A. 1994. Replacement of evaporites within the Permian Park City Formation, Bighorn basin, Wyoming, U.S.A. *Sedimentology*, **41**, 1203–1222.
- VAIL, P.R., 1987. Seismic stratigraphy interpretation using sequence stratigraphy, Part 1: Seismic stratigraphy interpretation procedure. In: BALLY, A.W. (ed.). *AAPG Studies in Geology*, **27**, 1–10.
- VAIL, P.R., MITCHUM, R.M., JR. & THOMPSON, S., III. 1977. Seismic stratigraphy and global changes of sea level, part four: global cycles of relative changes of sea level. *AAPG Memoir*, **26**, 83–98.
- VAIL, P.R., AUDEMARD, F., BOWMAN, S.A., EISNER, P.N. & PEREZ-CRUZ, C. 1991. The stratigraphic signatures of tectonics, eustasy and sedimentology — an overview. In: EINSELE, G., RICKEN, W. & SEILACHER, A. (eds). *Cycles and Events in Stratigraphy*. 617–659.
- VAN BREEMEN, O., AFTALION, M. & JOHNSON, M.R. 1979. Age of the Loch Borrolan complex, Assynt, and late movements along the Moine Thr. *Journal of the Geological Society of London*, **136**, 489–495.
- VAN WAGONER, J.C. 1985. Reservoir facies distribution as controlled by sea-level change. *SEPM. Annual. Midyear Meeting, Golden, CO*, **2**, 91–92.

- VAN WAGONER, J.C., MITCHUM, R.M., CAMPION, K.M., RAHMANIAN, V.D. 1990. Siliciclastic Sequence Stratigraphy in Well Logs, Cores, and Outcrops: Concepts for High-Resolution Correlation of Time and Facies. *AAPG Methods in Exploration*, **7**.
- VAN WAGONER J.C., POSAMENTIER, H.W., MITCHUM, R.M., VAIL, P.R., SARG, J.F., LOUITIT, T.S. & HARDENBOL, J. 1988. An overview of the fundamental of sequence stratigraphy and key definitions. *In*: WILGUS, C.K., HASTINGS, B.S., ROSS, C.A., POSAMENTIER, H.W., VAN WAGONER, J.C. & KENDALL, C.G.St.C. (eds). *Sea-level Changes: An Integrated Approach*, SEPM Special Publication, **42**, 39–45.
- WALTER, M.R. 1977. Interpreting stromatolites. *American Scientist*, **65**, 563–571
- WALTER, M.R. 1994. Stromatolites: the main geological source of information on the evolution of the early benthos. *In*: BENGTSOON, S. (ed.) *Early Life on Earth Nobel Symposium*, **84**, 270–286
- WALTER, M.R., & HEYS, G.R. 1985. Links between the rise of the metazoa and the decline of stromatolites. *Precambrian Research*, **29**, 149–174.
- WALTER, M.R. GROTZINGER, J.P. & SCHOPF, J.W. 1992. Proterozoic stromatolites. *In*: SCHOPF, J.W. & KLEIN, C. (eds), *The Proterozoic Biosphere; a Multidisciplinary Study*. Cambridge University Press, Cambridge, 253–260.
- WALTON, E.K. 1965. Lower Palaeozoic rocks — stratigraphy. *In*: CRAIG, G.Y. (ed.) *The Geology of Scotland*. 1st Edition, Oliver & Boyd, Edinburgh. 161–168.
- WANG, X, STOUGE, S., ERDTMANN, B. -D., CHEN, X, Li, Z., WANG, C., ZENG, Q., ZHOU, Z. & CHEN, H. 2005. A proposed GSSP for the base of the Middle Ordovician Series: the Huanghuachang section, Yichang, China. *Episodes*, **28**, 105–117.
- WANLESS, H.R. & TEDESCO, L.P. 1993. Comparison of oolitic sand bodies generated by tidal vs. wind-wave agitation. *In*: KEITH, B.D. & ZUPPANK, C.W. (eds) *Mississippian Oolites and Modern Analogues*. American Association of Petroleum Geologists, Studies in Geology, **35**, 199–225.
- WARREN, J.K. 2006. *Evaporites: Sediments, Resources and Hydrocarbons*. Springer, 1036 pp.
- WATERS, B.B., SPENCER, R.J. & DEMICCO, R.V. 1989. Three-dimensional architecture of shallowing-upward carbonate-cycles: Middle and Upper Cambrian Waterfowl Formation, Canmore, Alberta. *Bulletin of Canadian Petroleum Geology*, **37**, 198–209.
- WEBBY, B.D. 2002. Patterns of Ordovician reef development. *In* KIESSLING, W., FLÜGEL, E. & GOLONKA, J. (eds.) *Phanerozoic Reef Patterns*. SEPM Special Publication, **72**, 129 –179.
- WEBBY, B.D., COOPER, R.A., BERGSTÖM, S.M. & PARIS, F. 2004. Stratigraphic framework and time slices. *In*: WEBBY, B.D., PARIS, F., DROSER, M.L. & PERCIVAL, I.G. (eds) *The Great Ordovician Biodiversification Event*. Columbia University Press, New York, 41–47.

- WEST, I.M. 1964. Evaporite diagenesis in the Lower Purbeck Beds of Dorset. *Proceedings of the Yorkshire Geological Society*, **34**, 315–330.
- WESTROP, S.R. 1992. Upper Cambrian (Marjuman-Steptoean) trilobites from the Port au Port Group, Western Newfoundland. *Journal of Paleontology*, **66**, 228–255.
- WHISONANT, R.C. 1987. Paleocurrent and petrographic analysis of imbricate intraclasts in shallow-marine carbonates, Upper Cambrian, southwestern Virginia. *Journal of Sedimentary Research*, **57**, 983–994.
- WHITTINGTON, H.B. 1972. Scotland. In: WILLIAMS, A., STRACHAN, I., Bassett, D.A., DEAN, W.T., INGHAM, J.K., WRIGHT, A.D., & WHITTINGTON, H.B. *A Correlation of the Ordovician rocks in the British Isles*. Geological Society of London Special Report. **3**, 49–53.
- WILKINSON, B.H. 1982. Cyclic cratonic carbonates and Phanerozoic calcite seas. *Journal of Geological Education*, **30**, 189–203.
- WILKINSON, B.H., DIEDRICH, N.W. & DRUMMOND, C.N. 1996. Facies successions in peritidal carbonate sequences. *Journal of Sedimentary Research*, **66**, 1065–1078.
- WILLIAMS, H. 1979. Appalachian orogen in Canada. *Canadian Journal of Earth Sciences*, **16**, 792–807.
- WILLIAMS, H. & MAX, M.D. 1980. Zonal subdivision and regional correlation in the Appalachian/Caledonide orogen. In: WONES, D.R. (ed.). *The Caledonides of the USA: Proceedings of the International Geological Correlation Program—Caledonide Orogen Project 27, Blacksburg, VA*. Department of Geological Sciences, Virginia Polytechnic Institute and State University Memoir, **2**, 57–62.
- WILSON, I. 1971. Desert sandflow basins and a model for the development of ergs. *Geographical Journal*, **137**, 180–199.
- WONG, P.K. & OLDERSHAW, E.A. 1980. Causes of cyclicity in reef interior sediments, Kaybob Reef, Alberta. *Bulletin of Canadian Petroleum Geology*, **28**, 411–424.
- WORSLEY, T.R., NANCE, D., & MOODY, J.E. 1984. Global tectonics and eustasy for the past 2 billion years. *Marine Geology*, **58**, 373–400.
- WRIGHT, D.T. 1993. *Studies of the Cambrian Eilean Dubh Formation of North-West Scotland*. Unpublished PhD thesis, University of Oxford.
- WRIGHT, D.T. 1997. An organogenic origin for widespread dolomite in the Cambrian Eilean Dubh Formation, northwestern Scotland. *Journal of Sedimentary Research*, **67**, 54–64.
- WRIGHT, D.T. and KNIGHT, I. 1995. A revised chronostratigraphy for the lower Durness Group. *Scottish Journal of Geology*, **31**, 11–22.
- WRIGHT, S.C. 1985. *The study of the depositional environments and diagenesis in the Durness Group of N.W. Scotland*. Unpublished PhD thesis, University of Oxford.
- WRIGHT, V.P. 1984. Peritidal carbonate facies models: a review. *Geological Journal*, **19**, 309–325.

- WRIGHT, V.P. 1992. Speculations on the controls on cyclic peritidal carbonates: ice-house versus greenhouse eustatic controls. *Sedimentary Geology*, **76**, 1–5.
- YOCHELSON, E.L. 1964. The Early Ordovician gastropod *Ceratopea* from East Greenland. *Meddelelser om Grønland*, **164**, 1–10.
- YOCHELSON, E.L. 1983. *Salterella* (Early Cambrian: Agmata) from the Scottish Highlands. *Palaeontology*, **26**, 253–260.
- YOUNG, H.R. 1979. Evidence of former evaporites in the Cambro-Ordovician Durness Group, Northwest Scotland. *Sedimentary Geology*, **22**, 287–303.
- ZENGER, D.H. 1992. Burrowing and dolomitization patterns in the Steamboat Point Member, Bighorn Dolomite (Upper Ordovician), northeast Wyoming. *Contributions to Geology*, **29**, 133–142.
- ZHEN, Y.Y. & PERCIVAL, I.G. 2003 Ordovician conodont biogeography – reconsidered. *Lethaia*, **36**, 357–370.

APPENDIX 1

Section	Grid reference of base of section	Grid reference of top of section	Location	Lithostratigraphy Represented
030909.1	NC 3835 6886	NC 3850 6886	Balnakeil Bay	uppermost Sailmhor - Sangomore Formation
030909.2	NC3855 6887		Balnakeil Bay	Sangomore Formation
030909.3	NC 3882 6877	NC 3915 6869	Balnakeil Bay	Sangomore - Balnakeil Formation
030912.1/2/3	NC 3783 6877	NC 3835 6886	Balnakeil Bay	Eilean Dubh - Sailmhor Formation
030913.1	NC 4417 5812	NC 4400 5807	An t-Sròn	Pipe Rock Member to baseGhrudaidh Formation
030913.2	NC 4400 5807	NC 4396 5798	An t-Sròn	Ghrudaidh Formation
030914.1	NC 3599 6316	NC 3628 6319	Grudie	Ghrudaidh Formation and lowest Eilean Dubh? Formation
030917-1	NC 3718 6688	NC 3725 6680	Kyle of Durness	uppermost Eilean Dubh to lower Sailmhor
030918.1	NC 3741 6894		Eilean Dubh	lower Eilean Dubh
030918.2	NC 3757 6867		Balnakeil Bay	Middle to upper Eilean Dubh
060911-1/040912-1	NC 2355 2427	NC 2373 2405	Road section E of Skiag Bridge	Furoid Member
030923.2	NC 2662 2006	NC 26655 1996	Inchnadamph	Eilean Dubh-Sailmhor boundary
		NC 2448 2334	Ardvreck	Ghrudaidh - Eilean Dubh Formation boundary.
040523-1	NC 3839 6750		Loch Borrallie	Basal Balnakeil
040523-2	NC 1582 0384		road north of Ullapool	Furoid Member
040524-2	NC 2640 1870		Stronchrubie	Eilean Dubh - Sailmhor boundary
040525-2	NH 1504 9951		Reservoir	Furoid - Salterella Grit Member
040527-2	NG 9805 6517		Fuaran Mor	Furoid Member
040528-1	NC 1968 0999		Knockan Cliff	Furoid Member
040528-2	NC 1985 1010		small roadside quarry	upper Furoid Member
040906-3	NC 3851 6717	NC 3899 6696	E of Loch Borrallie	Croisaphuill Formation
040907-3/4	NC 3906 6870		Balnakeil Bay	Further Balnakeil logging
040908-1	NC 3731 5232		Head of Loch Eriboll	Furoid Member
040909-1	NC 3927 6749	NC 3929 6732	Track to old Manse.	upper Croisaphuill Formation - lower Durine Formation
040910-1	NC 3949 6719	NC 3953 6718	Small quarry, Durness road	mid Durine Formation
040910-2	NC 3952 6701	NC 3960 6705	shore of Caladail.	mid - upper Durine Formation
040910-3	NC 3967 8701	NC 3972 6697	shore of Caladail.	upper Durine Formation

APPENDIX 2

FORMATION/SAMPLE	FORMATION HEIGHT	PROCESSED	LAB NUMBER	WEIGHT PROCESSED	WEIGHT DISSOLVED
Eilean Dubh					
030912-1.1 ED01		yes	2005-38	3937 g	3936 g
Sailmhor					
030912-1.2 SM02	01.10 m	yes	2005-161	4212 g	4102 g
030912-1.3 SM03	03.80 m	yes	2007-45	4092 g	2938 g
030912-1.4 SM04	12.55 m	yes	2005-191	4168 g	3905 g
030912-1.5 SM05	18.75 m	yes	2007-46	4194.00	4119.00
030912-1.6 SM06	28.40 m	yes	2004-10	3995 g	3926 g
030912-1.8 SM08	48.05 m	yes	2005-190	4124.00	4058.00
030912-2.1 SM09	spot sample	yes	2005-164	4055 g	3786 g
030912-3.1 SM10	62.00 m	yes	2003-31	3996 g	3856 g
030912-3.2 SM11	70.75 m	yes	2005-163	4066 g	3767 g
030912-3.3 SM12	81.10 m	yes	2007-48	4019.00	3866.00
030912-3.4 SM13	93.95 m	yes	2003-33	3984 g	3900 g
030912-5.1 SM16	106.98 m	yes	2004-11	3990 g	3869 g
030909-1.1 SM01	108.90 m	yes	2005-160	4110 g	3916 g
Sangomore					
030909-1.2 SG01	01.45 m	yes	2003-09	3865 g	3828 g
030909-1.3 SG02	05.40 m	yes	2005-158	4027 g	3685 g
030909-1.4 SG03	10.45 m	yes	2004-37	4073 g	3837 g
030909-1.5 SG04	17.83 m	yes	2003-27	3926 g	3894 g
030909-1.6 SG05	21.00 m	yes	2004-03	3994 g	3946 g
030909-2.1 SG06	33.90 m	yes	2004-33	4166 g	3913 g
030909-2.2 SG07	34.40 m	yes	2004-45	4005 g	3915 g
030909-2.3 SG08	44.00 m	yes	2004-02	3998 g	3945 g
030909-3.1 SG09	45.20 m	yes	2004-09	3987 g	3886 g
030909-3.2 SG10	54.04 m	yes	2004-46	4172 g	3024 g
030909-2.4 (2005)	33.00 m	yes	2007-49	3976.00	3655.00
030909-2.5 (2005)	40.50 m	yes	2005-166	4182 g	3944 g
030909-2.6 (2005)	40.90 m	yes	2005-170	2686 g	2623 g
030909-3.9 (2005)	40.20 m	yes	2005-165	4134 g	3941 g
Balnakeil					
030909-3.3 BK01	00.85 m	yes	2004-04	3985 g	3985 g
030909-3.4 BK02	02.50 m	yes	2004-34	4045 g	3986 g
030909-3.5 BK03	07.25 m	yes	2004-31	3992 g	3926 g
030909-3.6 BK04	18.50 m	yes	2004-32	3932 g	3905 g
030909-3.7 BK05	30.42 m	yes	2004-36	3988 g	3958 g
030909-3.8 BK06	39.82 m	yes	2004-05	3881 g	3878 g
040907-3.1 BK07	64.90 m	yes	2003-34	3992 g	3865 g
040906-1.1	top	yes	2005-168	4117 g	4045 g
040907-4.2	spot sample	yes	2005-36	3957 g	3953 g
030909-3.11?	32.40 m	yes	2005-167	4165 g	4044 g
Croisaphuil					
040906-3.1	08.50 m	yes	2004-101	4195 g	4057 g
040906-3.2	17.9 m	yes	2005-22	3819 g	3789 g
040906-3.3	29.05 m	yes	2005-25	3573 g	3433 g
040906-3.4	38.25 m	yes	2005-29	3962 g	3834 g
040906-3.5	50.05 m	yes	2005-23	3162 g	3130 g
040906-3.6	58.55 m	yes	2005-27	3655 g	3655 g
040906-3.7	68.65 m	yes	2005-43	3934 g	3896 g
040906-3.8	78.85 m	yes	2005-31	3967 g	3967 g
060524-1.1	93.65 m	yes	2007-40	4123.00	3802.00

APPENDIX 2

060524-1.2	129.55 m	yes	2007-41	3850.00	3694.00
060524-1.3	133.45 m	yes	2007-39	3674 g	3662 g
060524-1.4	146.59 m	yes	2007-42	4063.00	3802.00
060524-1.5	164.29 m	yes	2007-43	4171.00	3679.00
060524-1.6	296.99 m	yes	2007-44	4128.00	3532.00
040909-1.1	10.00 m down	yes	2005-39	4126 g	3876 g
040909-1.2	00.10 m down	yes	2005-46	3495 g	3495 g
Durine					
040909-1.3	10.80 m	yes	2005-37	4002 g	4002 g
040909-1.4	20.70 m	yes	2005-48	4052 g	4052 g
040909-1.5	32.20 m	yes	2005-45	3975 g	3975 g
040909-1.6	34.30 m	yes	2005-44	3993 g	3795 g
040909-1.7	42.90 m	yes	2005-41	3986 g	3950 g
040909-1.8	53.40 m	yes	2005-173	4020 g	3957 g
040910-1.1	55.60 m	yes	2005-187	4021 g	3979 g
040910-1.2	66.20 m	yes	2007-47	3918 g	3897 g
040910-2.1	69.30 m	yes	2005-192	3977 g	3760 g
040910-2.2	80.45 m	yes	2005-189	4167 g	4018 g
040910-3.1	94.40 m	yes	2005-26	3666 g	3549 g
040910-3.2	102.00 m	yes	2005-28	4036 g	3896 g
040910-3.3	120.45 m	yes	2005-21	3904 g	3885 g
040910-4.1	spot sample	yes	2005-24	3889 g	3883 g
040910-6.1	spot sample	yes	2005-30	3983 g	3983 g
040909-2.1	top	yes	2005-20	2518 g	2500 g
040909-2.2	top	yes	2005-19	3882 g	3862 g